Process development for gelatinisation and enzymatic hydrolysis of starch at high concentrations

Process development for gelatinisation and enzymatic hydrolysis of starch at high concentrations

Tim Baks

Voor mijn ouders en broers

Contents

Chapter 1

Introduction

Enzymatic starch hydrolysis

Starch is a biopolymer that consists of approximately 25 w/w % linear (amylose) and 75 w/w % branched (amylopectin) glucose polymers. Amylose has an average molecular weight of 10^5-10^6 g·mol^{-1} built up from α-1,4-linked glucose units. Amylopectin is much larger and it has a molecular weight of 10^7-10^9 g·mol^{-1}. This molecule has a highly branched structure, because approximately 5 % of the glucose units in amylopectin are α-1,6-linked (Ellis *et al.*, 1998). The most important sources for starch are potatoes, maize, wheat and tapioca (Ellis *et al.*, 1998). The properties of the starches from these species differ considerably, not only in the relative proportions of amylose and amylopectin and the characteristics of these molecules, but also in the amount of non-starch components of starch granules, such as lipids, proteins and phosphate groups. Numerous industrial applications of starch exist, either in its native form or after modification. Starch is, for example, applied in adhesive, agrochemical, cosmetic, detergent, food, medical, oil drilling, paper and board, pharmaceutical, plastic, purification, and textile industries (Ellis *et al.*, 1998). Starch can be modified by thermal treatment, by chemical treatment, or by enzymatic treatment (Tharanathan, 2005; Ellis *et al.*, 1998). Several different thermal treatment methods can be distinguished depending on the moisture and treatment temperature: annealing, gelatinisation, and heat/moisture treatment (see Tester and Debon (2000) for details). Starch modification reactions employed for chemical treatment can be divided into four groups: oxidation, esterification, etherification, and crosslinking (Tharanathan, 2005). The most important enzymatic treatment method used to modify starch consists of treatment with hydrolytic enzymes during which glucosidic bonds are broken (Guzman-Maldonado and Paredes-Lopez, 1995).

One of these hydrolytic enzymes is α-amylase from *Bacillus licheniformis*, which is often used for large-scale starch hydrolysis (see *Figure 1*). Enzymatic treatment of starch with α-amylase is usually preceded by gelatinisation. Gelatinisation of starch is required to increase the accessibility of the substrate and to enhance the hydrolysis rate. In industry, a jet cooker is used to gelatinise starch by mixing the starch slurry with steam under pressure (Van der Maarel *et al.*, 2002). After gelatinisation, starch can be hydrolysed. During the first hydrolysis stage called liquefaction, the viscosity of the gelatinised starch mixture is reduced due to partial hydrolysis of the carbohydrate polymers. During the second hydrolysis stage called saccharification, these partially hydrolysed starch chains are broken down into glucose, maltose, maltotriose, and some higher oligomers.
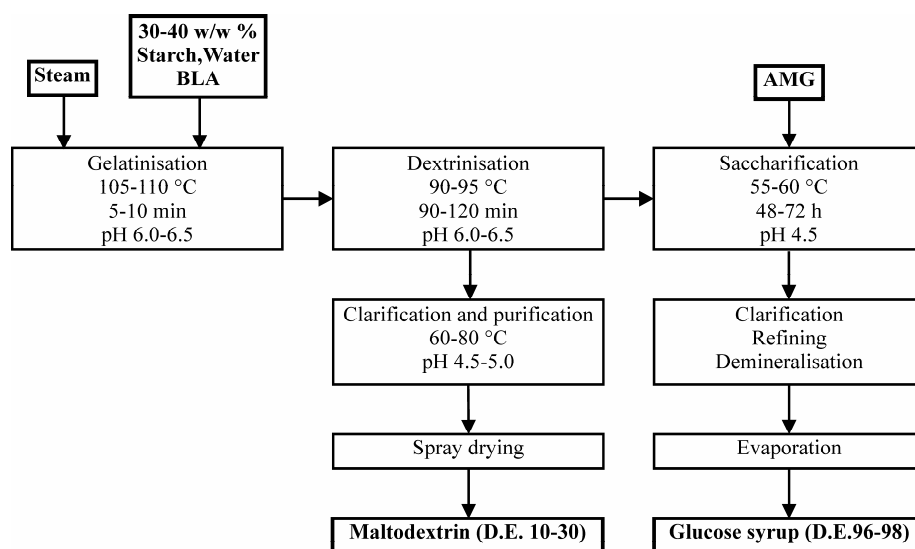
Figure 1: Main steps during production of maltodextrin and glucose syrup (and valid for enzymatic starch hydrolysis in general). Abbreviations: BLA = α-amylase from Bacillus licheniformis; AMG = amyloglucosidase. Based on Fullbrook (1984), Guzman-Maldonado and Paredes-Lopez (1995), and Kennedy et al. (1988).

The properties of the product formed during enzymatic hydrolysis of starch can be varied by using different enzymes (Guzman-Maldonado and Paredes-Lopez, 1995; Van der Maarel *et al.*, 2002). Hydrolysate products are usually characterised by their dextrose equivalent (D.E.), which is a measure for the amount of glucosidic linkages that have been hydrolysed (Chaplin and Bucke, 1990). Native starch has a dextrose equivalent of approximately 0 and glucose has a dextrose equivalent equal to 100. After liquefaction, a wide range of products can be formed with dextrose equivalents varying between 10 and 30 (Fullbrook, 1984). These hydrolysates are called maltodextrins and they are used as carrier or bulk agent, texture provider, fat replacer, ingredient for added nutritional value, etc (Kennedy *et al.*, 1988; Marchal, 1999). After saccharification, the dextrose equivalent of the products varies between 40 and 98 depending on the enzyme and the reaction conditions that were used. Three major product groups can be distinguished (Kennedy *et al.*, 1988). Firstly, high maltose syrups (dextrose equivalent between 40 and 55) are used in the confectionery industry for the manufacture of hard sweets, in industries producing frozen deserts to control the crystal formation, and in the brewing industry due to their high non-glucose fermentability (Fullbrook, 1984). Secondly, high dextrose equivalent syrups (dextrose equivalent between 56 and 68) are used in the confectionery industry; in brewing and fermentation industries, and in general food production (for soft drinks, jams,

conserves, and sauces) (Kennedy *et al.*, 1988). Thirdly, high glucose syrups (dextrose equivalent between 96 and 98) are used in brewing and fermentation industries, in beverage industry (Kennedy *et al.*, 1988), for the manufacture of crystalline D-glucose, and as starting material for the production of fructose syrup (Fullbrook, 1984).

Gelatinisation and hydrolysis at high starch concentrations

In industry, gelatinisation and liquefaction are often carried out simultaneously by adding a thermostable α-amylase to the starch slurry before gelatinisation in a jet cooker. The starch concentration during this process is limited to 30–35 w/w % dry solids, because higher concentrations cannot be processed in a jet-cooker. However, increasing the starch concentration during gelatinisation and enzymatic hydrolysis can potentially yield a higher volumetric productivity, a higher enzyme stability (De Cordt *et al.*, 1994; Klibanov, 1983), and lower energy costs (Grafelman and Meagher, 1995).

Besides the advantages of a higher substrate concentration, it also leads to an increase of the viscosity of the reaction mixture. Consequently, reactor concepts that are used in industry for 30–35 w/w % dry solids starch slurries cannot be used to process more concentrated starch slurries and therefore other reactor types have to be used.

Extruders have proven to be successful for processing of concentrated starch slurries. They have been used for non-enzymatic starch processing (Blanche and Sun, 2004; Cai *et al.*, 1995; Cai and Diosady, 1993; Colonna *et al.*, 1984; Davidson *et al.*, 1984; Gomez and Aguilera, 1984; Jackson *et al.*, 1990; Zheng and Wang, 1994) and enzymatic starch treatment (Ćurić *et al.*, 1998; Govindasamy *et al.*, 1997a,b; Komolprasert and Ofoli, 1991; Lee and Kim, 1990; Roussel *et al.*, 1991; Vasanthan *et al.*, 2001). Since it is not feasible to attain high residence times in an extruder, it is not possible to produce a hydrolysate with a high dextrose equivalent (more than 25) without using high enzyme concentrations. If a higher dextrose equivalent is desired, a second reactor is required that is linked to an extruder to increase the hydrolysis time (Chouvel *et al.*, 1983; Grafelman and Meagher, 1995; Linko *et al.*, 1980, 1983; Meagher and Grafelman, 1999; Reinikainen *et al.*, 1986; Van Zuilichem *et al.*, 1990). The use of separate process steps for gelatinisation and enzymatic hydrolysis may be beneficial, because it enables independent optimisation of these processes. On the other hand, it might also lead to higher equipment costs.

Research aim

The aim of this project was to develop a process for gelatinisation and enzymatic hydrolysis of wheat starch at high substrate concentrations (more than 40 w/w %) with α-amylase from *Bacillus licheniformis*. For this purpose, measurement procedures for the α-amylase activity, degree of gelatinisation, and carbohydrate composition at high starch concentrations were developed. In addition, gelatinisation phase diagrams had to be obtained to determine the temperature and pressure required to completely gelatinise starch in starch-water mixtures with different starch concentrations. Based on these phase diagrams, two main process concepts were investigated in more detail; a high pressure and a high temperature-based process for gelatinisation and enzymatic hydrolysis of starch.

Thesis outline

Measurement procedures used for aqueous solutions are often not applicable for concentrated starch-water mixtures. Consequently, the first part of this study was used to develop measurement techniques for the degree of gelatinisation, and the enzyme activity and stability at high substrate concentrations.

The effects of high concentrations of carbohydrates on α-amylase activity measurements were described in *Chapters 2* and *3*. The results in *Chapter 2* were explained by considering substrate inhibition and substrate competition. A simple kinetic model was used to describe the observed phenomena for starch and maltodextrins. For smaller carbohydrates, this model was not suitable and in *Chapter 3* a more general kinetic model is presented that can be used to describe all phenomena, including the observed maximum in the α-amylase activity measurements that has been observed in the presence of several carbohydrates. Besides substrate inhibition and substrate competition, this model takes into account the formation of a carbohydrate-enzyme complex that remains active.

Chapter 4 compares gelatinisation curves measured for aqueous (10 w/w %) and concentrated (60 w/w %) starch-water mixtures obtained with birefringence, differential scanning calorimetry, wide angle X-ray scattering, and amylose-iodine complex formation. In addition, an adapted version of the Flory equation was used to provide a quantitative explanation for the curves describing the degree of starch gelatinisation as a function of the starch-water ratio and the temperature. The results shown in *Chapter 4* are extended in *Chapter 5* by including the effect of pressure and treatment time on the degree of gelatinisation. In this chapter, a model based on the Gibbs energy difference was used to

describe the degree of gelatinisation as a function of both pressure and temperature at 5, 30, and 60 w/w % wheat starch in water.

Starch can be gelatinised by means of a temperature increase (*Chapters 4* and *5*) or by means of a pressure increase (*Chapter 5*). A comparison between the effects of both gelatinisation methods on the enzymatic hydrolysis of 5 w/w % starch-water mixtures was investigated in *Chapter 6*. The observed differences between thermally gelatinised, high pressure gelatinised, and native starch were explained by considering the accessibility of starch. These results show that the hydrolysate composition can be affected by choosing different process sequences and conditions.

With use of the analysis methods from *Chapters 2*, *3*, and *4* and the gelatinisation diagram in *Chapter 4*, an extruder-based process was developed that is described in *Chapter 7*. We found that it is possible to reach high hydrolysis yields after gelatinisation and hydrolysis of concentrated starch-water mixtures (50-70 w/w %) in this set up. This chapter provides a basis for detailed optimisation of this process for the development of an industrial-scale process at high substrate concentrations.

Instead of carrying out a large number of hydrolysis experiments, it is faster and more efficient to use a kinetic model that is based on literature sources concerning the substrate structure and hydrolysis mechanism. *Chapter 8* describes a stochastic model that was developed for this purpose. This model can be used to describe the formation and breakdown of all saccharides involved during enzymatic starch hydrolysis in time. This kinetic model takes into account the different affinity of α-amylase for different substrates by using the subsite mapping theory. In addition, the main structural characteristics of starch were also taken into account. The validity of the model was verified by comparing the modeled oligosaccharide composition and the dextrose equivalent in time with the corresponding experimental data.

While the process configuration described in *Chapter 7* proved to be successful for gelatinisation and enzymatic hydrolysis at high starch concentrations, other process configurations also seem to be feasible. Besides a description of these alternative processes, *Chapter 9* also discusses how the results that were obtained during this thesis can be used for other applications. In addition, this chapter mentions the remaining topics that have to be studied to apply these processes on an industrial scale.

References

Blanche S, Sun X. 2004. Physical characterization of starch extrudates as a function of melting transitions and extrusion conditions. Adv Polym Tech 23:277-290.

Cai W, Diosady LL. 1993. Model for gelatinization of wheat starch in a twin-screw extruder. J Food Sci 58:872-875, 887.

Cai W, Diosady LL, Rubin LJ. 1995. Degradation of wheat starch in a twin-screw extruder. J Food Eng 26:289-300.

Chaplin MF, Bucke C. 1990. The large-scale use of enzymes in solution. In: Chaplin MF, Bucke C. Enzyme technology. Cambridge: Cambridge University Press. 146-161.

Chouvel H, Chay PB, Cheftel JC. 1983. Enzymatic hydrolysis of starch and cereal flours at intermediate moisture contents in a continuous extrusion-reactor. Lebensmittel-Wissenschaft und -Technologie 16:346-53.

Colonna P, Doublier JL, Melcion JP, De Monredon F, Mercier C. 1984. Extrusion cooking and drum drying of wheat starch. I. Physical and macromolecular modifications. Cereal Chem 61:538-543.

Ćurić D, Karlović D, Tripalo B, Ježek D. 1998. Enzymatic conversion of corn starch in twin-screw extruder. Chem Biochem Eng Q 12:63-71.

Davidson VJ, Paton D, Diosady LL, Rubin LJ. 1984. A model for mechanical degradation of wheat starch in a single-screw extruder. J Food Sci 49:1154-1157.

De Cordt S, Hendrickx M, Maesmans G, Tobback P. 1994. The influence of polyalcohols and carbohydrates on the thermostability of α-amylase. Biotechnol Bioeng 43:107-114.

Ellis RP, Cochrane MP, Dale MFB, Duffus CM, Lynn A, Morrison IM, Prentice RDM, Swanston JS, Tiller SA. 1998. Starch production and industrial use. J Sci Food Agric 77:289-311.

Fullbrook PD. 1984. The enzymic production of glucose syrups. In: Dziedzic SZ; Kearsley MW, editors. Glucose syrups: science and technology. London: Elsevier. 65-115.

Gomez MH, Aguilera JM. 1984. A physicochemical model for extrusion of corn starch. J Food Sci 49:40-43,63.

Govindasamy S, Campanella OH, Oates CG. 1997a. Enzymatic hydrolysis of sago starch in a twin-screw extruder. J Food Eng 32:403-426.

Govindasamy S, Campanella OH, Oates CG. 1997b. The single screw extruder as a bioreactor for sago starch hydrolysis. Food Chem 60:1-11.

Grafelman DD, Meagher MM. 1995. Liquefaction of starch by a single-screw extruder and post-extrusion static-mixer reactor. J Food Eng 24:529-542.

Guzman-Maldonado H, Paredes-Lopez O. 1995. Amylolytic enzymes and products derived from starch: a review. Crit Rev Food Sci Nutr 35:373-403.

Jackson DS, Gomez MH, Waniska RD, Rooney LW. 1990. Effects of single-screw extrusion cooking on starch as measured by aqueous high-performance size-exclusion chromatography. Cereal Chem 67:529-532.

Kennedy JF, Cabalda VM, White CA. 1988. Enzymic starch utilization and genetic engineering. Trends Biotechnol 6:184-189.

Klibanov AM. 1983. Stabilization of enzymes against thermal inactivation. Adv Appl Microbiol 29:1-28.

Komolprasert V, Ofoli RY. 1991. Starch hydrolysis kinetics of *Bacillus licheniformis* α-amylase. J Chem Technol Biotechnol 51:209-223.

Lee YC, Kim KT. 1990. Gelatinization and liquefaction of starch with a heat stable α-amylase. J Food Sci 55:1365-1366, 1372.

Linko P, Linko Y-Y, Olkku J. 1983. Extrusion cooking and bioconversions. J Food Eng 2:243-257.

Linko Y-Y, Vuorinen H, Olkku J, Linko P. 1980. The effect of HTST-extrusion on retention of cereal α-amylase activity and on enzymatic hydrolysis of barley starch. In: Linko P, Larinkari J, editors. Food process engineering. Vol. 2: Enzyme engineering in food processing. London: Applied Science Publishers. 210-23.

Marchal LM. 1999. Towards a rational design of commercial maltodextrins: a mechanistic approach. PhD thesis, Wageningen University, Wageningen, the Netherlands. 197 p.

Meagher MM, Grafelman DD. 1999. Method for liquefaction of cereal grain starch substrate and apparatus therefor. U.S. patent 5,981,237.

Reinikainen P, Suortti T, Olkku J, Mälkki Y, Linko P. 1986. Extrusion cooking in enzymatic liquefaction of wheat starch. Starch/Stärke 38:20-26.

Roussel L, Vieille A, Billet I, Cheftel JC. 1991. Sequential heat gelatinization and enzymatic hydrolysis of corn starch in an extrusion reactor. Optimization for maximum dextrose equivalent. Lebensmittel-Wissenschaft und -Technologie 24:449-458.

Tester RF, Debon SJJ. 2000. Annealing of starch - a review. Int J Biol Macromol 27:1–12.

Tharanathan RN. 2005. Starch - value addition by modification. Crit Rev Food Sci 45:371-384.

Van der Maarel MJEC, Van der Veen B, Uitdehaag JCM, Leemhuis H, Dijkhuizen L. 2002. Properties and applications of starch-converting enzymes of the α-amylase family. J Biotechnol 94:137-155.

Van Zuilichem DJ, Van Roekel GJ, Stolp W, Van 't Riet K. 1990. Modelling of the enzymatic conversion of cracked corn by twin-screw extrusion cooking. J Food Eng 12:13-28.

Vasanthan T, Yeung J, Hoover R. 2001. Dextrinization of starch in barley flours with thermostable alpha-amylase by extrusion cooking. Starch/Stärke 53:616-622.

Zheng X, Wang SS. 1994. Shear induced starch conversion during extrusion. J Food Sci 59:1137-1143.

Chapter 2

The effect of carbohydrates on α-amylase activity measurements

Abstract

The Ceralpha method can be used for the α-amylase activity measurement during the hydrolysis of starch at high substrate concentrations (> 40 w/w %). However, the results are affected by the carbohydrates present in the samples. The effect of carbohydrates on the Ceralpha α-amylase activity measurements was measured over a broad concentration range. It was found that starch has the largest influence and glucose has the lowest influence on the Ceralpha assay procedure. These results were explained by considering substrate inhibition and substrate competition. A simple kinetic model was used to describe the observed phenomena quantitatively. This model was also used to estimate the Michaelis-Menten constant for a large number of substrates and it requires only a single experiment for each K_m determination.

Introduction

One of the most important enzymatic reactions that is carried out at an industrial scale is the enzymatic hydrolysis of starch. α-Amylase (1,4-α-D-glucanohydrolase, E.C. 3.2.1.1) is essential during this process and plays a role in the liquefaction of starch and the subsequent saccharification where larger carbohydrate chains are hydrolysed and converted into smaller carbohydrates (Chaplin and Bucke, 1990). It is therefore important to preserve the highest α-amylase activity during industrial operating conditions.

Currently, enzymatic starch hydrolysis is carried out at a substrate concentration of 35-40 w/w % (Schenck, 2002). Increasing the substrate concentration has several advantages; such as increased volumetric productivity and a higher α-amylase stability (Klibanov, 1983; Krishnan and Chandra, 1983; De Cordt *et al.*, 1994). However, the influence of these conditions on the enzyme activity also needs to be considered. A suitable assay procedure needs to be chosen to determine the residual α-amylase activity under these operating conditions.

Several assay procedures exist and they can be divided into three groups: reducing sugar methods, dyed starch substrate methods and defined substrate methods (Wong and Robertson, 2000). Working at high substrate concentrations leads to a high amount of reducing ends in the samples containing α-amylase and it is therefore difficult to achieve sufficient resolution. For this reason assay procedures based on reducing sugars are not desirable. Furthermore, the addition of more starch is also not advisable because it increases the viscosity of the samples even further. Therefore, a suitable defined substrate method is preferred. We chose for the Ceralpha method that was developed by McCleary and Sheehan (McCleary and Sheehan, 1987; Sheehan and McCleary, 1988) that is now commercialised by Megazyme. This is a rapid and accurate assay (McCleary *et al.*, 2002) that is assumed to be suitable for samples with high background levels of small carbohydrates.

The Ceralpha procedure employs Amylase HR reagent that contains a defined oligosaccharide 'non-reducing-end blocked p-nitrophenyl maltoheptaoside' in the presence of excess levels of a thermostable α-glucosidase. During the assay, endo α-amylase cleaves a bond somewhere in this defined oligosaccharide and due to the excess quantities of α-glucosidase present in the mixture the remaining p-nitrophenyl maltosaccharide is hydrolysed very rapidly to glucose and free p-nitrophenol. The amount of p-nitrophenol released is a measure for the α-amylase activity. The release of this compound leads to a yellow colour that can be measured with a spectrophotometer.

The ceralpha method from Megazyme is widely used, however, the influence of different carbohydrates on the outcome of this α-amylase activity assay has never been reported to our knowledge. In order to study this we chose for components that are also present in samples from hydrolysis experiments, e.g. soluble starch and various starch hydrolysates. A simple kinetic model describing substrate inhibition and substrate competition was used to explain and describe our observations. Furthermore, the same kinetic model was used to calculate estimates of Michaelis-Menten parameters of other substrates.

Materials and methods

Materials

Thermostable α-amylase from *Bacillus licheniformis* (EC 3.2.1.1, Termamyl 120L, type XII-A) was obtained from Sigma-Aldrich (Steinheim, Germany). The enzyme concentration used in the experiments is expressed in grams of this enzyme stock solution per liter. Anhydrous D(+)-glucose, maltotriose, maltodextrin from corn with dextrose equivalents of 4-7, 13-17 and 16.5-19.5 and soluble potato starch were obtained from Sigma-Aldrich (Steinheim, Germany). Maltose monohydrate, sodium chloride, calcium chloride dihydrate and tri-sodium phosphate were bought from Merck (Darmstadt, Germany). Maltotetraose, maltopentaose, maltoheptaose and maltohexaose were present in an oligosaccharide kit obtained from Supelco (Bellefonte, PA, USA). Maleic acid (di-sodium salt) was obtained from Acros Organics (Geel, Belgium). For the measurement of the α-amylase activity Amylase HR reagent was used and this is a product from Megazyme International Ireland (Bray, Republic of Ireland). The standard buffer used for all the experiments was 0.1 M maleic acid buffer (pH 6.5) with 2 mM $CaCl_2$ and 0.1 M NaCl. A solution of 0.06 M tri-sodium phosphate (pH 11) was used as stopping reagent during the Ceralpha end-point measurements.

α-Amylase activity

The α-amylase activity is defined as the amount of p-nitrophenol released in μmol per min per mg of enzyme solution at 40 ºC and pH 6.5. To determine this activity we calculated the release of p-nitrophenol by measuring the absorbance of the reaction mixture at 410 nm

after incubation at 40 ºC (end-point method) and pH 6.5:

$$A_E = \frac{(A - A_0) \cdot D}{\varepsilon_1 \cdot b \cdot C_E \cdot \Delta t} \tag{1}$$

where A_E is the α-amylase activity in μmol·mg^{-1}·min^{-1}, A is the absorbance at 410 nm and 25 ºC, A_0 is the absorbance of the blank solution at 410 nm and 25 ºC (reaction mixture before incubation), Δt is the incubation time in min, ε_1 is the molar absorptivity at 410 nm, 25 ºC and pH 11 in l·μmol^{-1}·cm^{-1}, b is the path length of the light in the cuvette in cm, C_E is the enzyme concentration in mg·l^{-1} and D is the dilution factor.

The release of p-nitrophenol as a result of enzymatic break down by α-amylase can also be determined by continuous measurement of the absorbance of the reaction mixture at 410 nm, 40 ºC and pH 6.5:

$$A_E = \frac{D}{\varepsilon_2 \cdot b \cdot C_E} \cdot \frac{dA}{dt} \tag{2}$$

where dA/dt is the slope of the linear part of the absorbance-time curve and ε_2 is the molar absorptivity at 410 nm, 40 ºC and pH 6.5 in l·μmol^{-1}·cm^{-1}. The continuous activity measurements have the advantage that the linear part of the graph can always be selected. The lag phase that is often observed (Rauscher *et al.*, 1985) during the beginning of the assay can be circumvented in this way. Determination of the activity with the original Ceralpha end-point method does not enable a correction of the lag phase and this makes it less accurate. However, the advantage of the end-point method is that the residual α-amylase activity can be determined in a large number of samples at once.

Measurement of molar absorptivity
The molar absorptivity of p-nitrophenol depends strongly on pH and temperature (Rauscher *et al.*, 1985) and to take this into account we determined the molar absorptivity of p-nitrophenol at our measurement conditions. Stock solutions with a p-nitrophenol concentration varying between $7.2 \cdot 10^{-6}$ and $4.9 \cdot 10^{-5}$ mol·l^{-1} were made in stopping reagent/maleic acid buffer (15/2 by volume). A second set of stock solutions was made with a p-nitrophenol concentration varying between $1.4 \cdot 10^{-5}$ and $9.7 \cdot 10^{-5}$ mol·l^{-1} in maleic acid buffer/demineralized water (7/3 by volume). The pH of these stock solutions were equal to pH of the solutions that were used during the experiments. The molar absorptivity for p-nitrophenol in stopping reagent/maleic acid buffer (pH 11) at room temperature is

$19.5 \cdot 10^{-3}$ l·μmol^{-1}·cm.$^{-1}$ and in maleic acid buffer/demineralized water (pH 6.5) at 40 ºC it amounts to $8.0 \cdot 10^{-3}$ l·μmol^{-1}·cm^{-1}.

Measurement of K_m and V_{max} for blocked p-nitrophenyl maltoheptaoside

A 0.32 g·l^{-1} α-amylase stock solution, Amylase HR reagent and maleic acid buffer were separately pre-incubated for 10 min at 40 ºC in a water bath. After pre-incubation 100 μl of alpha-amylase stock solution was added to respectively 10, 30, 50, 70, 100, 200, 300, 400, 500 and 800 μl of Amylase HR reagent. The volume was filled up to 1.7 ml with maleic acid buffer and incubated for 10 min at 40 ºC in a spectrophotometer while measuring the absorbance at 410 nm. With these data the initial reaction rates can be found at various concentrations of blocked p-nitrophenyl maltoheptaoside. The computer program 'Table Curve 2D' (Jandel Scientific, 1994, version 2.0, San Rafael, CA, USA) was used to determine the values of K_m and V_{max} by minimizing the sum of squared residuals. The enzyme solution that was used for the preparation of the stock solution for these measurements originated from a different batch than the enzyme solution that was used for the other measurements.

α-Amylase activity with different carbohydrates

Stock solutions of different carbohydrates (D(+)-glucose, maltodextrin and soluble starch) and with varying carbohydrate concentrations (between 0 and 286 g·l^{-1}) in maleic acid buffer were made. Enzyme stock solutions for the continuous method contained 35 mg enzyme·/(l solution) and for the end-point method they contained 480 mg enzyme·/(l solution). For each set of experiments a fresh enzyme stock solution was prepared. This solution was kept in the refrigerator for two hours before an experiment was carried out.

The α-amylase activity in the starch solutions was measured according to the Ceralpha end-point assay procedure of Megazyme. The starch stock solutions (0-45 g·l^{-1}) were first heated to 95 °C and they were kept at this temperature for 1 hour in order to gelatinize all the starch. After this treatment the starch was cooled to 40 ºC. The starch stock solutions, the enzyme stock solution and the Amylase HR stock solution were pre-incubated separately for 10 min at 40 ºC in a water bath. After this pre-incubation period 9 ml of the starch stock solutions and 1 ml of the enzyme stock solution were added together and 100 μl of this mixture was added to 100 μl Amylase HR reagent. After an incubation period of exactly 10 min at 40 ºC the reaction was stopped by adding 1.5 ml of stopping reagent

(pH 11) followed by the measurement of the absorbance at 410 nm and 25 ºC. The α-amylase activity in different maltodextrin solutions was also measured with the Ceralpha end-point assay procedure of Megazyme. In this case, the gelatinization step was not necessary and therefore omitted.

The α-amylase activity in all carbohydrate solutions except the starch solutions was measured using the continuous method. The carbohydrate stock solution, the enzyme stock solution and the Amylase HR stock solution were pre-incubated separately for 10 min at 40 ºC in a water bath. After pre-incubation equal volumes of the carbohydrate stock solution and the enzyme stock solution were added together. From this solution 700 μl were taken and added to 300 μl Amylase HR reagent and incubated for 10 min at 40 ºC in a spectrophotometer while measuring the absorbance at 410 nm. All the experiments were carried out in duplicate.

Determination of K_m values for different substrates

A carbohydrate stock solution that contained 100 g·l^{-1} of glucose, maltose, maltotriose, maltotetraose, maltopentaose, maltohexaose, maltoheptaose or maltodextrin in maleic acid buffer (pH 6.5) and an α-amylase stock solution, which contained 30 mg·l^{-1} in the same buffer, were prepared. The continuous method described in the previous section was used for the activity measurements. All experiments were repeated five times (in case of maltotetraose, maltopentaose, maltoheptaose and maltohexaose) or six times (in case of glucose, maltose, maltotriose and maltodextrin).

Kinetic calculations

Substrate inhibition or substrate competition can be described by the following general reaction scheme. Enzyme E attaches to substrate S_1 to form an enzyme-substrate complex (E-S_1). Then the enzyme cleaves the substrate and the products P_{11} and P_{12} are formed:

$$E + S_1 \rightleftharpoons E\text{-}S_1 \longrightarrow E + P_{11} + P_{12}$$
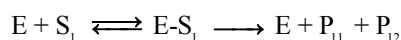
However, the enzyme can also catalyze the reaction of substrate S_2 towards P_{21} and P_{22} in the same manner.

$$E + S_2 \rightleftharpoons E\text{-}S_2 \longrightarrow E + P_{21} + P_{22} \qquad \text{(Substrate competition)}$$

If substrate S_2 cannot be converted into a product but does interact with the active center of the enzyme, substrate inhibition takes place:

$$E + S_2 \rightleftharpoons E\text{-}S_2 \qquad \text{(Substrate inhibition)}$$

These reaction equations form the basis for equation 3, which can be used to describe the initial reaction rate or α-amylase activity in case of substrate competition or substrate inhibition (Cornish-Bowden, 1995):

$$v_1 = \frac{V_{max,1} \cdot \dfrac{[S_1]}{K_{m,1}}}{1 + \dfrac{[S_1]}{K_{m,1}} + \dfrac{[S_2]}{K_{m,2}}} \tag{3}$$

where v_1 is the initial reaction rate in mol·l^{-1}·s^{-1} describing the break down rate of blocked p-nitrophenyl maltoheptaoside, $V_{max,1}$ is the maximum reaction rate in case of blocked p-nitrophenyl maltoheptaoside expressed in mol·l^{-1}·s^{-1}, $K_{m,1}$ and $K_{m,2}$ are the Michaelis-Menten parameters for blocked p-nitrophenyl maltoheptaoside and substrate S_2 in mol·l^{-1} and g·l^{-1} respectively and $[S_1]$ and $[S_2]$ are the concentrations of blocked p-nitrophenyl maltoheptaoside and a carbohydrate causing inhibition or substrate competition in mol·l^{-1} and g·l^{-1} respectively. The initial reaction rate in case of substrate competition and substrate inhibition can be described by the same kinetic equation, because these equations are derived without taking into account the influence of the products that are formed. This is allowed if the amount of conversion is low for both substrates.

Equation 3 can be rewritten to obtain an equation for the dimensionless initial reaction rate or α-amylase activity in case of substrate competition or substrate inhibition.

$$\frac{v_{1,\%}}{100} = \frac{1 + \dfrac{[S_1]}{K_{m,1}}}{1 + \dfrac{[S_1]}{K_{m,1}} + \dfrac{[S_2]}{K_{m,2}}} \tag{4}$$

where $v_{1,\%}$ is the initial reaction rate as a percentage of the initial reaction rate without addition of carbohydrates. Equation 4 does not depend on $V_{max,1}$ and it can be used to account for deviations between different α-amylase stock solutions. It is therefore required to measure the α-amylase actvity of the current α-amylase stock solution during each set of measurements.

Measurements with the spectrophotometer enable us to determine the dimensionless initial reaction rate of blocked p-nitrophenyl maltoheptaoside ($v_{1,\%}$). Because we have already determined $K_{m,1}$ and we know the initial concentrations of blocked p-nitrophenyl maltoheptaoside and S_2 the only unknown parameter in equations 4 is $K_{m,2}$. Equation 4 can

be used to fit the model data to the experimental data and the $K_{m,2}$ value was determined by minimizing the sum of the squared residuals.

Results and discussion

The influence of components on α-amylase has been investigated before, however, this research was mainly focused on the stability of α-amylase after addition of metal ions, ligands or carbohydrates (Asther and Meunier, 1990; Krishnan and Chandra, 1983; Lecker and Khan, 1998; Salieri *et al.*, 1995). The change in activity after addition of different components gained less interest. The influence of carbohydrates on the α-amylase activity determined with the Ceralpha assay procedure has not been investigated yet. Since we want to use this method for the measurement of the residual α-amylase activity during the hydrolysis of starch at high substrate concentrations, it is important to establish the effect of high carbohydrate concentrations on this assay procedure.

Measurement of K_m and V_{max} for blocked p-nitrophenyl maltoheptaoside
In order to use equation 3 or 4 the K_m and V_{max} for blocked p-nitrophenyl maltoheptaoside must be determined. This has been done by fitting the standard Michaelis-Menten equation to our experimental data points (*Figure 1*).
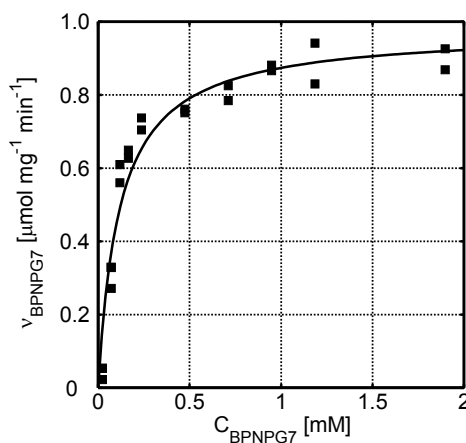
Figure 1: Initial reaction rate plotted vs. substrate concentration for hydrolysis of blocked p-nitrophenyl maltoheptaoside. The points indicate the experimental values and the line gives the values obeying the Michaelis-Menten equation with $K_{m,1}$ is 0.12 ± 0.03 mM (95 % confidence interval) and $V_{max,1}$ is equal to 0.98 ± 0.07 $\mu mol \cdot mg^{-1} \cdot min^{-1}$ (95 % confidence interval). Conditions: $C_E = 1.7 \cdot 10^{-2}\ g \cdot l^{-1}$, T = 40 °C, pH = 6.5.

This fit leads to a $K_{m,1}$ of 0.12 ± 0.03 mM (95 % confidence interval) and a maximum reaction rate $V_{max,1}$ that is equal to 0.98 ± 0.07 μmol·mg⁻¹·min⁻¹ (95 % confidence interval).

Effect of soluble starch on α-amylase activity
Starch is often present in samples that were taken during starch hydrolysis experiments and it is therefore essential to determine the influence of this carbohydrate on the α-amylase activity. *Figure 2* shows the α-amylase activity as a function of the soluble potato starch concentration.
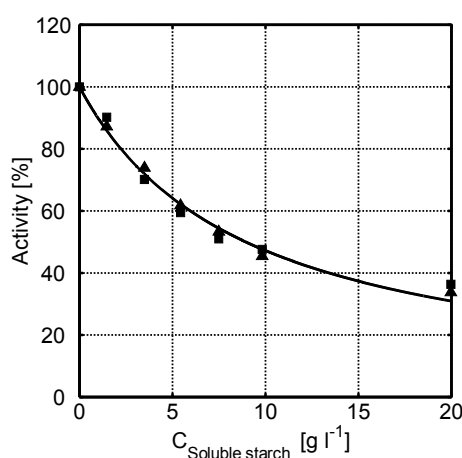
Figure 2: α-Amylase activity as function of the soluble potato starch concentration. Data obtained with duplicate experiments (experiment 1: ■, experiment 2: ▲). Conditions: C_E = 2.4·10⁻² g·l⁻¹, T = 40 °C, pH = 6.5. Without sugars ($C_{soluble\ starch}$ = 0) the α-amylase activity is 100 %, which equals 1.66 ± 0.07 μmol·mg⁻¹·min⁻¹.

The α-amylase activity in this figure is expressed as a percentage of the α-amylase activity without addition of carbohydrates. The latter value is equal to 1.66 ± 0.07 μmol·mg⁻¹·min⁻¹ (95 % confidence interval, based on 22 measurements). The α-amylase activity decreases with an increasing concentration of soluble starch. Besides blocked p-nitrophenyl maltoheptaoside, starch is a substrate for α-amylase as well. With the assumption of substrate competition, equation 4 can be used to describe the experimental data. For $K_{m,1}$ the value of blocked p-nitrophenyl maltoheptaoside is used. Equation 4 is fitted to the experimental data, which resulted in a $K_{m,2}$ 0.49 ± 0.04 g·l⁻¹ for soluble starch (*Table 1*).

17

Table 1: Affinity constants of several carbohydrates with 95 % confidence interval.

	$K_{m,2}$ [g·l^{-1}]	$K_{m,2}$ [mmol·l^{-1}]
Soluble potato starch	0.49 ± 0.04[a]	-
Maltodextrin D.E. 4-7	1.27 ± 0.08[a] 1.28 ± 0.09[b]	-
Maltodextrin D.E. 13-17	2.24 ± 0.19[b]	-
Maltodextrin D.E. 16.5-19.5	2.66 ± 0.49[b]	-
Maltotetraose	2.22 ± 0.19[b]	3.33 ± 0.28[b]
Maltopentaose	3.17 ± 0.77[b]	3.83 ± 0.93[b]
Maltohexaose	2.54 ± 0.25[b]	2.57 ± 0.25[b]
Maltoheptaose	1.93 ± 0.52[b]	1.67 ± 0.45[b]

[a] $K_{m,2}$ value obtained by fitting equation 4 to experimental data sets.

[b] $K_{m,2}$ value calculated with equation 4 by inserting experimental data from one single measurement.

Figure 2 also shows the α-amylase activity that was calculated with this model. The calculated values are in good agreement with the experimentally determined values. Furthermore, the K_m value obtained by fitting our model equation to the experimental data has the same order of magnitude as the values found in literature where K_m values of 1.2 (30 °C, pH 8.2; Asther and Meunier, 1990) and 0.9 g·l^{-1} (30 °C, pH 6.5; Dobreva *et al.*, 1994) were reported.

Effect of maltodextrin on α-amylase activity

As the starch hydrolysis proceeds starch is converted into several hydrolysates. One of these hydrolysis products is maltodextrin. The influence of maltodextrin (with a dextrose equivalent of 4-7) on the α-amylase activity assay is shown in *Figure 3*.
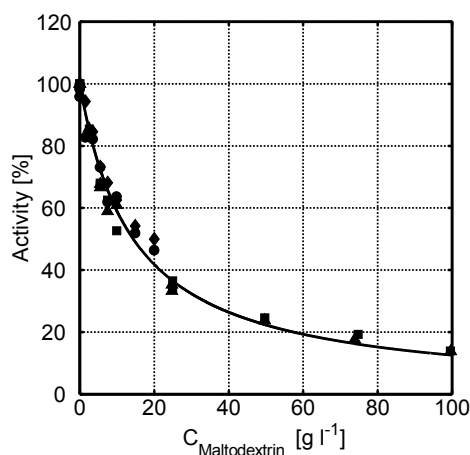
Figure 3: α-Amylase activity as function of the maltodextrin (with dextrose equivalent 4-7) concentration. Experiments 1 (▲) and 2 (■) were carried out with the continuous method. Experiments 3 (◆) and 4 (●) were carried out with the end-point method. Conditions: T = 40 °C, pH = 6.5, C_E = 1.2·10^{-2} g·l^{-1} (continuous method), C_E = 2.4·10^{-2} g·l^{-1} (end-point method). Without sugars ($C_{maltodextrin}$ = 0) the α-amylase activity is 100 %, which equals 1.66 ± 0.07 μmol·mg^{-1}·min^{-1}.

The α-amylase activity was measured with the Ceralpha end-point assay procedure as well as with the continuous method. The results obtained with both methods are comparable. As with starch the α-amylase activity decreases with increasing maltodextrin concentration. Maltodextrin can be hydrolysed by α-amylase and therefore substrate competition was assumed. The line in *Figure 3* shows the values that were obtained by using equation 4 to fit the experimental data and we obtained a $K_{m,2}$ of 1.27 ± 0.08 g·l^{-1} (*Table 1*).

Effect of glucose on α-amylase activity

The final product of starch hydrolysis is glucose. *Figure 4* shows the α-amylase activity as a function of the D(+)-glucose concentration. At low glucose concentrations, the α-amylase activity increases and after a maximum has been reached at 5.4 g·l^{-1} the activity starts to decrease slowly with increasing glucose concentration.
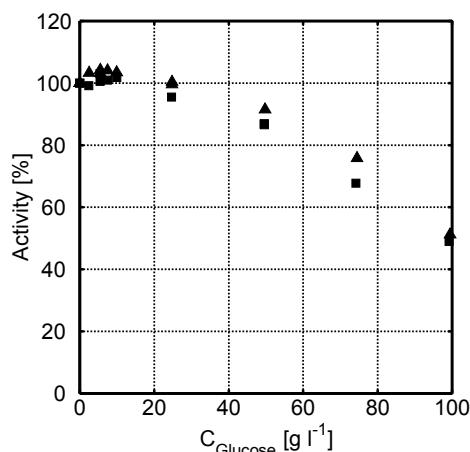
Figure 4: α-Amylase activity as function of the D(+)-glucose concentration. Data obtained with duplicate experiments (experiment 1: ■, experiment 2: ▲). Conditions: $C_E = 1.2 \cdot 10^{-2}$ g·l⁻¹, T = 40 ºC, pH = 6.5. Without sugars ($C_{glucose}$ = 0) the α-amylase activity is 100 %, which equals 1.66 ± 0.07 μmol·mg⁻¹·min⁻¹.

An increased activity in the presence of components has been observed before for other enzymes, e.g. increased pyruvate kinase activity in the presence of sorbitol (Xu *et al.*, 1990) and increased yeast alcohol dehydrogenase activity after addition of alcohols, polyols and carbohydrates (Larreta-Garde *et al.*, 1988). Gray (1988) states that if there is an equilibrium between the active, native form and an inactive unfolded conformer of the enzyme, the binding of the carbohydrate to the first one shifts the equilibrium towards the active native form with beneficial resulting effects on the overall enzyme activity. This might be an explanation for the observed behaviour at low glucose concentrations. The decrease in activity can be explained by assuming inhibition by glucose. Inhibition of α-amylase from *Bacillus licheniformis* by glucose was also reported by Yankov *et al.* (1986). Equation 4 can be used to describe product inhibition, but it cannot be used to describe the maximum in the enzyme activity as a function of the glucose concentration. A different kinetic equation is needed to describe this phenomenon.

Comparison of α-amylase activities in the presence of carbohydrates
Glucose, soluble starch and maltodextrin can all be present in starch hydrolysis samples. *Table 1* shows that α-amylase has a comparable affinity for soluble starch as for maltodextrin with a dextrose equivalent of 4-7. The decrease in activity after addition of glucose (*Figure 4*) is much lower as compared to the decrease shown in *Figures 2* and *3*. Therefore, the affinity of α-amylase for glucose is much lower than for starch and

maltodextrin. This might be explained by considering the subsite map of α-amylase from *Bacillus licheniformis*. This subsite map found by Kandra *et al.* (2002) suggest that this enzyme has at least 8 subsites and 1 catalytic site. Carbohydrate molecules that occupy more binding sites and thus lower the free energy will form a stronger enzyme-substrate complex. Glucose occupies only one binding site and will therefore form a weak enzyme-substrate complex. However, carbohydrate chains in maltodextrin and starch probably occupy all the subsites in the enzyme leading to a higher affinity.

The results shown in *Figures 2, 3* and *4* have a large influence on the results obtained with the Ceralpha method. Imagine that a starch hydrolysis experiment without α-amylase deactivation is carried out and samples are taken in time to determine the residual α-amylase activity. During such an experiment the starting material can be soluble starch and the end product D(+)-glucose. Although the amount of active enzyme and the total amount of carbohydrate is equal in all samples, one can find differences in residual α-amylase activity because D(+)-glucose influences the Ceralpha assay procedure differently than soluble starch. Even at low concentrations a deviation of 10 % from the desired value is easily achieved and at higher concentrations the deviations can even be more than 50 % although the amount of active enzyme in all the samples is equal.

Determination of K_m values for different substrates

Since the K_m for blocked p-nitrophenyl maltoheptaoside has already been determined by conventional kinetic measurements, equation 4 can be used to calculate the K_m values of other substrates by treating them as competitive substrates (Cornish-Bowden, 1995). This method enables us to calculate K_m values with a single measurement at a certain carbohydrate concentration. The concentration of this second substrate should be large enough to induce a significant change in α-amylase activity (more than 10 %).

Figure 5 shows the α-amylase activity as function for various types of carbohydrate at a carbohydrate concentration of 35 g·l⁻¹. Addition of glucose (DP1) has the smallest effect on the α-amylase activity and maltodextrin with a dextrose equivalent of 4-7 (MD3) leads to the highest activity change. This figure shows that the apparent change in α-amylase activity is more than 10 % for all carbohydrates except for glucose. However, not all measurements can be used to determine K_m values. The results from glucose showed a maximum in the actvity vs. glucose concentration curve that could not be fitted with equation 4. Preliminary results show that this behaviour is also observed in the presence of maltose and maltotriose. The K_m values were therefore only calculated for components that

could be hydrolysed by α-amylase and cause substrate competition (maltotetraose, maltopentaose, maltohexaose, maltoheptaose and several maltodextrins).
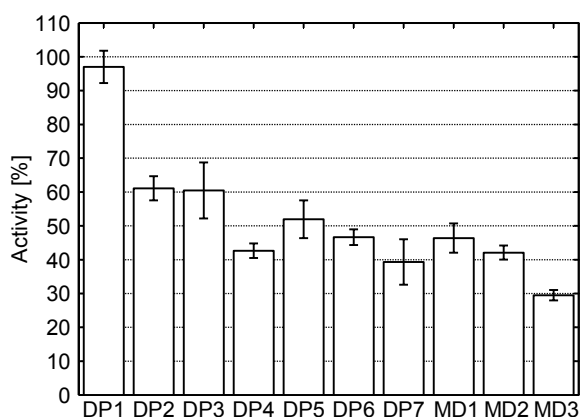
Figure 5: α-Amylase activity for various types of carbohydrates. The sugar concentration of all sugars was 35 g·l⁻¹ during the assay. Without sugars ($C_{carbohydrate}$ = 0) the α-amylase activity is 100 %, which equals 1.66 ± 0.07 µmol·mg⁻¹·min⁻¹. Conditions: C_E = 1.0·10⁻² g·l⁻¹, T = 40 ºC, pH = 6.5. Abbreviations: DP1 = glucose, DP2 = maltose, DP3 = maltotriose, DP4 = maltotetraose, DP5 = maltopentaose, DP6 = maltohexaose, DP7 = maltoheptaose, MD1 = maltodextrin with dextrose equivalent 4-7, MD2 = maltodextrin with dextrose equivalent 13-17, MD3 = maltodextrin with dextrose equivalent 16.5-19.5. Error bars show the 95 % confidence interval.

The K_m values that we have determined for various carbohydrates by using equation 4 are listed in *Table 1*. Maltopentaose has the highest K_m value and therefore the lowest affinity. The K_m value decreased as the chain length of the oligosaccharide increases. However, the K_m value of maltotetraose is slightly lower than that of maltopentaose. Maltotetraose is a poor substrate for α-amylase (Kandra *et al.*, 2002; Nakakuki *et al.*, 1984) and it might be acting as an inhibitor instead of second substrate for α-amylase. The behaviour of α-amylase in a maltotetraose solution might therefore be comparable with the behaviour observed in case of glucose (*Table 1*). A different model is therefore needed to describe these phenomena (Baks *et al.*, 2006) and in that case equation 4 cannot be used to find the K_m value for maltotetraose.

The K_m values that we have determined for maltopentaose, maltohexaose and maltoheptaose have the same order of magnitude as the ones reported by Kandra *et al.* (2002). However, these authors predict that the K_m values increase with increasing degree of polymerisation. This is not in agreement with the hydrolysis experiments that we carried out with pure oligosaccharides.

We have also determined the K_m values for various maltodextrins and these are also listed in *Table 1*. The K_m value for maltodextrin with a dextrose equivalent of 4-7 obtained from *Figure 3* (1.27 g·l⁻¹) has the same order of magnitude as the K_m value calculated here (1.28 g·l⁻¹). The affinity of α-amylase decreases with an increasing dextrose equivalent in case of maltodextrin. *Table 1* clearly shows that the carbohydrate chain length determines the affinity of α-amylase towards a certain substrate.

Conclusions

Carbohydrates can have a large effect on the Ceralpha α-amylase assay. The results have shown that maltodextrin and starch have the largest effect and glucose has the lowest effect on this method. The effect of carbohydrates during the Ceralpha α-amylase assay can be described and modeled quantitatively by considering substrate inhibition and substrate competition.

In general, substrate inhibition and substrate competition can be a source of errors during the activity measurements of any enzyme and this can be illustrated by the model shown in this paper. Especially enzyme activity measurements in samples with a high carbohydrate concentration can lead to large deviations from the true enzyme activity. However, by proper interpretation correct results can be obtained.

Due to the existence of substrate inhibition and substrate competition we were able to use the Ceralpha assay procedure to determine the K_m values of a broad range of α-amylase substrates. The K_m values that we have determined had the same order of magnitude as the ones obtained from literature.

Acknowledgements

References

Asther M, Meunier JC. 1990. Increased thermal stability of *Bacillus licheniformis* α-amylase in the presence of various sugars. Enzyme Microb Tech 12:902-905.

Baks T, Janssen AEM, Boom RM. 2006. A kinetic model to explain the maximum in α-amylase activity measurements in the presence of small carbohydrates. Biotechnol Bioeng 94:431-440.

Chaplin MF, Bucke C. 1990. The large-scale use of enzymes in solution. In: Chaplin MF, Bucke C. Enzyme technology. Cambridge: Cambridge University Press. 146-161.

Cornish-Bowden A. 1995. Fundamentals of enzyme kinetics. London: Portland Press. 343 p.

De Cordt S, Hendrickx M, Maesmans G, Tobback P. 1994. The influence of polyalcohols and carbohydrates on the thermostability of α-amylase. Biotechnol Bioeng 43:107-114.

Dobreva E, Ivanova V, Emanuilova E. 1994. Effect of temperature on some characteristics of the thermostable α-amylase from *Bacillus licheniformis*. World J Microbiol Biotechnol 10:547-550.

Gray CJ. 1988. Sugars and enzyme stability. Biocatalysis 1:187-196.

Kandra L, Gyémánt G, Remenyik J, Hovánszki G, Lipták A. 2002. Action pattern and subsite mapping of *Bacillus licheniformis* α-amylase (BLA) with modified maltooligosaccharide substrates. FEBS lett 518:79-82.

Klibanov AM. 1983. Stabilization of enzymes against thermal inactivation. Adv Appl Microbiol 29:1-28.

Krishnan T, Chandra AK. 1983. Purification and characterization of α-amylase from *Bacillus licheniformis* CUMC305. Appl Environ Microb 46:430-437.

Larreta-Garde V, Xu ZF, Thomas D. 1988. Behavior of enzymes in the presence of sugars. Influence of alcohols, polyols, and sugars on activity and stability of yeast alcohol dehydrogenase. Ann NY Acad Sci 542:294-298.

Lecker DN, Khan A. 1998. Model for the inactivation of α-amlyase in the presence of salts: theoretical and experimental studies. Biotechnol Progr 14:621-625.

McCleary BV, McNally M, Monaghan D, Mugford DC, Collaborators: Black C, Broadbent R, Chin M, Cormack M, Fox R, Gaines C, Gothard P, Home S, Howes E, Johnson C, Keeping R, Koliatsou M, Lindhauer M, Marins de Sa R, Martin R, Monaghan D, Nees U, Nishwitz R, Palmer G, Panozzo J, Recabarren J, Roumeliotis S, Seddig S, Solah V, Sonnet M, Themeier H. 2002. Measurement of α-amylase activity in white wheat flour, milled malt, and microbial enzyme preparations, using the Ceralpha assay: collaborative study. J AOAC Int 85:1096-1102.

McCleary BV, Sheehan H. 1987. Measurement of cereal α-amylase: a new assay procedure. J Cereal Sci 6:237-251.

Nakakuki T, Azuma K, Kainuma K. 1984. Action patterns of various exo-amylases and the anomeric configurations of their products. Carbohydr Res 128:297-310.

Rauscher E, Neumann U, Schaich E, Von Bülow S, Wahlefeld AW. 1985. Optimized conditions for determining activity concentration of α-amylase in serum, with 1,4-α-D-4-nitrophenylmalto-heptaoside as substrate. Clin Chem 31:14-19.

Salieri G, Vinci G, Antonelli ML. 1995. Microcalorimetric study of the enzymatic hydrolysis of starch: an α-amylase catalyzed reaction. Anal Chim Acta 300:287-292.

Schenck FW. 2002. Starch hydrolysates - An overview. Int Sugar J 104:82-89.

Sheehan H., McCleary BV. 1988. A new procedure for the measurement of fungal and bacterial α-amylase. Biotechnol Tech 2:289-292.

Wong DWS, Robertson GH. 2000. α-Amylases. In: Whitaker JR, Voragen AGJ, Wong DWS, editors. Handbook of food enzymology. New York: Marcel Dekker. 714-718.

Xu ZF, Thomas D, Larreta-Garde V. 1990. Kinetic indication for a conformational change of enzyme by a modified aqueous microenvironment. Ann NY Acad Sci 613:506-510.

Yankov D, Dobreva E, Beschkov V, Emanuilova E. 1986. Study of optimum conditions and kinetics of starch hydrolysis by means of thermostable α-amylase. Enzyme Microb Tech 8:665-667.

Chapter 3

A kinetic model to explain the maximum in α-amylase activity measurements in the presence of small carbohydrates

Abstract

The effect of the presence of several small carbohydrates on the measurement of the α-amylase activity was determined over a broad concentration range. At low carbohydrate concentrations, a distinct maximum in the α-amylase activity vs. concentration curves was observed in several cases. At higher concentrations, all carbohydrates show a decreasing α-amylase activity at increasing carbohydrate concentrations. A general kinetic model has been developed that can be used to describe and explain these phenomena. This model is based on the formation of a carbohydrate-enzyme complex that remains active. It is assumed that this complex is formed when a carbohydrate binds to α-amylase without blocking the catalytic site and its surrounding subsites. Furthermore, the kinetic model incorporates substrate inhibition and substrate competition. Depending on the carbohydrate type and concentration, the measured α-amylase activity can be 75 % lower than the actual α-amylase activity. The model that has been developed can be used to correct for these effects in order to obtain the actual amount of active enzyme.

Introduction

α-Amylase (1,4-α-D-glucanohydrolase, E.C. 3.2.1.1) plays an important role in the enzymatic hydrolysis of starch at an industrial scale (Chaplin and Bucke, 1990; Van der Maarel *et al.*, 2002). McCleary and Sheehan developed a rapid and accurate method to determine the residual α-amylase activity (McCleary and Sheehan, 1987; Sheehan and McCleary, 1988; McCleary *et al.*, 2002). This procedure is also known as the Ceralpha procedure (CER 07/00, Megazyme).

The Ceralpha procedure employs Amylase HR reagent that contains a defined oligosaccharide 'blocked (4,6-O-benzilidine)-p-nitrophenyl maltoheptaoside' (in the remainder of the article called blocked p-nitrophenyl maltoheptaoside) in the presence of excess levels of a thermostable α-glucosidase. During the assay, endo α-amylase cleaves a bond somewhere in this oligosaccharide. Due to the excess quantities of α-glucosidase present in the mixture the remaining p-nitrophenyl maltosaccharide is quickly hydrolysed to glucose and free p-nitrophenol. The amount of p-nitrophenol released is then a measure for the α-amylase activity. The release of this compound leads to a yellow colour that can be measured continuously with a spectrophotometer. Continuous measurement of p-nitrophenol gives the same results as the original end-point method (Baks *et al.*, 2006). However, the continuous method enables us to ascertain that the cleavage of α-amylase is the rate-determining step instead of the hydrolysis catalysed by α-glucosidase.

The Ceralpha method is used in several industries to measure the α-amylase activity. For example, it is the standard method for the measurement of the α-amylase activity of the International Association for Cereal Science and Technology, and the Association of Official Analytical Chemists International. The Ceralpha method is often used to measure the residual α-amylase activity in a reaction mixture where various carbohydrates are present. It is therefore important to know the effect of carbohydrates on this method. We investigated the effects of carbohydrates on the Ceralpha method before (Baks *et al.*, 2006). In that work, the effects of soluble potato starch, maltodextrin and glucose on α-amylase activity measurements with the Ceralpha method were determined over a broad concentration range. A simple kinetic model based on substrate competition or substrate inhibition was developed. This model was able to describe the decrease in α-amylase activity that was observed when the soluble starch or maltodextrin concentration was increased. However, this model could not explain the results that were obtained after glucose addition. The α-amylase activity showed a maximum in the activity vs. glucose

concentration curve that was not observed with larger saccharides. An increased activity in the presence of components had been observed before for other enzymes, e.g. increased pyruvate kinase activity in the presence of sorbitol (Xu *et al.*, 1990) and increased yeast alcohol dehydrogenase activity after addition of alcohols, polyols, and carbohydrates (Larreta-Garde *et al.*, 1988). The activity of pyruvate kinase was measured by coupling the pyruvate formation to the lactic dehydrogenase reaction. Sorbitol is supposed to accelerate the first reaction by decreasing the electrostatic repulsion between the reactants of the pyruvate formation, which is favourable for the catalytic function of pyruvate kinase and is accompanied by conformational changes of the enzyme. The increased activity of yeast alcohol dehydrogenase was assumed to be caused by changes in the microenvironment of the enzyme after addition of alcohols, polyols, and carbohydrates.

Since the kinetic model from our previous article (Baks *et al.*, 2006) could not explain the increased α-amylase activity that had been observed at low glucose concentrations, we propose here that substrate inhibition and substrate competition are not the only phenomena that take place under these conditions. We therefore extended the model by taking into account the formation of complexes between the added carbohydrates (e.g. glucose) and α-amylase. In this article, the extended model will be used to describe the experimental data from glucose and other small carbohydrates.

Kinetic model

According to the subsite theory, the active site of an α-amylase consists of a definite number of subsites (Hiromi, 1970; Allen and Thoma, 1976). This theory assumes that a saccharide can form a complex with the enzyme that results either in a non-productive or a productive complex (*Figures 1A* and *1B*). The formation of a productive complex will result in the cleavage of an α,1-4 glycosidic bond in the saccharide whereas the formation of a non-productive complex will not lead to cleavage. This knowledge forms the basis for the kinetic scheme shown in *Figure 2* that will be explained in detail below.
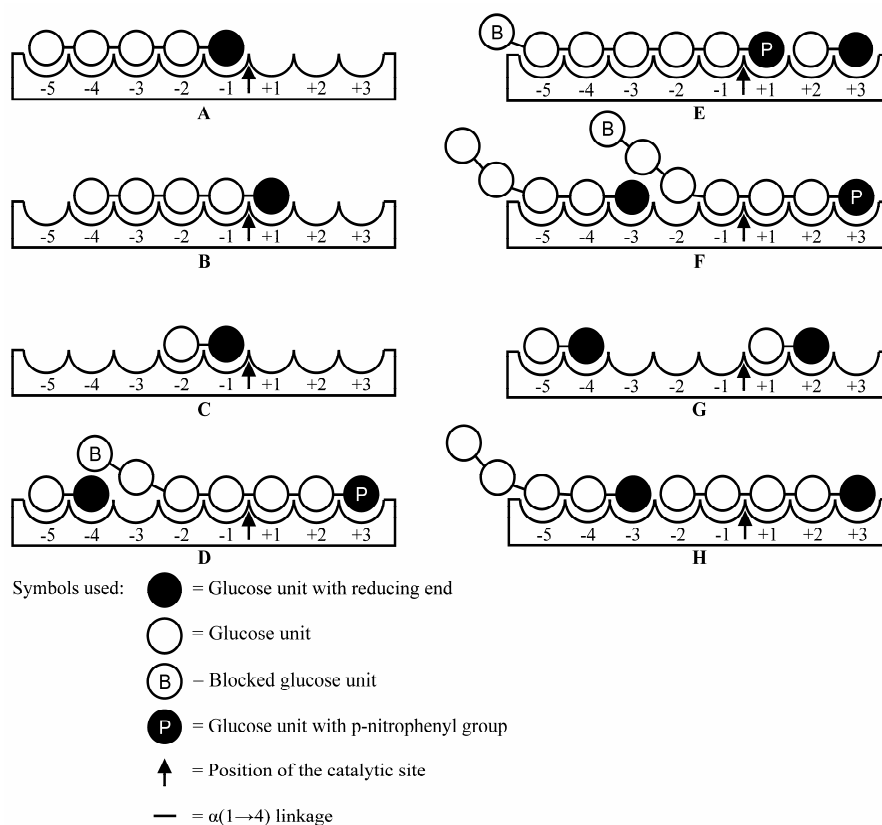
Figure 1: Several carbohydrate-α-amylase complexes based on the subsite mapping theory (Hiromi, 1970; Allen and Thoma, 1976): Non-productive complex with maltopentaose resulting in inhibition (Figure A); Productive complex with maltopentaose resulting in substrate competition (Figure B); Non-productive complex with maltose resulting in inhibition (Figure C); Active complex that consists of maltose and α-amylase that forms a productive complex with blocked p-nitrophenyl maltoheptaoside (Figure D); Active complex that consists of maltose and α-amylase that forms a productive complex with blocked p-nitrophenyl maltoheptaoside (Figure E); Active complex that consists of maltopentaose and α-amylase that forms a productive complex with blocked p-nitrophenyl maltoheptaoside (Figure F); Formation of complex between α-amylase and two maltose molecules leading to inhibition (Figure G); and complex that consists of maltopentaose and α-amylase that forms a productive complex with another maltopentaose resulting in substrate competition (with respect to blocked p-nitrophenyl maltoheptaoside) (Figure H).

Substrate S_1 (blocked p-nitrophenyl maltoheptaoside) attaches to enzyme E to form an enzyme-substrate complex (E-S_1). This complex can either decompose again in E and S_1, or it can lead to cleavage of substrate S_1 and subsequent formation of products P_1. The enzyme can also bind to carbohydrate S_2 and form enzyme-carbohydrate complex E-S_2. According to the subsite map of α-amylase from *Bacillus licheniformis* (Kandra *et al.*, 2002), small carbohydrates can bind at several places either leading to the cleavage of the substrate (*Figure 1B*) or to the formation of a non-productive complex (*Figures 1A* and *1C*). It is possible that these carbohydrates form a non-productive complex with the enzyme without blocking the catalytic site and the subsites surrounding it (*Figures 1D-1F*). It is therefore possible that the new enzyme-carbohydrate complex E-S_2 is still active. It can bind substrate S_1 and convert it into products P_1. If, however, a second small carbohydrate molecule attaches to other subsites surrounding the catalytic site (leading to the formation of E-S_2-S_2) the likelihood increases that the enzyme is blocked leading to substrate inhibition (*Figure 1G*) or substrate competition (*Figure 1H*) leading to subsequent release of products P_2 and enzyme complex E-S_2.
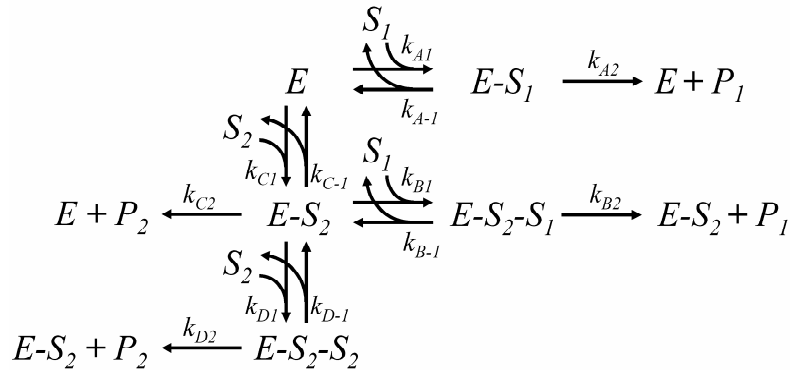
Figure 2: Reaction scheme for kinetic model. Symbols used: S_1 = blocked p-nitrophenyl maltoheptaoside; S_2 = small carbohydrate; P_1 = products from hydrolysis of blocked p-nitrophenyl maltoheptaoside; P_2 = products from hydrolysis of carbohydrate S_2; E = α-amylase; k_i = reaction rate constants.

The reaction scheme in *Figure 2* can be used to derive the mole balances for S_1, $E\text{-}S_1$, $E\text{-}S_2$, $E\text{-}S_2\text{-}S_2$, and $E\text{-}S_2\text{-}S_1$:

$$
\begin{aligned}
v_1 = -\frac{d[S_1]}{dt} &= k_{A1} \cdot [E] \cdot [S_1] - k_{A\text{-}1} \cdot [E\text{-}S_1] \\
&+ k_{B1} \cdot [E\text{-}S_2] \cdot [S_1] - k_{B\text{-}1} \cdot [E\text{-}S_2\text{-}S_1]
\end{aligned}
\tag{1}
$$

$$
\frac{d[E\text{-}S_1]}{dt} = k_{A1} \cdot [E] \cdot [S_1] - k_{A\text{-}1} \cdot [E\text{-}S_1] - k_{A2} \cdot [E\text{-}S_1]
\tag{2}
$$

$$
\begin{aligned}
\frac{d[E\text{-}S_2]}{dt} &= k_{C1} \cdot [E] \cdot [S_2] - k_{C\text{-}1} \cdot [E\text{-}S_2] - k_{C2} \cdot [E\text{-}S_2] \\
&- k_{B1} \cdot [E\text{-}S_2] \cdot [S_1] + k_{B\text{-}1} \cdot [E\text{-}S_2\text{-}S_1] + k_{B2} \cdot [E\text{-}S_2\text{-}S_1] \\
&- k_{D1} \cdot [E\text{-}S_2] \cdot [S_2] + k_{D\text{-}1} \cdot [E\text{-}S_2\text{-}S_2] + k_{D2} \cdot [E\text{-}S_2\text{-}S_2]
\end{aligned}
\tag{3}
$$

$$
\frac{d[E\text{-}S_2\text{-}S_1]}{dt} = k_{B1} \cdot [E\text{-}S_2] \cdot [S_1] - k_{B\text{-}1} \cdot [E\text{-}S_2\text{-}S_1] - k_{B2} \cdot [E\text{-}S_2\text{-}S_1]
\tag{4}
$$

$$
\frac{d[E\text{-}S_2\text{-}S_2]}{dt} = k_{D1} \cdot [E\text{-}S_2] \cdot [S_2] - k_{D\text{-}1} \cdot [E\text{-}S_2\text{-}S_2] - k_{D2} \cdot [E\text{-}S_2\text{-}S_2]
\tag{5}
$$

Applying the pseudo steady state assumption for species $E\text{-}S_1$, $E\text{-}S_2$, $E\text{-}S_2\text{-}S_2$, and $E\text{-}S_2\text{-}S_1$ leads to equation 6:

$$
v_1 = \frac{V_{\max,A} \cdot \dfrac{[S_1]}{K_{m,A}} + V_{\max,B} \cdot \dfrac{[S_1]}{K_{m,B}} \cdot \dfrac{[S_2]}{K_{m,C}}}{1 + \dfrac{[S_1]}{K_{m,A}} + \left(1 + \dfrac{[S_1]}{K_{m,B}}\right) \cdot \dfrac{[S_2]}{K_{m,C}} + \dfrac{1}{K_{m,C}} \cdot \dfrac{1}{K_{m,D}} \cdot [S_2]^2}
\tag{6}
$$

where v_1 is the initial reaction rate in $\text{mol·l}^{-1}\text{·s}^{-1}$ describing the break down rate of blocked p-nitrophenyl maltoheptaoside, and $V_{max,A}$ is the maximum reaction rate for blocked p-nitrophenyl maltoheptaoside catalysed by enzyme E expressed in $\text{mol·l}^{-1}\text{·s}^{-1}$. $V_{max,B}$ is the maximum reaction rate for blocked p-nitrophenyl maltoheptaoside catalysed by enzyme complex $E\text{-}S_2$ expressed in $\text{mol·l}^{-1}\text{·s}^{-1}$. $K_{m,A}$ and $K_{m,B}$ are the Michaelis-Menten parameters for blocked p-nitrophenyl maltoheptaoside in case of enzyme E and enzyme complex $E\text{-}S_2$ in mol·l^{-1} respectively. $K_{m,C}$ and $K_{m,D}$ are the Michaelis-Menten parameters for S_2 for enzyme E and enzyme complex $E\text{-}S_2$ respectively, and $[S_1]$ and $[S_2]$ are the concentrations of blocked p-nitrophenyl maltoheptaoside and the carbohydrate in mol·l^{-1}. For substrates that cannot be hydrolysed by α-amylase, k_{C2} and k_{D2} are equal to zero and in this case $K_{m,C}$ and $K_{m,D}$ become affinity constants.

Equation 6 can be rewritten to obtain an equation for the dimensionless initial reaction rate or α-amylase activity by dividing through the α-amylase activity in case no additional carbohydrates are added ($[S_2]=0$). This results in the following equation:

$$\frac{v_{1,\%}}{100} = \frac{\left(1 + \left(\frac{V_{\max,B}}{V_{\max,A}} \cdot \frac{K_{m,A}}{K_{m,B}}\right) \cdot \frac{[S_2]}{K_{m,C}}\right) \cdot \left(1 + \frac{[S_1]}{K_{m,A}}\right)}{1 + \frac{[S_1]}{K_{m,A}} + \left(1 + \frac{[S_1]}{K_{m,B}}\right) \cdot \frac{[S_2]}{K_{m,C}} + \frac{1}{K_{m,C}} \cdot \frac{1}{K_{m,D}} \cdot [S_2]^2}$$

(7)

where $v_{1,\%}$ is the initial reaction rate as a percentage of the initial reaction rate without addition of carbohydrates. Equation 7 can be used to account for variations between different α-amylase stock solutions.

Measurements with the spectrophotometer enable us to determine the dimensionless initial reaction rate of blocked p-nitrophenyl maltoheptaoside ($v_{1,\%}$) as a function of the carbohydrate concentration ($[S_2]$). Equation 7 depends on four parameters, if it is rewritten in the following manner:

$$\frac{v_{1,\%}}{100} = \frac{C \cdot \left(1 + U_1 \cdot [S_2]\right)}{C + U_2 \cdot [S_2] + U_3 \cdot [S_2]^2}$$

(8)

where C is a known parameter and U_1, U_2, and U_3 are unknown parameters. Parameter C can be calculated with $K_{m,A}$ and the initial concentration of blocked p-nitrophenyl maltoheptaoside:

$$C = 1 + \frac{[S_1]}{K_{m,A}}$$

(9)

The unknown parameters U_1, U_2, and U_3 are:

$$U_1 = \frac{V_{max,B}}{V_{max,A}} \cdot \frac{K_{m,A}}{K_{m,B}} \cdot \frac{1}{K_{m,C}}$$

(10a)

$$U_2 = \frac{1}{K_{m,C}} \cdot \left(1 + \frac{[S_1]}{K_{m,B}}\right)$$

(10b)

$$U_3 = \frac{1}{K_{m,C}} \cdot \frac{1}{K_{m,D}}$$

(10c)

U_1, U_2, and U_3 are independent although they all contain parameter $K_{m,C}$. The independency is caused by the presence of $V_{max,B}$, $K_{m,B}$, and $K_{m,D}$ in the equations of respectively U_1, U_2, and U_3.

If substrate competition or inhibition is the only phenomenon that takes place and the formation of an active complex does not take place, the following equation can be used (Cornish-Bowden, 1995):

$$\frac{v_{1,\%}}{100} = \frac{1 + \dfrac{[S_1]}{K_{m,A}}}{1 + \dfrac{[S_1]}{K_{m,A}} + \dfrac{[S_2]}{K_{m,B}}} \tag{11}$$

Equation 11 was used to describe the decrease in α-amylase activity that was observed when the soluble starch or maltodextrin concentration was increased (Baks *et al.*, 2006). Note that this equation can also be obtained from equation 7 if $K_{m,B}$ and $K_{m,D}$ approach infinity, and $V_{max,B}$ is equal to zero or, in other words, enzyme complex $E-S_2$ is not active.

Materials and methods

Materials

Thermostable α-amylase from *Bacillus licheniformis* (EC 3.2.1.1, Termamyl 120L, type XII-A) was obtained from Sigma-Aldrich (Steinheim, Germany). The enzyme concentration used in the experiments is expressed in grams of this α-amylase solution per liter. Anhydrous D(+)-glucose, maltotriose, maltotetraose, maltopentaose, maltohexaose, and maltoheptaose were obtained from Sigma-Aldrich (Steinheim, Germany). Maltose monohydrate, sodium chloride, and calcium chloride dihydrate were bought from Merck (Darmstadt, Germany). Maleic acid (di-sodium salt) and sucrose were obtained from Acros Organics (Geel, Belgium). For the measurement of the α-amylase activity Amylase HR reagent was used, and this is a product from Megazyme International Ireland (Bray, Republic of Ireland). Amylase HR is supplied as dry matter in vials containing 54.5 mg blocked (4,6-O-benzilidine)-p-nitrophenyl maltoheptaose and 125 units thermostable α-glucosidase. The contents was dissolved in 10 ml ultrapure water before use. The standard buffer used for all the experiments was 0.1 M maleic acid buffer (pH 6.5) with 2 mM $CaCl_2$ and 0.1 M NaCl.

α-Amylase activity measurements

The α-amylase activity is defined as the amount of p-nitrophenol released in μmol per min per mg of enzyme solution at 40 ºC and pH 6.5. The release of p-nitrophenol can be followed continuously by measuring the absorbance of the reaction mixture at 410 nm:

$$A_E = \frac{D}{\varepsilon \cdot b \cdot C_E} \cdot \frac{dA}{dt} \tag{12}$$

where dA/dt is the slope of the linear part of the absorbance-time curve; ε is the molar absorptivity at 410 nm, 40 ºC, and pH 6.5 in l·μmol^{-1}·cm^{-1}; b is the path length of the light in the cuvette in cm; C_E is the enzyme concentration in mg·l^{-1}; and D is the dilution factor. The molar absorptivity (ε) at these conditions is $8.0·10^{-3}$ l·μmol^{-1}·cm^{-1} (Baks *et al.*, 2006). The continuous activity measurements have the advantage that the linear part of the graph can always be selected.

Stock solutions of the different carbohydrates with varying carbohydrate concentrations (between 0 and 286 g·l^{-1}) were prepared. Enzyme stock solutions contained 35 mg α-amylase solution·l^{-1}. For each set of experiments, a fresh enzyme stock solution was prepared. Measurements showed that after preparation of such a stock solution, the α-amylase activity increased during the first two hours and after these 2 hours the activity remained constant for 6 hours. For this reason an α-amylase stock solution was kept in the refrigerator for approximately 2 hours before an experiment was carried out. According to Asther and Meunier (1989) α-amylase aggregates can be present in a concentrated α-amylase solution such as the stock solution of Sigma. If it takes some time before these aggregates fall apart into more active, individual enzyme molecules, it might explain the observed increase in enzyme activity during the first two hours after preparation of our stock solution. The carbohydrate stock solution, the enzyme stock solution and the Amylase HR stock solution were pre-incubated separately for 10 min at 40 ºC in a water bath. After pre-incubation, equal volumes of the carbohydrate stock solution and the enzyme stock solution were added together. From this solution 700 μl were taken and added to 300 μl Amylase HR reagent (corresponding to 1.2 mM blocked p-nitrophenyl maltoheptaoside, which is approximately $10·K_{m,A}$) and incubated for 10 min at 40ºC in a spectrophotometer while measuring the absorbance at 410 nm. During each set of measurements the α-amylase activity of the α-amylase stock solution was measured. The α-amylase activity of this solution was used as the 100 % level. All the experiments were carried out in duplicate.

Fitting procedure

Equation 8 was used to fit the model data to the experimental data. Parameter *C* (equation 9) can be calculated with $K_{m,A}$ and $[S_1]$. $K_{m,A}$ is equal to 0.12 ± 0.03 mM (95 % confidence interval) at 40 ºC and pH 6.5 (Baks *et al.*, 2006), and the initial blocked p-nitrophenyl maltoheptaoside concentration was equal to 1.21 mmol/l during our experiments. The values of U_1, U_2, and U_3 were determined by minimizing the sum of the squared residuals.

If $K_{m,C}$ is known, equation 7 depends on three unknown parameters: $V_{max,B}/V_{max,A}$, $1/K_{m,B}$, and $1/K_{m,D}$. This equation was also used to fit the model data to the experimental data. The reciprocals of $K_{m,B}$ and $K_{m,D}$ were used for the fitting procedure to avoid numerical instabilities.

The computer program 'Table Curve 2D' (Jandel Scientific, 1994, version 2.0, San Rafael, CA, USA) was used for all fitting procedures.

Results and discussion

The α-amylase activity determined with the Ceralpha assay procedure went through a maximum when the glucose concentration was increased (Baks *et al.*, 2006). It is also important to understand the behaviour of other carbohydrates on the Ceralpha assay procedure. The carbohydrates that were used for our experiments can be divided into two groups. The first group consists of glucose, sucrose, maltose, and maltotriose, which cannot be broken down by α-amylase from *Bacillus licheniformis* (Marchal *et al.*, 1999). The second group is composed of oligosaccharides that can be hydrolysed by this enzyme, such as maltotetraose, maltopentaose, maltohexaose, and maltoheptaose (Kandra *et al.*, 2002; Marchal *et al.*, 1999).

Experimental data

Figure 3A shows the α-amylase activity as a function of the D-(+)-glucose concentration. The α-amylase activity is expressed as a percentage of the α-amylase activity without addition of sugars. The latter value is equal to 1.51 ± 0.08 $\mu mol \cdot mg^{-1} \cdot min^{-1}$ (95 % confidence interval) and is based on 32 measurements. As the glucose concentration increases a maximum α-amylase activity was measured at a glucose concentration of 0.03 $mol \cdot l^{-1}$. This was followed by a gradual decrease towards an activity of 50 % at 0.55 $mol \cdot l^{-1}$.

Figures 3B and *3C* show the α-amylase activity as a function of the maltose and maltotriose concentration respectively, and both figures are qualitatively comparable to the experimental data obtained with glucose.
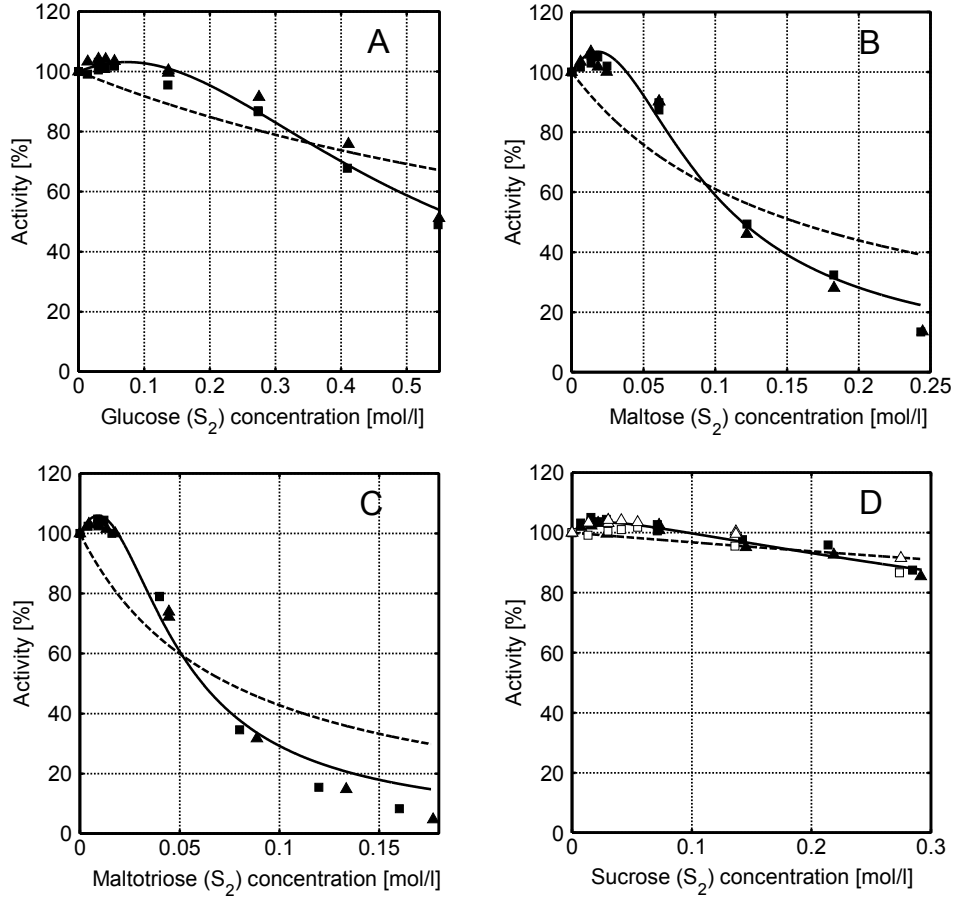
Figure 3: Apparent α-amylase activity towards blocked p-nitrophenyl maltoheptaoside as function of respectively the D(+)-glucose (Figure A), maltose (Figure B), maltotriose (Figure C) and sucrose (Figure D) concentration. Experimental data obtained with duplicate experiments (experiment 1: ■, experiment 2: ▲). The solid line describes the model data obtained with equation 8 and the dashed line describes the data obtained with equation 11. Experimental data of glucose (experiment 1: □, experiment 2: Δ) has been added to figure 3D to make the comparison between sucrose and glucose easier. Conditions: $C_E = 1.1 \cdot 10^{-2}$ $g \cdot l^{-1}$, T = 40 ºC, pH = 6.5. Without carbohydrates ([S_2] = 0) the α-amylase activity is 100 %, which equals 1.51 ± 0.08 $\mu mol \cdot mg^{-1} \cdot min^{-1}$.

However, the maximum activity is observed at a much lower concentration in comparison with glucose. In addition, the α-amylase activity decreases faster with the same increase in concentration if the chain length of the carbohydrate is increased.

Maltotetraose is the smallest oligosaccharide that can be hydrolyzed by α-amylase. *Figure 4A* shows the observed α-amylase activity vs. the maltotetraose concentration. The maximum α-amylase activity that was observed with the smaller oligosaccharides is not present in case of maltotetraose. Instead, the activity remains independent of the carbohydrate concentration at low concentrations. At higher concentrations, the α-amylase activity decreases rapidly with an increasing carbohydrate concentration.

Figures 4B, *4C,* and *4D* show the α-amylase activity at various concentrations of maltopentaose, maltohexaose, and maltoheptaose respectively. The trends in the experimental data shown in these figures are comparable to the data trend shown in *Figure 4A*. Furthermore, larger carbohydrates will lead to a larger activity decrease with an equal increase in carbohydrate concentration.

All carbohydrates used thus far consist of α-D-glucopyranosyl monomers that fit into the active site of α-amylase. *Figure 3D* shows the α-amylase activity at various sucrose concentrations. For comparison, the results of glucose are also plotted. The presence of the β-D-fructofuranoside group in the active site does not lead to significant changes in the α-amylase activity curve in comparison with glucose.
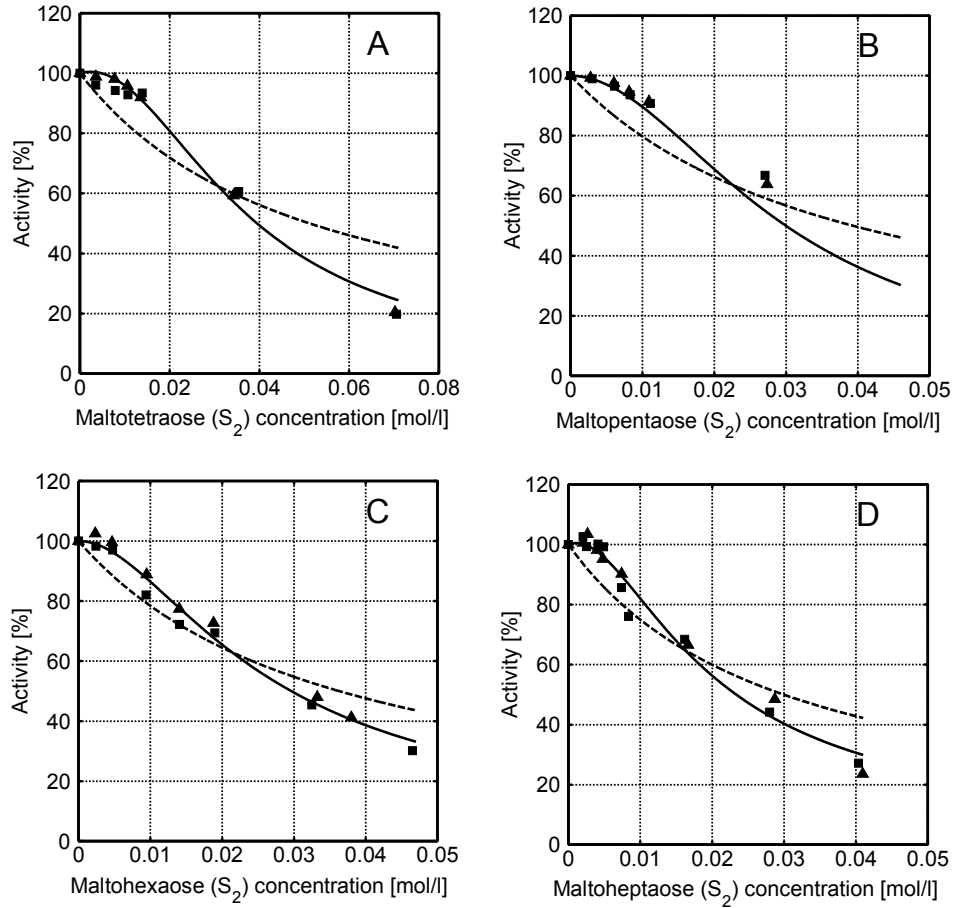
Figure 4: Apparent α-amylase activity towards blocked p-nitrophenyl maltoheptaoside as function of respectively the maltotetraose (Figure A), maltopentaose (Figure B), maltohexaose (Figure C) and maltoheptaose (Figure D) concentration. Experimental data obtained with duplicate experiments (experiment 1: ■, experiment 2: ▲). The solid line describes the model data obtained with equation 8 and the dashed line describes the data obtained with equation 11. Conditions: $C_E = 1.0 \cdot 10^{-2}$ g·l^{-1}, T = 40 °C, pH = 6.5. Without carbohydrates ([S_2] = 0) the α-amylase activity is 100 %, which equals 1.51 ± 0.08 μmol·mg^{-1}·min^{-1}.

Kinetic model

Equation 8 was fitted to the experimental data, and the results are shown in *Figures 3* and *4*. The parameters U_1, U_2 and U_3 that resulted in the lowest sum of the squared residuals are given in *Table 1*. The calculated α-amylase activity values (solid lines) are in good agreement with the experimentally determined activity values.

Table 1: The parameters (including 95 % confidence interval) that were obtained by fitting equation 8 to the experimental data sets.

Data set	n[a]	U_1 [l/mol]	U_2 [l/mol]	U_3 [10^3 (l/mol)^2]	SSR[b]
Glucose	21	0.87 ± 1.88	$1.10 \cdot 10^{-3} \pm 15.6$	0.06 ± 0.04	169.9
Maltose	21	7.58 ± 7.60	$7.03 \cdot 10^{-3} \pm 56.1$	2.23 ± 1.07	383.3
Maltotriose	21	13.2 ± 15.8	$4.46 \cdot 10^{-3} \pm 117$	7.80 ± 4.38	498.6
Maltotetraose	13	4.0 ± 17.1	$4.56 \cdot 10^{-3} \pm 126$	9.54 ± 7.89	121.2
Maltopentaose	13	$2.93 \cdot 10^{-3} \pm 8.19$	4.2 ± 64.4	12.43 ± 4.74	18.5
Maltohexaose	15	25.0 ± 57.4	277 ± 476	22.4 ± 28.6	133.6
Maltoheptaose	21	42.4 ± 84.3	373 ± 716	45.6 ± 53.6	288.1
Sucrose	21	63.7 ± 83.8	664 ± 894	0.55 ± 0.60	47.1

[a] n = number of data points

[b] SSR = sum of squared residuals

In some cases one of the parameters has a broad confidence interval (see *Table 1*): parameter U_2 in case of glucose, maltose, maltotriose, and maltotetraose and parameter U_1 in case of maltopentaose. This indicates that one of these parameters cannot be determined with sufficient certainty. If one of the parameters has a broad confidence interval, it can also indicate that the model contains too many parameters. However, we wanted to develop a generally applicable model based on a theoretical mechanism instead of an empirical model with fewer, more significant parameters.

The dotted lines in *Figures 3* and *4* show the resulting fit of equation 11 to the experimental data that was obtained by using one fit parameter ($K_{m,C}$). The α-amylase activity model values are in poor agreement with the experimentally determined activity values, because this model was not able to describe the maximum α-amylase activity that has been observed. *Figures 3* and *4* show that the resemblance between the experimental values and the model values increases with increasing chain length. In all cases, however,

the trend in the experimental data can be better described with equation 8 that depends on three fit parameters. This has also been statistically verified with the Akaike information criterion (AIC_c) adapted for small sample sizes (Hurvich and Tsai, 1995). In all cases, the model equation based on three fit parameters (equation 8) has a lower AIC_c value than the AIC_c value obtained with the one fit parameter model (equation 11) indicating that use of the more complex model with more than one parameter is justified (results not shown).

The $K_{m,C}$ values for maltopentaose, maltohexaose, and maltoheptaose were reported by Kandra *et al.* (2002) (respectively 2.5, 3.3, 4.0 mM). If the $K_{m,C}$ values are known, equation 7 can be fitted to the experimental data by varying $V_{max,B}/V_{max,A}$, $1/K_{m,B}$, and $1/K_{m,D}$. The parameters that resulted in the lowest sum of the squared residuals are given in *Table 2*. The resulting fits are not shown in *Figures 3* and *4*, because the resulting model values coincide with the model values that were obtained by fitting equation 8 to the experimental data.

Table 2: The parameters (including 95 % confidence interval) that were obtained by fitting equation 7 (with $K_{m,C}$ values taken form Kandra et al., 2002) to experimental data sets of maltopentaose, maltohexaose, and maltoheptaose.

Data set	n[a]	$V_{max,B}/V_{max,A}$ [-]	$1/K_{m,B}$ [l/mol]	$1/K_{m,D}$ [l/mmol]	SSR[b]
Maltopentaose	13	13.3 ± 727	$30.0 \pm 1.69 \cdot 10^3$	0.09 ± 0.11	112.1
Maltohexaose	15	2.89 ± 40.6	$94.4 \pm 1.52 \cdot 10^3$	0.09 ± 0.11	133.9
Maltoheptaose	21	0.89 ± 3.48	$403 \pm 2.36 \cdot 10^3$	0.18 ± 0.21	288.1

[a] n = number of data points

[b] SSR = sum of squared residuals

Discussion

The kinetic scheme in *Figure 2* is proposed to explain the observed α-amylase activity vs. concentration curves (*Figures 3* and *4*). After addition of a low amount of small carbohydrates, the sample not only contains free enzyme E, and complex E-S_1, but also E-S_2, E-S_2-S_2, and E-S_2-S_1. This can only take place if the Michaelis-Menten constant for binding S2 to the enzyme ($K_{m,C}$) is small enough to cause a noticeable shift towards E-S_2. The observed maxima can now appear if the conversion rate of blocked p-nitrophenyl maltoheptaoside catalyzed by complex E-S_2 is larger than the rate catalyzed by E. This requirement will be met if $K_{m,B}$ is low in comparison with $K_{m,A}$ or if $V_{max,B}$ is higher than

$V_{max,A}$. A $K_{m,B}$ value that is low in comparison with $K_{m,A}$ implies that the E-S$_2$ complex has a high affinity for substrate S$_1$. If $V_{max,B}$ is higher than $V_{max,A}$, the conversion rate of S$_1$ catalyzed by complex E-S$_2$ is higher than the conversion rate of S$_1$ catalyzed by E.

If a substrate is attached to a smaller number of subsites, the bond between the substrate and the enzyme is weaker. A weaker bond will probably result in a higher K_m value. In case of E-S$_2$, it is likely that there are less subsites available for a bond between the enzyme and blocked p-nitrophenyl maltoheptaoside in comparison with a bond between only the enzyme E and blocked p-nitrophenyl maltoheptaoside, because part of the subsites are already occupied by S$_2$. Therefore, it is unlikely that $K_{m,B}$ is smaller than $K_{m,A}$. It is more likely that $V_{max,B}$ is larger than $V_{max,A}$; after the hydrolysis of blocked p-nitrophenyl maltoheptaoside, the desorption of products from E-S$_2$ is expected to be faster than the desorption of products from α-amylase (E). The desorption from E-S$_2$ is faster, because part of the subsites are already occupied by S$_2$ and therefore the hydrolysis products are attached to a lower number of subsites resulting in a weaker bond between the products and enzyme complex E-S$_2$.

At higher carbohydrate concentrations, a decrease in activity is observed. We assumed that all the subsites around the catalytic site are occupied at higher carbohydrate concentrations. This results in inhibition or substrate competition.

The maximum in the α-amylase activity vs. concentration curves is less pronounced with oligosaccharides that are larger than maltotriose and it shifts to lower carbohydrate concentrations (compare *Figures 4A-4D* with *Figures 3A-3D*). A large carbohydrate can also form an active carbohydrate-enzyme complex, if part of the carbohydrate chain is outside the binding region of α-amylase (*Figure 1F*). However, the number of possibilities that an oligosaccharide can attach to any of the subsites of the enzyme without blocking the catalytic site and the surrounding subsites decreases if the chain length of the carbohydrate increases. Consequently, there are more options that will lead to inhibition. It is expected that with a certain chain length that is larger than a critical value, the maximum disappears completely and the α-amylase activity vs. concentration curves will be similar to the ones observed in case of starch and maltodextrin (Baks *et al.*, 2006). This expectation is supported by comparing the α-amylase activity vs. concentration curves of oligosaccharides with those curves of starch and maltodextrin (*Figure 5*).
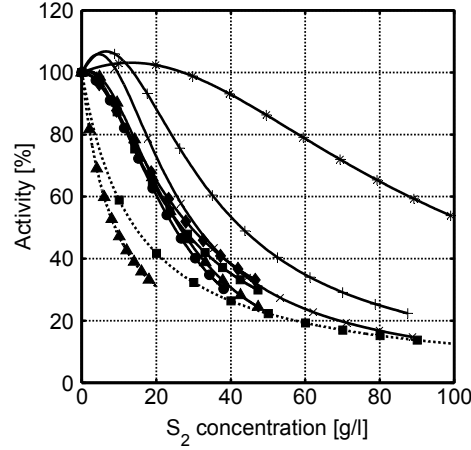
Figure 5: Comparison of the calculated apparent α-amylase activity towards blocked p-nitrophenyl maltoheptaoside as function of the carbohydrate concentration and carbohydrate type. Solid lines: α-amylase activity calculated with equation 8 and the parameters in Table 1 for glucose (∗), maltose (+), maltotriose (×), maltotetraose (▲), maltopentaose (●), maltohexaose (♦), maltoheptaose (■). Dotted lines: α-amylase activity calculated with equation 11 for maltodextrin (■) and soluble potato starch (▲).

It is hard to draw conclusions from a comparison between U_1, U_2, and U_3 of different carbohydrates, because several parameters are lumped within U_1, U_2, and U_3. In case of maltopentaose, maltohexaose and maltoheptaose parameters that can be compared ($K_{m,B}$, $V_{max,B}/V_{max,A}$ and $K_{m,D}$) could be determined with use of known $K_{m,C}$ values. As we expected, the values of $K_{m,B}$ are larger than the value $K_{m,A}$ (0.12 mM). The values of $V_{max,B}/V_{max,A}$ can provide an explanation as was previously discussed. *Table 2* shows that $V_{max,B}$ is 13.3 times higher than $V_{max,A}$ for maltopentaose and 2.9 times higher for maltohexaose. Although the exact values are uncertain due to the large confidence intervals, these values suggest that blocked p-nitrophenyl maltoheptoaside is converted faster if an E-S_2 complex is present. This explains a higher reaction rate in the presence of low concentrations of S_2. For maltoheptaose $V_{max,B}$ is lower than $V_{max,A}$. This can be expected because the maximum disappears if carbohydrates become larger.

The $K_{m,D}$ values, which are related to the affinity of S_2 for the E-S_2-complex, are slightly higher than the values of $K_{m,C}$, indicating a lower affinity of S_2 for the E-S_2-complex as compared to the affinity of S_2 for the enzyme itself. This agrees with our findings that the values of $K_{m,B}$ are larger than the value $K_{m,A}$.

If the Ceralpha method is used to determine the residual α-amylase activity in samples taken during a starch hydrolysis reaction, the total carbohydrate concentration (g·l^{-1}) in

these samples is approximately equal. However, samples taken during the hydrolysis reaction can contain either partially hydrolysed carbohydrates (e.g. maltoheptaose) in the beginning of a hydrolysis experiment or completely hydrolysed carbohydrates (e.g. glucose) at the end of a hydrolysis experiment. The results in *Figure 5* show that at equal concentrations (g·l^{-1}) the apparent α-amylase activity in samples with glucose can be 60 % larger than in a sample with maltoheptaose although the amount of active enzyme is equal.

Conclusions

Small carbohydrates can strongly affect activity measurements with the Ceralpha assay procedure. We have shown that the effect of carbohydrates on the α-amylase activity increases with an increasing chain length. The Ceralpha assay procedure is further affected by the carbohydrate concentration. For several carbohydrates we found that the α-amylase activity increases with an increasing carbohydrate concentration at low carbohydrate concentrations. At higher carbohydrate concentrations, however, all carbohydrates show a decreasing α-amylase activity at increasing carbohydrate concentration.

A kinetic model was developed to describe the α-amylase activity as a function of the carbohydrate concentration. This model takes into account the formation of a carbohydrate-enzyme complex that leads to a new, active enzyme species. It also takes into account substrate inhibition or substrate competition. This results in a kinetic model with 3 fit parameters (equation 8) that can be used to describe the maximum α-amylase activity at low concentrations of small carbohydrates and the subsequent decrease of the α-amylase activity at higher carbohydrate concentrations. The model data agree with the experimental α-amylase activity values and this supports our hypothesis that the adsorption of oligosaccharides in various subsites could influence the activity of the enzyme both positively and negatively. The values of the kinetic parameters give insight into the proposed reaction mechanism.

The kinetic model derived here can be used to correct for the effect of small carbohydrates on the α-amylase activity to obtain the actual α-amylase activity. These corrections are necessary because under certain conditions the difference between the actual α-amylase activity and the value determined with the Ceralpha method can be large (e.g. a 75 % decrease in activity if the sample contains 0.04 mol·l^{-1} maltoheptaose in comparison with the activity in a sample without carbohydrates).

Acknowledgements

References

Allen JD, Thoma JA. 1976. Subsite mapping of enzymes. Application of the depolymerase computer model to two α-amylases. Biochem J 159:121-132.

Asther M, Meunier JC. 1989. Kinetic study of the irreversible thermal denaturation of *Bacillus licheniformis* α-amylase. Biochem J 263:665-670.

Baks T, Janssen AEM, Boom RM. 2006. The effect of carbohydrates on α-amylase activity measurements. Enzyme Microb Technol 39:114-119.

Ceralpha: α-Amylase assay procedure (CER 07/00) Test Kit Booklet, Megazyme International Ireland Ltd., Bray, County Wicklow, Ireland.

Chaplin MF, Bucke C. 1990. The large-scale use of enzymes in solution. In: Chaplin MF, Bucke C. Enzyme technology. Cambridge: Cambridge University Press. 146-161.

Cornish-Bowden A. 1995. Fundamentals of enzyme kinetics. London: Portland Press. 343 p.

Hiromi K. 1970. Interpreatation of dependency of rate parameters of the degree of polymerization of substrate in enzyme-catalysed reactions. Evaluation of subsite affinities of exo-enzyme. Biochem Biophys Res Commun 40:1–6.

Hurvich CM, Tsai CL. 1995. Model selection for extended quasi-likelihood models in small samples. Biometrics 51:1077-1084.

Kandra L, Gyémánt G, Remenyik J, Hovánszki G, Lipták A. 2002. Action pattern and subsite mapping of *Bacillus licheniformis* α-amylase (BLA) with modified maltooligosaccharide substrates. FEBS lett 518:79-82.

Larreta-Garde V, Xu ZF, Thomas D. 1988. Behavior of enzymes in the presence of carbohydrates. Influence of alcohols, polyols, and carbohydrates on activity and stability of yeast alcohol dehydrogenase. Ann NY Acad Sci 542:294-298.

Marchal LM, Van de Laar AMJ, Goetheer E, Schimmelpennink EB, Bergsma J, Beeftink HH, Tramper J. 1999. Effect of temperature on the saccharide composition obtained after α-amylolysis of starch. Biotechnol Bioeng 63:344-355.

McCleary BV, Sheehan H. 1987. Measurement of cereal α-amylase: a new assay procedure. J Cereal Sci 6:237-251.

McCleary BV, McNally M, Monaghan D, Mugford DC. 2002. Measurement of α-amylase activity in white wheat flour, milled malt, and microbial enzyme preparations, using the Ceralpha assay: collaborative study. J AOAC Int 85:1096-1102.

Sheehan H, McCleary BV. 1988. A new procedure for the measurement of fungal and bacterial α-amylase. Biotechnol Tech 2:289-292.

Van der Maarel MJEC, Van der Veen B, Uitdehaag JCM, Leemhuis H, Dijkhuizen L. 2002. Properties and applications of starch-converting enzymes of the α-amylase family. J Biotechnol 94:137–155.

Xu ZF, Thomas D, Larreta-Garde V. 1990. Kinetic indication for a conformational change of enzyme by a modified aqueous microenvironment. Ann NY Acad Sci 613:506-510.

Chapter 4

Comparison of methods to determine the degree of gelatinisation for both high and low starch concentrations

Abstract

A general procedure was developed to measure the degree of gelatinisation in samples over a broad concentration range. Measurements based on birefringence, differential scanning calorimetry (DSC), wide angle X-ray scattering (WAXS), and amylose-iodine complex formation were used. If a 10 w/w % wheat starch-water mixture was used, each method resulted in approximately the same degree of gelatinisation vs. temperature curve. In case of 60 w/w % wheat starch-water mixtures, each method resulted in a different degree of gelatinisation vs. temperature curve. DSC and WAXS measurements are preferred, because they can be used to determine when the final stage of the gelatinisation process has been completed. The differences between the methods can be explained by considering the phenomena that take place during the gelatinisation at limiting water conditions. Gelatinisation of 10 w/w % and 60 w/w % wheat starch-water mixtures started at the same temperature. However, complete gelatinisation was reached at different temperatures. These results are in accordance with independent DSC measurements that were carried out. The Flory equation was adapted to provide a quantitative explanation for the gelatinisation curves as function of starch-water ratio and temperature. The gelatinisation curves that were obtained with the model are in good agreement with the experimentally determined curves.

Introduction

Starch is a biopolymer that occurs naturally as water-insoluble and birefringent granules. Each granule consists of concentric growth rings of alternating amorphous and semi-crystalline composition. The semi-crystalline growth rings contain stacks of amorphous and crystalline lamellae. The crystalline lamellae consist of chain sections of amylopectin that form double helices (type A), while other chain sections of amylopectin form connections between the helices (type B). Branching points of both A and B chains of amylopectin are usually found within the amorphous lamellae (Jenkins *et al.*, 1994; Waigh *et al.*, 2000).

When a suspension of starch is heated in the presence of excess quantities of water, an irreversible order-disorder transition called gelatinisation takes place (Cooke and Gidley, 1992; Jenkins and Donald, 1998; Liu and Lelievre, 1993). During gelatinisation, starch granules take up water, swell, lose crystallinity and leach amylose (Parker and Ring, 2001). In addition, heat is taken up, according to the characteristic gelatinisation endotherm that can be measured with differential scanning calorimetry (DSC). If the amount of water is insufficient to provide complete swelling and disruption of the starch granules, only part of the crystallinity of the starch granules is lost. The remaining crystallinity only disappears after heating to higher temperatures. A melting transition occurs giving rise to an additional DSC endotherm (Donovan, 1979; Eliasson, 1980; Randzio *et al.*, 2002; Whittam *et al.*, 1990). For a brief overview of the qualitative models describing the gelatinisation of starch we refer to Jenkins *et al.* (1998). A more recent qualitative model was developed by Waigh *et al.* (2000) using a liquid-crystalline approach to describe the gelatinisation of starch. The Flory equation has been used by several authors for a quantitative description of the gelatinization or melting temperature as a function of the starch concentration (Burt and Russell, 1983; Donovan, 1979; Donovan, Lorenz and Kulp, 1983; Donovan and Mapes, 1980; Parker *et al.*, 2001; Russell, 1987; Whittam *et al.*, 1990).

Several analysis techniques are used to study different aspects of the gelatinisation process. Birefringence is used to follow the ordering in the granule on the length scale of the wavelength of light (approximately 500 nm) (Lelievre, 1974; Waigh *et al.*, 2000). Wide angle X-ray scattering (WAXS) and short angle X-ray scattering (SAXS) can be used to follow respectively short-range order (crystalline double helices) and long-range order (alternating crystalline and amorphous lamellae) (Jenkins *et al.*, 1994). Where X-ray scattering probes the double helices packed in regular arrays, solid state NMR detects the double helix content at a molecular order level (Cooke *et al.*, 1992; Gidley and Bociek,

1985). IR spectroscopy can also be used to follow the gelatinisation of starch on a short-range molecular level, because the IR spectrum of starch is affected by changes in structure such as starch chain conformation, helicity and crystallinity (Van Soest *et al.*, 1995). Liu *et al.* (1991) have found a quantitative correlation between crystallinity loss and thermal transitions during the gelatinisation of starch, since melting is a first order transition accompanied by a heat effect that can be measured well. Therefore, DSC measurements can also be used to follow the loss of order that takes place during the gelatinisation process. Amylose chains are released during the gelatinisation process and these chains can be determined colorimetrically (Birch and Priestley, 1973), as dissolved amylose forms a blue complex with iodine (Calabrese and Khan, 1999). When a starch-water mixture gelatinises, the water distribution and manner at which water is bound to the starch matrix changes (Tang and Hills, 2001). These changes affect the dielectric properties of the starch-water system and for this reason conductance measurements can be used to monitor the gelatinisation process (Karapantsios *et al.*, 2000). Besides the conductance, the viscosity of the starch-water mixture also changes during gelatinisation due to swelling of the granules. Monitoring the viscosity can therefore also be used to follow the gelatinisation. After starch has been gelatinised, it is susceptible to hydrolytic enzymes (Tester and Sommerville, 2000). For this reason, enzymatic methods have also been used to investigate the gelatinisation process indirectly (Roussel *et al.*, 1991).

Comparisons between the analysis methods were made to elucidate the mechanisms that take place during the order-disorder transition of the gelatinisation process (Chaiwanichsiri *et al.*, 2001; Cooke *et al.*, 1992; Liu *et al.*, 1991; Waigh *et al.*, 2000). Liu *et al.* compared birefringence and X-ray measurements during the gelatinisation of a 2 w/w % corn starch suspension. However, these authors did not compare these measurements at higher starch concentrations.

In this article, DSC, X-ray, birefringence and amylose-iodine complex formation measurements will be used to determine the degree of gelatinisation in 10 w/w % and 60 w/w % starch suspensions in water. A general procedure was developed to measure the degree of gelatinisation at both low and high starch concentrations. Furthermore, the observed differences between the analysis techniques will be discussed. In addition, the differences between the gelatinisation behaviour of diluted and concentrated starch suspensions will be explained based on the Flory equation. The Flory equation is adapted to describe the degree of gelatinization as function of both temperature and starch concentration.

Theory

The Flory equation is often used to relate the melting temperature T_m of a polymer in a polymer-diluent mixture to the volume fraction ϕ_1 of the diluent (Flory, 1953):

$$\frac{1}{T_m} - \frac{1}{T_m^0} = \left(\frac{R}{\Delta H_u} \frac{V_2}{V_1} \right) \cdot \left[\phi_1 - \chi_{12} \phi_1^2 \right] \tag{1}$$

where T_m^0 is the melting point of the pure polymer, R is the gas constant, ΔH_u the heat of fusion per repeating unit, V_1 and V_2 are the molar volumes of the diluent and the repeating unit of the polymer and χ_{12} is the Flory-Huggins polymer-diluent interaction parameter. In addition, we have assumed that the ratio V_2/V_1 and χ_{12} are temperature independent. The Flory-Huggins interaction parameter is known to depend linearly on the reciprocal of the absolute temperature (Rudin, 1999). Therefore, χ_{12} decreases with 20 % over the temperature interval of interest (50-115 °C). This variation is not too large and for this reason the assumption of a constant χ_{12} parameter seems justified. In the derivation of equation 1, it is assumed that the heat of fusion and the entropy of fusion do not depend on the temperature. According to Hoffman (1958), Van Krevelen (1976) and Mandelkern (1989), this assumption is not justified anymore for large differences in T_m and T_m^0. Hoffman (1958) assumed that the enthalpy of fusion depends linearly on the temperature. In turn, this enthalpy equation can be used to derive an equation to describe the entropy of fusion as a function of the temperature. The Flory equation can now be derived by taking into account the temperature dependency of the free energy difference involved in the melting transition (composed of the enthalpy and entropy equations). Application of Hoffman's approximation is only valid when the temperature that is considered is larger than the glass transition temperature and smaller than T_m^0. Application of Hoffman's approximation leads to the following equation:

$$\frac{1}{T_m} - \frac{1}{T_m^0} = \left(\frac{R}{\Delta H_u} \frac{V_2}{V_1} \right) \cdot \left(\frac{T_m^0}{T_m} \right) \cdot \left[\phi_1 - \chi_{12} \phi_1^2 \right] \tag{2a}$$

This equation can be rewritten in a more useful form leading to equation 2b:

$$T_m = T_m^0 - \left(\frac{R}{\Delta H_u} \frac{V_2}{V_1} \right) \cdot \left(T_m^0 \right)^2 \cdot \left[\phi_1 - \chi_{12} \phi_1^2 \right] \tag{2b}$$

We would like to use equation 2b to describe the relation between the starch concentration, melting temperature and degree of gelatinization of starch in starch-water mixtures. To achieve this aim, the procedure described below can be followed.

The degree of crystallinity (α_c) of the polymer (starch) is given by:

$$\alpha_c = \frac{v_2^c}{v_2^a + v_2^c} \tag{3}$$

where v_2^a is the volume of amorphous starch and v_2^c is the volume of crystalline starch. This equation can be rewritten to obtain:

$$v_2^a = \left(v_2^a + v_2^c\right)\left(1 - \alpha_c\right) \tag{4}$$

The volume fraction of the solvent in the amorphous part of the system (ϕ_1) and the overall volume fractions of the solvent (ϕ_1^T) can be calculated with:

$$\phi_1 = \frac{v_1}{v_1 + v_2^a} \quad , \quad \phi_1^T = \frac{v_1}{v_1 + v_2^a + v_2^c} \tag{5a,b}$$

where v_1 is equal to the volume occupied by the solvent.

Substitution of equation 4, dividing the denominator and numerator through $v_1 + v_2^a + v_2^c$, substitution of equation 5b, and substitution $\phi_1^T = 1 - \phi_2^T$ changes equation 5a into:

$$\phi_1 = \frac{1 - \phi_2^T}{1 - \alpha_c \cdot \phi_2^T} \tag{6}$$

where ϕ_2^T is the overall volume fraction (averaged over the crystalline and amorphous part of the system) of the starch. Only part of the native starch is crystalline (Cooke *et al.*, 1992) and the remaining non-crystalline fraction cannot crystallize, e.g. those chain sections close to a branching point. This non-crystalline fraction acts as an inert part of the system. For this reason, the relative crystallinity can be used instead of the degree of crystallinity. Therefore, α_c in equation 6 can be replaced with *1-DG*, in which *DG* stands for the degree of gelatinisation. This replacement results in the following equation after substitution in equation 2b:

$$T_m = T_m^0 - \left(\frac{R}{\Delta H_u}\frac{V_2}{V_1}\right) \cdot \left(T_m^0\right)^2 \cdot \left[\left(\frac{1 - \phi_2^T}{1 - \left(1 - DG\right) \cdot \phi_2^T}\right) - \chi_{12}\left(\frac{1 - \phi_2^T}{1 - \left(1 - DG\right) \cdot \phi_2^T}\right)^2\right] \tag{7}$$

Equation 7 gives a relationship between the melting temperature, the starch concentration and the degree of gelatinization of starch in starch-water mixtures.

Materials and methods

Materials

Wheat starch (S5127) and potato starch (S2630) were obtained from Sigma-Aldrich (Steinheim, Germany). The wheat starch had a moisture content of 9.95 ± 0.43 w/w % (based on 22 measurements, 95 % confidence interval). The moisture content was determined by drying the wheat starch in a hot air oven at 105 °C or in a vacuum oven at 80 °C until the mass of the samples was constant in time. The water content of wheat starch was taken into account during all experiments.

All other chemicals (potassium hydroxide, fuming hydrochloric acid, potassium iodide, iodine crystals) were at least analytical grade and they were purchased from Merck (Darmstadt, Germany). Milli-Q water was used for all experiments.

Gelatinisation of starch in starch-water mixtures

For the gelatinisation of 10 w/w % starch-water mixtures, a temperature controlled batch reactor equipped with anchor stirrer was used. A Philips HR 7638 kitchen machine (Amsterdam, the Netherlands) was used to prepare 60 w/w % starch slurries (also for DSC measurements). These slurries were gelatinised or melted in a compression molder from PHI (City of Industry, U.S.A.). The mould consisted of 3 stainless steel plates with dimensions 300x350 mm. The upper and lower plate had a thickness of 4 mm. The middle plate had a rectangular hole with dimensions 180x120x5 mm. To facilitate the removal of the sample from the mould, the sample was covered with printable plastic overhead slides on both sides of the middle plate. The pressure applied to the mould was 6 tonnes, which was sufficient to keep water loss due to evaporation negligible.

During all gelatinisation experiments, the starch solutions or slurries were first heated to the desired temperature and held at this temperature for 45 min to equilibrate the starch-water mixture.

Handling of samples

To reduce recrystallisation, samples taken from the batch reactor or compression molder were immediately transferred to a vessel with liquid nitrogen. After the samples were completely frozen, they were stored in an -80 °C freezer until further use.

After storage, the samples were freeze-dried in a Christ Epsilon 2-6D freeze dryer (Osterode am Harz, Germany) prior to analysis. Freeze-drying was started at -20 °C and 1.030 mbar for 7 h followed by a second drying stage at -5 °C and 0.01 mbar for 12 h. The

freeze-dried samples were grinded in an analytical mill (type A10) from IKA (Staufen, Germany) and sieved to obtain a fine powder that could be dissolved easily. The powder obtained after sieving was stored in a desiccator before further use.

Birefringence measurements

A 1 w/w % solution of the freeze-dried starch powder was stirred for 1 h. After mixing, approximately 20 μl of this solution was transferred to a microscopic slide and viewed under normal and polarized light using a Zeiss Axioscop 50 (Jena, Germany) equipped with a CCD camera module. Pictures of different locations on the slide were taken randomly both under normal and polarized light. The total number of granules (n_t) and the number of granules that had not lost their polarization or Maltese crosses (n_m) was determined. The ratio n_m/n_t can be used as a measure for the degree of gelatinisation of the sample (Bauer and Knorr, 2005; Burt *et al.*, 1983; Liu *et al.*, 1991). Granules or parts of granules with part of the Maltese cross still present were taken as ungelatinised granules during the analysis.

Amylose-iodine complex formation

The amylose-iodine method used in this article is an adapted version of the method developed by Birch *et al.* (1973). A freeze dried sample (0.04 g) was dissolved in 50 ml of 0.15 M KOH and the solution was mixed for 15 min. The resulting solution is centrifuged to remove the insoluble part of the sample. After centrifugation, 1 ml of the supernatant is removed and neutralized with 9 ml 0.017 M HCl. Subsequently, 0.1 ml iodine reagent (1 g iodine and 4 g potassium iodide in 100 ml water) was added to form a blue complex with the dissolved amylose present in the sample. The absorbance was measured at 25 °C and 600 nm (A_1). The procedure was repeated, however, in this case 0.40 M KOH was used to ensure complete solubilisation of all the amylose present in the sample. The supernatant was neutralized with 0.045 M HCl. After adding 0.1 ml iodine reagent, the absorbance at 25 °C and 600 nm was measured (A_2). The ratio A_1(0.15 M KOH)/A_2(0.40 M KOH) can be used as a measure for the degree of gelatinisation of the sample.

Wide-angle X-ray diffraction

Diffractograms were recorded with a Philips PC-APD diffractometer. The scattered X-ray radiation was recorded by a proportional moving detector over a 4° and 40° (2θ) angular range with an angular scanning velocity of 1.2°/min and a measurement frequency of 1 s^{-1}. The Cu-Ka radiation from the anode operating at 40 kV and 50 mA was monochromated with use of a 15-mm thick Ni foil. The diffractograms were smoothened with the computer

program 'Table Curve 2D' (Jandel Scientific, 1994, version 2.0, San Rafael, USA) by applying Savitsky-Golay data smoothening (5 % smoothening). The procedure of Van Soest *et al.* (1995) was used for the determination of the relative crystallinity. For wheat starch, the characteristic peak at $2\theta = 22.9°$ was selected. A straight line was used to approach the baseline below the characteristic peak. A Matlab script was used to calculate the slope and y-intercept of the baseline. In addition, this script was used to calculate the total area below the characteristic peak (A_t), the total area below the characteristic peak minus the area below the baseline (A_c), the height of the characteristic peak (H_t), and the total height of the characteristic peak minus the height of the baseline at the diffraction angle at $2\theta = 22.9°$ (H_c). The ratios $R_A = A_c/A_t$ and $R_H = H_c/H_t$ were obtained for native wheat starch (100 % relative crystallinity) and for completely gelatinised or molten wheat starch (0 % relative crystallinity) The relative crystallinity of a sample based on peak areas (X_{rA}) or peak heights (X_{rH}) can now be determined with the following equations:

$$X_{rA} = \frac{(R_A)_s}{(R_A)_n} \; ; \; X_{rH} = \frac{(R_H)_s}{(R_H)_n} \tag{8a, 8b}$$

Where the subscript n stands for native wheat starch and the subscript s stands for sample. The relative crystallinity can be used as a measure for the degree of gelatinisation by applying the following equation:

$$DG = 1 - X_r \tag{9}$$

where X_r can be either X_{rA} or X_{rH}. The difference between the degree of gelatinisation calculated with X_{rA} and the degree of gelatinisation calculated with X_{rH} is equal to 5.9 ± 2.7 % (95 % confidence interval based on 26 measurements). This difference seems negligible. We have used the calculation based upon X_{rA} to determine the degree of gelatinisation.

Differential Scanning Calorimetry

First, freeze dried starch sample was transferred to a stainless steel DSC cup, dissolved in milli-Q water to obtain a 10 w/w % starch solution (approximately) and hermetically sealed. Thermograms of the resulting solutions were made using a Perkin-Elmer DSC-7 equipped with a PE model TAC7/DX Thermal Analysis Controller (Boston, USA). An empty pan was used as reference. Before the actual measurement, samples were held at 0 °C for 5 min in the DSC measuring cell. Subsequently, the sample was heated at 10°C/min from 0-150°C. The raw data was processed with Pyris 6 (Perkin-Elmer) to obtain the enthalpy needed to gelatinise the remaining crystalline part of the starch in the sample (ΔH_s). The characteristic gelatinisation endotherm occurs in the thermogram between 51 °C

and 76 °C. With use of the gelatinisation enthalpy of native wheat starch (ΔH_n), the degree of gelatinisation of the sample can be determined (Qu and Wang, 1994; Wang and Sastry, 1997):

$$DG = 1 - \frac{\Delta H_s}{\Delta H_n} \tag{10}$$

DSC measurements were also used to determine the temperature at which the first crystallites start to gelatinise (T_{oc}) and the temperature at which the most perfect crystallites have just been gelatinised or melted (T_{cc}) for 10 and 60 w/w % wheat starch-water mixtures. In case of the 10 w/w % wheat starch-water mixtures, wheat starch and water were added to the DSC cup before the measurement. In case of the 60 w/w % wheat starch-water mixtures, wheat starch and water were mixed as mentioned above and left to rest for at least 36 hours. This wheat starch-water mixture was used for the DSC measurements.

The onset temperature (T_o) and conclusion temperature (T_c) of gelatinisation or melting peaks often encountered in literature differ from T_{oc} and T_{cc}. The differences between T_{oc} and T_o and between T_{cc} and T_c are shown in the DSC thermograms in *Figure 1*. The onset and conclusion temperatures were obtained with the procedure that has been used by Eliasson and Karlsson (1983).
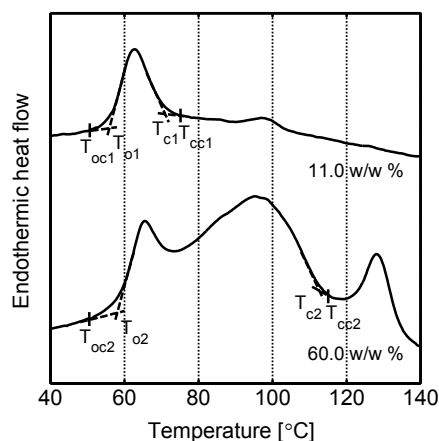
Figure 1: DSC thermograms of different wheat starch-water mixtures. Symbols used: T_{oc} = temperature at which the first crystallites gelatinise or melt, T_o = onset temperature of gelatinisation or melting peak, T_{cc} = temperature at which the most perfect crystallites gelatinise or melt, T_c = conclusion temperature of gelatinisation or melting peak, 1 = index for 11.0 w/w % wheat starch-water mixture, and 2 = index for 60.0 w/w % wheat starch-water mixture. Note: the peak at 95 °C in the upper thermogram and the peak at 130 °C in the lower thermogram are caused by amylose-lipid complexes that are melting.

Curve fitting procedure

Equation 7 can be used to calculate the melting temperature as a function of the degree of gelatinisation and starch concentration. These model values were fitted to experimental data in the temperature range between T_{oc} and T_{cc} (51-75 °C in case of 10 w/w % starch and 50-114 °C in case of 60 w/w % starch) with Mathcad (Mathsoft Engineering & Education, version 11.2, Cambridge, U.S.A.). These temperature ranges were determined by means of DSC. We have used 18.1 cm^3·mol^{-1} for V_1 (Lepori and Gianni, 2000) and 97.5 cm^3·mol^{-1} for V_2 (Shahidi *et al.*, 1976) at 25 °C for all calculations and the ratio V_2/V_1 was assumed to be independent of temperature. To calculate the volume fractions of water during our experiments, we have used 1.65 g/cm^3 and 0.997 g/cm^3 for respectively the density of wheat starch (Mark, 1999) and water (Atkins, 1997). It was assumed that these densities do not depend on temperature. In addition, it was assumed that the densities of crystalline and amorphous wheat starch are equal. Three fit parameters were used (T_m^0, ΔH_u and χ_{12}) and the values of these parameters were determined by minimizing the sum of the squared residuals.

Results

Handling of samples

Throughout the sample handling process, care was taken that the samples remain frozen to make sure that recrystallisation did not take place. X-ray measurements can be used to determine whether recrystallisation has occurred (Karim *et al.*, 2000; Ottenhof *et al.*, 2005). Our X-ray diffractograms showed that recrystallisation had not taken place prior to analysis (results not shown).

Gelatinisation of 10 and 60 w/w % wheat starch-water mixtures

Birefringence, DSC, wide angle X-ray diffraction and amylose-iodine complex formation measurements were applied for the measurement of the degree of gelatinisation of both a diluted (10 w/w %) and a concentrated (60 w/w %) starch-water mixture.

The enthalpy of gelatinisation of a 11.0 ± 1.0 w/w % (95 % confidence interval) wheat starch-water mixture is equal to 13.4 ± 2.0 J/g (95 % confidence interval) based on 4 DSC measurements (*Table 1*). This gelatinisation enthalpy is in good agreement with the value reported in literature (see *Table 1*).

Table 1: Temperature at which the first crystallites gelatinise or melt (T_{oc}), temperature at which the most perfect crystallites gelatinise or melt (T_{cc}) and enthalpy (ΔH) of the gelatinisation or melting for different wheat starch-water mixtures determined with DSC measurements with a heating rate of 10 °C/min.

C_{starch} [w/w %]	T_{oc} [°C]	T_{cc} [°C]	ΔH[a] [J/g]	Reference
11	51	75	13.4 ± 2.0[b]	This article
16	51	63	17.9	Douzals *et al.* (1996)
60	50	114	-	This article
55	56	101	-	Eliasson (1980)
57	45	103	-	Svensson and Eliasson (1995)
58	53	104	-	Rolee and Le Meste (1997)
65	49	116	-	Eliasson (1980)

[a] Gelatinisation enthalpy in J per g dry starch

[b] 95 % confidence interval

Figure 2A shows the degree of gelatinisation of 10 w/w % wheat starch-water mixtures that have been kept at a constant temperature for 45 min obtained with microscopy (birefringence), DSC, wide angle X-ray diffraction and amylose-iodine compleximetry. The values found with these methods give comparable degree of gelatinisation vs. treatment temperature curves. The temperature at which the gelatinisation of a 10 w/w % starch-water mixture starts, is equal to approximately 50 °C and the maximum degree of gelatinisation is reached at approximately 75 °C.
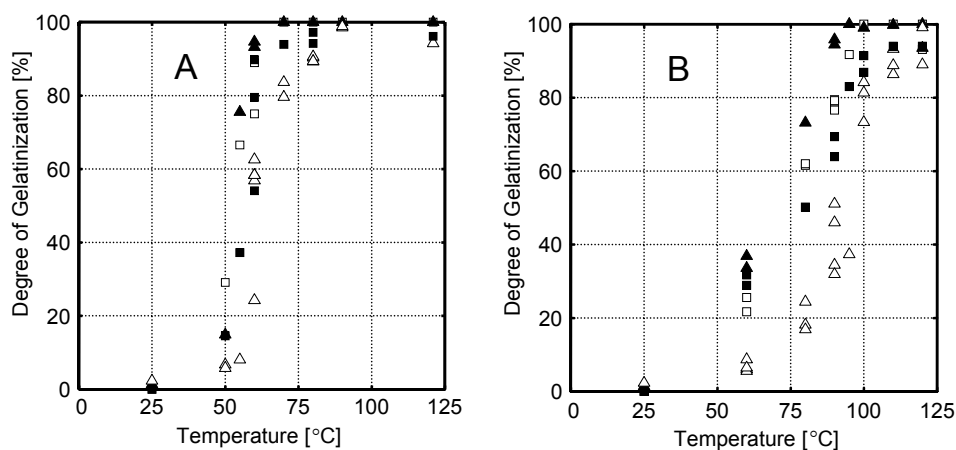
Figure 2: Degree of gelatinisation of starch in 10 w/w % (Figure A) and 60 w/w % (Figure B) wheat starch-water mixtures as function of the treatment temperature (treatment time 45 min). Experimental data determined with birefringence (▲), DSC (□), X-ray (■), and amylose-iodine complex formation (△) measurements.

Figure 2B shows the degree of gelatinisation of a 60 w/w % wheat starch-water mixture that has been measured with microscopy (birefringence), DSC, wide angle X-ray diffraction and amylose-iodine compleximetry after various treatments at constant temperature have been applied for 45 min. The degree of gelatinisation of the 60 w/w % starch-water mixture that is found, depends on the method used. Measurement of the degree of gelatinisation with birefringence leads to a high estimate, while measurement with amylose-iodine compleximetry provides a low estimate. DSC and wide angle X-ray measurements provide values of the degree of gelatinisation that are in between the ones obtained with birefringence measurements and amylose-iodine compleximetry. Gelatinisation of starch in a 60 w/w % starch-water mixture starts before 60 °C and the maximum degree of gelatinisation is obtained at approximately 110 °C.
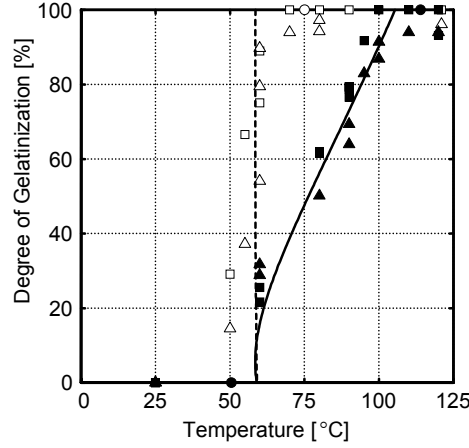
Figure 3: Degree of gelatinisation of starch as function of the treatment temperature (treatment time 45 min) for 10 w/w % (□: DSC data, △: X-ray data) and 60 w/w % (■: DSC data, ▲: X-ray data) wheat starch-water mixtures. Dotted line: calculated values for a 10 w/w % wheat starch-water mixture, solid line: calculated values for a 60 w/w % wheat starch-water mixture. T_{oc1} and T_{cc1} of a 11.0 w/w % wheat starch-water mixture (○) and T_{oc2} and T_{cc2} of a 60.0 w/w % wheat starch-water mixture (●) obtained with DSC have also been added to this graph.

Figure 3 shows the degree of gelatinisation as a function of the treatment temperature for a 10 w/w % and a 60 w/w % wheat starch-water mixture. This figure shows the results that were obtained with DSC and X-ray measurements. The temperature at which the gelatinisation process starts, seems to depend on the starch concentration. However, the number of measurements in this region is limited and for this reason it is hard to draw firm conclusions. The temperature at which maximum degree of gelatinisation is reached, clearly depends on the starch concentration.

The temperature at which the gelatinisation starts and ends can also be obtained from DSC thermograms (see *Figure 1* and *Table 1*). The temperatures that we have found are comparable with the values reported in literature (see *Table 1*). *Figure 3* shows that T_{oc} and T_{cc} are also in line with the DSC and X-ray measurements.

Equation 7 was fitted to the experimental data for which holds that the temperature is in between T_{oc} and T_{cc} and the results are shown in *Figure 3*. The parameters T_m^0, ΔH_u and χ_{12} that resulted in the lowest sum of the squared residuals are given in *Table 2*. The calculated degree of gelatinisation vs. treatment temperature curves agree with the experimentally determined curves.

Table 2: Parameters of the Flory equation.

$T_m^{\ 0}$ [°C]	ΔH_u [kJ/mol]	χ_{12} [-]	Reference
291 ± 63^a	29.2 ± 3.9^a	0.53 ± 0.05^a	This article
210	29.4	0.04	Lelievre (1974)
181	52.8	0	Donovan *et al.* (1980)
227 ± 13^a	37.3	0	Burt *et al.* (1983); Russell (1987)
263	22	0.57	Whittam *et al.* (1990); Moates *et al.* (1998)

[a] 95 % confidence interval

Discussion

According to Donovan (1979), the loss of crystallinity of the granule, the uptake of heat accompanied by the conformation change of starch, take up of water resulting in swelling of the granule and a decrease in the relaxation time of the water molecules occur simultaneously (or nearly so) during starch gelatinisation in excess water. Each method that can be used to study the gelatinisation of starch focuses on one or several of these specific aspects of the starch gelatinisation. During gelatinisation of a 10 w/w % wheat starch-water mixture, the microscopic changes in the crystallinity of the granule measured with the birefringence measurements, the endothermic gelatinisation transition measured with DSC, the long-range order determined with wide angle X-ray diffraction and the leaching of amylose chains with the amylose-iodine compleximetry occur more or less simultaneously. Because all these phenomena occur at the same time at these conditions, it does not matter which method is used for the determination of the degree of gelatinisation of starch in 10 w/w % wheat starch-water mixtures (see *Figure 2A*).

Similar results were obtained by Liu *et al.* (1991) and Cooke *et al.* (1992). Liu *et al.* (1991) observed small differences between birefringence and relative crystallinity (measured with X-ray) values of a 2 w/w % corn starch mixture as a function of the temperature that are comparable to the differences that are shown in *Figure 1*. Cooke *et al.* (1992) have shown that the crystallinity loss (measured with X-ray) and the loss in endothermic peak area (measured with DSC) of starch in 5 w/v % aqueous wheat starch suspensions (they have also used maize, potato, waxy maize and tapioca) as a function of the treatment temperature are comparable.

At the beginning of the gelatinization process, the same phenomenon occurs whether the amount of water is abundant (e.g. in case of a 10 w/w % wheat starch-water mixture) or limiting (e.g. in case of a 60 w/w % wheat starch-water mixture). Assuming that we have prepared a homogeneous starch-water mixture, every starch granule (independent of size) is surrounded by a thin layer of water and it increases in size due to the uptake of water by the amorphous growth rings (Waigh *et al.*, 2000). Because the granule consists of alternating amorphous and semi-crystalline growth rings, increase of the amorphous growth rings due to the uptake of water results in disruption of the semi-crystalline growth rings and loss of crystallinity. The similarity between the beginning of the gelatinisation process at high and limiting water concentrations can be explained as follows. The semi-crystalline, concentric growth rings on the outside of the granule are the first growth rings that have access to the available water. This part of the granule will gelatinise and hold the available water. As a result, there is an excess of water at the outside of the granule at both high and limiting water concentrations during the onset of the gelatinisation process. For this reason, the same process can take place initially in both cases resulting in the same starting temperature for gelatinisation. Therefore, the first peaks in the DSC thermograms of both diluted and concentrated starch-water mixtures start at the same temperature (see *Figure 1*). Because all water has been absorbed and bound by the gelatinised starch fraction in the concentric growth rings on the outside of the granule, there is no water available to induce swelling and disruption of the remainder of the starch granule at high starch-water ratios. For this reason, a heterogeneous mixture is formed that consists of amorphous, gelatinised starch and a part that has remained semi-crystalline. Complete loss of crystallinity can only be achieved by further increasing the temperature resulting in melting of the remaining semi-crystalline starch fraction (Waigh *et al.*, 2000). An increased temperature is required because the amount of water in the remaining starch fraction is very low. This can also be observed in the additional peak in the DSC thermogram of 60 w/w % wheat starch in water in *Figure 1*. In addition, equation 1 also predicts that the temperature required for complete loss of crystallinity increases with an increasing starch-water ratio.

At a wheat starch-water concentration of 60 w/w %, the differences between the curves obtained with birefringence, X-ray, DSC and amylose-iodine complex formation measurements become significant. Apparently, the phenomena that take place during the gelatinisation process at higher starch concentrations do not occur simultaneously anymore. The qualitative model based on a liquid crystalline theory presented by Waigh *et al.* (2000) might provide an explanation here. They suggest that the gelatinisation of starch is a two-stage process. In the first stage, the amylopectin side chains that form double helices

become separated from their duplex helical neighbours. In the second stage, a helix-random coil transition takes place resulting in the unwinding of the double helix. According to these authors the intermediate phase between the first stage and the second stage is not birefringent for A-type starches (e.g. wheat starch) and therefore birefringence measurements will already indicate that gelatinisation has taken place after the first stage. The unwinding of the double helices during the second stage is followed with WAXS and for this reason it is expected that the typical degree of gelatinisation determined with WAXS is lower than the degree of gelatinisation determined with birefringence at the same temperature. Both stages during the gelatinisation process give rise to an endothermic DSC peak. Only after the second stage has taken place, the sample is completely gelatinised and the DSC thermogram will not show an endothermic peak anymore. For this reason, the gelatinisation curve that is obtained with DSC is comparable to the curve obtained with WAXS. The theory of Waigh *et al.* (2000) does not provide a direct explanation for the observation that the amylose chains seem to be released after all ordening has disappeared. The behaviour of amylose during the gelatinisation of a concentrated starch-water mixture might be explained by considering the reduced mobility of the amylose chains in the granule (or part of the granule) caused by the low amount of water. Perhaps the disappearance of all ordening in the granule is needed to increase the mobility of the amylose chains within the granule to enable the release of amylose.

Based on the section above, it is expected that all birefringence is completely lost before X-ray measurements indicate that the gelatinization process starts, because the first stage of the gelatinization process should be completed before the second stage of the gelatinization process can start. However, granules in wheat starch do not gelatinise at the same temperature due to the bimodal granule size distribution (Eliasson *et al.*, 1983). Small granules gelatinise over a broader temperature interval than large granules. These differences can be caused by differences in composition between small and large granules. Meredith (1981) found that the distribution of saturated and unsaturated lipid is different for small granules and this author also found that the total lipid concentration varies with granule size. Morrison (1995) mentioned that the amount of lipid might affect the gelatinisation temperature and therefore differences in lipid content between small and large granules might affect the gelatinisation temperature. Furthermore, the chain length distribution of amylose chains might differ between small and large granules. Amylose chain length results in a different gelatinisation temperature (Moates *et al.*, 1997). For these reasons, it seems that within different granules different stages of the gelatinisation process can take place. Therefore, X-ray measurements can indicate that the gelatinization process

has started, although birefringence measurements indicate that part of the granules have not been gelatinised yet.

DSC and X-ray measurements can be used to determine whether the final stage of the gelatinisation process (unwinding of the double helices) has been completed. For this reason, we have used the experimental data based on these measurements for comparison between the 10 and 60 w/w % wheat starch-water mixtures and for fitting of the adapted Flory equation. To our knowledge, this is the first time that the Flory equation has been adapted in such way that it can quantitatively describe the degree of starch gelatinisation as a function of temperature and the starch-water ratio, even at very high ratios. According to this equation, the gelatinisation process starts at the same temperature independent of the concentration. This behaviour was also expected based on the theory mentioned above and the thermograms of 11 w/w % and 60 w/w % wheat starch-water mixtures (see *Table 1* and *Figure 1*). Furthermore, equation 7 predicts a steep increase in the degree of gelatinisation with increasing temperature for a 10 w/w % wheat starch-water mixture and a more gradual increase of the degree of gelatinisation with increasing temperature in case of a 60 w/w % wheat starch-water mixture. These differences are also present in our experimental data.

Fitting equation 7 to the experimental data resulted in useful T_m^0, ΔH_u and χ_{12} values. We have determined the degree of gelatinisation of an 80 w/w % wheat starch solution as a function of the treatment temperature (results not shown). At the maximum temperature that has been applied (180 °C), the degree of gelatinization was slightly higher than 50 %. Extrapolation of the trend indicates that the temperature to achieve complete gelatinization of this starch-water mixture is much higher than 200 °C. For this reason, the value of T_m^0 should be much higher and therefore our value of T_m^0 seems reasonable. The Flory-Huggins interaction parameter χ_{12} that we have obtained is close to 0.5. A negative or small positive χ_{12} value is a characteristic of a stable mixture (Rudin, 1999), which is the case for a starch-water mixture. In addition, a χ_{12} value close to 0.5 indicates that the second virial constant is close to zero (Rudin, 1999). Banks *et al.* (1969) have also found that the second virial coefficient is equal to zero for both amylose and amylopectin with use of light scattering experiments. It is expected that starch, a mixture of amylopectin and amylose, will therefore also have a second virial coefficient that is approximately equal to zero indicating that χ_{12} is close to 0.5.

The parameters that we have obtained with the adapted version of Flory's equation (equation 7) are comparable to the values of other researchers that were obtained after they have fitted the original Flory equation (equation 1) to their experimental data (see *Table 1*). It should be noted that the majority of reported values did not contain a confidence interval.

In addition, in other publications the Flory equation was not modified to account for the temperature dependence of the heat of fusion and entropy of fusion. The parameters obtained by these researchers should therefore be used with caution. The T_m^0 value that we have obtained is higher than the values reported by others (see *Table 2*), but the values reported by Burt *et al.* (1983) and Whittam *et al.* (1990) fall within our confidence interval and therefore one cannot conclude that our value is different. The value of ΔH_u is lower than the value reported by Donovan *et al.* (1980), but close to the values reported by other researchers (see *Table 2*). All reported χ_{12} values are in this range 0-0.6 indicating that starch-water mixtures are stable. The Flory-Huggins interaction parameter of Whittam *et al.* (1990) is close to the value that we have found and falls within our confidence interval. The χ_{12} value obtained by Lelievre (1974) is closer to zero. Other authors have assumed that χ_{12} is zero (e.g. Burt *et al.*, 1983; Donovan *et al.*, 1980), but do not verify this assumption.

We have included the parameters reported by Whittam *et al.* (1990) in our comparison, although they have used A-type crystalline starch instead of native wheat starch. However, since we have assumed that the non-crystalline part of native starch is an inert part of the system, we only consider that part of the starch, which is crystalline in native starch, and that is therefore comparable with A-type crystalline starch.

The parameters that have been obtained with the fitting procedure appear to be reasonable. In addition, the model values are in good agreement with the experimental values. Thus, in our view equation 7 can be used as a practical and reliable way to quantitatively estimate the degree of gelatinization of a starch-water mixture as a function of the starch concentration and treatment temperature.

Conclusions

Measurement of the degree of gelatinisation of starch in a 10 w/w % wheat starch-water mixture as a function of the treatment temperature based on birefringence, DSC, X-ray or amylose-iodine complex formation measurements give similar curves, because the physical-chemical processes involved occur simultaneously. If a 60 w/w % wheat starch-water mixture is used, however, the degree of gelatinisation vs. temperature curves are affected by the methods used to calculate the degree of gelatinisation. The highest values are obtained with birefringence measurements. Calculations based on DSC and X-ray measurements resulted in slightly lower values. Finally, amylose-iodine complex formation resulted in the lowest degree of gelatinisation. These differences were explained by

considering the phenomena that take place during the gelatinisation at limiting water conditions.

Gelatinisation of 10 w/w % and 60 w/w % wheat starch-water mixtures started at approximately the same temperature. However, complete gelatinisation was reached at different temperatures. These results are in accordance with DSC measurements that were carried out independently.

An adapted version of the Flory equation provides a quantitative description of the degree of starch gelatinisation as a function of the starch-water ratio and the temperature. Fitting this equation to our experimental data results in T_m^0, ΔH_u and χ_{12} values that are reasonable and comparable to the values reported in literature. The adapted Flory equation can be used as a means to estimate the temperature that is needed to completely gelatinise starch in a starch-water mixture over the whole concentration range.

The procedure followed for the handling of the samples can be used for diluted and concentrated starch-water mixtures and makes sure that recrystallisation is prevented. At low starch concentration it does not matter which method is selected to determine the degree of gelatinisation. However, at higher concentrations the degree of gelatinisation that is calculated depends on the analysis method used. DSC and X-ray measurements can be used to determine whether the final stage of the gelatinisation process has been completed. Birefringence and amylose-iodine complex formation measurements do not require specialized equipment and for this reason they are suitable alternatives. However, use of birefringence and amylose-iodine complex formation measurements will lead to different results.

Acknowledgements

References

Atkins PW. 1997. Physical chemistry. Oxford: Oxford University Press. 1031 p.

Banks W, Greenwood CT, Sloss J. 1969. Light-scattering studies on aqueous solutions of amylose and amylopectin. Carbohydr Res 11:399-406.

Bauer BA, Knorr D. 2005. The impact of pressure, temperature and treatment time on starches: pressure-induced starch gelatinisation as pressure time temperature indicator for high hydrostatic pressure processing. J Food Eng 68:329–334.

Birch GG, Priestley RJ. 1973. Degree of gelatinisation of cooked rice. Starch/Stärke 25:98-100.

Burt DJ, Russell PL. 1983. Gelatinization of low water content wheat starch-water mixtures. A combined study by differential scanning calorimetry and light microscopy. Starch/Stärke 35:354-360.

Calabrese VT, Khan A. 1999. Amylose-iodine complex formation without KI: evidence for absence of iodide ions within the complex. J Polymer Sci: Part A Polym Chem 37:2711–2717.

Chaiwanichsiri S, Ohnishi S, Suzuki T, Takai R, Miyawaki O. 2001. Measurement of electrical conductivity, differential scanning calorimetry and viscosity of starch and flour suspensions during gelatinisation process. J Sci Food Agric 81:1586-1591.

Cooke D, Gidley MJ. 1992. Loss of crystalline and molecular order during starchgelatinisation: origin of the enthalpic transition. Carbohydr Res 227:103-112.

Donovan JW. 1979. Phase transitions of the starch-water system. Biopolymers 18:263-275.

Donovan JW, Mapes CJ. 1980. Mutiple phase transitions of starches and nägeli amylodextrins. Starch/Stärke 32:190-193.

Donovan JW, Lorenz K, Kulp K. 1983. Differential scanning calorimetry of heat-moisture treatment of starches. Cereal Chem 60:381-387.

Douzals JP, Marechal PA, Coquille JC, Gervais P. 1996. Microscopic study of starch gelatinization under high hydrostatic pressure. J Agric Food Chem 44:1403-1408.

Eliasson AC. 1980. Effect of water content on the gelatinization of wheat starch. Starch/Stärke 32:270-272.

Eliasson AC, Karlsson R. 1983. Gelatinization properties of different size classes of wheat starch granules measured with differential scanning calorimeter. Starch/Stärke 35:130–133.

Flory PJ. 1953. Principles of polymer chemistry. Ithaca:Cornell University Press. 672 p.

Gidley MJ, Bociek SM. 1985. Molecular organization in starches: a carbon 13CP/MAS NMR study. J Amer Chem Soc 107:7040-7044.

Hoffman JD. 1958. Thermodynamic driving force in nucleation and growth processes. J Chem Phys 29:1192-1193.

Jenkins PJ, Donald AM. 1998. Gelation of starch: a combined SAXS/WAXS/DSC and SANS study. Carbohydr Res 308:133-147.

Jenkins PJ, Cameron RE, Donald AM, Bras W, Derbyshire GE, Mant GR, Ryan AJ. 1994. In situ simultaneous small and wide angle x-ray scattering: a new technique to study starch gelatinization. J Polymer Sci Part B: Polym Phys 32:1579-1583.

Karapantsios TD, Sakonidou EP, Raphaelides SN. 2000. Electrical conductance study of fluid motion and heat transport during starch gelatinization. J Food Sci 65:144-150.

Karim AA, Norziah MH, Seow CC. 2000. Methods for the study of starch recrystallization. Food Chem 71:9-36.

Lelievre J. 1974. Starch gelatinization. J Appl Polym Sci 18:293-296.

Lepori L, Gianni P. 2000. Partial molar volumes of ionic and nonionic organic solutes in water: a simple additivity scheme based on the intrinsic volume approach. J Solution Chem 29:405-447.

Liu H, Lelievre J. 1993. A model of starch gelatinization linking differential scanning calorimetry and birefringence measurements. Carbohydr Polym 20:1-5.

Liu H, Lelievre J, Ayoung-Chee W. 1991. A study of starch gelatinization using differential scanning calorimetry, X-ray, and birefringence measurements. Carbohydr Res 210:79-87.

Mandelkern L. 1989. Crystallization and melting. In: Booth C, Price C, editors. Comprehensive polymer science: the synthesis, characterization, reactions and applications of polymers. Vol 2. Polymer Properties. Oxford: Pergamon Press. 363-414.

Mark JE. 1999. Polymer data handbook. Oxford: Oxford University Press. 1040 p.

Meredith P. 1981. Large and small starch granules in wheat - Are they really different? Starch/Stärke 33:40-44.

Moates GK, Noel TR, Parker R, Ring SG. 1997. The effect of chain length and solvent interactions on the dissolution of the B-type crystalline polymorph of amylose in water. Carbohydr Res 298:327-333.

Moates GK, Parker R, Ring SG. 1998. Preferential solvent interactions and the dissolution of the B-type crystalline polymorph of starch in aqueous solutions. Carbohydr Res 313:225-234.

Morrison WR. 1995. Starch lipids and how they relate to starch granule structure and functionality. Cereal Food World 40:437-438, 440-441, 443-446.

Ottenhof M-A, Hill SE, Farhat IA. 2005. Comparative study of the recrystallization of intermediate water content waxy maize, wheat, and potato starches. J Agric Food Chem 53:631-638.

Parker R, Ring SG. 2001. Aspects of the physical chemistry of starch. J Cereal Sci 34:1-17.

Qu D, Wang SS. 1994. Kinetics of the formations of gelatinized and melted starch at extrusion cooking conditions. Starch/Stärke 46:225-229.

Randzio SL, Flis-Kabulska I, Grolier J-PE. 2002. Reexamination of phase transformations in the starch-water system. Macromolecules 35:8852-8859.

Rolee A, Le Meste M. 1997. Thermomechanical behavior of concentrated starch-water preparations. Cereal Chem 74:581-588.

Roussel L, Vieille A, Billet I, Cheftel JC. 1991. Sequential heat gelatinization and enzymic hydrolysis of corn starch in an extrusion reactor. Optimization for maximum dextrose equivalent. Lebensmittel-Wissenschaft und -Technologie 24:449-58.

Rudin A. 1999. The elements of polymer science and engineering. New York: Academic Press.

Russell PL. 1987. Gelatinization of starches of different amylose/amylopectin content. A study by differential scanning calorimetry. J Cereal Sci 6:133-145.

Shahidi F, Farrell PG, Edward JT. 1976. Partial molar volumes of organic compounds in water. III. Carbohydrates. J Solution Chem 5:807-816.

Svensson E, Eliasson A-C. 1995. Crystalline changes in native wheat and potato starches at intermediate water levels during gelatinization. Carbohydr Polym 26:171-176.

Tang H, Hills B. 2001. Starch granules. A multinuclear magnetic resonance study. Special Publication - Royal Society of Chemistry 262:157-164.

Tester RF, Sommerville MD. 2001. Swelling and enzymatic hydrolysis of starch in low water systems. J Cereal Sci 33:193-203.

Van Krevelen DW. 1976. Properties of polymers : their estimation and correlation with chemical structure. Amsterdam: Elsevier. 620 p.

Van Soest JJG, Tournois H, De Wit D, Vliegenthart JFG. 1995. Short-range structure in (partially) crystalline potato starch determined with attenuated total reflectance Fourier-transform IR spectroscopy. Carbohydr Res 279:201-214.

Waigh TA, Gidley MJ, Komanshek BU, Donald AM. 2000. The phase transformations in starch during gelatinisation: a liquid crystalline approach. Carbohydr Res 328:165-176.

Wang W-C, Sastry SK. 1997. Starch gelatinization in ohmic heating. J Food Eng 34:225-242.

Whittam MA, Noel TR, Ring SG. 1990. Melting behaviour of A- and B-type crystalline starch. Int J Biol Macromol 12:359-362.

Chapter 5

The effect of pressure and temperature on the gelatinisation of starch at various starch concentrations

Abstract

The effects of pressure, temperature, and treatment time on the degree of gelatinisation were determined with differential scanning calorimetry measurements for wheat starch-water mixtures with starch concentrations varying between 5 and 80 w/w %. Although simple models could be used to describe the degree of starch gelatinisation as function of pressure or temperature, a more complex model based on the Gibbs energy difference had to be used to describe the degree of gelatinisation as a function of both pressure and temperature. The experimental and model data were used to construct a phase diagram for 5, 30, and 60 w/w % wheat starch-water mixtures. Data obtained from literature were in accordance with our phase diagrams. These phase diagrams can be used to estimate the degree of gelatinisation after applying a certain pressure and temperature on a starch-water mixture with starch concentrations in the range of 5 and 60 w/w %.

Introduction

Gelatinisation of starch is required for many industrial and food applications. For example, gelatinisation of starch is required prior to enzymatic hydrolysis to make starch accessible for the enzyme. In this case, the industrial gelatinisation process is usually carried out with a 30–35 w/w % dry solids starch slurry. Higher starch concentrations may yield higher volumetric efficiencies and lower energy consumption.

When the temperature of an aqueous starch-water suspension is increased, gelatinisation takes place. During thermal gelatinisation, starch granules take up water, swell, lose crystallinity, and leach amylose (Parker and Ring, 2001). In addition, differential scanning calorimetry (DSC) measurements indicate that heat is taken up during this temperature increase (Donovan, 1979). Together with all these phenomena occurring during gelatinisation, an irreversible order-disorder transition takes place (Cooke and Gidley, 1992; Jenkins and Donald, 1998; Liu and Lelievre, 1993). Gelatinisation of starch is affected by the starch-water ratio (Parker and Ring, 2001; Burt and Russell, 1983; Donovan, 1979; Donovan and Mapes, 1980; Donovan *et al.*, 1983; Russell, 1987; Whittam *et al.*, 1990). When the moisture content of the starch-water mixture is low, complete swelling and disruption of the starch granules is not possible and only part of the crystallinity of the starch granules is lost. The remaining crystallinity only disappears after heating to higher temperatures. This could be quantitatively described by a model based on the Flory equation that was developed for the description of the degree of gelatinisation as a function of temperature and starch concentration (Baks *et al.*, 2007). The article of Jenkins and Donald (1998) provides an overview of the various theories that provide explanations for the phenomena that take place during thermal gelatinisation of starch.

Starch can also be gelatinised by application of high pressures (Thevelein *et al.*, 1981). In certain aspects, high pressure gelatinisation differs from thermal gelatinisation. During high pressure gelatinisation, disintegration of the granules is less (or the granules even remain intact), amylose solubilisation is less, and swelling of the granules is limited (Douzals *et al.*, 1998; Katopo *et al.*, 2002; Knorr *et al.*, 2006; Stolt *et al.*, 2002; Stute *et al.*, 1996). On the other hand, the effect of the starch-water ratio on high pressure gelatinisation is similar. In case of thermal gelatinisation, a higher temperature is required to achieve complete gelatinisation and in case of high pressure gelatinisation a higher pressure is required to achieve complete gelatinisation (Kawai *et al.*, 2007; Muhr and Blanshard, 1982; Stute *et al.*, 1996). Knorr *et al.* (2006) developed a theory for the similarities and differences between thermal gelatinisation and high pressure gelatinisation.

The degree of gelatinisation can also be affected by the treatment time (Bauer and Knorr, 2004, 2005; Stolt *et al.*, 2000). Stolt *et al.* kept 25 w/w % barley starch-water mixtures at 30 °C and different pressures varying between 400 and 550 MPa; while Bauer and Knorr (2004; 2005) kept 5 w/w % wheat starch-water mixtures at 29 °C at pressures varying between 250 and 450 MPa. In both cases, the time required to reach an equilibrium value for the degree of gelatinisation varied from several minutes to more than six hours. It was observed that the final degree of gelatinisation was reached faster when a higher pressures was applied during gelatinisation.

The effect of pressure and temperature on the equilibrium degree of gelatinisation of starch-water mixtures can be depicted in a phase diagram. Up to now, these phase diagrams were only obtained for dilute starch-water mixtures (1-5 w/w %) (Bauer and Knorr, 2005; Douzals *et al.*, 2001; Knorr *et al.*, 2006; Rubens and Heremans, 2000) or for potato starch-water mixtures over a wide range of concentrations (10-70 w/w %) at a fixed temperature (Kawai *et al.*, 2007). In some cases, a treatment time of 15 minutes was used (Bauer and Knorr, 2005; Douzals *et al.*, 2001; Knorr *et al.*, 2006) and it is not clear whether this treatment time is sufficient to reach an equilibrium value for the degree of gelatinisation. Phase diagrams that relate the degree of gelatinisation to pressure and temperature were not determined for higher starch-water ratios. For that reason, the effect of the starch-water ratio over a broad pressure and temperature range is not yet known.

Hawley (1971) developed a thermodynamic model to describe the reversible denaturation of chymotrypsinogen as a function of pressure and temperature. The standard Gibbs energy change of reaction was used as a starting point for the derivation of this model (Hawley, 1971; Heremans and Smeller, 1998; Knorr *et al.*, 2006; Smeller, 2002). This model has also been used to describe the effect of pressure and temperature on the degree of gelatinisation (Knorr *et al.*, 2006; Rubens and Heremans, 2000)

The aim of this article is to measure the degree of gelatinisation as a function of pressure, temperature, and treatment time for wheat starch-water mixtures with starch concentrations varying between 5 and 80 w/w %. DSC measurements are used to determine the degree of gelatinisation. In addition, various models are used to describe the degree of gelatinisation as a function of pressure and temperature separately and as function of both of these variables. The experimental and model data are used to construct a phase diagram that shows the effect of pressure, temperature and concentration on the degree of gelatinisation over a broad range of experimental conditions.

Theory

If we assume that native starch is in equilibrium with gelatinised starch, the apparent equilibrium constant of the gelatinisation reaction can be defined as a function of the degree of gelatinisation:

$$K' = \frac{x_G}{x_N} = \frac{DG}{100\text{-}DG} \tag{1}$$

where K' is the apparent equilibrium constant (dimensionless), x_N is the mole fraction of native starch (dimensionless), x_G is the mole fraction of gelatinised starch (dimensionless), and DG is the degree of gelatinisation (in %). The temperature dependency of the apparent equilibrium constant is given by (Atkins, 1997):

$$\left(\frac{\partial (lnK')}{\partial T} \right)_P = \frac{\Delta H(P_r)}{R \cdot T^2} \tag{2}$$

where $\Delta H(P_r)$ is the enthalpy change of reaction at the reference pressure P_r (in J·mol^{-1}), and R is the gas constant (in J·mol^{-1}·K^{-1}), and T is the temperature (in K). The apparent equilibrium constant (for reactions in solutions) also depends on pressure P (in Pa). The pressure dependency of the apparent equilibrium constant is given by the following equation (Atkins, 1997):

$$\left(\frac{\partial (lnK')}{\partial P} \right)_T = \frac{\Delta V(P_r)}{-R \cdot T} \tag{3}$$

where $\Delta V(P_r)$ is the volume change of reaction at the reference pressure P_r (in m^3·mol^{-1}), and P is the absolute pressure (in Pa).

After combining equation 1 and equation 2, assuming that $\Delta H(P_r)$ does not depend on temperature (so $\Delta H(P_r,T) = \Delta H(P_r,T_r)$), and integrating from T to T_r, a relationship between the degree of gelatinisation and temperature is obtained (for constant pressure):

$$DG = \frac{100}{1 + exp\left[-lnK_r + \frac{\Delta H(P_r,T_r)}{R} \cdot \left(\frac{1}{T} - \frac{1}{T_r} \right) \right]} \tag{4}$$

where K_r is the apparent equilibrium constant at a reference point with pressure P_r and temperature T_r. Similarly, a relationship between the degree of gelatinisation and pressure is obtained (for constant temperature) after inserting equation 1 into equation 3, assuming

that $\Delta V(P_r)$ is independent of pressure and temperature (so $\Delta V(P_r,T) = \Delta V(P_r,T_r)$), and integrating from P to P_r:

$$DG = \frac{100}{1 + \exp\left[-\ln K_r + \dfrac{\Delta V\left(P_r,T_r\right)}{RT_r}\cdot\left(P-P_r\right)\right]} \tag{5}$$

Equations 4 and 5 cannot be used to describe the degree of gelatinisation as a function of both pressure and temperature. Muhr and Blanshard (1982) already found that ΔV depended on temperature and they stated that more complex models were required to describe the effect of pressure on the degree of gelatinisation.

According to Hawley (1971), equation 6 can be used to relate the apparent equilibrium constant to pressure and temperature in the vicinity of an arbitrarily chosen reference point (T_r, P_r)[1]:

$$\Delta G = \Delta G\left(P_r,T_r\right) - \Delta S\left(P_r,T_r\right)\cdot\left(T-T_r\right) - \frac{\Delta C_p}{2T_r}\cdot\left(T-T_r\right)^2$$
$$+ \Delta V\left(P_r,T_r\right)\cdot\left(P-P_r\right) + \frac{\Delta\beta}{2}\cdot\left(P-P_r\right)^2 + \Delta\alpha\cdot\left(T-T_r\right)\cdot\left(P-P_r\right) \tag{6}$$

where $\Delta G(P_r,T_r)$ is the Gibbs energy change of reaction at reference pressure P_r and reference temperature T_r (in J·mol^{-1}); $\Delta S(P_r,T_r)$ is the entropy change of reaction at reference pressure P_r and reference temperature T_r (in J·mol^{-1}·K^{-1}); ΔC_p is the heat capacity change of reaction (in J·mol^{-1}·K^{-1}); $\Delta V(P_r,T_r)$ is the volume change of reaction at reference pressure P_r and reference temperature T_r (in m^3·mol^{-1}); $\Delta\beta$ is the isothermal compressibility change of reaction (in m^6·mol^{-1}·J^{-1}); and $\Delta\alpha$ is the thermal expansion factor change of reaction (in m^3·mol^{-1}·K^{-1}). Combining equations 1, 6, and $-R\cdot T\cdot \ln K = \Delta G$ results in an equation that relates the degree of gelatinisation to pressure and temperature:

$$DG = \frac{100}{1 + \exp\left(\dfrac{\Delta G}{RT}\right)} \tag{7}$$

Where ΔG is defined in equation 6. Plotting lines with the same degree of gelatinisation as function of the temperature and pressure results in the characteristic elliptic phase

---

[1] Although equation 6 was used by several others (Hawley, 1971; Heremans and Smeller, 1998; Knorr *et al.*, 2006; Smeller, 2002), the derivation has not been published before. The derivation of this equation is therefore given in the appendix.

diagrams that have been observed for several proteins and other biopolymers (Hawley, 1971; Heremans and Smeller, 1998; Knorr *et al.*, 2006; Smeller, 2002).

Experimental

Materials

Wheat starch (S5127) was obtained from Sigma-Aldrich (Steinheim, Germany). The moisture content was 9.95 ± 0.43 w/w % (based on 22 measurements, 95 % confidence interval). The moisture content was determined by drying the wheat starch in a hot air oven at 105 °C or in a vacuum oven at 80 °C until the mass of the samples was constant in time. The water content of wheat starch was taken into account during all experiments. Milli-Q water was used for all experiments.

Gelatinisation experiments

Gelatinisation experiments were carried out with starch concentrations varying from 5 to 80 w/w % wheat starch in water with treatment temperatures between 20 and 180 °C and with operating pressures between 0.1 and 900 MPa. Wheat starch-water mixtures were prepared one day in advance. An analytical mill (type A10) from IKA (Staufen, Germany) was used to prepare the 60-80 w/w % wheat starch-water mixtures

For gelatinisation experiments at 0.1 MPa, a temperature controlled batch reactor equipped with an anchor stirrer was used for the experiments with 10 w/w % wheat starch-water slurries and a compression molder from PHI (City of Industry, U.S.A.) was used for the experiments with 60, 70, and 80 w/w % wheat starch-water mixtures. The compression molder setup is described in more detail elsewhere (Baks *et al.*, 2007). The treatment time in the batch reactor was 45 min and the treatment time in the compression molder was 45 min for 60 w/w % wheat starch-water mixtures and 20 min for 70 and 80 w/w % wheat starch-water mixtures. For all gelatinisation experiments at 0.1 MPa holds that the degree of gelatinisation became constant after a treatment time of approximately 5 min.

Gelatinisation experiments at higher pressures were carried out in a multi vessel high-pressure apparatus (Resato FPU 100-50, Resato International B.V., Roden, the Netherlands). Glycol was used as pressure medium. Wheat starch-water mixtures (5, 30, 60 w/w % wheat starch in water) were transferred to custom made polyethylene bags sealed with a minimum amount of air. These bags were placed in the high pressure equipment. During the experiments, set point pressures of 100, 200, 300, 400, 600, and 800 MPa were

built up in respectively 1, 2, 2.5, 3, 3, and 4 min. The temperature overshoot after pressure build-up varied from 1 to 10 °C depending on the pressure (higher pressures resulted in a higher temperature overshoot). After the set point pressure was reached, the starch-water mixture was held at this pressure for 2 min, which proved to be enough time to let the temperature decrease to the set point temperature. This point was taken as the starting time of the gelatinisation reaction. In case the degree of gelatinisation was followed in time, samples were taken 0, 15, 30, 45, 60, and 120 min after this starting point. In case the treatment time was kept constant, 60 min was used. Samples that were taken immediately after the holding time of 2 min were used to determine the effect of the start-up procedure on the degree of gelatinisation.

Handling of samples

To avoid retrogradation as much as possible, samples were transferred to a vessel with liquid nitrogen immediately after they were taken. When the samples were completely frozen, they were stored in an -80 °C freezer until further use.

After storage and prior to analysis, the samples were freeze-dried in a Christ Epsilon 2-6D freeze dryer (Osterode am Harz, Germany). Freeze-drying was started at -20 °C and 1.030 mbar for 20 h, followed by a second drying stage at -5 °C and 0.05 mbar for 20 h. During the third drying stage, the temperature was kept at -5 °C and the pressure was kept at 0.001 mbar for 28 h. The freeze-dried samples were submerged in liquid nitrogen for several minutes and subsequently grinded in a Retsch ZM 100 rotor mill (Retsch Gmbh, Haan, Germany) with a 0.5 mm ring sieve. The powder obtained after the grinding step was stored in a desiccator at room temperature until further use.

Measurement of the degree of gelatinisation

Differential Scanning Calorimetric measurements were used to measure the degree of gelatinisation. This procedure was described in a previous article (Baks *et al.* 2007).

Curve fitting procedure and selection of data for curve fitting

The model data obtained with equation 4 were fitted to our own experimental values of the degree of gelatinisation as a function of temperature at atmospheric pressure. The experimental data from Kawai *et al.* (2007) were used to calculate the degree of gelatinisation as described elsewhere (Baks *et al.*, 2007). Equation 5 was used to fit the model data to the experimental degree of gelatinisation values of Kawai. Table Curve 2D (Jandel Scientific, 1994, version 2.0, San Rafael, CA, USA) was used for the fitting

procedure of equations 4 and 5 (based on minimizing the sum of squared residuals). Two fit parameters were used for each equation (K_r and $\Delta H(P_r, T_r)$ in case of equation 4 and K_r and $\Delta V(P_r, T_r)$ in case of equation 5). Note that it is not necessary to use K_r as a fitting parameter: an average of experimental K_r values that have been measured at the same conditions can be used. However, we chose not to use experimental values because an error in this average K_r value greatly affects the model output.

Model data obtained with equation 7 were fitted to the experimental degree of gelatinisation data where both pressure and temperature were varied. Six fit parameters were used ($\Delta G(P_r, T_r)$, $\Delta V(P_r, T_r)$, $\Delta H(P_r, T_r)$, $\Delta \alpha$, $\Delta \beta$, ΔC_p). Tablecurve 3D was used for the fitting procedure (Jandel Scientific, 1993, version 1.04, San Rafael, CA, USA). Besides our own experimental data, part of the experimental data of Douzals *et al.* (2001) and Randzio *et al.* (2002) were also used. The onset temperature from the DSC thermograms of Randzio *et al.* (2002) (for explanation see Baks *et al.*, 2007) obtained at 0.1 MPa was used as the highest temperature at which the degree of gelatinisation was still equal to zero. At temperatures below the onset temperature, the degree of gelatinisation was equal to zero. Several points at temperatures below the onset temperature were used for the curve fitting procedure to make sure that the degree of gelatinisation was equal to zero in between 20 °C and the onset temperature.

The degree of gelatinisation was followed in time. The following procedure was used to determine which experimental data points were at equilibrium. It was assumed that the gelatinisation can be described as a first order reaction (Lund, 1984):

$$\frac{dDG}{dt} = k \cdot \left(DG_f - DG \right) \tag{8A}$$

$$DG_t = DG_f - \left(DG_f - DG_0 \right) \cdot exp \left(- k \cdot t \right) \tag{8B}$$

where DG_t is the degree of gelatinisation (%) at time t, DG_f is the degree of gelatinisation at equilibrium (%), DG_0 the initial degree of gelatinisation (%) at $t = 0$ min, and k is the first order reaction rate constant (min^{-1}). Second, DG_f and k were determined by fitting the model data from equation 8B to the experimental values for each time course experiment. The experimental values for which holds that the degree of gelatinisation does not differ more than 5 % from DG_f are assumed to be at equilibrium. For all curve fitting procedures related to equations 4, 5, 6, and 7, equilibrium data were used exclusively.

In equations 4, 5, 6, and 7, the reference pressure P_r is equal to 400 MPa and the reference temperature T_r is equal to 313 K (except for model used in *Figure 3A*; T_r was equal to 298 K in this case). This reference point was chosen, because the temperatures and

pressures used during the experiments with the different starch-water mixtures are close to this point.

Results

Effect of treatment time on the degree of gelatinisation
Figure 1 shows the degree of gelatinisation as function of time when 30 and 60 w/w % starch-water mixtures are held at 400 MPa and 20 °C. At these conditions, the time required to reach 95 % of the equilibrium value is significantly lower for a 60 w/w % starch-water mixture than for a 30 w/w % starch-water mixture. *Table 1* shows the results of all time course experiments. The time required to reach an equilibrium value for the degree of gelatinisation is also affected by the operating conditions. In many cases, this time was zero or close to zero. In such cases, the equilibrium values were reached immediately or very soon after the set point pressure and temperature were reached. If the temperature is kept constant, increasing the pressure results in a shorter time to reach an equilibrium value for the degree of gelatinisation. However, in case of a starch concentration of 60 w/w %, the time to reach equilibrium increases when the temperature is increased. At a starch concentration of 5, 30, and 60 w/w %, the longest time to reach equilibrium value for the degree of gelatinisation was respectively 27 min (300 MPa, 40 °C), 54 min (400 MPa, 20 °C), and 47 min (400 MPa, 60 °C).

Table 1: Main characteristics of time course experiments, in which the degree of gelatinisation was followed as function of treatment time at a specific temperature and pressure.

P [a] [MPa]	T [b] [°C]	$t_{e,5}$ [c] [min]	$t_{e,30}$ [c] [min]	$t_{e,60}$ [c] [min]
100	80	0	0	0.2
200	40	n.d.[d]	0.6	2.0
300	40	27	0	n.d.[d]
400	20	n.d.[d]	54.0	2.0
400	60	0	0	47.0
600	40	0	0	0.1
800	20	0	0	0.1

[a] Set point pressure; the deviation from the set point was smaller than 1.5 MPa.

[b] Set point temperature; the deviation from the set point was smaller than 1 °C.

[c] $t_{e,5}$, $t_{e,30}$, and $t_{e,60}$ are the times required to reach 95 % of the equilibrium degree of gelatinisation at a certain pressure and temperature for starch-water mixture with starch concentrations with respectively 5, 30, and 60 w/w % starch in water. In case t_e is equal to zero, the equilibrium value was reached directly after the time required for pressure build-up and the holding time were passed.

[d] Not determined.
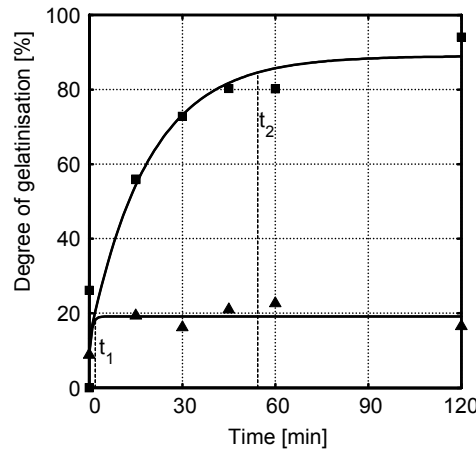
Figure 1: Degree of starch gelatinisation of wheat starch-water mixtures held at 400 MPa and 20 °C for 120 minutes, with experimental data of respectively 30 (■) and 60 (▲) w/w % starch in water and solid lines for model values obtained with equation 8. The time required to reach an equilibrium value for the degree of gelatinisation is depicted by t_1 and t_2 for respectively 60 and 30 w/w % starch-water mixtures.

For the fitting procedure of equation 7, data of Douzals *et al.* (2001) were used. The holding time during their gelatinisation experiments was fixed at 15 min. In some cases, such a period of time is enough to reach an equilibrium value, while in other cases it is not. For that reason, only data in which the degree of gelatinisation was equal to 100 % were used, because only at this degree of gelatinisation we can be certain that equilibrium was reached.

Effect of temperature on the degree of gelatinisation
Figure 2 shows the degree of gelatinisation as a function of the temperature at 0.1 MPa for 10, 60, 70, and 80 w/w % wheat starch-water mixtures. The model data calculated with equation 4 that were fitted to the experimental data agree well with the experimental data for 10, 60, and 70 w/w % starch-water mixtures. The deviation between the model values and the experimental values is larger in case of 80 w/w %. For each starch-water mixture, the lowest sum of squared errors was obtained with the values of $\Delta H(P_r,T_r)$ and K_r given in *Table 2*. According to model values in *Figure 2*, the temperature at which gelatinisation starts at 0.1 MPa is roughly the same for starch-water mixtures with different concentrations. Contrary to the onset temperature of the gelatinisation curve, the temperature at which 100 % gelatinisation is reached differs for each starch-water mixture. The temperature for complete gelatinisation increases with an increasing starch concentration.
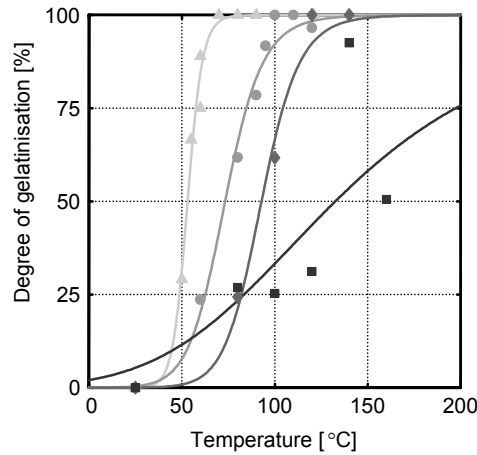
Figure 2: Degree of starch gelatinisation in 10 (△), 60 (●), 70 (◆), and 80 (■) w/w % wheat starch-water mixtures as a function of temperature at 0.1 MPa. Points indicate the experimental data while lines indicate model values obtained with equation 4.

Table 2: Standard enthalpy change of reaction ($\Delta H(P_r, T_r)$) and apparent equilibrium constant (K_r) for different wheat starch-water ratios at 0.1 MPa obtained after fitting model values (equation 4) to our experimental data.

C_s [w/w %]	$\Delta H(P_r, T_r)$ [a] [10^4 J·mol^{-1}]	K_r [a,b] [-]
10	22.1 ± 6.0	$(3.4 \pm 3.6) \cdot 10^{-2}$
60	9.9 ± 2.8	$(2.6 \pm 3.2) \cdot 10^{-2}$
70	11.0 ± 6.0	$(2.3 \pm 7.8) \cdot 10^{-3}$
80	2.7 ± 3.8	$(9.5 \pm 31.6) \cdot 10^{-2}$

[a] 95 % confidence interval.

[b] Apparent equilibrium constant at 0.1 MPa and 313 K.

Effect of pressure on the degree of gelatinisation

Figure 3A shows the degree of gelatinisation as a function of pressure at 25 °C for 5, 30, and 60 w/w % wheat starch-water mixtures. The model data calculated with equation 5 that were fitted to the experimental data agree with the experimental data. For each starch-water mixture, the lowest sum of squared errors was obtained with the values of $\Delta V(P_r, T_r)$ and K_r given in *Table 3*.
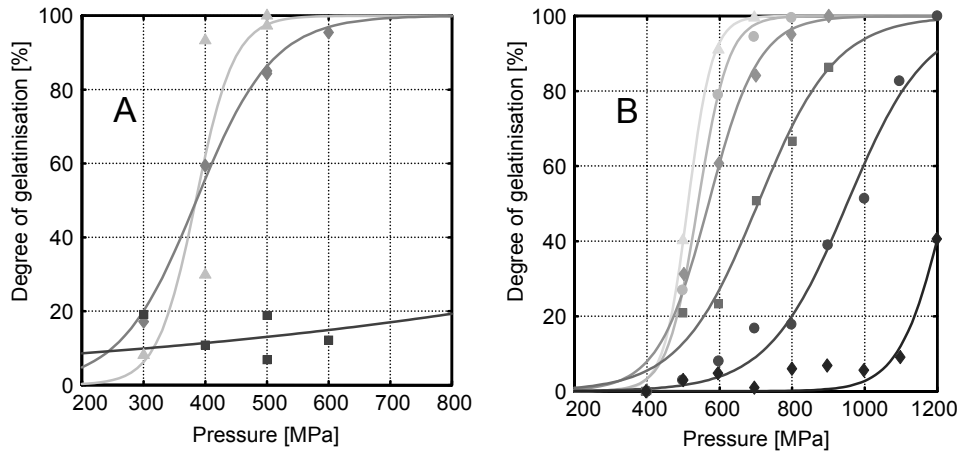
Figure 3: Degree of starch gelatinisation in 5 (△), 30 (◆), and 60 (◆) w/w % wheat starch-water mixtures as a function of pressure at 298 K (Figure A, own data) and in 10 (△), 20 (●), 30 (◆), 40 (■), 50 (●), and 60 (◆) w/w % potato starch-water mixtures as a function of pressure at 313 K (Figure B, data Kawai et al., 2007). Points indicate the experimental data while lines indicate model values obtained with equation 5. The gelatinisation enthalpy at 400 MPa was used as the gelatinisation enthalpy for native potato starch.

The data of Kawai *et al.* (2007) were also used to determine the degree of gelatinisation as a function of pressure for 10, 20, 30, 40, 50, and 60 w/w % potato starch-water mixtures at 40 °C (*Figure 3B*). The model data obtained with equation 5 agree well with the experimental data. The parameters $\Delta V(P_r, T_r)$ and K_r that resulted in the lowest sum of squared errors for each starch-water mixture are given in *Table 3*. The pressure, at which the gelatinisation starts, was approximately equal for all starch-water mixtures. However, the pressure at which starch was completely gelatinised, increased with an increasing starch-water ratio.

Table 3: *Standard volume change of reaction ($\Delta V(P_r, T_r)$) and apparent equilibrium constant (K_r) for different wheat starch-water ratios at 298 K and potato starch-water ratios at 313 K obtained after fitting model values (equation 5) to experimental data.*

T [K]	C_s [w/w %]	$\Delta V(P_r, T_r)$ [a] [10^{-6} m^3·mol^{-1}]	K_r [a] [-]
298	5	-79.4 ± 181.3	1.6 ± 2.5 [b]
	30	-40.0 ± 7.9	1.3 ± 0.3 [b]
	60	-3.9 ± 13.4	0.1 ± 0.1 [b]
313	10	-77.7 ± 34.8	$(3.4 \pm 4.9) \cdot 10^{-2}$ [c]
	20	-62.4 ± 15.9	$(3.4 \pm 3.1) \cdot 10^{-2}$ [c]
	30	-37.6 ± 13.1	$(8.6 \pm 8.1) \cdot 10^{-2}$ [c]
	40	-24.2 ± 7.9	$(5.8 \pm 5.8) \cdot 10^{-2}$ [c]
	50	-23.7 ± 7.7	$(6.5 \pm 10.8) \cdot 10^{-3}$ [c]
	60	-41.5 ± 24.1	$(2.0 \pm 14.2) \cdot 10^{-6}$ [c]

[a] 95 % confidence interval.

[b] Apparent equilibrium constant at 400 MPa and 298 K.

[c] Apparent equilibrium constant at 400 MPa and 313 K.

Degree of gelatinisation vs. T and p for 5, 30, and 60 w/w % starch-water mixtures
In *Figures 4A, 5A*, and *6A*, the degree of gelatinisation of respectively 5, 30, and 60 w/w % wheat starch-water mixtures is shown as a function of pressure and temperature. The location of each experimental data point in these graphs represents the pressure and temperature that was used during the experiment, while the degree of greyness (greyscale) of the marker indicates what the degree of gelatinisation is.

Model values obtained with equation 7 were fitted to the experimental data shown in *Figures 4A, 5A*, and *6A*. *Table 4* shows the values of $\Delta G(P_r,T_r)$, $\Delta V(P_r,T_r)$, $\Delta S(P_r,T_r)$, $\Delta\alpha$, $\Delta\beta$, and ΔC_p that resulted in the lowest sum of squared residuals after fitting the data calculated with the model equation (equation 7) to the experimental data. The calculated degrees of gelatinisation were compared with the experimental data in two different types of two-dimensional plots. Firstly, lines were plotted that show the pressure and temperature combination that results in the same degree of gelatinisation (10, 25, 50, 75, 99 %). The lines calculated with the model resemble the characteristic elliptic phase diagrams that have been observed for several proteins (Heremans and Smeller, 1998). In addition, parity plots (*Figures 4B, 5B*, and *6B*) are shown to compare the degree of gelatinisation that was found in the experiments with the model values.

Figure 4: Degree of starch gelatinisation as function of temperature and pressure obtained with experiments and calculations (Figure A) and comparison of calculated values (DG_{model}) with experimental values (DG_{exp}) in parity plot (Figure B) for 5 w/w % wheat starch-water mixtures. Our own experimental data are depicted with: □: DG = 0 %; ▪: 0 % < DG ≤ 25 %; ▪: 25 % < DG ≤ 50 %; ▪: 50 % < DG ≤ 75 %; ▪: 75 % < DG < 100 %; ▪: DG=100%. The experimental data of others are depicted as followed: ◇: DG = 0 %, Randzio et al. (2002); and ◆: DG = 100 %, Douzals et al. (2001) The model data (obtained with equation 6 inserted into equation 7 and parameters from Table 4) shown in Figure A are depicted with the solid lines and the index represents the degree of hydrolysis.

The parity plots (*Figures 4B, 5B*, and *6B*) show that the degree of gelatinisation of 5, 30, and 60 w/w % wheat starch-water mixtures calculated with equation 7 agree with the experimental data. *Figures 4A, 5A*, and *6A* show the degree of gelatinisation of 5, 30, and 60 w/w % wheat starch-water mixtures as a function of pressure and temperature. All lines in these figures, which connect the operating conditions that result in the same degree of

gelatinisation, have the characteristic elliptic shape. A smaller ellipse (shorter major and minor axis) was observed for lower degrees of gelatinisation.

Figure 4A shows that when the temperature of a 5 w/w % wheat starch-water mixture was increased from respectively -20 °C to approximately 20 °C, the pressure required to maintain a certain degree of gelatinisation increased. A similar trend was observed for 30 w/w % wheat starch-water mixtures (*Figure 5A*). In this case, the pressure required to obtain the same degree of gelatinisation increased when the temperature increased from approximately 0 to 30 °C. Such a trend could not be observed for 60 w/w % wheat starch-water mixtures.

For all wheat starch-water mixtures, we observed that above approximately 20 °C, the pressure required to maintain the same degree of gelatinisation decreases with increasing temperature. However, only in case of 5 w/w % wheat starch-water mixtures it seemed that above a certain temperature, two operating pressures can be found that result in the same degree of gelatinisation.
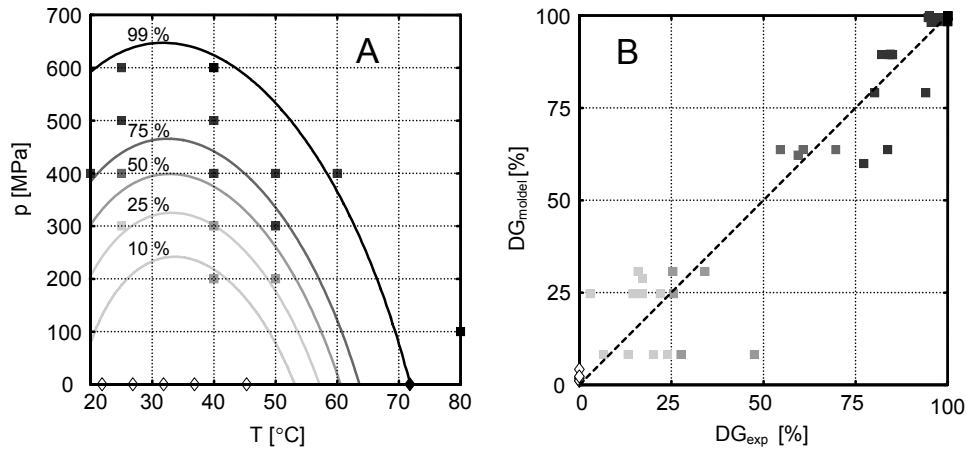
Figure 5: Degree of starch gelatinisation as function of temperature and pressure obtained with experiments and calculations (Figure A) and comparison of calculated values (DG_{model}) with experimental values (DG_{exp}) in parity plot (Figure B) for 30 w/w % wheat starch-water mixtures. Our own experimental data are depicted with: □: DG = 0 %; ■: 0 % < DG ≤ 25%; ■: 25 % < DG ≤ 50 %; ■: 50 % < DG ≤ 75 %; ■: 75 % < DG < 100 %; ■: DG = 100 %. The experimental data of Randzio et al. (2002) are depicted with: ◇: DG = 0 %. The model data (obtained with equation 6 inserted into equation 7 and parameters from Table 4) shown in Figure A are depicted with the solid lines and the index represents the degree of hydrolysis.
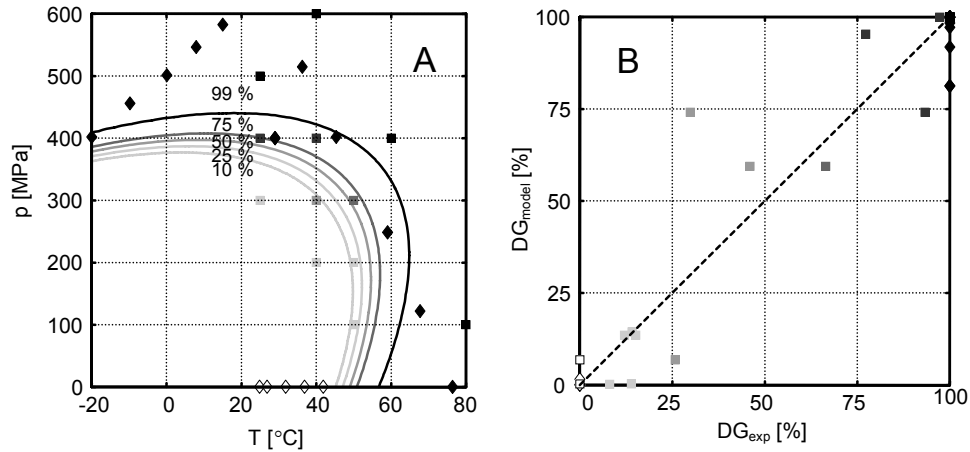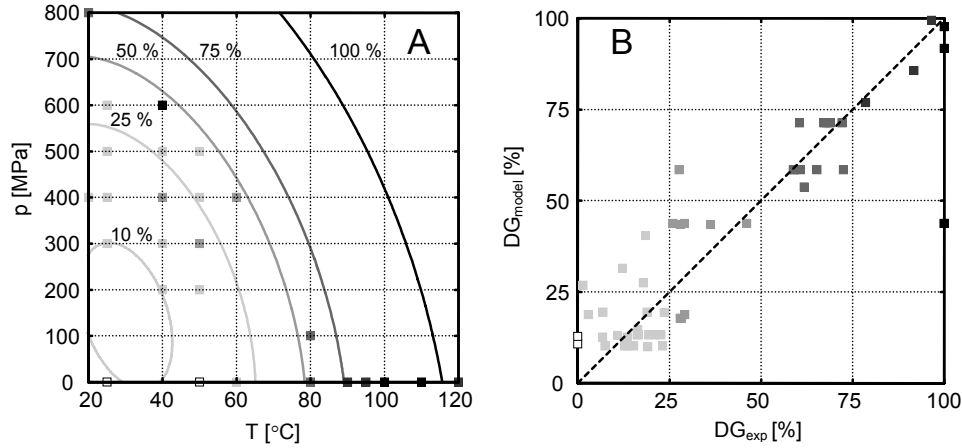
Figure 6: Degree of starch gelatinisation as function of temperature and pressure obtained with experiments and calculations (Figure A) and comparison of calculated values (DG$_{model}$) with experimental values (DG$_{exp}$) in parity plot (Figure B) for 60 w/w % wheat starch-water mixtures. The experimental data is depicted with: □: DG = 0 %; ■: 0 %< DG ≤ 25 %; ■: 25 % < DG ≤ 50 %; ■: 50 % < DG ≤ 75 %; ■: 75 % < DG < 100 %; ■: DG = 100 %. The model data (obtained with equation 6 inserted into equation 7 and parameters from Table 4) shown in Figure A are depicted with the solid lines and the index represents the degree of hydrolysis.

Table 4: Parameters for description of the degree of gelatinisation as function of the pressure and temperature (equation 6 inserted into equation 7).

C_s	[w/w %]	5	30	60
$\Delta G(P_r, T_r)$ [a]	$[10^3 \text{ J·mol}^{-1}]$	-7.88 ± 4.13	-1.05 ± 1.23	3.99 ± 1.35
$\Delta S(P_r, T_r)$ [a]	$[10^2 \text{ J·mol}^{-1}\text{·K}^{-1}]$	4.63 ± 3.75	2.79 ± 1.26	0.97 ± 0.68
$\Delta V(P_r, T_r)$ [a]	$[10^{-4} \text{ m}^3\text{·mol}^{-1}]$	-1.78 ± 0.89	-0.42 ± 0.15	-0.13 ± 0.05
$\Delta \alpha$ [a]	$[10^{-6} \text{ m}^3\text{·mol}^{-1}\text{·K}^{-1}]$	2.45 ± 4.48	-0.32 ± 0.93	-0.19 ± 0.55
$\Delta \beta$ [a]	$[10^{-12} \text{ m}^6\text{·mol}^{-1}\text{·J}^{-1}]$	-0.62 ± 0.55	-0.06 ± 0.12	-0.04 ± 0.05
ΔC_p [a]	$[10^4 \text{ J·mol}^{-1}\text{·K}^{-1}]$	0.47 ± 0.45	1.22 ± 0.49	0.21 ± 0.25

[a] 95 % confidence interval.

Phase diagram for the gelatinisation of starch

The pressures and temperatures required to obtain a degree of gelatinisation equal to 10 and 99.99 % for 5, 30, and 60 w/w % starch-water mixtures are depicted in *Figure 7*. This figure shows that the conditions required to obtain a degree of gelatinisation that is equal to 10 % were relatively close together irrespective of the starch-water ratio. However, the pressure and temperature required for complete gelatinisation increased as the starch

concentration was increased and these conditions differ significantly for different starch concentrations.
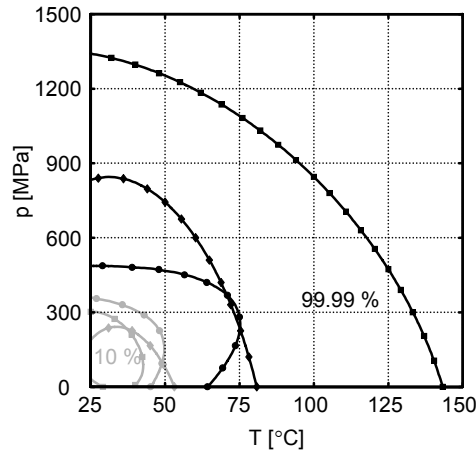
Figure 7: Degree of starch gelatinisation (black: 99.99 % gelatinisation and gray: 10 % gelatinisation) as function of temperature, pressure, and starch-water ratio (5 w/w %: ●, 30 w/w %: ◆, 60 w/w %: ■). Values based on model calculations with parameters from Table 4 used in equation 6 inserted into equation 7.

Discussion

Effect of treatment time on the degree of gelatinisation

When 30 and 60 w/w % starch-water mixtures were held at 400 MPa and 20 °C, the time required to reach 95 % of the equilibrium value was lower for a 60 w/w % starch-water mixture than for a 30 w/w % starch-water mixture. If the gelatinisation rate is independent of the starch concentration, the time required to reach an equilibrium value would be the same because gelatinisation was assumed to be a first order process (equations 8A and 8B). However, different times were observed indicating that the gelatinisation rate depends on concentration. One would expect that a higher concentration leads to a lower gelatinisation rate due to an increased viscosity, which leads to a lower mobility of the carbohydrate chains and a lower diffusion rate of water. Nevertheless, we found that a lower starch concentration results in a longer time required to reach an equilibrium value for the degree of gelatinisation.

The experiments, in which the degree of gelatinisation was followed as function of time, showed that in most cases the time required to reach an equilibrium value was less than 2 min. In some cases, this time was much longer. When 5 w/w % wheat starch

suspensions were kept at 29 °C and different pressures, Bauer and Knorr (2005) found that in some cases the time required to reach steady state was long, but that it could be decreased by increasing the pressure (a decrease in t_e from 240 to 30 min when the pressure was increased from 250 to 400 MPa). Our results have also indicated that at constant temperature, a pressure increase resulted in a rapid decrease in the time required to reach equilibrium.

Effect of temperature on the degree of gelatinisation

When equilibrium values are used, the experimental degree of gelatinisation vs. temperature curves can be described with equation 4 leading to sigmoidal curves, both at atmospheric pressure (*Figure 2*) and at higher pressures (results not shown). The sigmoidal shape of these gelatinisation curves was also observed by Thevelein *et al.* (1981) and Muhr and Blanshard (1982). In a previous article (Baks *et al.*, 2007), we observed that the degree of gelatinisation of starch as a function of temperature for 10 and 60 w/w % wheat starch-water mixtures at 0.1 MPa could also be described with an adapted version of the Flory equation. Both the output values of the adapted Flory equation and equation 4 agree well with the experimental values.

Experimental data, both our own and from Randzio *et al.* (2002), showed that at 40 °C and 0.1 MPa the degree of gelatinisation is very low for all starch-water mixtures. This results in low K_r values when fitting the model data to the experimental data. The $\Delta H(P_r, T_r)$ values that were obtained after fitting (*Table 2*) seem to decrease when the starch concentration was increased. Randzio *et al.* (2002) and Eliasson (1980) also observed that $\Delta H(P_r, T_r)$ decreased when the starch concentration was increased at 0.1 MPa.

Effect of pressure on the degree of gelatinisation

Similar to the degree of gelatinisation as function of temperature, the degree of gelatinisation as function of pressure for several different starch-water ratios at 40 °C could be described by sigmoidal curves (*Figure 3*). Similar shaped gelatinisation curves were also observed by others (Stute *et al.*, 1996; Bauer and Knorr, 2005).

Equation 5 is based on two parameters ($\Delta V(P_r, T_r)$ and K_r) for each starch concentration (*Table* 3). According to our experimental data (*Figure 3A*), the degree of gelatinisation increases with an increasing starch concentration at 400 MPa and 25 °C, which is also reflected by the K_r values obtained after fitting. According to the experimental data of Kawai *et al.* (2007) (*Figure 3*), the degree of gelatinisation is approximately zero at 400

MPa and 40 °C for all potato starch-water mixtures. As a result, low K_r values are obtained (see *Table 3*).

The $\Delta V(P_r, T_r)$ values for wheat starch and potato starch shown in *Table 3* have the same order of magnitude. This table also shows that the $\Delta V(P_r, T_r)$ values are negative, which can be explained by considering the results of Douzals *et al.* (1996). They also found that the total suspension volume of wheat starch suspensions decreased during high pressure gelatinisation (16 w/w % wheat starch in water). In addition, they observed that the granule size increased as a result of the uptake of water. Consequently, they concluded that water molecules linked with starch occupy a smaller volume than water molecules in pure water. As a result, the negative $\Delta V(P_r, T_r)$ values can be explained by considering the role of water during gelatinisation. At pressures equal to or above 272 MPa and temperatures close to 65 °C, Muhr *et al.* (1982) also found that $\Delta V(P_r, T_r)$ is negative. When the starch concentration is increased, $\Delta V(P_r, T_r)$ increases (see *Table 3*). This implies that the molar volume of native starch and the molar volume of gelatinised starch start to resemble each other more and more when the starch concentration is increased. Perhaps the limited amount of water prevents the starch granule from swelling, leading to a more compact amorphous phase after gelatinisation. The $\Delta V(P_r, T_r)$ value at 60 w/w % deviates from the described trend. However, this value is less reliable, since it is based on measurements at too low pressures.

Degree of gelatinisation vs. T and p for 5, 30, and 60 w/w % starch-water mixtures
Phase diagrams for biopolymers in the pressure-temperature plane often have an elliptic shape (Hawley, 1971; Heremans and Smeller, 1998; Smeller, 2002). The elliptic shapes in our phase diagram (*Figure* 4A) are similar to the shape of other phase diagrams for starch gelatinisation in 5 w/w % wheat starch-water mixtures (Bauer and Knorr, 2005; Knorr *et al.*, 2006). The phase diagram of the group of Knorr (Bauer and Knorr, 2005; Douzals *et al.*, 2001; Knorr *et al.*, 2006) gives the pressure and temperature that is required to reach complete gelatinisation after 15 min of treatment. These equilibrium measurements agree well with our phase diagram. The phase diagram of Douzals *et al.* (2001) shows the pressure and temperature that leads to 10, 50, and 100 % gelatinisation after a treatment time of 15 min. Their data deviate from the model data in our phase diagrams and these deviations cannot be explained by assuming that equilibrium was not reached. Douzals *et al.* (2001) have predominantly used birefringence measurements, which lead to an overestimation of the degree of gelatinisation in comparison with DSC measurements (Douzals *et al.*, 2001). DSC measurements might have showed that higher temperatures and

pressures would be required to reach 10 and 50 % gelatinisation, which would lead to better agreement between the data of Douzals *et al.* (2001) and our own data at 10 % gelatinisation. However, in case of 100 % gelatinisation the differences would increase.

In case of concentrated starch-water mixtures, measurements of the degree of gelatinisation at a large number of pressure-temperature combinations are not available in literature. Muhr *et al.* (1982) found that the temperatures required to completely gelatinise starch in 33 w/w % wheat starch-water mixtures were close to 65 °C between 0.1 and 329 MPa. Their measurements agree with the phase diagram shown in *Figure 5* in that region.

The degree of gelatinisation vs. temperature curve and degree of gelatinisation vs. pressure curve could be described with respectively equation 4 and equation 5. Based on these results, it is expected that ΔC_p and $\Delta \beta$ in equation 6 are close or equal to zero, because that would result in a similar pressure and temperature dependency of equation 7 after insertion of equation 6. After removal of the second order pressure and temperature terms in equation 6, however, the model values calculated with equation 7 could not be fitted to the experimental values. It seems that the assumptions that the enthalpy (or entropy) and molar volume are not dependent on pressure and temperature (resulting in the second order pressure and temperature terms) are not valid when both the pressure and temperature dependency are taken into account. For that reason, higher order terms in equation 6 seem to be of importance.

Knorr *et al.* (2006) and Rubens and Heremans (2000) also used equation 6 combined with equation 7 to calculate the degree of gelatinisation as function of pressure and temperature. Rubens and Heremans (2000) fitted the model values to the experimental data at which 50 % gelatinisation was observed. We have used their values of $\Delta G(P_r,T_r)$, $\Delta V(P_r,T_r)$, $\Delta H(P_r,T_r)$, $\Delta \alpha$, $\Delta \beta$, and ΔC_p to calculate the degree of gelatinization as function of pressure and temperature. These calculations showed that a hyperbolic phase diagram would appear instead of the expected elliptical phase diagram. A phase diagram with a hyperbolic shape suggests that at higher pressures and temperatures recrystallisation can occur again, which is unlikely. Knorr *et al.* (2006) did not focus on the model for the description of the degree of gelatinisation and the values of $\Delta G(P_r,T_r)$, $\Delta V(P_r,T_r)$, $\Delta H(P_r,T_r)$, $\Delta \alpha$, $\Delta \beta$, and ΔC_p were not given. Unfortunately, the experimental data was not shown together with the values calculated with the model. For that reason, it is not possible to determine whether their model values lead to an accurate prediction.

The $\Delta V(P_r,T_r)$ values in *Table 4* cannot be compared directly with the values in *Table 3*, because in case of wheat starch a different reference temperature was used and in case of

potato starch the difference in starch species might cause differences. However, the order of magnitude of $\Delta V(P_r,T_r)$ for wheat and potato starch at the same reference temperature is expected to be the same and this is confirmed by our data. With use of $\Delta G(P_r,T_r)$ (*Table 4*), $\Delta S(P_r,T_r)$ (*Table* 4), and T_r, $\Delta H(P_r,T_r)$ can be calculated (137, 86, and 34 kJ·mol^{-1} for respectively 5, 30, 60 w/w % starch in water). These values are higher than the values obtained with equation 4 (*Table 2*), but the order of magnitude is comparable.

It is not possible to determine the quantitative relationship between the starch concentration and the parameters $\Delta G(P_r,T_r)$, $\Delta V(P_r,T_r)$, $\Delta S(P_r,T_r)$, $\Delta \alpha$, $\Delta \beta$, and ΔC_p, because we have measured at a limited number of starch concentrations . However, it can be established how these parameters are affected by the starch concentration in a qualitative manner. At the reference pressure and temperature (40 °C and 400 MPa), the standard Gibbs energy change of reaction increases with an increasing starch concentration. This trend implies that the degree of gelatinisation decreases with an increasing starch concentration (equation 1), which is in accordance with the results shown in *Figure 3*. At the reference conditions, the standard volume change of reaction $\Delta V(P_r,T_r)$ is negative for all starch-water ratios and increases with an increasing starch concentration, which is in accordance with the results shown in *Table 3*. At 40 °C and 400 MPa, the standard entropy change of reaction decreases with an increasing starch-water ratio. At higher starch concentrations, the standard isothermal compressibility change of reaction increases with an increasing starch concentration. Such a change in $\Delta \beta$ implies that the volume change during the reaction decreases as a result of an increasing pressure, but the decrease in the volume change during the reaction is less for more concentrated starch-water mixtures. In case of ΔC_p and $\Delta \alpha$, the effect of the starch concentration could not be established.

Some assumptions were implicitly made by using the equilibrium equation defined in equation 1 to keep the model equation as simple as possible and to make a comparison with other literature sources possible (Knorr *et al.*, 2006; Rubens and Heremans, 2000). Firstly, it was assumed that water is an inert component during the gelatinisation reaction. However, water affects starch gelatinisation and the distribution of water in the granules changes during gelatinisation (Tananuwong and Reid, 2004; Tang *et al.*, 2001). Water should therefore be taken into account, for example by including the concentration of unbound water in the nominator and the concentration of water attached to starch in the denominator. Another assumption is that the activity coefficients of native starch and gelatinised starch are either approximately equal or constant with varying temperature, pressure, and composition. Consequently, their contribution in the apparent equilibrium

constant can be neglected. Implicitly, this assumption has also been made by several others (Hawley *et al.*, 1971; Knorr *et al.*, 2006; Rubens and Heremans, 2000). In reality, however, the activity coefficients might change during gelatinisation as a result of varying fractions of native and gelatinised starch, temperature, and pressure (the effects of these changes are unknown).

Phase diagram for the gelatinisation of starch

According to *Figures 2-7*, the onset conditions for gelatinisation are close together for all wheat starch-water mixtures, while the pressures and temperatures required for complete gelatinisation differ significantly in most cases. These observations might be explained by considering the following theories. Jenkins *et al.* (1994) have proposed a scheme for the starch granule structure. According to them, starch granules consist of alternating amorphous and semi-crystalline growth rings. These semi-crystalline growth rings consist of amorphous and crystalline lamellae. These crystalline lamellae consist of double helices of amylopectin side chains that are ordered side by side. According to Jenkins *et al.* (1998) and Waigh *et al.* (2000), gelatinisation in excess water starts with the uptake of water by the amorphous growth rings resulting in a size expansion. The uptake of water can either be achieved by increasing the temperature or by increasing the pressure according to Rubens and Heremans (2000). Because the granule consists of an alternating system of amorphous and semi-crystalline growth rings, uptake of water by the amorphous growth rings results in disruption of the semi-crystalline growth rings, which leads to a reduction of the granule's crystallinity. When the amount of water is limiting, the swelling capability of the granule is reduced. Consequently, only part of the crystallinity is lost by the swelling process as the amount of water is insufficient to permit full swelling and disruption of the crystalline phase. However, up to the point where water becomes a limiting factor, the process that causes the reduction in crystallinity is the same. As a result, the same onset conditions are observed for gelatinsation at all starch-water ratios. In case the amount of water is insufficient to remove all crystallinity by swelling, the remaining crystallinity caused by the presence of double helices can only be lost by increasing the temperature. An increase in temperature results in an increased thermal energy of the amylopectin double helices and therefore sufficient mobility of these double helices to unwind (Waigh *et al.*, 2000).

When the starch concentration is increased at the reference temperature during high pressure gelatinisation, the volume change during gelatinisation was less negative whilst the ΔC_p values were positive in all cases (see *Table 4*). At higher starch concentrations, the amount of water linked to starch is lower. Because water linked to starch seems to occupy a

smaller volume than water surrounded by itself (Douzals *et al.*, 1996), a less negative volume change at higher starch concentrations can be explained by the lower amount of water that is available during gelatinisation. As a result, a higher pressure is required to reach the same degree of gelatinisation at high starch concentrations (equations 6 and 7).

As shown in the previous paragraphs, the gelatinisation diagrams for 5, 30, and 60 w/w % starch-water mixtures agree with the experimental data. For those reasons, the combined gelatinisation diagrams (*Figure 7*), or the model equations that were used to construct them, can be used to predict the degree of gelatinisation as a function of pressure and temperature for 5, 30, and 60 w/w % starch-water mixtures. Moreover, the pressures and temperatures required to gelatinise starch-water mixtures with a concentration between 5 and 60 w/w %, can be roughly estimated with use of *Figure 7*.

Conclusions

The results in this article confirmed earlier findings that the degree of gelatinisation depends on temperature, pressure, starch concentration, and treatment time. The time course experiments showed that after a certain treatment time the degree of gelatinisation became constant. In many cases, the time required to reach an equilibrium value was less than 5 min. In some other cases, this time was much larger, but always shorter than one hour. For that reason, the degree of starch gelatinisation values of starch-water mixtures that were held at a certain temperature and pressure for 60 min were assumed to be at equilibrium. In general, an increase in the pressure or temperature results in a shorter time to reach an equilibrium value for the degree of gelatinisation.

Sigmoidal curves were obtained when the degree of gelatinisation was plotted as function of temperature or pressure for different starch concentrations. Simple model equations (equation 4 for temperature dependency and equation 5 for pressure dependency) could be used to describe these curves.

Phase diagrams that relate the degree of gelatinisation for 5, 30, and 60 w/w % wheat starch-water mixtures to both pressure and temperature were obtained. The experimental data for 5 w/w % starch-water mixtures agree with the existing literature data. The experimental data for mixtures with 30 and 60 w/w % starch content extend the knowledge for the gelatinisation behaviour at higher concentrations.

The simple models could not be used to describe the degree of gelatinisation as function of both pressure and temperature. Therefore, a model based on the Gibbs free energy difference was used. The values of the parameters in this model, $\Delta G(P_r, T_r)$,

$\Delta V(P_r, T_r)$, $\Delta\alpha$, $\Delta\beta$, and ΔC_p, seem to comply with general theory. In addition, the effect of the starch concentration on $\Delta G(P_r, T_r)$, $\Delta V(P_r, T_r)$, $\Delta S(P_r, T_r)$, and $\Delta\beta$ could be established in a qualitative manner. Both the pressure-temperature plots and the parity plots show that the model data agree well with the experimental values.

The model data of 5, 30, and 60 w/w % wheat starch-water mixtures were combined to construct a phase diagram that shows the effect of pressure, temperature and concentration on the degree of gelatinisation over a broad range of experimental conditions. Such a phase diagram can be used to estimate the degree of gelatinisation after applying a certain pressure and temperature on a starch-water mixture with starch concentrations somewhere in between 5 and 60 w/w %.

Acknowledgements

References

Atkins PW. 1997. Physical Chemistry. Oxford: Oxford University Press. 1031 p.

Baks T, Ngene IS, Van Soest JJG, Janssen AEM, Boom RM. 2007. Comparison of methods to determine the degree of gelatinisation for both high and low starch concentrations. Carbohydr Polym 67:481-490.

Bauer BA, Knorr D. 2004. Electrical conductivity: a new tool for the determination of high hydrostatic pressure-induced starch gelatinisation. Innov Food Sci Emerg Technol 5:437-442.

Bauer BA, Knorr D. 2005. The impact of pressure, temperature and treatment time on starches: Pressure-induced starch gelatinisation as pressure time temperature integrator for high hydrostatic pressure processing. J Food Eng 68:329-334.

Burt DJ, Russell PL. 1983. Gelatinization of low water content wheat starch-water mixtures. A combined study by differential scanning calorimetry and light microscopy. Starch/Stärke 35:354-360.

Cooke D, Gidley MJ. 1992. Loss of crystalline and molecular order during starch gelatinisation: origin of the enthalpic transition. Carbohydr Res 227:103-112.

Donovan JW. 1979. Phase transitions of the starch-water system. Biopolymers 18:263-275.

Donovan JW, Lorenz K, Kulp K. 1983. Differential scanning calorimetry of heat-moisture treatment of starches. Cereal Chem 60:381-387.

Donovan JW, Mapes CJ. 1980. Mutiple phase transitions of starches and nägeli amylodextrins. Starch/Stärke 32:190-193.

Douzals JP, Perrier-Cornet JM, Gervais P, Coquille JC. 1998. High-pressure gelatinization of wheat starch and properties of pressure-induced gels. J Agric Food Chem 46:4824-4829.

Douzals JP, Coquille JC, Gervais P, Perrier-Cornet JM. 2001. Pressure-temperature phase transition diagram for wheat starch. J Agric Food Chem 49:873-876.

Douzals JP, Marechal PA, Coquille JC, Gervais P. 1996. Microscopic study of starch gelatinization under high hydrostatic pressure. J Agric Food Chem 44:1403-1408.

Eliasson A-C. 1980. Effect of water content on the gelatinization of wheat starch. Starch/Stärke 32:270-272.

Hawley SA. 1971. Reversible pressure–temperature denaturation of chymotrypsinogen. Biochemistry 10:2436-2442.

Heremans K, Smeller L. 1998. Protein structure and dynamics at high pressure. Biochim Biophys Acta 1386:353-370.

Jenkins PJ, Cameron RE, Donald AM, Bras W, Derbyshire GE, Mant GR, Ryan AJJ. 1994. In situ simultaneous small and wide angle x-ray scattering: a new technique to study starch gelatinization. Polym Sci Part B: Polym Phys 32:1579-1583.

Jenkins PJ, Donald AM. 1998. Gelation of starch: a combined SAXS/WAXS/DSC and SANS study. Carbohydr Res 308:133-147.

Katopo H, Song Y, Jane J-L. 2002. Effect and mechanism of ultrahigh hydrostatic pressure on the structure and properties of starches. Carbohydr Polym 47:233-244.

Kawai K, Fukami K, Yamamoto K. 2007. Effect and mechanism of ultrahigh hydrostatic pressure on the structure and properties of starches. Carbohydr Polym 67:530-535.

Knorr D, Heinz V, Buckow R. 2006. High pressure application for food biopolymers. Biochim Biophys Acta 1764:619-631.

Liu H, Lelievre JA. 1993. model of starch gelatinization linking differential scanning calorimetry and birefringence measurements. Carbohydr Polym 20:1-5.

Lund D. 1984. Influence of time, temperature, moisture, ingredients, and processing conditions on starch gelatinization. Crit Rev Food Sci Nutr 20:249-273.

Muhr AH, Blanshard JMV. 1982. Effect of hydrostatic pressure on gelatinisation of starch. Carbohydr Polym 2:61-74.

Muhr AH, Wetton RE, Blanshard JMV. 1982. Effect of hydrostatic pressure on starch gelatinisation, as determined by DTA. Carbohydr Polym 2:91-102.

Parker R, Ring SG. 2001. Aspects of the physical chemistry of starch. J Cereal Sci 34:1-17.

Randzio SL, Flis-Kabulska I, Grollier J-PE. 2002. Reexamination of phase transformations in the starch-water system. Macromolecules 35:8852-8859.

Rubens P, Heremans K. 2000. Pressure-temperature gelatinization phase diagram of starch: an in situ fourier transform infrared study. Biopolymers 54:524-530.

Russell PL. 1987. Gelatinization of starches of different amylose/amylopectin content. A study by differential scanning calorimetry. Starch/Stärke 6:133-145.

Smeller L. 2002. Pressure-temperature phase diagrams of biomolecules Biochim Biophys Acta 1595:11-29.

Appendix: derivation of equation 6

The equilibrium constant is defined by the following equation (Smith *et al.*, 1996):

$$\prod_i (a_i)^{v_i} = \frac{\sum_i v_i G_i (P_r)}{RT} \equiv K \tag{A1}$$

In case a parameter was evaluated at a certain reference pressure and/or temperature, the reference pressure and/or temperature is mentioned in between brackets behind the symbol of the parameter. The equilibrium constant can be related to the Gibbs energy change of reaction at the reference pressure (Smith *et al.*, 1996):

$$-RTlnK = \sum_i v_i G_i (P_r) \equiv \Delta G (P_r) \tag{A2}$$

Other property changes of reaction are defined in a similar fashion as the Gibbs energy change of reaction at the reference pressure (Smith *et al.*, 1996):

$$\Delta M (P_r) = \sum_i v_i M_i (P_r) \tag{A3}$$

The activity of species *i* in a solution mentioned in equation A1 is defined as follows (Smith *et al.*, 1996):

$$a_i = \frac{\hat{f}_i}{f(P_r)} = \gamma_i x_i \frac{f_i}{f_i(P_r)} \tag{A4}$$

In the part below, a relationship is derived that can be substituted in equation A4 for $f_i/f_i(P_r)$. For the Gibbs energy of a real fluid, the following equation is valid (Smith *et al.*, 1996):

$$G_i \equiv \Gamma_i (T) + RT \cdot ln (f_i) \tag{A5}$$

This equation can be written twice, first for a pure liquid i at temperature T and pressure P, and second for pure liquid i at the same temperature but at standard-state pressure. After taking the difference of these equations, the following result is obtained (Smith *et al.*, 1996):

$$G_i - G_i\left(P_r\right) = RT \cdot ln \frac{f_i}{f_i\left(P_r\right)} \tag{A6}$$

The difference $G_i - G_i(P_r)$ can also be derived starting from the following equation (Smith *et al.*, 1996):

$$dG = V\,dP - S\,dT \tag{A7}$$

At constant temperature, equation A7 can be integrated leading to the following equation:

$$G_i\left(P\right) - G_i\left(P_r\right) = \int_{P_r}^{P} V_i dP \tag{A8}$$

Note that $G_i(P)$ and $G_i(P_r)$ are considered at the same temperature and for that reason dT is zero. If we assume that V_i does not depend on pressure ($V_i\left(P\right) = V_i(P_r)$), A8 can be solved leading to:

$$G_i - G_i\left(P_r\right) = V_i\left(P_r\right) \cdot \left(P - P_r\right) \tag{A9}$$

Combination of equation A6 with A9 leads to:

$$RT \cdot ln \frac{f_i}{f_i\left(P_r\right)} = V_i\left(P_r\right) \cdot \left(P - P_r\right) \tag{A10}$$

Combining equation A10 with equation A4 leads to equation A11:

$$a_i = \frac{\hat{f}_i}{f_i\left(P_r\right)} = \frac{\gamma_i x_i f_i}{f_i\left(P_r\right)} = \gamma_i x_i \left(exp\left[\frac{V_i\left(P_r\right) \cdot \left(P - P_r\right)}{RT} \right] \right) \tag{A11}$$

Equation A11 can be used to substitute the activity of species i in equation A1:

$$K = \left[\prod_i \left(\gamma_i x_i\right)^{\nu_i} \right] \cdot exp\left[\frac{1}{RT} \sum_i \nu_i V_i\left(P_r\right) \cdot \left(P - P_r\right) \right] \tag{A12}$$

Application of equation A3 results in equation A13:

$$K = \left[\prod_i \left(\gamma_i x_i\right)^{\nu_i} \right] \cdot exp\left[\frac{\left(P - P_r\right) \cdot \Delta V\left(P_r\right)}{RT} \right] \tag{A13}$$

We can now define an alternative equilibrium constant K' in the following manner:

$$K' = \prod_i \left(\gamma_i x_i\right)^{\nu_i} \tag{A14}$$

Combining equation A13, A14 and A2 results in:

$$K' = exp\left[-\frac{\Delta G(P_r)}{RT} - \frac{(P\text{-}P_r)\cdot\Delta V(P_r)}{RT} \right] \tag{A15}$$

An equation for the pressure dependency of the equilibrium constant K' can now be obtained after differentation of equation A15 with respect to the pressure at constant temperature:

$$\left(\frac{\partial lnK'}{\partial P}\right)_T = \left(\frac{\partial}{\partial P}\left[-\frac{\Delta G(P_r)}{RT} - \frac{(P\text{-}P_r)\cdot\Delta V(P_r)}{RT} \right]\right)_T = -\frac{\Delta V(P_r)}{RT} \tag{A16}$$

In the vicinity of the reference pressure, the exponential term in equation A13 is close to unity and may be omitted ($K \approx K'$). The temperature dependency of the equilibrium constant K (and at low pressures K') is depicted by the following equation (Smith *et al.*, 1996):

$$\left(\frac{\partial lnK'}{\partial T}\right)_P = \frac{\partial}{\partial T}\left[-\frac{\Delta G(P_r)}{RT} \right]_P = \frac{\partial}{\partial T}\left[-\frac{\Delta H(P_r)}{RT} + \frac{T\cdot\Delta S(P_r)}{RT} \right]_P = \frac{\Delta H(P_r)}{RT^2} \tag{A17}$$

However, when high pressures are applied, the temperature and pressure dependency of V_i should be taken into account. The following procedure is used to derive an equation for:

$$dV_i = \left(\frac{\partial V_i}{\partial T}\right)_P dT + \left(\frac{\partial V_i}{\partial P}\right)_T dP = \alpha_i dT + \beta_i dP \tag{A18.A}$$

$$V_i = V_i(P_r,T_r) + \alpha_i(T\text{-}T_r) + \beta_i(P\text{-}P_r) \tag{A18.B}$$

Note that it is assumed that α_i and β_i are constants independent of temperature and pressure. Insertion of equation A18.B in A8 followed by integration from P_r to P, leads to:

$$G_i - G_i(P_r) = V_i(P_r,T_r)\cdot(P\text{-}P_r) + \alpha_i(T\text{-}T_r)(P\text{-}P_r) + \frac{\beta_i}{2}(P\text{-}P_r)^2 \tag{A19}$$

Substitution of equation A19 into equation A6 leads to an equation for $f_i/f_i(P_r)$:

$$\frac{f_i}{f_i(P_r)} = exp\left(\frac{1}{RT}\int_{P_r}^{P} V_i dP \right)$$

$$= exp\left(\frac{V_i(P_r)\cdot(P\text{-}P_r) + \alpha_i(T\text{-}T_r)(P\text{-}P_r) + \frac{\beta_i}{2}(P\text{-}P_r)^2}{RT} \right) \tag{A20}$$

Insertion of equation A20 into equation A4 leads to equation A21:

$$a_i = \frac{\hat{f}_i}{f_i(P_r)} = \frac{\gamma_i x_i f_i}{f_i(P_r)}$$

$$= \gamma_i x_i \left(exp \left[\frac{V_i(P_r) \cdot (P\text{-}P_r) + \alpha_i (T\text{-}T_r)(P\text{-}P_r) + \frac{\beta_i}{2}(P\text{-}P_r)^2}{RT} \right] \right) \tag{A21}$$

Equation A21 can be used to substitute the activity of species i in equation A1:

$$K = \left[\prod_i \left[\gamma_i x_i \right]^{v_i} \right]$$

$$\cdot exp \left[\frac{1}{RT} \sum_i v_i \left(V_i(P_r) \cdot (P\text{-}P_r) + \alpha_i (T\text{-}T_r)(P\text{-}P_r) + \frac{\beta_i}{2}(P\text{-}P_r)^2 \right) \right] \tag{A22}$$

Rearrangement leads to:

$$K = \left[\prod_i (\gamma_i x_i)^{v_i} \right]$$

$$\cdot exp \left[\frac{(P\text{-}P_r)}{RT} \sum_i v_i V_i(P_r, T_r) + \frac{(T\text{-}T_r)(P\text{-}P_r)}{RT} \sum_i v_i \alpha_i + \frac{(P\text{-}P_r)^2}{2RT} \sum_i v_i \beta_i \right] \tag{A23}$$

Taking into account equation A3 leads to:

$$K = \left[\prod_i (\gamma_i x_i)^{v_i} \right] \cdot exp \left[\frac{(P\text{-}P_r)}{RT} \Delta V(P_r, T_r) + \frac{(T\text{-}T_r)(P\text{-}P_r)}{RT} \Delta\alpha + \frac{(P\text{-}P_r)^2}{2RT} \Delta\beta \right] \tag{A24}$$

At the reference pressure, the Gibbs energy change of reaction can be related to the enthalpy change of reaction, the entropy change of reaction, and temperature in the following manner:

$$\Delta G(P_r) = \Delta H(P_r) - T \cdot \Delta S(P_r) \tag{A25}$$

The standard enthalpy change of reaction can be calculated relative to a known reference point:

$$\Delta H(P_r) = \Delta H(P_r, T_r) + R \int_{T_r}^{T} \frac{\Delta C_p}{R} dT \tag{A26}$$

Similarly, the standard entropy change of reaction can be calculated relative to a known reference point:

$$\Delta S\left(P_r\right) = \Delta S\left(P_r, T_r\right) + R\int_{T_r}^{T}\frac{\Delta C_p}{R}\frac{dT}{T} \tag{A27}$$

Insertion of equations A26 and A27 into A25 and substitution of $\Delta H(P_r, T_r) = \Delta G(P_r, T_r) + T_r\cdot\Delta S(P_r, T_r)$ results in:

$$\Delta G\left(P_r\right) = \Delta G\left(P_r, T_r\right) + T_r\cdot\Delta S\left(P_r, T_r\right) + R\int_{T_r}^{T}\frac{\Delta C_p}{R}\,dT$$
$$- T\left[\Delta S\left(P_r, T_r\right) + R\int_{T_r}^{T}\frac{\Delta C_p}{R}\frac{dT}{T}\right] \tag{A28}$$

Insertion of A24 and A28 into equation A2 leads to the following equation:

$$-RTln\left(\left[\prod_i\left(\gamma_i x_i\right)^{v_i}\right]\cdot exp\left[\frac{\left(P\text{-}P_r\right)}{RT}\Delta V\left(P_r, T_r\right) + \frac{\left(T\text{-}T_r\right)\left(P\text{-}P_r\right)}{RT}\Delta\alpha + \frac{\left(P\text{-}P_r\right)^2}{2RT}\Delta\beta\right]\right) =$$
$$\Delta G\left(P_r, T_r\right) + T_r\cdot\Delta S\left(P_r, T_r\right) + R\int_{T_r}^{T}\frac{\Delta C_p}{R}dT - T\left[\Delta S\left(P_r, T_r\right) + R\int_{T_r}^{T}\frac{\Delta C_p}{R}\frac{dT}{T}\right] \tag{A29}$$

Rearrangement results in:

$$-RTln\left(\prod_i\left(\gamma_i x_i\right)^{v_i}\right) =$$
$$\Delta G\left(P_r, T_r\right) - \Delta S\left(P_r, T_r\right)\cdot\left(T\text{-}T_r\right) + \int_{T_r}^{T}\Delta C_p dT - T\int_{T_r}^{T}\Delta C_p\frac{dT}{T} \tag{A30}$$
$$+ \Delta V\left(P_r, T_r\right)\cdot\left(P\text{-}P_r\right) + \Delta\alpha\left(T\text{-}T_r\right)\left(P\text{-}P_r\right) + \frac{\Delta\beta}{2}\left(P\text{-}P_r\right)^2$$

After assuming that ΔC_p is independent of pressure and temperature, the following equation is obtained:

$$-RTln\left(\prod_i\left(\gamma_i x_i\right)^{v_i}\right) =$$
$$\Delta G\left(P_r, T_r\right) - \Delta S\left(P_r, T_r\right)\cdot\left(T\text{-}T_r\right) - \Delta C_p\left(T\left(ln\frac{T}{T_r} - 1\right) + T_r\right) \tag{A31}$$
$$+ \Delta V\left(P_r, T_r\right)\cdot\left(P\text{-}P_r\right) + \Delta\alpha\left(T\text{-}T_r\right)\left(P\text{-}P_r\right) + \frac{\Delta\beta}{2}\left(P\text{-}P_r\right)^2$$

In the vicinity of T_r, equation A31 can be simplified (Hawley, 1971):

$$\Delta C_p \left[T \left(ln\frac{T}{T_r} - 1 \right) + T_r \right] \approx \frac{\Delta C_p}{2T_r} \left(T\text{-}T_r \right)^2 \tag{A32}$$

After insertion of equation A32 in equation A31, the following equation is obtained:

$$-RTln\left(\prod_i \left(\gamma_i x_i \right)^{\nu_i} \right) =$$

$$\Delta G\left(P_r, T_r \right) - \Delta S\left(P_r, T \right) \cdot \left(T\text{-}T_r \right) - \frac{\Delta C_p}{2T_r} \left(T\text{-}T_r \right)^2 \tag{A33}$$

$$+ \Delta V\left(P_r, T_r \right) \cdot \left(P\text{-}P_r \right) + \Delta\alpha\left(T\text{-}T_r \right)\left(P\text{-}P_r \right) + \frac{\Delta\beta}{2}\left(P\text{-}P_r \right)^2$$

When $\Delta\beta$ and ΔC_p have opposite signs, this equation results in an elliptic paraboloid. The cross section in the pressure-temperature plane of such an elliptic paraboloid results in the characteristic elliptic phase diagrams that have been observed for several proteins (Heremans and Smeller, 1998). Insertion of equation A14 in equation A33 leads to:

$$-RTlnK' = \Delta G\left(P_r, T_r \right) - S\left(P_r, T_r \right) \cdot \left(T\text{-}T_r \right) - \frac{\Delta C_p}{2T_r} \left(T\text{-}T_r \right)^2$$

$$+ \Delta V\left(P_r, T_r \right) \cdot \left(P\text{-}P_r \right) + \Delta\alpha\left(T\text{-}T_r \right) \cdot \left(P\text{-}P_r \right) + \frac{\Delta\beta}{2}\left(P\text{-}P_r \right)^2 \tag{A34}$$

Comparison of equation A34 with equation A2, shows that the right term in equation A34 is equal to the Gibbs energy of reaction (but not the standard Gibbs energy change of reaction):

$$\Delta G = \Delta G\left(P_r, T_r \right) - \Delta S\left(P_r, T_r \right) \cdot \left(T\text{-}T_r \right) - \frac{\Delta C_p}{2T_r} \left(T\text{-}T_r \right)^2$$

$$+ \Delta V\left(P_r, T_r \right) \cdot \left(P\text{-}P_r \right) + \Delta\alpha\left(T\text{-}T_r \right) \cdot \left(P\text{-}P_r \right) + \frac{\Delta\beta}{2}\left(P\text{-}P_r \right)^2 \tag{A35}$$

This equation was published by Hawley (1971). In the evaluation of K' by Hawley, the γ_i's are not mentioned, which implies that they are close to unity, equal to each other ($\gamma_{\text{native starch}} = \gamma_{\text{gelatinised starch}}$), or constant. In such way, the equilibrium constant can be simplified further. We can now define the apparent equilibrium constant K' in the following manner:

$$K' \approx \prod_i \left(x_i \right)^{\nu_i} \tag{A36}$$

Insertion of A36 into A34 leads to the equation that has been used for the fitting procedure in our article.

References appendix

Atkins PW. 1997. Physical chemistry. Oxford: Oxford University Press. 1031 p.

Hawley SA. 1971. Reversible pressure–temperature denaturation of chymotrypsinogen. Biochemistry 10:2436-2442.

Heremans K, Smeller L. 1998. Protein structure and dynamics at high pressure. Biochim Biophys Acta 1386:353-370.

Knorr D, Heinz V, Buckow R. 2006. High pressure application for food biopolymers. Biochim Biophys Acta 1764:619-631.

Smeller L. 2002. Pressure-temperature phase diagrams of biomolecules Biochim Biophys Acta 1595:11-29.

Smith JM, Van Ness HC, Abbott MM. 1996. Introduction to chemical engineering thermodynamics. Singapore: McGraw-Hill. 763 p.

List of symbols

$\hat{a}_i$	:	Activity of species i in solution (-)
ΔC_p	:	Heat capacity change of reaction ($J \cdot mol^{-1} \cdot K^{-1}$)
$\hat{f}_i$	:	Fugacity of species i in solution (Pa)
f_i	:	Fugacity of pure species i (Pa)
$f_i(P_r)$		Standard state fugacity at the reference pressure P_r (Pa)
G_i	:	Gibbs energy of species i ($J \cdot mol^{-1}$)
$G_i(P_r)$	:	Gibbs energy of species i at the reference pressure P_r ($J \cdot mol^{-1}$)
ΔG	:	Gibbs energy change ($J \cdot mol^{-1}$)
$\Delta G(P_r)$	:	Gibbs energy change of reaction at the reference pressure P_r ($J \cdot mol^{-1}$)
$\Delta G(P_r, T_r)$	:	Gibbs energy change of reaction at reference temperature T_r and reference pressure P_r ($J \cdot mol^{-1}$)
$\Delta H(P_r, T_r)$	:	Enthalpy change of reaction at reference temperature T_r and reference pressure P_r ($J \cdot mol^{-1}$)
$\Delta H(P_r)$	:	Standard enthalpy change of reaction at the reference pressure P_r ($J \cdot mol^{-1}$)
K	:	Equilibrium constant (-)
K'	:	Apparent equilibrium constant (-)
$M_i(P_r)$	:	Molar property of species i at the reference pressure P_r
$\Delta M(P_r)$	:	Property change of reaction at the reference pressure P_r
P	:	Pressure (Pa)
P_r	:	Reference pressure (Pa)
R	:	Universal gas constant ($J \cdot mol^{-1} \cdot K$)
$\Delta S(P_r)$	:	Entropy change of reaction at the reference pressure P_r ($J \cdot mol^{-1} \cdot K^{-1}$)
$\Delta S(P_r, T_r)$	:	Entropy change of reaction at reference temperature T_r and reference pressure P_r ($J \cdot mol^{-1} \cdot K^{-1}$)
T	:	Absolute temperature (K)
V_i	:	Molar volume of species i ($m^3 \cdot mol^{-1}$)
$V_i(P_r)$	:	Molar volume of species i at standard pressure at the reference pressure P_r ($m^3 \cdot mol^{-1}$)
$\Delta V(P_r)$	:	Volume change of reaction at the reference pressure P_r ($m^3 \cdot mol^{-1}$)
$\Delta V(P_r, T_r)$	:	Volume change of reaction at reference temperature T_r and reference pressure P_r ($m^3 \cdot mol^{-1}$)
x_i	:	Mole fraction of species i in a liquid phase (-)

Greek letters

α_i	:	Molar, thermal expansion factor for species i ($m^3 \cdot mol^{-1} \cdot K^{-1}$)
$\Delta\alpha$	:	Thermal expansion factor change of reaction ($m^3 \cdot mol^{-1} \cdot K^{-1}$)
β_i		Molar, isothermal compressibility for species i ($m^6 \cdot mol^{-1} \cdot J^{-1}$)
$\Delta\beta$	:	Isothermal compressibility change of reaction ($m^6 \cdot mol^{-1} \cdot J^{-1}$)
Γ_i	:	Integration constant ($J \cdot mol^{-1}$)
γ_i	:	Activity coefficient of species i in solution (-)
μ_i	:	Chemical potential of species i ($J \cdot mol^{-1}$)
ν_i	:	Stoichiometric number of species i (-)

Chapter 6

Effect of gelatinisation and hydrolysis conditions on the selectivity of starch hydrolysis with α-amylase from *B. licheniformis*

Abstract

Enzymatic hydrolysis of starch can be used to obtain various valuable hydrolysates with different compositions. The effects of starch pretreatment, enzyme addition point, and hydrolysis conditions on the hydrolysate composition and reaction rate during wheat starch hydrolysis with α-amylase from *B. licheniformis* were compared. Suspensions of native starch or starch gelatinised at different conditions either with or without enzyme were hydrolysed. During hydrolysis, the oligosaccharide concentration, the dextrose equivalent, and the enzyme activity were determined. We found that the hydrolysate composition was affected by the type of starch pretreatment and the enzyme addition point, but it was not affected by the hydrolysis pressure, as long as gelatinization was complete. The differences between thermally gelatinised, high pressure gelatinised and native starch were explained by considering the accessibility of starch during the hydrolysis. These results show that the hydrolysate composition can be influenced by choosing different process sequences and conditions.

Introduction

Starch can be hydrolysed enzymatically to yield several commercially relevant hydrolysates (Kennedy *et al.*, 1988; Marchal, 1999). The enzymatic hydrolysis of starch consists of three steps: gelatinisation, liquefaction and saccharification. Gelatinisation of starch is required to increase the accessibility of the substrate and to enhance the hydrolysis rate. During liquefaction, the viscosity of the reaction mixture is reduced and gelatinised starch is partially hydrolysed to form a product with a dextrose equivalent that varies between 15 and 30. During saccharification, these partially hydrolysed starch chains are broken down into glucose, maltose, maltotriose, and some higher oligomers. The dextrose equivalent varies between 40 and 98 depending on the enzyme that was used.

The degree of gelatinisation is an important parameter during the enzymatic hydrolysis of starch. The degree of gelatinisation is affected by temperature, pressure, starch concentration, and treatment time (Baks *et al.*, 2007a,c; Bauer and Knorr, 2005; Douzals *et al.*, 2001; Knorr *et al.*, 2006). Besides the degree of gelatinisation, the activity and stability of the enzyme are also very important. α-Amylase (1,4-α-D-glucanohydrolase, E.C. 3.2.1.1) is often used for the enzymatic hydrolysis of starch. The activity and stability of α-amylase are affected by temperature, pressure, pH, substrate concentration, and additives (De Cordt *et al.*, 1994; Fitter *et al.*, 2001; Raabe and Knorr, 1996; Weemaes *et al.*, 1996).

Although the individual behaviour of starch and α-amylase in aqueous solutions has been studied over a broad range of pressures and temperatures, the behaviour of a system that consists of both starch and α-amylase has received less attention. The relevance of such a combined system emerges when the relation between starch gelatinisation and enzymatic hydrolysis is investigated. The effects of high pressure gelatinisation and high temperature gelatinisation on the glucose production rate, the hydrolysis yield, and the enzyme activity during enzymatic hydrolysis at atmospheric pressure have been investigated before (Hayashi and Hayashida, 1989; Selmi *et al.*, 2000; Stute *et al.*, 1996; Tester and Sommerville, 2001). However, the effects of these gelatinisation conditions on the hydrolysate composition were not determined.

The hydrolysate composition can also be affected by the hydrolysis pressure according to Matsumoto *et al.* (1997a,b). They studied the hydrolysis of various oligosaccharides by porcine pancreatic α-amylase by following the carbohydrate concentration in time at 200-400 MPa. Raabe and Knorr (1996) hydrolysed starch with α-amylase from *B. amolyliquefaciens* using the same pressure range, but they only measured the maltose

concentration in time. The effect of an increased pressure on the hydrolysate composition during enzymatic starch hydrolysis with α-amylase from *B. licheniformis* has not been determined before.

In the articles mentioned above, the raw materials required for enzymatic hydrolysis (starch, water, and enzymes) could be added anywhere during the process, because individually isolated components were used. It might be easier to mix all of them before gelatinisation, because mixing of the enzyme with starch and water after gelatinisation can be omitted. In some other cases, the raw materials required for enzymatic hydrolysis are only available as mixture, for example in mashing during brewing. It is therefore also relevant to determine whether the presence of the enzyme during gelatinisation affects enzymatic starch hydrolysis.

The aim of this article was to investigate the effect of starch pretreatment, enzyme addition point, and hydrolysis conditions on the hydrolysate composition and reaction rate during enzymatic starch hydrolysis with α-amylase from *B. licheniformis*. For this purpose, the concentration of oligosaccharides (with a degree of polymerisation smaller than eight), the dextrose equivalent, and the residual enzyme activity were determined as function of time. These results can be used to determine whether the process configuration can be used to change the hydrolysate composition.

Experimental

Materials

Wheat starch (S5127) was obtained from Sigma-Aldrich (Steinheim, Germany). The moisture content was 9.95 ± 0.43 w/w % (based on 22 measurements, 95 % confidence interval). The moisture content was determined by drying the wheat starch in a hot air oven at 105 °C or in a vacuum oven at 80 °C until the mass of the samples was constant in time. The water content of wheat starch was taken into account during all experiments. Thermostable α-amylase from *B. licheniformis* (Termamyl 120L) was donated by Novozymes (Bagsværd, Denmark). The enzyme concentration used during the experiments is expressed in mass percent of this enzyme stock solution per equivalent mass of substrate (w/w %). Maltose monohydrate, fuming hydrochloric acid, sodium hydroxide, sodium chloride, calcium chloride dihydrate, calcium chloride and tri-sodium phosphate were bought from Merck (Darmstadt, Germany). Maleic acid (di-sodium salt) was obtained from

Acros Organics (Geel, Belgium). Glucose was obtained from Sigma-Aldrich (Steinheim, Germany). Milli-Q water was used for all experiments and measurements.

Amylase HR reagent was used for measurement of the α-amylase activity and this is a product form Megazyme International Ireland (Bray, Republic of Ireland). The standard buffer used for all enzyme activity measurements was 0.1 M maleic acid buffer (pH 6.5) with 2 mM $CaCl_2.2H_2O$ and 0.1 M NaCl. A solution of 0.06 M tri-sodium phosphate (pH 11) was used as stopping reagent.

Microcon YM-30 centrifuge filters (Millipore Corporation, Bedford, MA, United States) were used to remove the enzyme from the hydrolysate. Before the actual filtration, these filters were washed by centrifugation with 500 µl milli-Q water during 40 minutes at 25 °C and 13000 g.

Experimental set up

For all experiments, 5 w/w % wheat starch-water mixtures were used, because the gelatinisation behaviour at this starch concentration is well investigated (Baks *et al.*, 2007c; Bauer and Knorr, 2005; Douzals *et al.*, 2001; Knorr *et al.*, 2006). In addition, 5 w/w % wheat starch-water mixtures can be handled easily due to the low viscosity of these mixtures. Calcium chloride (1.8 mM) was added to each reaction mixture.

High pressure experiments (450 MPa) were carried out in a multi vessel high-pressure apparatus (Resato FPU 100-50, Resato International B.V., Roden, the Netherlands). During these experiments, the pressure build-up rate was equal to 2.5 MPa/s. Glycol was used as pressure medium. Reaction mixtures were transferred to custom made polyethylene bags that were sealed with a minimum amount of air inside. Two bags were placed in each high pressure vessel. In order to gelatinise starch completely, starch-water mixtures were held at 450 MPa and 50 °C for 15 minutes (referred to as HP treatment) (Baks *et al.*, 2007c; Douzals *et al.*, 2001).

For gelatinisation at 0.1 MPa, a temperature controlled batch reactor equipped with an anchor stirrer was used (stirrer speed was 300 rpm). Firstly, wheat starch and water were mixed at room temperature in this reactor. In case the enzyme was present during gelatinisation, the enzyme was also added at this point. Secondly, the reaction mixture was heated to 90 °C in 30 minutes. Subsequently, the reaction mixture was held at 90 °C for 60 minutes. A temperature of 90 °C is known to be sufficient to gelatinise starch completely in a 5 w/w % wheat starch-water mixture after holding it for 60 minutes (Baks *et al.*, 2007a,c; Douzals *et al.*, 2001; Randzio *et al.*, 2002). Finally, the contents of the

reaction vessels were cooled down to 50 °C in 60 minutes. The complete heating and cooling treatment used for thermal gelatinisation is referred to as the HT treatment.

In case enzyme was not present during gelatinisation or gelatinisation was not carried out, the enzyme was added when the temperature of the reaction mixture was 50 °C. During all experiments, the starting time of the experiment ($t = 0$) was the point at which the enzyme was added. Immediately after this point in time (in case enzyme was not present during gelatinisation) or after the hydrolysis temperature was reached (in case the enzyme was present during gelatinisation), 1.5 ml safe-lock tubes (Eppendorf AG, Hamburg, Germany) were filled with the reaction mixture and placed in a water bath to keep the contents of the safe-lock tubes at 50 °C. Because the reaction mixtures in the high pressure vessels could not be stirred, the reaction mixtures that were treated at 0.1 MPa were also not stirred.

In case high pressure gelatinised starch was used for hydrolysis at atmospheric pressure or thermally gelatinised starch was used for hydrolysis at high pressure, the gelatinised starch suspension had to be transported. During the 15 minutes required for transport, the temperature of the suspension was kept at 50 °C by using a thermos flask filled with water. After transportation, enzyme was mixed with the gelatinised starch suspension and subsequently safe-lock tubes or sample bags were filled with this mixture and placed in the water bath or high pressure equipment for hydrolysis. The remainder of the procedure is equal to the procedures described above.

A hydrolysis temperature of 50 °C was used, because is below the gelatinisation onset temperature at atmospheric pressure (Baks *et al.*, 2007c; Douzals *et al.*, 2001; Randzio *et al.*, 2002). In this case, gelatinisation would not take place during hydrolysis at atmospheric pressure and the effect of incomplete gelatinisation could be investigated.

The hydrolysate composition and enzyme activity were determined for each measurement point in time and for that reason two safe-lock tubes or two sample bags were used. At each sample point, sample safe-lock tubes and bags were submerged in liquid nitrogen to stop the enzyme reaction. After holding them in liquid nitrogen for approximately 15 minutes, the safe-lock tubes or bags were stored in a -80 °C freezer until further use.

Sample handling
Samples from the -80 °C freezer that were taken to determine the carbohydrate composition or enzyme activity were submerged in liquid nitrogen for several minutes. Subsequently,

the sample was grinded in a mortar with a pestle while submerging the sample in liquid nitrogen.

Measurement of the carbohydrate composition

For measurement of the carbohydrate composition, approximately 0.3 g of the grinded sample was mixed with 1125 μl milli-Q water and 75 μl 2 M NaOH to obtain a carbohydrate concentration of 50 g·l⁻¹ and a NaOH concentration of 0.1 M. Samples were stored in ice, before part of this solution was transferred to a 1.5 ml safe-lock tube and centrifuged in a CS-15R centrifuge (Beckman Coulter Inc., Fullerton, CA, United States of America) during 15 minutes at 4 °C and 14000 g to remove undissolved material. After this centrifugation step, 500 μl of the supernatant was pipetted to a pre-washed microcon YM 30 filter and centrifuged for 1 h and 45 minutes at 4 °C and 13000 g to remove the enzyme. After centrifugation, 300 μl of the filtrate was taken and neutralized with 50 μl 0.6 M HCl. This solution was analysed with HPLC to determine the carbohydrate composition. The HPLC column was an Aminex HPX-42A column (300 mm x 7.8 mm) from Bio-Rad (Veenendaal, the Netherlands) operated at 85 °C with milli-Q water eluent at 0.3 ml/min. The amount of carbohydrates was determined with a refractive index detector. Calibration curves for glucose and maltose were approximately equal and it was assumed that the calibration curves of maltotriose, maltotetraose, maltopentaose, maltohexaose and maltoheptaose were also the same. The weight fraction $x_{w,i}$ of a carbohydrate with a degree of polymerisation (D.P.) equal to i was calculated with:

$$x_{w,i} = \frac{\left(\dfrac{C_{DP_i}}{M_{w,DP_i}} \cdot i \right)}{\left(\dfrac{C_{tot}}{M_{w,g}} \right)} \cdot 100\ \% \tag{1}$$

where C_{DPi} (in g·l⁻¹) and $M_{w,DPi}$ (in g·mol⁻¹) are respectively the concentration and molar mass of a maltooligosaccharide with a degree of polymerisation equal to i, C_{tot} is the total carbohydrate concentration (in g·l⁻¹), and $M_{w,g}$ is the molar mass of a D-glucopyranoside unit (162 g·mol⁻¹). The total carbohydrate concentration was corrected for the increase in dry matter during the reaction caused by the formation of maltooligosaccharides smaller than maltooctaose (for each maltooligosaccharide that is formed one molecule of water is used). Note that for the derivation of equation 1, the contribution of the molar mass of

water ($M_{w,w}$) to the molar mass of carbohydrate polymers in native starch with degree of polymerisation n was neglected ($n \cdot M_{w,g} \gg M_{w,w}$). The carbohydrate composition was used to determine the yield and dextrose equivalent (D.E.) (for procedures see Baks *et al.*, 2007b).

Model data were fitted to the experimentally determined weight fractions of oligosaccharides. The model equations were taken from (Paolucci-Jeanjean *et al.*, 2000) and fitted to our own data to guide the eye.

Measurement of the enzyme activity

For measurement of the residual enzyme activity, the grinded, frozen samples were dissolved in 0.1 M maleic acid buffer (final concentration approximately 25 mg enzyme solution$\cdot$l^{-1}) and stored in ice water if it was not used directly for the enzyme activity assay. The Ceralpha end-point assay procedure, which was used to measure the α-amylase activity, is described elsewhere (Baks *et al.*, 2006a). In this case, the α-amylase activity is defined as the amount of p-nitrophenol that is released (in μmol$\cdot$mg$^{-1}\cdot$min^{-1} of enzyme solution) at 40 °C and pH 6.5 after hydrolysis of blocked p-nitrophenyl maltoheptaoside. Samples often contain various carbohydrates that affect the measurement of the α-amylase activity (Baks *et al.*, 2006a,b). The experimentally determined α-amylase activity should be corrected for the presence of carbohydrates in the sample to obtain the true α-amylase activity. The method used to obtain the actual α-amylase activity is described elsewhere (Baks *et al.*, 2007b).

Results

Effect of enzyme to substrate ratio on enzymatic hydrolysis

Three different enzyme to substrate ratios were used for the enzymatic hydrolysis of HT gelatinised wheat starch (experiment 3, 6, and 8 in *Table 1*). The highest enzyme to substrate ratio (10 w/w %) resulted in the highest dextrose equivalent (*Figure 1*). In addition, the initial rate of increase of the dextrose equivalent as function of time was largest for the highest enzyme to substrate ratio.

Table 1: *Overview experiments. Abbreviations: Exp = experiment number; C_e/C_s = enzyme to substrate ratio; T_G = gelatinisation temperature; P_G = gelatinisation pressure; t_G = gelatinisation time; T_H = hydrolysis temperature; P_H = hydrolysis pressure; v = average enzyme activity; and E.A.P. = enzyme addition point, with a and b standing for respectively addition of the enzyme after and before gelatinisation.*

Exp	C_e/C_s	T_G	P_G	t_G	T_H	P_H	v^a	E.A.P.
	[w/w %]	[°C]	[MPa]	[min]	[°C]	[MPa]	[μmol·mg^{-1}·min^{-1}]	
1	0.1	-	-	-	50	0.1	1.41 ± 0.07^b	-
2	0.1	50	450	15	50	0.1	1.27 ± 0.05^b	a
3	0.1	90	0.1	60	50	0.1	1.78 ± 0.17^b	a
4	0.1	90	0.1	5	50	450^e	1.40 ± 0.06^d	a
5	1	-	-	-	50	0.1	1.11 ± 0.06^b	-
6	1	90	0.1	60	50	0.1	1.14 ± 0.03^b	a
7	1	90	0.1	60	50	0.1	1.23 ± 0.05^c	b
8	10	90	0.1	60	50	0.1	1.32 ± 0.06^b	a

[a] 95 % confidence interval.

[b] Average over 24 hours.

[c] Average over 6 hours.

[d] Average over 1.5 hours.

[e] During the first 15 minutes, the pressure was not equal to 450 MPa (approximately 12 minutes sample preparation and 3 minutes for pressure build up).

The enzyme activity was also measured during the complete time course of these hydrolysis reactions. The scatter in these enzyme activity measurements was small and did not follow a pattern (see confidence intervals *Table 1*) and for that reason it was assumed that the amount of enzyme inactivation was negligible under these reaction conditions.
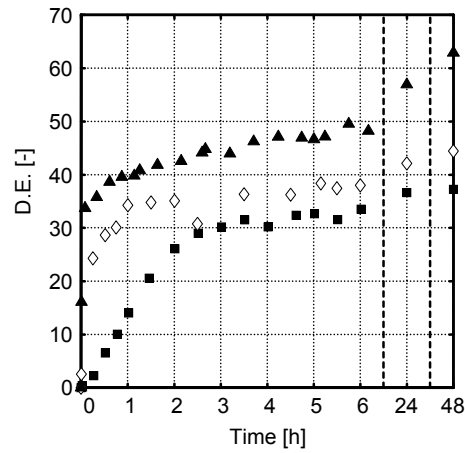
Figure 1: Dextrose equivalent as a function of hydrolysis time for three different enzyme to substrate ratios after HT gelatinisation. Symbols used: ▲ = 10.0 w/w % (Table 1, experiment 8); ◇ = 1.0 w/w % (Table 1, experiment 6); ■ = 0.1 w/w % (Table 1, experiment 3). Hydrolysis conditions: α-amylase from B. licheniformis, 50 °C, 5 w/w % wheat starch in water.

Effect of starch pretreatment on enzymatic hydrolysis

Figure 2 shows the dextrose equivalent as function of time during enzymatic hydrolysis of native, HP gelatinised, and HT gelatinised starches (experiment 1, 2, and 3 in *Table 1*, respectively). The initial slope of the dextrose equivalent vs. time curve is comparable for native and HP gelatinised starch. The largest initial slope of the dextrose equivalent vs. time curve was obtained with HT gelatinised starch. The lowest dextrose equivalent is obtained after enzymatic hydrolysis of native starch and the highest dextrose equivalent is obtained after hydrolysis of HT gelatinised starch, while the dextrose equivalent of HP gelatinised starch falls in between.

The enzyme was stable over the complete time course of the experiments with native, HP gelatinised, and HP gelatinised starch, since the scatter in the enzyme activity measurements was random and small (see confidence intervals *Table 1*). As a consequence, differences between hydrolysis experiments with native, HP gelatinised, and HT gelatinised starches cannot be explained by considering the enzyme activity.

Figure 2: Dextrose equivalent as a function of hydrolysis time for native (■) (Table 1, experiment 1), HP gelatinised (◇) (Table 1, experiment 2), and HT gelatin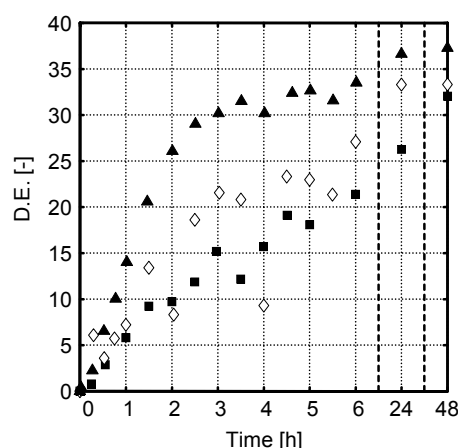ised (▲) (Table 1, experiment 3) starches. Gelatinisation conditions: HP = 450 MPa and 50 °C; HT = 0.1 MPa and 90 °C. Hydrolysis conditions: α-amylase from B. licheniformis, 50 °C, 5 w/w % wheat starch in water, enzyme to substrate ratio = 0.1 w/w %.

Figure 3 shows the weight fractions of various oligosaccharides as function of time during the experiments of which the dextrose equivalents are shown in *Figure 2*. Hydrolysis of native, HP, and HT gelatinised starches results in similar weight fraction profiles for maltotetraose, maltopentaose, maltohexaose, and maltoheptaose. However, the weight fractions of these oligosaccharides during enzymatic hydrolysis are higher in the following order of used substrates: native starch < HP gelatinised starch < HT gelatinised starch. The weight fractions of maltose and maltotriose are approximately equal during the hydrolysis of HP gelatinised starch. During the hydrolysis of HT gelatinised starch, the maltotriose weight fraction is higher than the maltose weight fraction. Hydrolysis of native starch resulted in a maltose weight fraction that is higher than the maltotriose weight fraction. The weight fraction of glucose is lower than the weight fraction of maltose and maltotriose and of comparable magnitude in all cases. The yield of glucose, maltose, and maltotriose after 48 hours of hydrolysis decreases in the following order: native starch (51 %), HP gelatinised starch (46 %), and HT gelatinised starch (44 %). The yields of maltotetraose, maltopentaose, maltohexaose, and maltheptaose show the reverse trend (respectively 10, 26, and 44 % for native starch, HP gelatinised starch, and HT gelatinised starch).

Figure 3: Weight fraction of glucose (■), maltose (◆), maltotriose (▲), maltotetraose (□), maltopentaose (◇), maltohexaose (△), and maltoheptaose (○) as function of time for native (Figures A and B) (Table 1, experiment 1), HP gelatinised (Figures C and D) (Table 1, experiment 2) and HT gelatinised (Figures E and F) (Table 1, experiment 3) starches. The lines were added to guide the eye and they are based on model equations from Paolucci-Jeanjean et al. (2000). Gelatinisation conditions: HP = 450 MPa and 50 °C; HT = 0.1 MPa and 90 °C. Hydrolysis conditions: α-amylase from B. licheniformis, 50 °C, 5 w/w % wheat starch in water, enzyme to substrate ratio = 0.1 w/w %.

In case an enzyme to substrate ratio of 1.0 w/w % was used for enzymatic hydrolysis of native starch (experiment 5, *Table* 1) instead of 0.1 w/w %, the dextrose equivalent and weight fractions were approximately the same as those in respectively *Figure 2* and *Figures 3C-3D*. The yield of glucose, maltose, and maltotriose after 48 hours of hydrolysis was 56 %, while the yield of maltotetraose, maltopentaose, maltohexaose, and maltheptaose was 12 %.

Effect of enzyme addition point on enzymatic hydrolysis

With the enzyme present during gelatinisation at 90 °C (experiment 7, *Table 1*), the dextrose equivalent was higher (see *Figure 4*) than the dextrose equivalent obtained after hydrolysis of starch gelatinised at the same temperature in the absence of enzyme (experiment 6, *Table 1*).
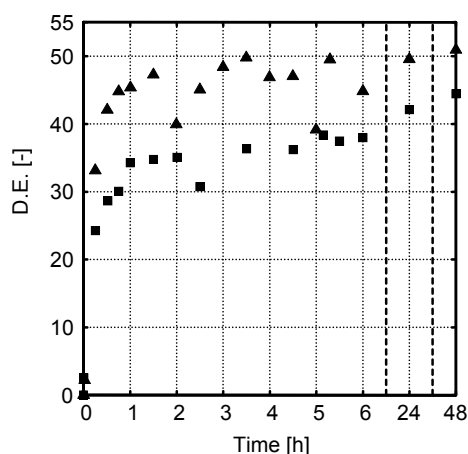
Figure 4: Dextrose equivalent as a function of starch hydrolysis time when the enzyme was present during gelatinisation (▲) (Table 1, experiment 7) and when the enzyme was added after gelatinisation (■) (Table 1, experiment 6). Gelatinisation conditions: 0.1 MPa and 90 °C. Hydrolysis conditions: α-amylase from B. licheniformis, 50 °C, 5 w/w % wheat starch in water, enzyme to substrate ratio = 1.0 w/w %.

Figure 5 shows the weight fractions of various oligosaccharides in time for these experiments. In both cases, the weight fraction profiles of maltose, maltotetraose, maltopentaose, maltohexaose, and maltoheptaose were similar. However, the weight fractions of glucose, maltotriose, and maltopentaose were much higher when the enzyme was already present during gelatinisation.
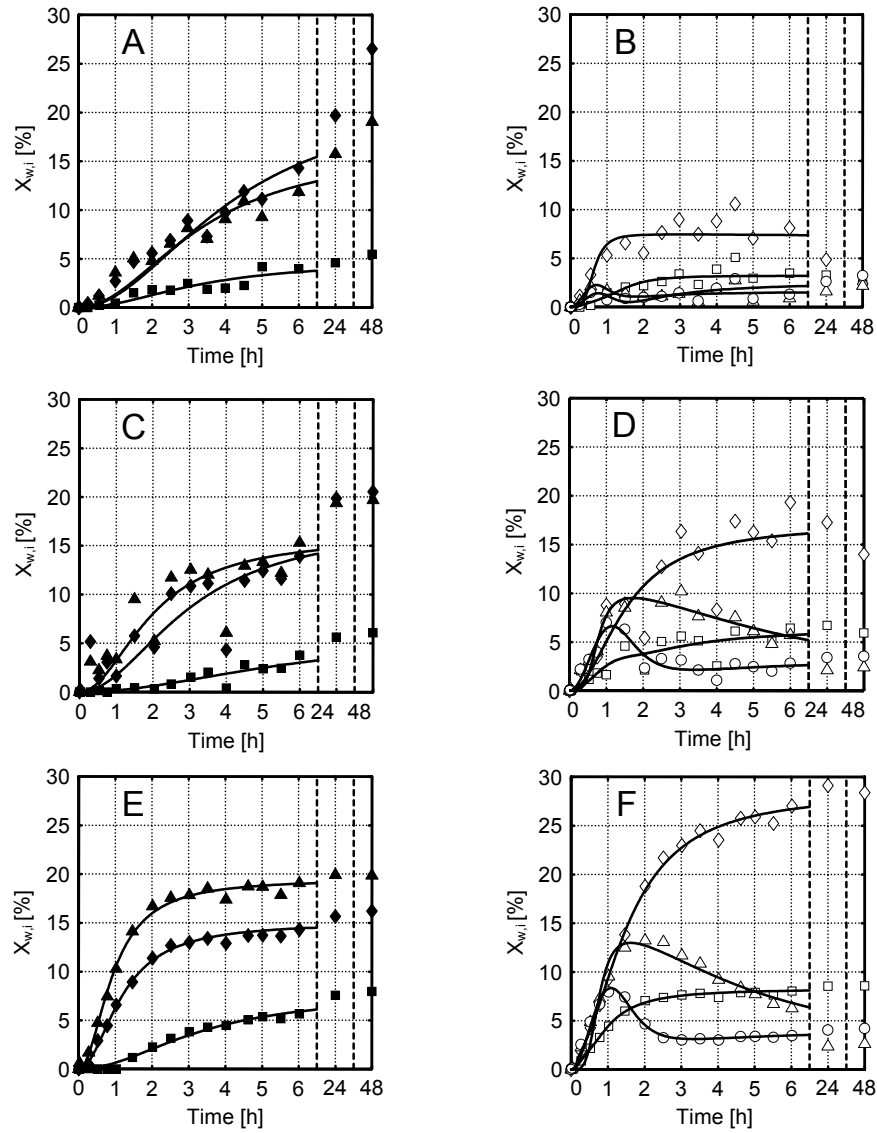
Figure 5: Weight fractions of glucose (■), maltose (◆), maltotriose (▲), maltotetraose (□), maltopentaose (◇), maltohexaose (△), and maltoheptaose (○) as function of time when the enzyme was added after gelatinisation (Figures A and B) (Table 1, experiment 7) and when the enzyme was present during gelatinisation (Figures C and D) (Table 1, experiment 6). The lines were added to guide the eye and they are based on model equations from Paolucci-Jeanjean et al. (2000). Gelatinisation conditions: 0.1 MPa and 90 °C. Hydrolysis conditions: α-amylase from B. licheniformis, 50 °C, 5 w/w % wheat starch in water, enzyme to substrate ratio = 1.0 w/w %.

Enzyme deactivation did not take place during the first six hours of these experiments, because the scatter in the enzyme activity measurements was random and small (see confidence intervals *Table 1*). However, after 24 and 48 hours the residual enzyme activity was equal to respectively 90 and 60 % in case the enzyme was present during

gelatinisation, while no enzyme deactivation could be observed if the enzyme was added after gelatinisation.

When the holding time of the starch-water mixture at 90 °C in the presence of α-amylase was decreased from 60 to 5 minutes kept (results not shown), the weight fractions of the measured oligosaccharides were the same during the complete time course of the experiment.

When the enzyme was present during gelatinisation at 450 MPa and 50 °C, starch sedimented during gelatinisation. As a result, starch was not well mixed with the enzyme and this experiment did not lead to reliable results.

Effect of pressure on enzymatic hydrolysis

In *Figure 6*, the results are shown for the hydrolysis of HT gelatinised starch that was hydrolysed at ambient pressure (experiment 3, *Table 1*) and 450 MPa (experiment 4, *Table 1*). *Figure 6A* shows that the initial increase of the dextrose equivalent in time was approximately the same for both conditions. *Figures 6B* and *6C* show that the initial increase of the weight fractions of all measured oligosaccharides was approximately the same when a hydrolysis pressure of 450 MPa was used instead of 0.1 MPa. The weight fractions of all other measured oligosaccharides are comparable during the experiment, except for glucose and maltotriose. The weight fractions of these carbohydrates are lower when the enzymatic hydrolysis is carried out at 450 MPa instead of 0.1 MPa.

During hydrolysis at 450 MPa, we found that the enzym was stable over the complete time course of the experiment. The enzyme activity measurements showed some (random) scatter, but the variability was small (see confidence intervals *Table 1*).

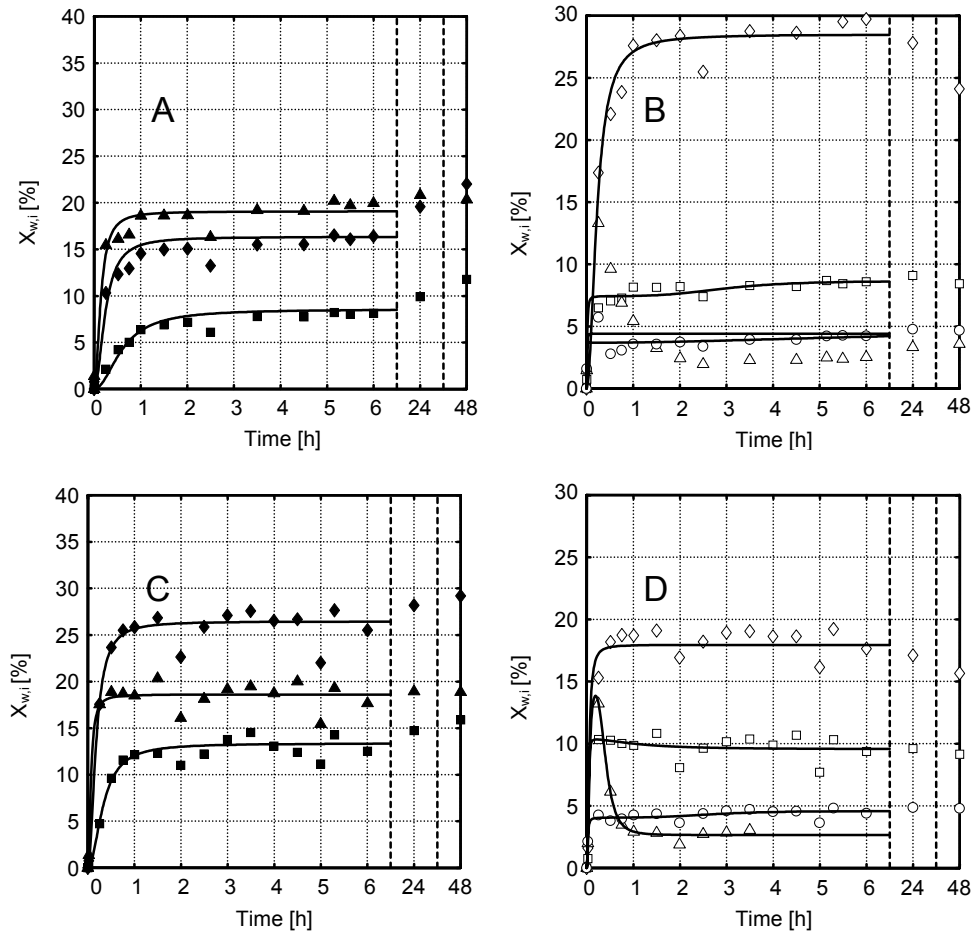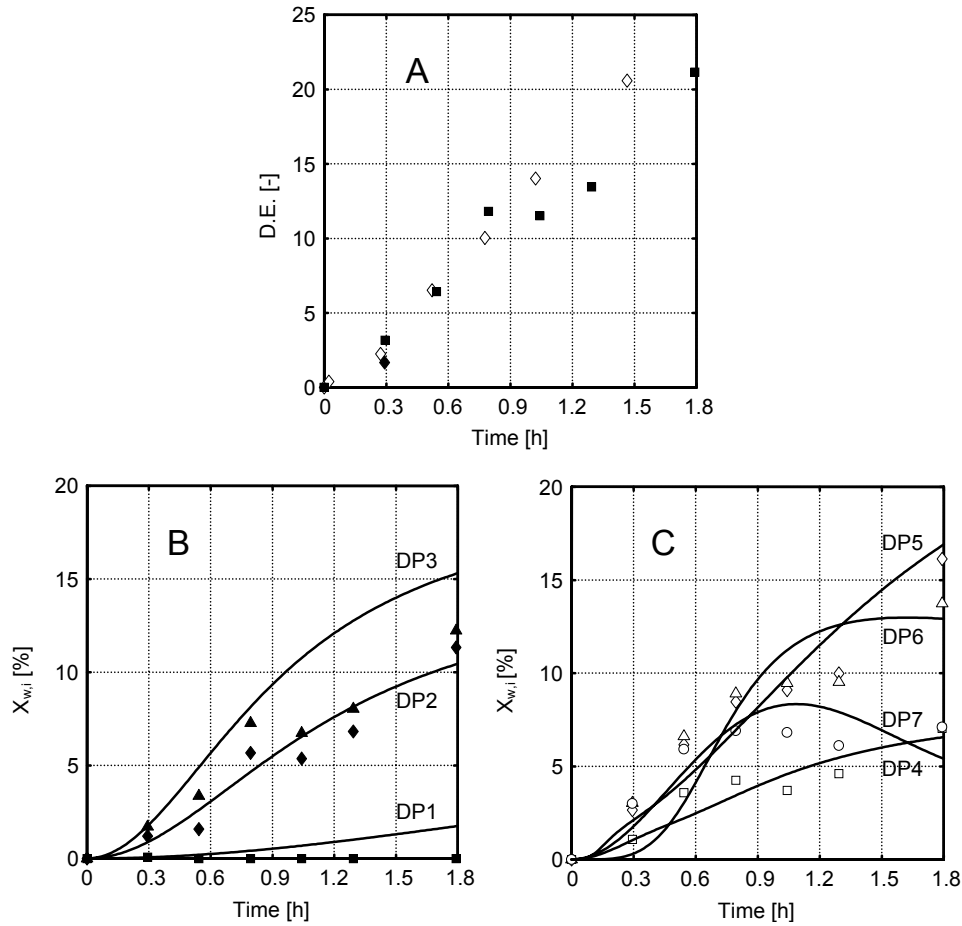*Figure 6: Dextrose equivalent (■) (Figure A) and mole fractions of glucose (■), maltose (♦), maltotriose (▲) (Figure B), maltotetraose (□), maltopentaose (◇), maltohexaose (△), and maltoheptaose (○) (Figure C) as function of time when HT gelatinised starch was hydrolysed at 450 MPa and 50 ℃ (Table 1, experiment 4). The experimental dextrose equivalent (◇) (Figure A), and the lines from Figures 3E and 3F for mole fractions of glucose (DP1), maltose (DP2), maltotriose (DP3) (Figure B), maltotetraose (DP4), maltopentaose (DP5), maltohexaose (DP6), and maltoheptaose (DP7) (Figure C) found during hydrolysis of HT gelatinised starch at atmospheric pressure and 50 °C were added (Table 1, experiment 3). Gelatinisation conditions: 0.1 MPa and 90 °C. Additional hydrolysis conditions: α-amylase from B. licheniformis, 5 w/w % wheat starch in water, enzyme to substrate ratio = 0.1 w/w %.*

Discussion

Effect of enzyme to substrate ratio on enzymatic hydrolysis

When the enzyme to substrate ratio was increased, the initial slope of the dextrose equivalent vs. time curve increased and the dextrose equivalent over the complete time course of the experiment increased. The initial slope of the dextrose equivalent vs. time curve could be determined accurately at an enzyme to substrate ratio of 0.1 w/w %. In this case, the amount of substrate is in excess and therefore the initial hydrolysis rate should be investigated at this enzyme to substrate ratio. The high enzyme concentrations can be used to determine the maximum dextrose equivalent that can be reached with α-amylase from *B. licheniformis* at these reaction conditions.

Effect of starch pretreatment on enzymatic hydrolysis

Use of HT gelatinised starch instead of native starch resulted in a more rapid increase of the dextrose equivalent and oligosaccharide weight fractions in time. These differences cannot be explained by differences in enzyme activity, because the ratio of the initial slopes (1.0:2.3) differs from the ratio of the enzyme activities (1.0:1.3). The initial slope of the dextrose equivalent vs. time curve and the increase in the oligosaccharide weight fractions are approximately the same during hydrolysis of native starch and HP gelatinised starch. In this case, the enzyme activities were equal and therefore comparable hydrolysis rates could be expected.

Studies in literature have shown that native starch can be hydrolysed enzymatically (Colonna *et al.*, 1988; Guerrieri *et al.*, 2000; Sarikaya *et al.*, 2000; Tester *et al.*, 2006). Guerrieri *et al.* (2000) found that use of native starch instead of temperature gelatinised starch resulted in a much lower hydrolysis rate and final glucose yield during hydrolysis with amyloglucosidase at 60 °C. However, we observed that the hydrolysis rate of native starch with α-amylase from *B. licheniformis* was quite high and that the differences between native and HT gelatinised starch were not as large as observed by Guerrieri *et al.* (2000). Native starch is partly crystalline and although these crystalline regions can be broken down (Planchot *et al.*, 1997), the hydrolysis rate is slow. According to Colonna *et al.* (1988), the accessibility and the crystallinity are the main limiting factors for the hydrolysis rate of native starch. Tester *et al.* (2006) also state that the accessibility of the enzyme to the interior of the granules regulates the hydrolysis. When native starch granules are hydrolysed, carbohydrates are slowly released or solubilised (Manelius *et al.*, 1997). As

a result, the availability of carbohydrates is limiting during hydrolysis of native starch and all carbohydrates that become available will be broken down rapidly by the enzyme (Manelius *et al.*, 1997). For that reason, the weight fractions of intermediates, such as oligosaccharides with D.P. 4-7, are low and the weight fractions of end products, oligosaccharides with D.P. 1-3, increase only gradually during hydrolysis. Because the available substrate is the limiting factor during hydrolysis of native starch, an increase in the enzyme to substrate ratio should not affect the results. Comparison of the results of experiments 1 and 5 indeed showed that the weight fractions of small oligosaccharides (and therefore the yield and the dextrose equivalent) did not change over the complete time course of the experiment.

During thermal gelatinisation at 90 °C, granules become completely gelatinised and amorphous inside (Baks *et al.*, 2007c; Douzals *et al.*, 2001). The carbohydrate chains are therefore much better accessible for the enzyme in comparison with native starch. Consequently, the number of accessible carbohydrate chains per enzyme molecule is so large that the enzyme concentration limits the hydrolysis rate. A higher enzyme to substrate ratio therefore leads to an increased hydrolysis rate (see *Figure 1*) and a faster increase in the oligosaccharide weight fractions. The enzyme has a preference for large carbohydrates (Baks *et al.*, 2006a,b) and they are hydrolysed first. After the large carbohydrates have been broken down into oligosaccharides, the oligosaccharides themselves are hydrolysed. As a result of the large quantity of large carbohydrates, the weight fractions of oligosaccharides with D.P. 4-7 will remain relatively high during the course of the experiment in comparison with native and starch. After some time, the large carbohydrates have been hydrolysed and the oligosaccharides with D.P. 4-7 are the largest carbohydrates available for hydrolysis. The hydrolysis profiles shown in *Figures 3E* and *3F* agree with the results of Nakakuki *et al.* (1984) and Saito (1973), and the description given by Guzman-Maldonado and Paredes-Lopez (1995).

The enzymatic hydrolysis of pressure gelatinised starch falls in between the hydrolysis of native starch and heat gelatinised starch. Consequently, it seems that the accessibility of the substrate of HP gelatinised starch also falls in between that of HT gelatinised and native starch. Douzals *et al.* (1998), Stolt *et al.* (2000), Katopo *et al.* (2002), and Knorr *et al.* (2006) mentioned that pressure gelatinised granules do not disintegrate. In addition, double helices in amylopectin do not unwind during high pressure treatment according to Knorr *et al.* (2006). These two factors combined may lead to a lower accessibility of carbohydrates for the enzyme and consequently a lower amount of oligosaccharides with D.P. 4-7 when HP gelatinised starch is hydrolysed instead of HT gelatinised starch. Our results agree with

the results of Hayashi and Hayashida (1989), who found that hydrolysis of pressure treated starch instead of native starch resulted in a higher hydrolysis yield when α-amylase from *Bacillus* sp. was used. In addition, Stute *et al.* (1996) found that the degree of hydrolysis with amyloglucosidase was slightly lower when pressure gelatinised starch (550 MPa) was hydrolysed instead of thermally gelatinised starch, which agrees with our results obtained with our enzyme. However, Selmi *et al.* (2000) found that use of pressure gelatinised starch instead of thermally gelatinised starch resulted in a higher glucose production yield during hydrolysis with amyloglucosidase. They suggest that this difference can be explained by structural differences between high pressure and high temperature gelatinised starches, and the presence of amylose-lipid complexes formed during thermal gelatinisation. Although the rate at which these amylose-lipid complexes are broken down might be low (*35*), they can be hydrolysed enzymatically (Ciu and Oates, 1999; Eliasson and Krog, 1985; Nebesny *et al.*, 2002). As a result, we expect that the presence of amylose-lipid complexes cannot lead to a lower glucose yield, it can only result in a slower increase of the glucose production in time.

It is expected that the hydrolysis mechanism is the same for native, HP gelatinised, and HT gelatinised starch. However, the differences in accessibility of the hydrolysable carbohydrates during enzymatic hydrolysis causes the differences in oligosaccharide weight fractions. Apparently, limited accessibility results in a more gradual release of carbohydrates that are immediately converted to glucose, maltose, and maltotriose by excess quantities of enzyme.

Effect of enzyme addition point on enzymatic hydrolysis

When the enzyme was added before instead of after gelatinisation, the dextrose equivalent is higher over the complete time course. During gelatinisation at 90 °C, the initial enzyme activity is approximately 40 % higher than at 50 °C (Fitter *et al.*, 2001). Our measurements indicated that the enzyme was also stable at these conditions (probably due to the presence of substrate). Because of the high activity and high stability, a higher hydrolysis rate is expected resulting in a higher dextrose equivalent as observed. However, we also observed a difference in the oligosaccharide weight fractions of experiment 6 and experiment 7. If this difference is only caused by a higher reaction rate and not by a change in hydrolysis mechanism, a higher enzyme concentration (experiment 8) should lead to similar results as observed for experiment 7. The weight fractions of all oligosaccharides during experiment 8 (results not shown) are comparable to those observed in *Figures 5C* and *5D*. However,

the weight fraction of maltose is lower and the weight fraction of maltopentaose is higher. As a result, the higher hydrolysis rate cannot explain our results.

Our results might be related to differences in substrate accessibility during gelatinisation in the presence of the enzyme. In the beginning of the process, the starch granules are not yet gelatinised, because the reaction mixture is first heated from 20 to 90 °C (30 minutes). Consequently, enzymatic hydrolysis proceeds according to the hydrolysis of native starch (as shown in *Figures 3A* and *3B*) as long as the temperature in the reaction mixture is below the gelatinisation onset temperature (approximately 50 °C). Two aspects that confirm this hypothesis are the high glucose and maltose weight fractions and the low maltopentaose weight fraction. During heating, the accessibility of carbohydrates for the enzyme increases. Consequently, the hydrolysis starts to proceed according to the hydrolysis of HP gelatinised starch (as shown in *Figures 3C* and *3D*). This is confirmed by the high weight fractions of oligosaccharides with D.P. 4-7. When the temperature has become 90 °C, which is sufficient to gelatinise starch completely, the hydrolysis proceeds according to the hydrolysis of HT gelatinised starch (*Figures 3E* and *3F*). Note that the combination of a high temperature during gelatinisation and a high enzyme to substrate ratio decreases the time to reach a more or less stable carbohydrate composition from two hours to one hour of hydrolysis.

Enzymatic hydrolysis of native cassava starch at 80 °C (Paolucci-Jeanjean *et al.*, 2000), which also results in gelatinisation and hydrolysis at the same time, resulted in similar oligosaccharide profile as we found in *Figures 5C* and *5D*.

Effect of pressure on enzymatic hydrolysis
When the pressure during hydrolysis of HT gelatinised starch was increased from 0.1 to 450 MPa (temperature was kept constant at 50 °C), all results remained approximately the same, except for the weight fractions of glucose and maltotriose. The weight fractions of these carbohydrates were lower than the weight fractions obtained with hydrolysis at 0.1 MPa. Additional experiments are required to draw more definite conclusions about the selectivity on larger time scale. Based on the results, it seems that α-amylase from *B. licheniformis* is stable at 450 MPa, which agrees with the results obtained by Weemaes *et al.* (1996). With the results that we have obtained, it seems that use of high pressure for hydrolysis does not lead to significantly different results in comparison to hydrolysis at atmospheric pressure. For that reason, additional experiments were not pursued.

Consequences for process design

The pretreatment of starch and the enzyme addition point strongly influence the hydrolysis rate and the weight fractions of oligosaccharides that are formed. In case the weight fraction of oligosaccharides with D.P. 4-7 should be low in comparison to the weight fraction of non-hydrolysable carbohydrates, native starch should be used as a substrate. In addition, the ratio between glucose, maltose, and maltotriose can be altered by choosing different process conditions. Hydrolysis of native starch can be used for obtaining the highest maltose weight fraction (it seems at the cost of longer reaction times and lower conversion), while hydrolysis of HT gelatinised starch can be used to yield the lowest maltose weight fraction. Having α-amylase present during gelatinisation resulted in higher glucose and maltose weight fractions and a lower weight fraction of maltopentaose as compared to the hydrolysis where the enzyme was added after gelatinisation. Approximately the same weight fractions of oligosaccharides with D.P. 4, 5, and 7 were obtained.

The hydrolysis rate can also be affected by the process. In case high weight fractions of all oligosaccharides with D.P. 1-7 are required in a short period of time, HT gelatinised starch should be used (either in the presence or in the absence of enzyme). It is therefore used during liquefaction (Kennedy *et al.*, 1988; Van der Maarel *et al.*, 2002) to supply partially hydrolysed carbohydrates for subsequent saccharification with other enzymes. In case the amount of glucose, maltose, and maltotriose should increase gradually in time, native starch should be used as a substrate. Hydrolysis of native starch might be combined with fermentation to provide a steady state supply of fermentable carbohydrates (glucose, maltose, and maltotriose) to a yeast to avoid inhibition by these small carbohydrates (Verstrepen *et al.*, 2004).

During one of the gelatinisation experiments, α-amylase from *B. licheniformis* was present during gelatinisation. This enzyme is stable at high temperatures and high pressures. Many starch converting enzymes are less stable at high temperatures or high pressures. However, stability measurements are usually carried out in the absence of substrate, whilst the presence of substrate results in a higher stability (Klibanov, 1983) due to stabilisation of the enzyme by the substrate. In addition, we have used 60 minutes to gelatinise starch in the presence of the enzyme. However, the gelatinisation conditions can be chosen in such way that complete gelatinisation is reached in a shorter period of time, thus further minimizing the amount of enzyme deactivation. If, for example, glucoamylase is used to hydrolyse starch, the starch gelatinisation diagram of Douzals *et al.* (2001) together with the activity measurements of Buckow *et al.* (2005) can be used to select the

conditions (pressure, temperature, and treatment time) that result in complete gelatinisation while limiting or even preventing enzyme deactivation. Finally, the stability of the enzyme can be increased by using a higher substrate concentration (Baks *et al.*, 2007b) enabling the user to retain complete enzyme activity during gelatinisation.

Acknowledgements

References

Baks T, Janssen AEM, Boom RM. 2006a. A kinetic model to explain the maximum in α-amylase activity measurements in the presence of small carbohydrates. Biotechnol Bioeng 94:431-440.

Baks T, Janssen AEM, Boom RM. 2006b. The effect of carbohydrates on α-amylase activity measurements. Enzyme Microb Technol 39:114-119.

Baks T, Ngene IS, Van Soest JJG, Janssen AEM, Boom RM. 2007a. Comparison of methods to determine the degree of gelatinisation for both high and low starch concentrations. Carbohydr Polym 67:481-490.

Baks T, Kappen FHJ, Janssen AEM, Boom RM. 2007b. Towards an optimal process for gelatinisation and enzymatic hydrolysis of highly concentrated starch-water mixtures. Accepted for publication in J Cereal Sci.

Baks T, Bruins ME, Janssen AEM, Boom RM. 2007c. The effect of pressure and temperature on the gelatinisation of starch at various starch concentrations. Submitted for publication.

Bauer BA, Knorr D. 2005. The impact of pressure, temperature and treatment time on starches: pressure-induced starch gelatinisation as pressure time temperature indicator for high hydrostatic pressure processing. J Food Eng 68:329-334.

Buckow R, Heinz V, Knorr D. 2005. Two fractional model for evaluating the activity of glucoamylase from *Aspergillus niger* under combined pressure and temperature conditions. Food Bioprod Process 83:220-228.

Colonna P, Buleon A, Lemarie F. 1988. Action of *Bacillus subtilis* α-amylase on native wheat starch. Biotechnol Bioeng 31:895-904.

Cui R, Oates CG. 1999. The effect of amylose-lipid complex formation on enzyme susceptibility of sago starch. Food Chem 65:417-425.

De Cordt S, Hendrickx M, Maesmans G, Tobback P. 1994. The influence of polyalcohols and carbohydrates on the thermostablity of α-amylase. Biotechnol Bioeng 43:107-114.

Douzals JP, Perrier Cornet JM, Gervais P, Coquille JC. 1998. High-pressure gelatinization of wheat starch and properties of pressure-induced gels. J Agric Food Chem 46:4824-4829.

Douzals JP, Coquille JC, Gervais P, Perrier-Cornet JM. 2001. Pressure-temperature phase transition diagram for wheat starch. J Agric Food Chem 49:873-876.

Eliasson AC, Krog N. 1985. Physical properties of amylose-monoglyceride complexes. J Cereal Sci 3:239-248.

Fitter J, Herrmann R, Dencher NA, Blume A, Hauss T. 2001. Activity and stability of a thermostable α-amylase compared to its mesophilic homologue: mechanisms of thermal adaptation. Biochemistry 40:10723 - 10731.

Guerrieri N, Eynard L, Lavelli V, Gerletti P. 1997. Interactions of protein and starch studied through amyloglucosidase action. Cereal Chem 74:846-850.

Guzman-Maldonado H, Paredes-Lopez O. 1995. Amylolytic enzymes and products derived from starch: a review. Crit Rev Food Sci Nutr 35:373–403.

Hayashi R, Hayashida A. 1989. Increased amylase digestibility of pressure-treated starch. Agric Biol Chem 53:2543-2544.

Katopo H, Song Y, Jane J-L. 2002. Effect and mechanism of ultrahigh hydrostatic pressure on the structure and properties of starches. Carbohydr Polym 47:233-244.

Kennedy JF, Cabalda VM, White CA. 1988. Enzymic starch utilization and genetic engineering. Trends Biotechnol 6:184-189.

Klibanov AM. 1983. Stabilization of enzymes against thermal inactivation. Adv Appl Microbiol 29:1-28.

Knorr D, Heinz V, Buckow R. 2006. High pressure application for food biopolymers. Biochim Biophys Acta 1764:619-631.

Manelius R, Qin Z, Avall A-K, Andtfolk H, Bertoft E. 1997. The mode of action on granular wheat starch by bacterial α-amylase. Starch/Stärke 49:142-147.

Marchal LM. 1999. General introduction. In: Marchal LM. Towards a rational design of commercial maltodextrins: a mechanistic approach. PhD thesis. Wageningen:Wageningen University. 1-9.

Matsumoto T, Makimoto S, Taniguchi Y. 1997a. Effect of pressure on the mechanism of hydrolysis of maltotetraose, maltopentaose and maltohexaose catalyzed by porcine pancreatic α-amylase. Biochim Biophys Acta 1343:243-250.

Matsumoto T, Makimoto S, Taniguchi Y. 1997b. Effect of pressure on the mechanism of hydrolysis of maltoheptaose and amylose catalyzed by porcine pancreatic α–amylase. J Agric Food Chem 45:3431-3436.

Nakakuki T, Azuma K, Kainuma K. 1984. Action patterns of various exo-amylases and the anomeric configurations of their products. Carbohydr Res 128:297-310.

Nebesny E, Rosicka J, Tkaczyk M. 2002. Effect of enzymatic hydrolysis of wheat starch on amylose-lipid complexes stability. Starch/Stärke 54:603-608.

Paolucci-Jeanjean D, Belleville M-P, Zakhia N, Rios GM. 2000. Kinetics of cassava starch hydrolysis with Termamyl enzyme. Biotechnol Bioeng 68:71-77.

Planchot V, Colonna P, Buleon A. 1997. Enzymatic hydrolysis of α-glucan crystallites. Carbohydr Res 298:319-326.

Raabe E, Knorr D. 1996. Kinetics of starch hydrolysis with *Bacillus amyloliquefaciens* α-amylase under high hydrostatic pressure. Starch/Stärke 48:409-414.

Randzio SL, Flis-Kabulska I, Grollier J-PE. 2002. Reexamination of phase transformations in the starch-water system. Macromolecules 35:8852-8859.

Saito N. 1973. A thermophilic extracellular α-amylase from *Bacillus licheniformis*. Arch Biochem Biophys 155:290-298.

Sarikaya E, Higasa T, Adachi M, Mikami B. 2000. Comparison of degradation abilities of α- and β-amylases on raw starch granules. Process Biochem 35:711-715.

Selmi B, Marion D, Perrier Cornet JM, Douzals JP, Gervais P. 2000. Amyloglucosidase hydrolysis of high-pressure and thermally gelatinized corn and wheat starches. J Agric Food Chem 48:2629-2633.

Stolt M, Oinonen S, Autio K. 2000. Effect of high pressure on the physical properties of barley starch. Innov Food Sci Emerg 1:167-175.

Stute R, Klingler RW, Boguslawsli S, Eshtiaghi NM, Knorr D. 1996. Effects of high-pressure treatments on starches. Starch/Stärke 48:399-408.

Tester RF, Qi X, Karkalas J. 2006. Hydrolysis of native starches with amylases. Anim Feed Sci Technol 130:39-54.

Tester RF, Sommerville MD. 2001. Swelling and enzymatic hydrolysis of starch in low water systems. J Cereal Sci 33:193-203.

Van der Maarel MJEC, Van der Veen B, Uitdehaag JCM, Leemhuis H, Dijkhuizen L. 2002. Properties and applications of starch-converting enzymes of the α-amylase family. J Biotechnol 94:137-155.

Verstrepen KJ, Iserentant D, Malcorps P, Derdelinckx G, Van Dijck P, Winderickx J, Pretorius IS, Thevelein JM, Delvaux FR. 2004. Glucose and sucrose: hazardous fast-food for industrial yeast? Trends Biotechnol 22:531-537.

Weemaes C, De Cordt S, Goossens K, Ludikhuyze L, Hendrickx M, Heremans K, Tobback P. 1996. High pressure, thermal, and combined pressure-temperature stabilities of α-amylases from Bacillus species. Biotechnol Bioeng 50:49-56.

Chapter 7

Towards an optimal process for gelatinisation and hydrolysis of highly concentrated starch-water mixtures with α-amylase from *B. licheniformis*

Abstract

The enzymatic hydrolysis of starch is usually carried out with 30-35 w/w % starch in water. Higher substrate concentrations (50-70 w/w %) were reached by using a twin-screw extruder for gelatinisation and for mixing enzyme with gelatinised starch prior to enzymatic hydrolysis in a batch reactor. The aim of this study was to determine which parameters are important for gelatinisation of wheat starch and to investigate the effects of different extrusion conditions on the enzymatic hydrolysis. After extrusion, the degree of gelatinisation was measured. During hydrolysis, the carbohydrate composition, the dextrose equivalent, and the α-amylase activity were measured. Gelatinisation measurements showed that mechanical forces lowered the temperature required for complete gelatinisation. During hydrolysis experiments, high dextrose equivalents were observed even if starch was not completely gelatinised during extrusion. Due to high substrate concentrations, the residual α-amylase activity remained high throughout enzymatic hydrolysis, although high temperatures were used. Increased substrate concentrations did not affect the carbohydrate composition of the product. Furthermore, the time required for the batch hydrolysis step could be varied by choosing a different enzyme to substrate ratio. This article provides a basis for detailed optimisation of this process to develop an industrial-scale process at high substrate concentrations.

Introduction

The enzymatic hydrolysis of starch is an important industrial process that consists of three steps: gelatinisation, liquefaction and saccharification. In industry, a jet cooker is used to gelatinise starch by mixing the starch slurry with steam under pressure at 100-175 °C (Van der Maarel *et al.*, 2002). The residence time in such a jet cooker is in the order of seconds. After gelatinisation, liquefaction and saccharification can take place in a hydrolysis reactor. Usually, a thermostable α-amylase is used that is mixed with the starch slurry before passing through the jet cooker. The dextrose equivalent of the product depends on the time of incubation and the amount and type of enzyme being used. Two major hydrolysis products are maltodextrins that consist of partly hydrolysed starch chains with a dextrose equivalent below 30 and glucose and maltose syrups with a dextrose equivalent above 40 that contain mono- di- and some higher saccharides (Kennedy *et al.*, 1988).

The industrial gelatinisation process described above is usually carried out with a 30-35% dry solids starch slurry. Increasing the substrate concentration during the enzymatic hydrolysis can yield a higher productivity, and a higher enzyme stability (Klibanov, 1983; De Cordt *et al.*, 1994). When the starch concentration increases, the temperature required to reach complete gelatinisation increases rapidly (Donovan, 1979). Moreover, the viscosity of the starch slurry increases with increasing starch content and this complicates further processing. Conventional jet cookers cannot be used anymore at high substrate concentrations due to the increased viscosity. Since the gelatinisation temperature increases, addition of the enzyme during the gelatinisation process is unfavourable, because it can lead to enzyme inactivation. A different process is therefore needed to handle more concentrated starch slurries. Extruders appear to be suitable for this purpose.

Several authors have used extruders for non-enzymatic starch processing (Blanche and Sun, 2004; Cai and Diosady, 1993; Cai *et al.*, 1995; Colonna *et al.*, 1984; Davidson *et al.*, 1984; Gomez and Aguilera, 1984; Jackson *et al.*, 1990; Zheng and Wang, 1994). Other researchers used an extruder to gelatinise native starch and hydrolyse it enzymatically (Curic *et al.*, 1998; Govindasamy *et al.*, 1997a,b; Lee and Kim, 1990; Roussel *et al.*, 1991; Vasanthan *et al.*, 2001) or used it only to hydrolyse pre-gelatinised starch (Komolprasert and Ofoli, 1991a). Because the residence time in an extruder is limited, it is not possible to produce a hydrolysate with a high dextrose equivalent (more than 25). If a higher dextrose equivalent is desired, a batch reactor is often linked to an extruder to increase the hydrolysis time (Chouvel *et al.*, 1983; Linko *et al.*, 1980, 1983; Reinikainen *et al.*, 1986; Van

Zuilichem *et al.*, 1990). Komolprasert and Ofoli (1991b) also used the combination of an extruder and a batch reactor, but they started with pre-gelatinised starch. The extruder was used to mix pre-gelatinised starch with the enzyme and perform the liquefaction before saccharification in the batch reactor. Note that the use of separate process steps for gelatinisation and enzymatic hydrolysis makes it possible to optimise both processes independently.

In many cases, the enzyme was added at the beginning of the extruder together with the starch-water mixture (Chouvel *et al.*, 1983; Curic *et al.*, 1998; Govindasamy *et al.*, 1997a, 1997b; Komolprasert and Ofoli, 1991a; Lee and Kim, 1990; Linko *et al.*, 1980, 1981, 1983; Reinikainen *et al.*, 1986; Vasanthan *et al.*, 2001). Chouvel *et al.* (1983) also carried out experiments where the enzyme was added to the extruder approximately half-way along its length. Curic *et al.* (1998) and Linko *et al.* (1980, 1981) found that the residual α-amylase activity after extrusion decreased under several extrusion conditions. To reduce the amount of enzyme deactivation during extrusion, the enzyme should be added at the end of the gelatinisation section and not at the beginning of the extruder.

For optimisation of a process suitable for gelatinisation and enzymatic hydrolysis at high starch concentrations, it is important to know; whether complete gelatinisation is achieved (to reach a high degree of hydrolysis in the following steps), whether the enzyme is still active during the hydrolysis reaction (to maintain a high hydrolysis rate) and whether the desired product is formed (to decide how much time is needed for the hydrolysis reaction). It is therefore essential to measure the degree of gelatinisation, the enzyme activity, and the carbohydrate composition. The residual α-amylase activity during the enzymatic hydrolysis of starch in a batch reactor at high starch concentrations was not measured before. When the enzyme is added at the end of the extruder, the residence time of the enzyme is small in comparison with the time it spends in the batch reactor. As a result, a much larger decrease in α-amylase activity can be expected during the enzymatic hydrolysis in a batch reactor in comparison with the decrease in α-amylase activity during extrusion. Furthermore, in the literature the dextrose equivalent was often determined instead of the carbohydrate composition. Dextrose equivalent measurements alone are not suitable for the purpose of defining the product, because the same dextrose equivalent can be found for products with a different carbohydrate composition.

Besides the required changes in the process, an increased starch content can also affect measurements of the degree of gelatinisation (Baks *et al.*, 2007), the enzyme activity and stability (Baks *et al.*, 2006a, 2006b; Linko *et al.*, 1983), and the carbohydrate composition.

The objective of this article is to determine which process parameters are important for gelatinisation of starch in a twin-screw extruder and how extrusion conditions can affect the subsequent enzymatic hydrolysis of starch in a batch reactor at high starch concentrations. We will focus on several output parameters: the degree of gelatinisation, the enzyme activity, the dextrose equivalent and the carbohydrate composition. The enzyme activity and carbohydrate concentration will be measured at different times during the hydrolysis of the gelatinised starch slurry. The knowledge gathered during this study can be used for more detailed process optimisation.

Experimental

Materials

Native wheat starch (Excelsior) was obtained from Latenstein (Nijmegen, the Netherlands) and contained 10.0 ± 0.1 w/w % water (95 % confidence interval, based on 3 measurements). The moisture content was determined by drying wheat starch in a hot air oven at 105 °C until the mass of the samples was constant in time. The water content of wheat starch was taken into account during all experiments. Thermostable α-amylase from *B. licheniformis* (Termamyl 120 L) was donated by Novozymes (Bagsværd, Denmark). The enzyme concentration used during the experiments is expressed in mass percent of this enzyme stock solution per equivalent mass of substrate (w/w %). Maltose monohydrate, fuming hydrochloric acid, sodium hydroxide, sodium chloride, calcium chloride dihydrate, calcium chloride and tri-sodium phosphate were bought from Merck (Darmstadt, Germany). Maleic acid (di-sodium salt) was obtained from Acros Organics (Geel, Belgium). Glucose and maltodextrin from corn with dextrose equivalents of 4-7, 13-17, and 16.5-19.5 were obtained from Sigma-Aldrich (Steinheim, Germany).

For the measurement of the α-amylase activity, Amylase HR reagent (Megazyme International Ireland, Bray, Republic of Ireland) was used. The standard buffer used for all enzyme activity measurements was 0.1 M maleic acid buffer (pH 6.5) with 2 mM $CaCl_2.2H_2O$ and 0.1 M NaCl. A solution of 0.06 M tri-sodium phosphate (pH 11) was used as stopping reagent.

Milli-Q water was used for all enzyme activity measurements and for HPLC sample preparation and analysis. Demineralized water was used for the extrusion experiments.

Microcon YM-30 centrifuge filters (Millipore Corporation, Bedford, MA, United States) were used to remove the enzyme from the hydrolysate. Before the actual filtration, these filters were washed by centrifugation with 500 μl milli-Q water for 40 min at 25 °C and 13000 g.

Methods

Experimental set up

Figure 1 shows a schematic representation of the corotating twin-screw extruder (Berstorff, Hannover, Germany, $D = 25$ mm and $L = 40D$) that was used. This twin screw extruder (TSE) consists of 10 sections that can be heated or cooled individually to obtain a certain temperature profile (see *Table 1*). The temperature in sections 1 and 2 was always kept at 20 and 60 °C to make sure that water evaporation did not take place.
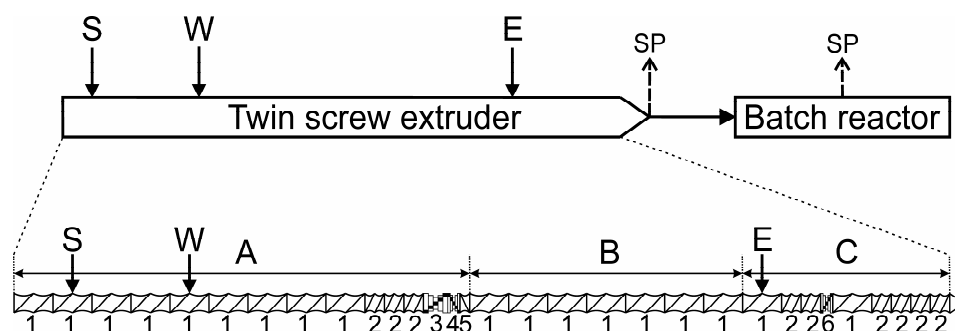
Figure 1: Overview of experimental setup including twin screw extruder configuration and location of sampling points (SP). Description of different zones in extruder: zone A = mixing of starch (S) with water (W) and subsequent gelatinsation of starch; zone B = cooling down to 90 °C; zone C = mixing of gelatinised starch with enzyme (E). Screw elements used: 1 = transport element; 2 = transport element to increase pressure; 3 = large kneading discs to provide positive pumping; 4 = small kneading disc inducing negative pumping; 5 = reverse screw element; 6 = small kneading discs for positive pumping.

131

Table 1: Temperature profiles of the corotating twin screw extruder.

Zone A[a]					Zone B[a]		Zone C[a]			Die	Experiment number[b]
T_1	T_2	T_3	T_4	T_5	T_6	T_7	T_8	T_9	T_{10}		
20	60	60	60	60	60	60	60	60	60	60	G8, G9, G10
20	60	80	80	80	80	80	80	80	80	80	G1, G11, G12, G13
20	60	90	90	90	90	90	90	90	90	90	G14
20	60	100	100	100	100	90	90	90	90	90	G2, G3, G15, G16, G17
20	60	100	110	120	110	90	90	90	90	90	G4, G5, G6
20	60	100	120	140	120	90	90	90	90	90	G7

[a] Zones A, B, and C refer to the sections depicted in *Figure 1*. $T_1,...,T_{10}$ are the set temperatures (°C) of the barrel in sections 1,…,10.

[b] Experiment number refers to gelatinisation experiments in *Table 2*.

The first zone (A) was used to mix wheat starch with water to obtain a 50, 60, or 70 w/w % wheat starch-water mixture and to subsequently gelatinise starch. Starch was fed with a single screw flex wall gravimetrical feeder (Brabender Technology KG, Duisburg, Germany) and water was added with a peristaltic pump (Watson-Marlow Bredel Inc, Wilmington, Massachusetts, USA). The starch feed rate was equal to 2.0 kg/h (dry weight) for all concentrations. The water feed rate was equal to 1.8, 1.1, and 0.6 kg/h for respectively 50, 60, and 70 w/w % wheat starch-water mixtures. The $CaCl_2$ concentration in the final starch-water mixture was kept constant at 70 ppm. After gelatinisation, the starch-water mixture was cooled down to 90 °C in zone B. In the remaining 3 sections (zone C), the starch-water mixture was kept at this temperature and mixed with the enzyme solution. When hydrolysis experiments were carried out, the enzyme solution was added with a Pharmacia/LKB HPLC pump (Delta Technical Products Company, Des Plaines, Illinois, USA). Enzyme stock solutions with different concentrations (3.3, 16.9, and 71.0 w/w % Novozymes liquid enzyme solution in demineralised water) were added at a constant flow rate of 0.065 kg/h to obtain 0.1, 0.5, or 2.5 w/w % Novozymes liquid enzyme/starch mixture (dry weight). In the case where gelatinisation experiments were carried out, the enzyme solution was replaced by water. Firstly, because the degree of gelatinisation measurements can be affected by enzymatic hydrolysis. Secondly, with the addition of enzyme to the mixing section of the extruder, additional water is added, which affects the degree of gelatinisation (Donovan, 1979). During the gelatinisation experiments in the extruder, we wanted to replicate as closely as possible conditions in which enzymes would

be added. For that reason, the same amount of water was added to the extruder as would be added by addition of the enzyme solution.

Representative samples were taken when the temperature in the different sections, the screw speed, the torque and the feed rate of the pumps of the extruder remained constant in time. The sample flowing out of the extruder die was immediately frozen in liquid nitrogen and stored in a -80 °C freezer to reduce recrystallisation and to stop the hydrolysis reaction. Although the residence time of the enzyme in the extruder is probably very short, part of the gelatinised starch slurry is expected to be hydrolysed in the extruder especially at high enzyme to substrate ratios. For that reason, samples were taken immediately after extrusion to quantify how much carbohydrates are broken down in the extruder. For the hydrolysis experiments, the extrudate was collected in a small 50 ml polypropylene Cellstar flask (Greiner Bio-One GmbH, Frickenhausen, Germany) and transferred to a water bath to keep the contents of the flask at 90 °C for the hydrolysis time that was required. The hydrolysis reaction was stopped by submerging the flask in liquid nitrogen. After the sample was completely frozen (at least 15 min), it was stored in a -80 °C freezer.

Handling of samples

After storage, the samples used for measuring the degree of gelatinisation were freeze-dried in a Christ Epsilon 2-6D freeze dryer (Osterode am Harz, Germany) prior to analysis. Freeze-drying was started at -20 °C and 1.030 mbar for 20 h followed by a second drying stage at -5 °C and 0.05 mbar for 20 h. During the third drying stage, the temperature was kept at -5 °C and the pressure was kept at 0.001 mbar for 28 h. The freeze-dried samples were submerged in liquid nitrogen for several minutes and subsequently ground in a Retsch ZM 100 rotor mill (Retsch Gmbh, Haan, Germany) with a 0.5 mm ring sieve. The obtained powder was stored in a desiccator until further use.

Samples from the -80 °C freezer that were taken to determine the carbohydrate composition or enzyme activity were submerged in liquid nitrogen for several minutes. Subsequently, a sample and some liquid nitrogen were transferred to an analytical mill (type A10) from IKA (Staufen, Germany). Liquid nitrogen was added before grinding to ensure that the sample remained frozen and that hydrolysis did not take place. After grinding, the samples were stored in a -80 °C freezer until further use.

Measurement of the degree of gelatinisation

Differential Scanning Calorimetry measurements were used to measure the degree of gelatinisation. This procedure has been described in a previous article (Baks *et al.*, 2007).

Measurement of the carbohydrate composition

The fine powder that was obtained during the grinding step was dissolved in 0.1 M NaOH (final concentration approximately 8 g·l⁻¹) and stored in ice water if necessary. Part of this solution was transferred to a 1.5 ml safe-lock tube (Eppendorf AG, Hamburg, Germany) and centrifuged on a CS-15R centrifuge (Beckman Coulter Inc., Fullerton, CA, United States of America) during 15 min at 4 °C and 14000 g to remove undissolved material. The undissolved material probably consists of lipids or amylose-lipid complexes that can lead to an opalescence, haze, and impaired clarity (Nebesny *et al.*, 2002). DSC measurements also proved that amylose-lipid complexes were present in the gelatinised starch mixtures. After this centrifugation step, 500 μl of the supernatant was pipetted to a pre-washed microcon YM 30 filter and centrifuged for 1 h and 45 min at 4 °C and 13000 g to remove the enzyme. After centrifugation, 300 μl of the filtrate was taken and neutralized with 50 μl 0.6 M HCl. This solution was analysed with HPLC to determine the carbohydrate concentration. The HPLC column was an Aminex HPX-42A column (300 mm x 7.8 mm) from Bio-Rad (Veenendaal, the Netherlands) operated at 85 °C with milli-Q water eluent at 0.3 ml/min. The amount of carbohydrates was determined with a refractive index detector. Calibration curves for glucose and maltose were approximately equal and it was assumed that maltotriose, tetrasaccharide, pentasaccharide, hexasaccharide and heptasaccharide responded in the same manner.

Calculation of yield and maltooligosaccharide concentration

The overall yield of maltooligosaccharides with a degree of polymerisation from 1 to 7 (%) was calculated with the following equation:

$$Y = \sum_{i=1}^{7} x_{m,i} \tag{1A}$$

where $x_{m,i}$ is the maltooligosaccharide fraction (%) calculated with:

$$x_{m,i} = \frac{\left(\dfrac{C_{DP_i}}{M_{w,DP_i}} \cdot i \right)}{\left(\dfrac{C_{tot}}{M_{w,g}} \right)} \cdot 100\,\% \tag{1B}$$

where C_{DPi} (in g·l⁻¹) and $M_{w,DPi}$ (in g·mol⁻¹) are respectively the concentration and molar mass of a maltooligosaccharide with a degree of polymerisation equal to i, C_{tot} is the total

carbohydrate concentration (in $g \cdot l^{-1}$) and $M_{w,g}$ is the molar mass of a D-glucopyranoside unit (162 $g \cdot mol^{-1}$). The total carbohydrate concentration was corrected for the increase in dry matter during the reaction caused by the formation of maltooligosaccharides smaller than maltooctaose by using the measured carbohydrate composition determined with HPLC (for each maltooligosaccharide that is formed one molecule of water is used). Note that for the derivation of equation 1B, the contribution of the molar mass of water ($M_{w,w}$) to the molar mass of carbohydrate polymers in native starch with degree of polymerisation n was neglected ($n \cdot M_{w,g} \gg M_{w,w}$).

Calculation of dextrose equivalent

The carbohydrate composition determined with HPLC can be used to calculate the dextrose equivalent (*DE*) by using the following equation (Kiser and Hagy, 1979):

$$DE = DE_r + \sum_{i=1}^{6} x_{w,i} \cdot DE_i \tag{2A}$$

where DE_r is the overall contribution to the *DE* of all carbohydrates larger than a hexasaccharide, $x_{w,i}$ is the weight fraction of a maltooligosaccharide with a degree of polymerization i and DE_i is the individual contribution to the *DE* of maltooligosaccharides smaller than heptasaccharides (Kiser and Hagy, 1979). DE_r was calculated with the following equation based on the experimental data from Kiser and Hagy (1979):

$$DE_r = -0.002 \cdot x_{w,DP>6} + 0.207 \tag{2B}$$

This equation was derived by assuming a linear relationship between the weight fraction of carbohydrates (in %) larger than a hexasaccharide ($x_{w,DP>6}$) and the contribution of this group of carbohydrates to the dextrose equivalent, The validity of this procedure used to calculate the dextrose equivalent was checked with maltodextrins with known dextrose equivalent.

Measurement of the α-amylase activity

The ground, frozen samples were dissolved in 0.1 M maleic acid buffer (final concentration approximately 30 mg enzyme solution$\cdot l^{-1}$) and stored in ice water if necessary. The end-point assay procedure that we have used to measure the α-amylase activity is described elsewhere (Baks *et al.*, 2006a).

The Ceralpha method is often used to measure the residual α-amylase activity in a reaction mixture. The α-amylase activity v is defined as the amount of p-nitrophenol released in $\mu mol \cdot mg^{-1} \cdot min^{-1}$ of enzyme solution at 40 °C and pH 6.5 when only blocked p-

nitrophenyl maltoheptaoside is present. However, samples often contain various carbohydrates that affect the measurement of the α-amylase activity due to substrate inhibition and substrate competition (Baks *et al.*, 2006a, 2006b). The experimentally determined α-amylase activity (v') should be corrected for the presence of carbohydrates in the sample to obtain the true α-amylase activity (v):

$$v = v' \cdot \frac{C + \sum_{i=1}^{7} \left(U_{i,2} \cdot [DP_i] + U_{i,3} \cdot [DP_i]^2 \right)}{C \cdot \sum_{i=1}^{7} \left(1 + U_{i,1} \cdot [DP_i] \right)} \tag{3a}$$

where C (dimensionless), $U_{i,1}$ (in $l \cdot mol^{-1}$), $U_{i,2}$, (in $l \cdot mol^{-1}$) and $U_{i,3}$ (in $l^{-2} \cdot mol^{-2}$) are known parameters for maltooligosaccharides smaller than maltooctaose (Baks *et al.*, 2006b) and $[DP_i]$ is the concentration of maltooligosaccharides with a degree of polymerisation i present during the enzyme assay (in $mol \cdot l^{-1}$). The parameters $U_{i,1}$, $U_{i,2}$, and $U_{i,3}$ are not known for larger carbohydrates. If samples contain predominantly large carbohydrates (*DE* smaller than 21), a different model was used to obtain the true enzyme activity:

$$v = v' \cdot \frac{C + \dfrac{[j]}{K_{m,j}}}{C} \tag{3b}$$

where $[j]$ is the overall carbohydrate concentration during the enzyme assay (in $g \cdot l^{-1}$) and $K_{m,j}$ is the overall Michaelis-Menten parameters (in $l \cdot g^{-1}$) for a carbohydrate mixture with a certain dextrose equivalent. $K_{m,j}$ values were determined by using:

$$K_{m,j} = 0.096 \cdot DE + 0.629 \tag{4}$$

This equation is based upon K_m measurements from Baks *et al.* (2006a) and it is valid for carbohydrate mixtures with a DE smaller than 21.

Calculation of specific mechanical energy

The specific mechanical energy (SME) was calculated (in $J \cdot g^{-1}$) with the following equation:

$$SME = \frac{2\pi \cdot N/60 \cdot \tau}{F} \tag{5}$$

where N is the rotation speed of the screw (rpm), τ is the torque (Nm) and F is the total feed rate of the extruder ($g \cdot s^{-1}$).

Calculation of productivity

The productivity is defined as the number of glucosidic bonds that have been broken per unit total mass:

$$P = \frac{DE}{100} \cdot \frac{C_s}{100} \cdot \frac{1000}{M_{w,g}} \tag{6}$$

where C_s (w/w %) is the initial starch concentration.

Results

Gelatinisation in TSE

The temperatures required for complete gelatinisation of starch in 50, 60, and 70 w/w % starch-water mixtures (approximately 85, 105, and 130 °C, respectively) were predicted by the adapted Flory equation that was derived in a previous article (Baks *et al.*, 2007). The first extrusion experiments (G1-G7 in *Table 2*) were carried out with set point temperatures (T_5) below and above the predicted temperatures required for complete gelatinisation. Extrusion at all these temperatures resulted in complete gelatinisation of starch for the three different starch concentrations. Note that in the case of 60 w/w % starch in water, two screw speeds were used (100 and 150 rpm for respectively G5 and G4). We observed that at a screw speed of 100 rpm steady state operation of the extruder was reached much faster in comparison with 150 rpm, while the product was the same based on the degree of gelatinisation and the appearance of the extrudate. For that reason, it was decided to perform the gelatinisation of 70 w/w % starch-water mixtures at 100 rpm.

Table 2: Degree of gelatinisation (DG) and specific mechanical energy (SME) at various conditions in a corotating twin screw extruder in the absence of enzyme.

Experiment number [a]	C_s [b] [w/w %]	T_5 [c] [°C]	N [d] [rpm]	SME [10^2 J/g]	DG [%]	Hydrolysis experiment number [e]
G1	50	81	156	3.0	98	1
G2	51	94	150	3.3	93	2
G3	61	100	152	4.1	100	3
G4	60	120	153	4.9	100	4
G5 [f]	60 ± 1	120 ± 3	101 ± 3	5.5 ± 1.0	99 ± 1	5
G6	68	123	102	12.2	98	6
G7	68	142	101	11.8	98	7
G8	61	60	48	2.0	65	8
G9	61	60	73	3.4	75	9
G10	63	60	102	4.7	85	10
G11	61	80	48	2.5	92	11
G12	62	80	74	3.2	96	12
G13	62	78	102	5.0	98	13
G14	62	87	99	4.3	100	17, 18
G15	61	102	51	1.8	97	14
G16	60	98	76	2.5	100	15
G17	62	101	102	3.5	100	16

[a] Experiment number refers to the gelatinisation experiments in which no enzymes were added.

[b] Starch concentration based on dry weight of starch.

[c] Actual temperature in section 5.

[d] Rotation speed of screw.

[e] Hydrolysis experiment number refers to the hydrolysis experiments mentioned in *Table 3*, for which the same extrusion conditions were used to gelatinise starch and to mix the enzyme with starch followed by hydrolysis in a batch reactor.

[f] Gelatinisation experiment G5 was repeated three times (95 % confidence interval).

Because the degree of gelatinisation after extrusion was the same for all starch concentrations, the highest amount of gelatinised starch produced per unit of mass fed to the extruder was found at 70 w/w % wheat starch in water. However, although the screw speed was decreased to improve operation at 70 w/w %, it remained difficult to reach steady state operation without crossing the maximum torque value that resulted in

automatic shutdown of the extruder. For that reason, it was decided to focus on the gelatinisation of 60 w/w % starch-water mixtures.

The effect of screw speed during the extrusion of a 60 w/w % starch-water mixture was investigated at 60, 80, and 100 °C. The degree of gelatinisation increased with increasing screw speed at an extrusion temperature of 60 °C (*Table 2*: G8-G10). When a temperature of 80 °C was used (*Table 2*: G11-G13), the degree of gelatinisation was close to 100 % for all screw speeds used. These samples were all considered to be completely gelatinised, because the difference between these samples is close to the experimental error encountered with DSC measurements. After extrusion of 60 w/w % starch-water mixtures with a maximum temperature of 100 °C (*Table 2*: G15-G17), complete gelatinisation of starch was achieved at all screw speeds. According to gelatinisation experiments G8-G17, the degree of gelatinisation also increased when the extrusion temperature was increased (*Table 3*: for example G8 vs. G11, G9 vs. G12, and G10 vs. G13).

Hydrolysis of extrudates

After gelatinisation, starch-water slurries were mixed with α-amylase for the enzymatic hydrolysis. The effects of the substrate concentration, degree of gelatinisation, and enzyme to substrate ratio were investigated.

Effect of substrate concentration
Experiments 1-7 were used to determine the effect of the substrate concentration on the main output parameters of the enzymatic hydrolysis. When the enzyme to substrate ratio and hydrolysis time were kept constant, the dextrose equivalent decreased with increasing starch concentration (see *Table 3*). However, variation of the substrate concentration between 50 and 70 w/w % did not seem to affect the residual α-amylase activity.

The productivity (equation 6) was also used to compare the performance of our process at different substrate concentrations (average values were used). At low enzyme to substrate ratios (see *Table 3*: experiments 1-7), the productivity obtained after one hour of hydrolysis decreased when the substrate concentration was increased (0.8, 0.7, and 0.5 mmol·g^{-1} for respectively 50, 60, and 70 w/w %). At high enzyme to substrate ratios, the highest productivity obtained after one hour of hydrolysis was found at 60 w/w % (1.1, 1.2, and 0.5 mmol·g^{-1} for respectively 50, 60, and 70 w/w %). After 24 h, hydrolysis of starch in a 60 w/w % starch-water mixture resulted in the highest productivity at both low (1.3, 1.4, and

1.2 mmol·g^{-1} for respectively 50, 60, and 70 w/w %) and high enzyme to substrate ratios (1.4, 1.6, 1.4 mmol·g^{-1} for respectively 50, 60, and 70 w/w %).

Effect of degree of gelatinisation

During experiments 1-7, completely gelatinised starch was used as a substrate for the enzymatic hydrolysis. However, in the second set of hydrolysis experiments (experiments 8-16) the starch extrudate used for the enzymatic hydrolysis was not completely gelatinised. The degree of gelatinisation varied from 65 to 100 % (*Table 3*). During the experiments, it was found that the dextrose equivalents obtained after enzymatic hydrolysis did not depend on the degree of gelatinisation of the substrate. In addition, the residual α-amylase activity was not affected by changes in the degree of gelatinisation.

Effect of enzyme to substrate ratio

Increasing the enzyme to substrate ratio resulted in an increased dextrose equivalent obtained after enzymatic hydrolysis for all cases reported in *Table 3* (except for experiment 6). The same trend was observed after measuring the dextrose equivalent during the hydrolysis of 60 w/w % wheat starch-water mixtures with three different enzyme to substrate ratios (*Figure 2*). The initial slopes of the dextrose equivalent vs. time curves (0.11, 0.58 and 1.98 min^{-1}) were proportional to the enzyme to substrate ratios (respectively 0.1, 0.5, and 2.5 w/w %). Furthermore, the dextrose equivalents obtained after 3 h were smaller than the dextrose equivalents obtained after 24 h of hydrolysis for the same enzyme dosage indicating that the hydrolysis reaction was not finished after 3 h.

Table 3: Effect of processing conditions on starch hydrolysis and α-amylase stability at 90 °C.

Hydr. exp. number [a]	C_s [b] [w/w %]	C_e/C_s [c,h] [w/w %]		SME [d,h] $[10^2 \text{ J/g}]$		DE_0 [e,h] [1]		DE_1 [f,h] [-]		DE_{24} [f,h] [-]		A_1/A_0 [g,h] [%]		A_{24}/A_0 [g,h] [%]	
1	50	0.5	2.2	2.7	2.6			27	33	41	43	79[i]	89[i]	47[i]	31[i]
2	51	0.5	2.2	2.2	2.1			26	35	41	48	106[i]	125[i]	60[i]	59[i]
3	60	0.5	2.5	4.9	4.5		9	21	31	36	46	105	84	63	62
4	60	0.5		4.6		2		21		34		102		72	
5	60	0.6	2.4	4.9	4.9	1	4	15	32	41	43	32	86	129	
6	69	0.6	2.4	13.6	9.9	2	4	12	9	22	31	56	54	18	80
7	69	0.6	2.5	10.2	10.3	1	8	12	14	33	36	70	52	59	63
8	61	0.5	2.4	1.7	1.8	1	5	20	30			79	99		
9	61	0.6	2.3	3.1	3.2	1	4	22	34			65	112		
10	61	0.5	2.4	4.3	3.7	1	6	22	33			63	101		
11	60	0.5	2.5	2.1	1.9	2	6	21	37	44	57	85	90	72	75
12	62	0.5	2.3	2.9	2.9	2	6	22	28			47	87		
13	61	0.5	2.5	1.6	1.5	1	6	18	40	43	55	107	94	84	88
14	62	0.5	2.2	3.9	4.1	2	6	18	32			52	79		
15	61	0.5	2.4	3.5	3.6	1	5	21	32	40	44	97	91	63	69
16	61	0.5	2.5	2.5	2.9	1	6	23	35	41	53	116	109	102	65
17	61	0.5	2.5	3.7	3.2	1	6	27	36	41	53	57[j]	81	52	67
18	61	0.1		4.0		0		8		32		102		36	

[a] Hydr. Exp. number refers to the hydrolysis experiments, for which the extrusion conditions mentioned in *Table 2* were used to gelatinise starch and to mix the enzyme with starch.

[b] Starch concentration based on dry weight of starch.

[c] Enzyme to substrate ratio.

[d] Specific mechanical energy during the extrusion process.

[e] Dextrose equivalent of the extrudate used as starting material for the batch hydrolysis.

[f] DE_1 and DE_{24} are the dextrose equivalent obtained after respectively 1 h and 24 h of hydrolysis.

[g] Residual activity of α-amylase after respectively 1 h and 24 h of hydrolysis. A_0 is the α-amylase activity in the mixture flowing out of the extruder used as starting material for the batch hydrolysis.

[h] The columns belonging to experiments 1-3 and 5-17 contain two values; one for a low enzyme to substrate ratio (left number in column) and the other one for a high enzyme to substrate ratio (right number in column).

[i] A_0 was not measured in 50 w/w % extrudate. A_0 in 60 w/w % extrudate with the same enzyme to substrate ratio was used for calculation of residual enzyme activity.
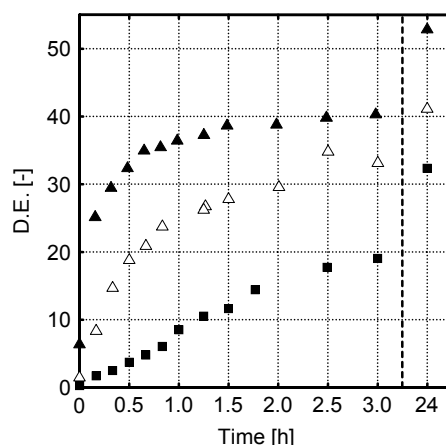
[j] Sample was taken after 76 min.

Figure 2: Dextrose equivalent as a function of hydrolysis time for three different enzyme to substrate ratios after gelatinisation (Table 2: G14). Symbols used: ▲ = 2.5 w/w %; △ = 0.5 w/w %; ■ = 0.1 w/w %. Hydrolysis conditions: α-amylase from B. licheniformis, 90 °C, 62 w/w % wheat starch in water, 70 ppm CaCl$_2$.

Although the dextrose equivalent gives some insight into the carbohydrate composition, additional data was required to specify the composition of the hydrolysate. *Figures 3A-3D* show the concentration of maltooligosaccharides with a degree of polymerisation smaller than 8 as a function of time for enzyme to substrate ratios of 0.1 (*Figures 3A* and *3B*) and 2.5 w/w % (*Figures 3C* and *3D*). During the first 3 h of hydrolysis with a low enzyme to substrate ratio, the concentrations of all maltooligosaccharides (except for heptasaccharides) shown in *Figures 3A-3B* increased in time. Between 3 h and 24 h of hydrolysis, the hexasaccharide and heptasaccharide concentrations decreased, which indicates that these components are broken down after 3 h of hydrolysis. At a higher enzyme to substrate ratio, the concentration of maltooligosaccharides smaller than a pentasaccharide increased during the first 3 h of hydrolysis. The concentration of pentasaccharides, hexasaccharides and heptasaccharides first increased, followed by a decrease in concentration (*Figure 4D*). The concentrations of these compounds decreased faster when the chain length was larger. After 24 h of hydrolysis with an enzyme to substrate ratio of 0.1 w/w %, 74 % of the initial substrate was converted into maltooligosaccharides with a degree of polymerisation smaller than 8 of which 40 mol % consists of glucose, maltose and maltotriose (*Figure 3A*). At an enzyme to substrate ratio of 2.5 w/w %, nearly all of the substrate was converted into maltooligosaccharides with a degree of polymerisation smaller than 8. In this case, the yield

of glucose, maltose and maltotriose was equal to 67 mol % (*Figure 3C*). Although the enzyme to substrate ratio affected the dextrose equivalent and the yield of maltooligosaccharides during hydrolysis, it did not seem to affect the residual α-amylase activities that were measured after 1 h and after 24 h of hydrolysis.
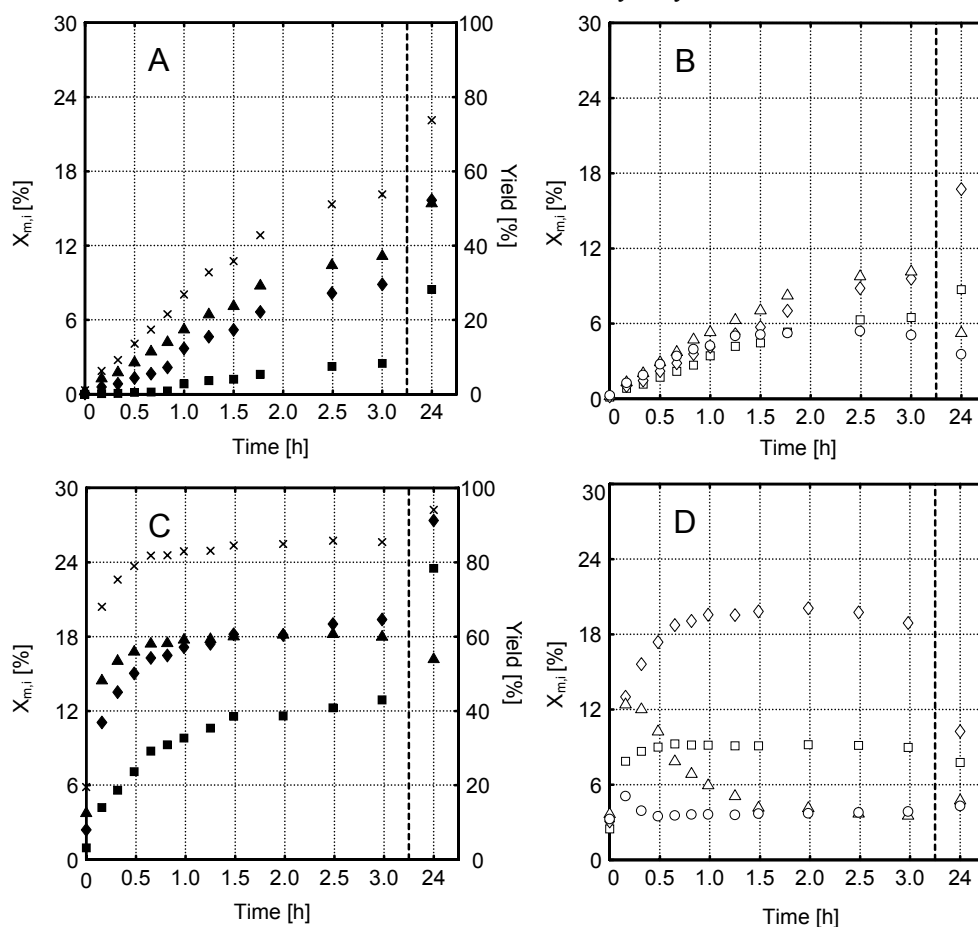
Figure 3: Concentration of glucose (■), maltose (◆), maltotriose (▲), and overall yield of maltooligosaccharides with a degree of polymerisation from 1 to 7 (✖) [Figures 3A and 3C]; and concentration of tetrasaccharide (□), pentasaccharide (◇), hexasaccharide (△), and heptasaccharide (○) [Figures 3B and 3D] as a function of time during the hydrolysis of wheat starch. Enzyme to substrate ratios of 0.1 w/w % [Figures 3A and 3B] and 2.5 w/w % [Figures 3C and 3D] were used. The gelatinisation conditions are mentioned in Table 2, experiment G14. Hydrolysis conditions: α-amylase from B. licheniformis, 90 °C, 62 w/w % wheat starch in water, 70 ppm CaCl₂.

Discussion

Gelatinisation in TSE

During the gelatinisation experiments, the maximum temperature in the extruder was chosen to be 5-10 °C below the temperature required for complete thermal gelatinisation that was predicted in a previous publication (Baks *et al.*, 2007). Use of these temperatures resulted in complete gelatinisation of starch in the extruder. The adapted Flory equation therefore provides a high estimate for the temperature needed to completely gelatinise starch when shear forces are applied.

During the gelatinisation experiments, it was found that the degree of gelatinisation increased with an increasing temperature, an increasing screw speed (at 60 °C), and a decreasing starch concentration. The effect of temperature on the degree of gelatinisation was also observed by Cai and Diosady (1993), Lee and Kim (1990), and Zheng and Wang (1994). An increased degree of gelatinisation after increasing the screw speed was observed by Zheng and Wang (1994) as well. Contrary to our findings, Cai and Diosady (1993) and Gomez and Aguilera (1983, 1984) found that the degree of gelatinisation increased with a decreasing moisture content, when high screw speeds (200-750 rpm) and low moisture contents (8-33 w/w %) were used. It seems that during gelatinisation at our extrusion conditions (screw speed range: 50-150 rpm; moisture content: 30-50 w/w %), two phenomena took place that had an opposite effect. On the one hand, decreasing the moisture content decreased the degree of thermal gelatinisation. This trend has been observed by several researchers in the case where no mechanical forces were applied (e.g. Baks *et al.*, 2007, Blanche and Sun, 2004; Donovan, 1979). On the other hand, a decrease in the moisture content increased the viscosity leading to a higher SME input. In turn, a higher SME input increases the degree of (mechanical) gelatinisation (Barron *et al.*, 2001; Van den Einde *et al.*, 2004). According to Barron *et al.* (2001), application of mechanical forces (including shear forces) leads to disruption of the starch granules. In turn, disruption of the granules leads to disruption of the granular structure and for that reason it might lead to a loss of order that also takes place in the case of gelatinisation. Application of higher mechanical forces (either by lowering the moisture content or increasing the screw speed) in combination with thermal treatment seems to lower the temperature needed for complete loss of order leading to complete gelatinisation in comparison to gelatinisation without the application of mechanical forces.

Complete gelatinisation can be achieved in a TSE at low temperatures in comparison with gelatinisation in a reactor in which mechanical forces are not applied. When the screw speed is increased, the temperature at which complete gelatinisation is reached can be decreased further due to the mechanical forces applied on the material. However, increasing the screw speed leads to a higher SME input and might therefore result in enzyme deactivation during mixing of the enzyme solution with the starch-water mixture. On the other hand, an increased screw speed might also result in less enzyme deactivation as the increased screw speed might decrease the residence time in the extruder. If enzyme deactivation cannot be permitted, a low screw speed should be used to lower the mechanical forces applied on the material. When the SME input is kept at a minimum, a higher extrusion temperature is required to achieve complete gelatinisation. Moreover, a longer extruder is required, because a cooling section is needed prior to the section at which the gelatinised starch slurry is mixed with the enzyme.

Preliminary experiments with a compression molder indicated that the final degree of gelatinisation was reached directly after the set point temperature was reached (results not shown). Apparently, it is not necessary to hold the starch-water mixture at a certain temperature for a minimum amount of time. For that reason, it is expected that a shorter extruder can be used for the gelatinisation step in comparison with the extruder that we have used. The length of the extruder can be decreased further, when it is operated at a low temperature together with a high screw speed. In that case, less heating sections are required for heating the contents to the desired set point temperature.

Hydrolysis of extrudates

During the hydrolysis experiments, we observed that the dextrose equivalent decreased when the substrate concentration was increased. The K_m value of α-amylase from *B. licheniformis* for starch is equal to 1.2 g·l^{-1} (Asther and Meunier, 1990) and it is independent of temperature (Dobreva *et al.*, 1994). The substrate concentration used during our hydrolysis experiments is much larger than K_m. For that reason, the initial reaction rate was expected to be approximately equal to V_{max} (based on the Michaelis-Menten equation). As a result, the same dextrose equivalent would be obtained after a short hydrolysis time, because the starch feed rate to the extruder was equal for all starch concentrations. However, increasing the starch concentration at a constant enzyme to substrate ratio resulted in a lower dextrose equivalent after equal hydrolysis time. This behaviour might be explained by assuming that diffusion limitation takes place due to an increased viscosity

caused by an increasing substrate concentration. Cheng and Prud'Homme (2000) found that diffusion limitation took place during the enzymatic hydrolysis of guar polysaccharides at higher substrate concentrations leading to a decrease of the initial hydrolysis rate. The enzymatic hydrolysis reactions of starch and guar polysaccharides were assumed to be similar, because both systems consist of an enzyme in a highly viscous polysaccharide-water mixture (Lindsay, 1996). Yankov *et al.* (1986) found that starch concentrations above 300 g·l^{-1} resulted in inhibition of the starch hydrolysis reaction catalysed by α-amylase from *B. licheniformis*. In addition, they found that addition of glucose resulted in a lower rate of hydrolysis. A decreased reaction rate caused by a higher substrate concentration might therefore also be explained by considering product inhibition. Based on the dextrose equivalent, it seems that increasing the substrate concentration is not always beneficial. However, the productivity increased in most cases when the substrate concentration was increased from 50 to 60 w/w %.

Although the dextrose equivalent and productivity were affected by changes in the substrate concentration, the observed concentration profile of carbohydrates smaller than maltooctaose remained approximately the same. The maltooligosaccharide profile that was obtained during the enzymatic hydrolysis at 60 w/w % and 90 °C with an enzyme to substrate ratio of 2.5 w/w % is comparable to the profile observed when a 10 w/w % wheat starch solution is hydrolysed at 90 °C with 0.7 w/w % α-amylase from *B. licheniformis* (unpublished results) and when a 10 w/w % cassava starch solution was hydrolysed at 80 °C with 1.2 w/w % α-amylase from *B. licheniformis* (Paolucci-Jeanjean *et al.*, 2000). It seems that increasing the substrate concentration does not affect the selectivity of the enzymatic hydrolysis process.

Based on the findings of Planchot *et al.* (1997) and Tester and Sommerville (2000), it was expected that ungelatinised or crystalline starch would not be hydrolysed completely by α-amylase. Consequently, it was expected that the dextrose equivalent obtained after enzymatic hydrolysis would be affected by the degree of gelatinisation. Such an effect of degree of gelatinisation was not observed during our experiments, probably because we have used a higher hydrolysis temperature (90 °C) in comparison with Planchot *et al.* (1997) (25 °C) and Tester and Sommerville (2000) (40-70 °C). In our case, the hydrolysis temperature was higher than the onset temperature of gelatinisation (Baks *et al.*, 2007) and for that reason both gelatinisation and hydrolysis might have taken place in the hydrolysis vessel. As long as the amount of gelatinised starch is abundant during the time required to reach complete gelatinisation in the hydrolysis vessel, the degree of gelatinisation will not

affect the dextrose equivalent obtained after enzymatic hydrolysis. These results can also be explained by considering the work of Barron *et al.* (2001), Helbert *et al.* (1996) and Kong *et al.* (2003). Barron *et al.* (2001) found that mechanical forces can disrupt the granules and granular structure. Helbert *et al.* (1996) proposed that enzymatic degradation of starch granules with α-amylase from *B. licheniformis* starts with the adsorption of the enzymes randomly at the surface of the granules. Kong *et al.* (2003) found that the reciprocal of the initial hydrolysis rate of porcine pancreatic α-amylase increases linearly with the specific surface area of starch granules. Assuming that the results of Kong *et al.* (2003) also hold for α-amylase from *B. licheniformis*, mechanical break down of the granules increases the specific surface area of the substrate. In turn, the accessibility of the granules to α-amylase and water are increased and this might lead to a higher reaction rate. The increased surface area that was created by the application of mechanical forces might cancel out the effect of a lower degree of gelatinisation of the substrate. For that reason, the yield after the enzymatic hydrolysis step will be high when the starch granules are completely gelatinised or their granular structure is broken down during the gelatinisation step prior to hydrolysis.

The dextrose equivalents increased with an increasing enzyme to substrate ratio. The proportionality between the initial slopes of the dextrose equivalent vs. time curves and the enzyme to substrate ratios was expected, because the initial slope of the dextrose equivalent vs. time curves can be used as a measure of the initial enzyme activity, which depends linearly on the enzyme to substrate ratio. The slight deviation at an enzyme to substrate ratio of 2.5 w/w % can be explained by the initial frequency of measurement points, which is too low to determine the initial reaction rate accurately. Roussel *et al.* (1991) also observed that the dextrose equivalent of the product flowing out of the extruder increased after increasing the enzyme to substrate ratio in the extruder. The dextrose equivalents that they observed were higher, because a larger part of the enzymatic hydrolysis reaction was also carried out in the extruder.

The substrate concentration, degree of hydrolysis, and enzyme to substrate ratio did not affect the residual α-amylase activity. For this reason, all measurements (1-18, see *Table 3*) can be used to calculate the average residual α-amylase activity, which was equal to 84 and 67 % after 1 h and 24 h of hydrolysis, respectively. When a 20 w/w % wheat starch-water mixture was used as a starting point for the enzymatic hydrolysis, the residual α-amylase activity measured after 1 h and 24 h was equal to, respectively, 63 and 2 %. The stability of the enzyme therefore increased when the enzymatic hydrolysis of starch was carried out at a starch concentration of 50-70 w/w % instead of 20 w/w %. For that reason, use of higher

147

substrate concentrations seems to have potential for a future process for the enzymatic hydrolysis.

The residual α-amylase activities that were measured after 1 h and after 24 h of hydrolysis for hydrolysis experiments, in which the carbohydrate composition and degree of gelatinisation of the substrate were equal, showed some variation (e.g. 15, 16, and 17 in *Table 3*). Although the carbohydrate composition and degree of gelatinisation of the substrate were approximately the same, the properties of the samples seemed to differ (as assessed during visual inspection and handling of the samples), probably because the extrusion conditions were not the same. We suspect that these differences in the nature of the samples affected the sample preparation leading to differences in the α-amylase activity measurements.

Process design considerations

Komolprasert and Ofoli (1991b) used the same process setup and similar conditions as those in the current study (50 w/w % pre-gelatinised starch, hydrolysis temperature 95 °C, enzyme to substrate ratio 0.2 w/w %). The dextrose equivalent that was obtained after 24 h of hydrolysis was approximately the same as the value that they found (*Table 3*: 1 and 2). Although the shapes of the dextrose equivalent vs. time curves obtained by others that used the same setup were comparable (Chouvel *et al.*, 1983; Komolprasert and Ofoli, 1991b; Linko *et al.*, 1980; Reinikainen *et al.*, 1986), the absolute values were different (after 3 h respectively: 49, 31, 14, and 13). Chouvel *et al.* (1983), Linko *et al.* (1980), and Reinikainen *et al.* (1986) used the same enzyme (Termamyl 60 L) and a moisture content of 50 w/w %, but the extrusion temperatures (respectively, 112, 112 and 125 °C), enzyme to substrate ratios (respectively, 0.36, 0.36, and 3.6 w/w %), screw speeds (respectively, 150, 150, and 25 rpm), and starch types (barley, barley, and corn starch) were different. Since the extrusion temperatures were high enough to completely gelatinise 50 w/w % starch-water mixtures in the absence of mechanical forces (according to DSC data from Ellis *et al.*, 1998), the degree of gelatinisation was equal to 100 % in all cases. Differences in the screw speed could result in a different residual α-amylase activity after extrusion. However, the differences in the enzyme to substrate ratios probably caused the differences in the dextrose equivalent. Besides our own results, comparison of the experiments of Chouvel *et al.* (1983), Linko *et al.* (1980), and Reinikainen *et al.* (1986) showed that the enzyme to substrate ratio is an important parameter. For a future industrial process, the most suitable enzyme concentration will depend on the user's preference; a higher enzyme to substrate

ratio will decrease the time required for the hydrolysis reaction making it possible to carry out more batch hydrolysis reactions in the same amount of time, but it increases the amount of enzyme that is required.

Grafelman and Meagher (1995) and Meagher and Grafelman (1999) used an extruder for gelatinisation and a static mixer (Gahlstrom *et al.*, 1997) for mixing the enzyme with a corn starch-water mixture and for liquefaction and compared this setup with a conventional jet cooker system. They obtained a maximum dextrose equivalent of approximately 6 with their process, which is comparable to the dextrose equivalent obtained after using a jet cooker. Although they gelatinised a starch-water mixture with 17 w/w % moisture content at 120 °C, which was approximately 40 °C too low to reach complete gelatinisation if mechanical forces were not applied (Blanche and Sun, 2004), a screw speed of 140 rpm was assumed to be sufficient to provide complete gelatinisation or complete break down of the granular structure providing a substrate that can be hydrolysed completely. It was therefore expected that the gelatinisation conditions will not be the limiting factor to reach higher dextrose equivalents. Grafelman and Meagher (1995) also mentioned that an increased length of the static mixer results in a higher dextrose equivalent. In addition, it will lead to better mixing and a more homogeneous reaction mixture. For those reasons, it seems that increasing the length of the static mixer or adding a tube reactor behind the static mixer to increase the residence time for the hydrolysis reaction, yields a continuous process that produces hydrolysates with a high dextrose equivalent. In addition, use of a static mixer instead of mixing the enzyme in the extruder might lead to a higher residual α-amylase activity, because the mechanical forces applied to the enzyme are probably lower in a static mixer compared to an extruder.

This study has shown that extrusion processes at higher substrate concentrations are feasible. Although we have focussed on a process that is based on 60 w/w % wheat starch in water, it is still possible that this process can also be carried out at higher starch concentrations. Perhaps a steady state operation might have been reached faster at higher starch concentrations (70 w/w % or more) and a lower screw speed. In addition, increasing the enzyme concentration might lower the effect of diffusion limitation and it might lead to a higher productivity in comparison with operation at lower starch concentrations.

Measurement of the degree of gelatinisation, the enzyme activity, carbohydrate composition, dextrose equivalent, and residual α-amylase activity is very useful for the investigation of a process for the conversion of native starch to small oligosaccharides. Moreover, the results in this article provide a basis for detailed optimisation of the gelatinisation and enzymatic hydrolysis at high substrate concentrations to develop an

industrial-scale process. The use of different enzymes or a combination of enzymes should be considered as well. In addition, more alternatives for the batch hydrolysis reactor (besides the static mixer) that can be operated in a continuous fashion should be considered.

Acknowledgements

References

Asther M, Meunier JC. 1990. Increased thermal stability of *Bacillus licheniformis* α-amylase in the presence of various sugars. Enzyme Microb Tech 12:902-905.

Baks T, Janssen AEM, Boom RM. 2006a. The effect of carbohydrates on α-amylase activity measurements. Enzyme Microb Technol 39:114-119.

Baks T, Janssen AEM, Boom RM. 2006b. A kinetic model to explain the maximum in α-amylase activity measurements in the presence of small carbohydrates. Biotechnol Bioeng 94:431-440.

Baks T, Ngene IS, Van Soest JJG, Janssen AEM, Boom RM. 2007a. Comparison of methods to determine the degree of gelatinisation for both high and low starch concentrations. Carbohydr Polym 67:481-490.

Barron C, Bouchet B, Della Valle G, Gallant DJ, Planchot V. 2001. Microscopical study of the destructering of waxy maize and smooth pea starches by shear and heat at low hydration. J Cereal Sci 33:289-300.

Blanche S, Sun X. 2004. Physical characterization of starch extrudates as a function of melting transitions and extrusion conditions. Adv Polym Tech 23:277-290.

Cai W, Diosady LL. 1993. Model for gelatinization of wheat starch in a twin-screw extruder. J Food Sci 58:872-875, 887.

Cai W, Diosady LL, Rubin LJ. 1995. Degradation of wheat starch in a twin-screw extruder. J Food Eng 26:289-300.

Cheng Y, Prud'Homme RK. 2000. Enzymatic degradation of guar and substituted guar galactomannans. Biomacromolecules 1:782-788.

Chouvel H, Chay PB, Cheftel JC. 1983. Enzymatic hydrolysis of starch and cereal flours at intermediate moisture contents in a continuous extrusion-reactor. Lebensmittel-Wissenschaft und -Technologie 16:346-53.

Colonna P, Doublier JL, Melcion JP, De Monredon F, Mercier C. 1984. Extrusion cooking and drum drying of wheat starch. I. Physical and macromolecular modifications. Cereal Chem 61:538-543.

Ćurić D, Karlović D, Tripalo B, Ježek D. 1998. Enzymatic conversion of corn starch in twin-screw extruder. Chem Biochem Eng Q 12:63-71.

Davidson VJ, Paton D, Diosady LL, Rubin LJ. 1984. A model for mechanical degradation of wheat starch in a single-screw extruder. J Food Sci 49:1154-1157.

De Cordt S, Hendrickx M, Maesmans G, Tobback P. 1994. The influence of polyalcohols and carbohydrates on the thermostability of α-amylase. Biotechnol Bioeng 43:107-114.

Dobreva E, Ivanova V, Emanuilova E. 1994. Effect of temperature on some characteristics of the thermostable α-amylase from *Bacillus licheniformis*. World J Microbiol Biotechnol 10:547-550.

Donovan JW. 1979. Phase transitions of the starch-water system. Biopolymers 18:263-275.

Ellis RP, Cochrane MP, Dale MFB, Duffus CM, Lynn A, Morrison IM, Prentice RDM, Swanston JS, Tiller SA. 1998. Starch production and industrial use. J Sci Food Agric 77:289-311.

Gahlstrom DA, Bennett RC, Emmett RC, Harriott P, Laros T, Leung W, McCleary C, Miller SA, Morey B, Oldshue JY, Priday G, Silverblatt CE, Slottee JS, Smith JC, Todd DB. 1997. Liquid-solid operations and equipment. In: Perry RH, Green DW, Maloney JO, editors. Perry's chemical engineers' handbook (7th edition). New York: McGraw-Hill. 2581 p.

Gomez MH, Aguilera JM. 1983. Changes in the starch fraction during extrusion-cooking of corn. J Food Sci 48, 378-381.

Gomez MH, Aguilera JM. 1984. A physicochemical model for extrusion of corn starch. J Food Sci 49:40-43,63.

Govindasamy S, Campanella OH, Oates CG. 1997a. Enzymatic hydrolysis of sago starch in a twin-screw extruder. J Food Eng 32:403-426.

Govindasamy S, Campanella OH, Oates CG. 1997b. The single screw extruder as a bioreactor for sago starch hydrolysis. Food Chem 60:1-11.

Grafelman DD, Meagher MM. 1995. Liquefaction of starch by a single-screw extruder and post-extrusion static-mixer reactor. J Food Eng 24:529-542.

Helbert W, Schulein M, Henrissat B. 1996. Electron microscopic investigation of the diffusion of *Bacillus licheniformis* α-amylase into corn starch granules. Int J Biol Macromol 19:165-169.

Jackson DS, Gomez MH, Waniska RD, Rooney LW. 1990. Effects of single-screw extrusion cooking on starch as measured by aqueous high-performance size-exclusion chromatography. Cereal Chem 67:529-532.

Kennedy JF, Cabalda VM, White CA. 1988. Enzymic starch utilization and genetic engineering. Trends Biotechnol 6:184-189.

Kiser DL, Hagy RL. 1979. Estimation of dextrose equivalent value of starch hydrolysates from liquid chromatographic profiles. In: Charalambous G, editor. Liquid chromatographic analysis of food and beverages (volume 2). New York: Academic press. 363-378.

Klibanov AM. 1983. Stabilization of enzymes against thermal inactivation. Adv Appl Microbiol 29:1-28.

Komolprasert V, Ofoli RY. 1991a. A dispersion model for predicting the extent ofstarch liquefaction by *Bacillus licheniformis* α-amylase during reactive extrusion. Biotechnol Bioeng 37:681-690.

Komolprasert V, Ofoli RY. 1991b. Starch hydrolysis kinetics of *Bacillus licheniformis* α-amylase. J Chem Technol Biotechnol 51:209-223.

Kong B-W, Kim J-I, Kim M-J, Kim JC. 2003. Porcine pancreatic α-amylase hydrolysis of native starch granules as a function of granule surface area. Biotechnol Progr 19:1162-1166.

Lee YC, Kim KT. 1990. Gelatinization and liquefaction of starch with a heat stable α-amylase. J Food Sci 55:1365-1366, 1372.

Lindsay RC. 1996. Food Additives. In: Fennema OR, editor. Food chemistry (3rd edition). New York: Marcel Dekker. 767-823.

Linko P, Linko Y-Y, Olkku J. 1983. Extrusion cooking and bioconversions. J Food Eng 2:243-257.

Linko Y-Y, Vuorinen H, Olkku J, Linko P. 1980. The effect of HTST-extrusion on retention of cereal α-amylase activity and on enzymatic hydrolysis of barley starch. In: Linko P, Larinkari J, editor. Food process engineering. Vol. 2: Enzyme engineering in food processing. London: Applied Science Publishers. 210-23.

Linko P, Colonna P, Mercier C. 1981. High-temperature, short-time extrusion cooking. In: Pomeranz Y, editor. Advances in Cereal Science and Technology (volume 4). St. Paul: AACC. 145-235.

Meagher MM, Grafelman DD. 1999. Method for liquefaction of cereal grain starch substrate and apparatus therefor. U.S.patent 5,981,237.

Nebesny E, Rosicka J, Tkaczyk M. 2002. Effect of enzymatic hydrolysis of wheat starch on amylose-lipid complexes stability. Starch/Stärke 54:603-608.

Paolucci-Jeanjean D, Belleville M-P, Zakhia N, Rios GM. 2000. Kinetics of cassava starch hydrolysis with termamyl enzyme. Biotechnol Bioeng 68:71-77.

Planchot V, Colonna P, Buleon A. 1997. Enzymatic hydrolysis of α-glucan crystallites. Carbohydr Res 298:319-326.

Reinikainen P, Suortti T, Olkku J, Mälkki Y, Linko P. 1986. Extrusion cooking in enzymatic liquefaction of wheat starch. Starch/Stärke 38:20-26.

Roussel L, Vieille A, Billet I, Cheftel JC. 1991. Sequential heat gelatinization and enzymatic hydrolysis of corn starch in an extrusion reactor. Optimization for maximum dextrose equivalent. Lebensmittel-Wissenschaft und -Technologie 24:449-458.

Tester RF, Sommerville MD. 2000. Swelling and enzymatic hydrolysis of starch in low water systems. J Cereal Sci 33:193-203.

Van der Maarel MJEC, Van der Veen B, Uitdehaag JCM, Leemhuis H, Dijkhuizen L. 2002. Properties and applications of starch-converting enzymes of the α-amylase family. J Biotechnol 94:137-155.

Van den Einde RM, Bolius A, Van Soest JJG, Janssen LPBM, Van der Goot AJ, Boom RM. 2004. The effect of thermomechanical treatment on starch breakdown and the consequences for process design. Carbohydr Polym 55:57-63.

Van Zuilichem DJ, Van Roekel GJ, Stolp W, Van 't Riet K. 1990. Modelling of the enzymatic conversion of cracked corn by twin-scew extrusion cooking. J Food Eng 12:13-28.

Vasanthan T, Yeung J, Hoover R. 2001. Dextrinization of starch in barley flours with thermostable α-amylase by extrusion cooking. Starch/Stärke 53:616-622.

Yankov D, Dobreva E, Beschkov V, Emanuilova E. 1986. Study of optimum conditions and kinetics of starch hydrolysis by means of thermostable α-amylase. Enzyme Microb Technol 8:665-667.

Zheng X, Wang SS. 1994. Shear induced starch conversion during extrusion. J Food Sci 59:1137-1143.

Chapter 8

A stochastic model for predicting dextrose equivalent and saccharide composition during enzymatic starch hydrolysis

Abstract

A stochastic model was developed that was used to describe the formation and breakdown of all saccharides involved during α-amylolytic starch hydrolysis in time. This model is based on the subsite maps found in literature for *Bacillus amyloliquefaciens* α-amylase (BAA) and *Bacillus licheniformis* α-amylase (BLA). Carbohydrate substrates were modelled in a relatively simple two-dimensional matrix. The predicted weight fractions of carbohydrates ranging from glucose to heptasaccharides and the predicted dextrose equivalent showed the same trend and order of magnitude as the corresponding experimental values. However, the absolute values were not the same. In case a well defined substrate such as maltohexaose was used, comparable differences between the experimental and simulated data were observed indicating that the substrate model for starch does not cause these deviations. After changing the subsite map of BLA and the ratio between the time required for a productive and a non-productive attack for BAA, a better agreement between the model data and the experimental data was observed. Although the model input should be improved for more accurate predictions, the model can already be used to gain knowledge about the concentrations of all carbohydrates during hydrolysis with an α-amylase. In addition, this model also seems to be applicable to other depolymerase-based systems.

Introduction

The hydrolysis of starch by amylolytic enzymes is one of the most important enzymatic processes on industrial scale. Starch can be completely hydrolyzed to produce glucose syrups or, alternatively, it can be partly hydrolyzed to yield maltodextrins. Many models have been developed to predict the concentrations of the different hydrolysis products and to optimize the hydrolysis process. These models can be roughly divided into two groups.

The first group of models is based on continuous (differential) equations (Brandam *et al.*, 2003; Komolprasert and Ofoli, 1991; Kusunoki *et al.*, 1982; Park and Rollings, 1994; Rodríguez *et al.*, 2006a; Rollings and Thompson, 1984) or empirical relations (Paolucci-Jeanjean *et al.*, 2000) for the description of the enzymatic starch hydrolysis. Most of these models only predict the breakdown and/or formation of a limited number of carbohydrates, because each prediction requires a differential equation or empirical relation. The number of predictions that can be made is therefore limited to computational power. In addition, the parameters in the equations have to be obtained by fitting model output to the experimental data. This type of kinetic modelling is therefore also limited to data that can be obtained with measurements and it is only valid for specific experimental conditions.

The other group of models simulates the hydrolysis process by translating each hydrolysis reaction into a discrete event (Marchal *et al.*, 2003; Nakatani, 1996; Wojciechowski *et al.*, 2001). During each event, a carbohydrate is chosen randomly to form a complex with the enzyme. Whether a bond in the carbohydrate is hydrolyzed, depends on enzyme characteristics. It is important that the substrate and the enzyme specificities are clearly defined in order to make accurate predictions of product profiles. This stochastic method can be used to describe the formation and breakdown of all carbohydrates without determination of numerous parameters and evaluation of large numbers of (dependent) equations. Contrary to the output of the first group of kinetic models, the output of the second group can vary even though the input parameters are kept the same, which resembles real-life hydrolysis.

An example of the models belonging to the second group is the stochastic model developed by Wojciechowski *et al.* (2001). They used the Monte Carlo method to describe the products formed during multi-enzymatic starch hydrolysis in time. They proposed that each enzyme has a certain reaction time and specificity for hydrolysis (e.g. hydrolysis near a branch point is not possible). Differences in substrate affinities were not taken into account. Furthermore, the authors did not focus on the amylopectin and amylose model structure (e.g. percentage of branched glucose units and chain length distribution). The

validity of their model was evaluated by comparing the reducing power of the reaction mixture predicted by the model with the experimental values at various points in time.

Another model belonging to the second group was developed by Marchal *et al.* (2001; 2003). These authors proposed a method to model amylopectin and the subsequent α-amylolysis by *Bacillus amyloliquefaciens* α-amylase. They used stochastic Monte Carlo simulation in combination with the subsite theory (Allen and Thoma, 1976a; 1976b; MacGregor and MacGregor, 1985) to describe the carbohydrate composition as a function of the dextrose equivalent (DE). The data obtained with the model simulations were compared to experimental data for the formation and breakdown of carbohydrates up to a degree of polymerization (DP) of 10. With the model of Marchal *et al.* (2003), it is possible to predict the carbohydrate composition at a certain dextrose equivalent. However, it was not possible to predict the concentration of hydrolysis products in time.

Although several models have thus been developed to describe enzymatic starch hydrolysis, a kinetic model that takes the structure and composition of starch into account and that predicts the concentration of all carbohydrates in time has not been developed yet.

The aim of this article was to develop a stochastic model to predict the formation and breakdown of all carbohydrates involved in the amylolytic hydrolysis of amylopectin and amylose in time with a minimum number of experiments. The subsite maps of *Bacillus licheniformis* α-amylase (BLA) from Kandra *et al.* (2002) and of *Bacillus amyloliquefaciens* α-amylase (BAA) from Allen and Thoma (1976b) were used as input for this model. In addition, a method to model the structure of starch was developed. This starch model was used as input for the kinetic model. Since the subsite maps used for our model were experimentally determined using small linear carbohydrates (DP up to 12 for BAA, Allen and Thoma (1976b); and up to 10 for BLA, Kandra *et al.* (2002)), we also wanted to investigate whether these subsite maps could be used to describe the breakdown of large carbohydrates in time. The data calculated with the model are compared with experimental data for wheat starch hydrolysis by both BAA and BLA.

Modelling

Modelling of starch

Marchal *et al.* (2001) proposed that the structure of starch can be captured using a two-dimensional array in which letters were used to describe the glucose units in amylopectin.

Wojciechowski *et al.* (2001) used two numbers to describe each glucose unit, which makes the data set for the description of amylopectin larger than necessary.

In our model, we have used numbers to distinguish five different types of glucose units in amylopectin and amylose. A reducing end is given the number 1, the number 3 is used for the non-reducing end. The number 2 stands for a glucose unit in a linear α-1,4-linked chain. A branched monomer is denoted with a negative number. The same number but positive points to the row in which the branch is located. This branch starts with the number 4 to distinguish it from a reducing end. An example of the amylopectin model structure and the representative matrix is given in *Figure 1*.

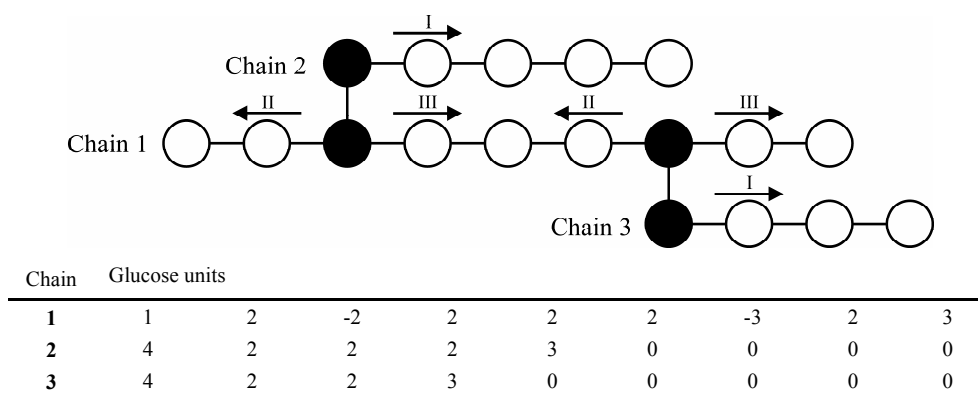| Chain	Glucose units								
1	1	2	-2	2	2	2	-3	2	3
2	4	2	2	2	3	0	0	0	0
3	4	2	2	3	0	0	0	0	0

Figure 1: Example of amylopectin model structure and matrix. The carbohydrate is drawn with the reducing end to the left and the non-reducing ends to the right. Filled circles indicate α-1,6-linked glucose units. The arrows with Roman numbers I, II and III indicate the type of inhibition from α-1,6-linked glucose units. See text for more details on nomenclature and inhibition.

The model described in this article takes into account several structural aspects of starch. Firstly, the model includes the fact that starch consists of approximately 25 w/w % amylose and 75 w/w % amylopectin. Secondly, amylose is an almost linear polymer with an average molecular weight of 10^5-10^6 g·mol^{-1} built up from α-1,4-linked glucose units. Thirdly, the much larger amylopectin (molecular weight of 10^7-10^9 g·mol^{-1}) has a highly branched structure, because about 5 % of the glucose units in amylopectin are α-1,6-linked (Ellis *et al.*, 1998). Finally, the modelled amylopectin has to comply with four constraints with respect to glycosidic α-1,6-linkages, as stated by Thompson (2000): amylopectin does not contain linear α-1,6-linked regions; α-1,4-linkages are more abundant than α-1,6-linkages; glucose units cannot have more than one side chain; and branch points are always at least one glucose unit apart. An additional assumption was that branching can

only occur when the glucose unit is at least 1 glucose unit apart from a reducing or non-reducing end.

To model starch, we started with a model for amylopectin. At the start, the largest chain in amylopectin is placed on the first row of the substrate array. A random number generator was used to generate a number between 0 and 1 for the first glucose unit capable of branching. If the number was smaller than the chance of branching, a side chain was attached to this glucose unit. If branching did not occur, the program proceeded to the next glucose unit. The restrictions stated by Thompson (2000) were taken into account during this procedure. It was assumed that the probability that a branch chain of a certain length is implemented in the molecule is proportional to its molar fraction in amylopectin.

If a branch chain was attached to the glucose unit, a new row was added to the bottom of the array. The number representing the glucose unit changed into a negative number that directed to index of the row in the matrix that contained the description of the newly implemented chain. This procedure was continued until the desired size of amylopectin was reached. It was possible that no more branch points were created, even though the desired size was not yet reached. In that case, the last row in the array was forced to branch. As a result, the actual fraction of branched glucose units could be slightly higher than desired.

Subsequently, amylose chains were added to the substrate matrix until the desired fraction of amylose was obtained. This fraction could vary depending on the size of the chains implemented. The starch model described here was used as input for the modelling of enzymatic starch hydrolysis.

Modelling of enzymatic starch hydrolysis

The subsite theory for depolymerising enzymes (Allen and Thoma, 1976; Torgerson *et al.*, 1979; MacGregor and MacGregor, 1985) was used as the basis for the hydrolysis model. According to this theory, the enzyme is composed of several subsites to which the monomers (in this case glucose units) can bind. Each subsite can increase or decrease the free energy of the enzyme-substrate complex. The following reaction scheme is used to describe the hydrolysis of substrate S_n with degree of polymerization n by the enzyme E into products P_{n-m} and P_m (the use of water is not shown):

$$E + S_n \underset{k_{-1,r,n}}{\overset{k_{+1,r,n}}{\rightleftharpoons}} ES_{r,n} \xrightarrow{k_{+2,r,n}} E + P_{n-m} + P_m \tag{1}$$
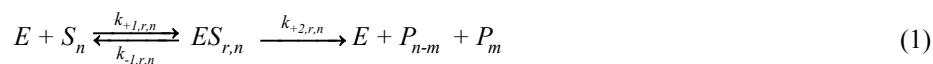
where r refers to the position of the reducing end of the saccharide in the subsite map. The subsite theory assumes that $k_{+2,r,n} << k_{-1,r,n}$, which implies that $K_{r,n}$ (the association constant for the enzyme-substrate complex) is equal to $k_{+1,r,n}/k_{-1,r,n}$. $K_{r,n}$ can be calculated from the

binding energies of the occupied subsites (Allen and Thoma, 1976a; Torgerson *et al.*, 1979; MacGregor and MacGregor, 1985; Marchal *et al.*, 2003) with the following equation:

$$-RT \cdot ln\left(K_{r,n}\right) = \sum_{i=r-n+1}^{r} \Delta G_i + \Delta G_{mix} \tag{2}$$

where R is the gas constant, T the absolute temperature (K), ΔG_i the binding energy of subsite i and $\Delta G_{mix} = 8.4 \cdot T \cdot ln(55.5)$ J·mol^{-1} for bimolecular processes (Gurney, 1953 by Marchal *et al.*, 2003). Note that subsite r might be a virtual subsite with zero binding energy, because it is located outside the subsite map.

If a substrate forms a complex with the enzyme, the complex is only productive when the substrate occupies the subsites to the left and right of the location of hydrolysis (subsites -1 and +1 according to the nomenclature defined by Davies *et al.*, 1997). If all enzymes in the reaction mixture are saturated with substrate, the rate of hydrolysis is limited by $k_{+2,r,n}$. The value of $k_{+2,r,n}$ may be assumed constant for all substrate sizes and binding modes, or it may be varied. To enhance the agreement between model data and experimental data, some subsite maps use an acceleration factor proportional to the number of subsites occupied (x) using the following relation:

$$k_{+2,r,n} = k_{+2} \cdot exp\left(\frac{x \cdot \Delta G_a}{RT}\right) \tag{3}$$

where ΔG_a is the acceleration factor of the subsite map (Allen and Thoma, 1976a; Torgerson *et al.*, 1979). For more details on the subsite theory, we refer to literature (Allen and Thoma, 1976a; 1976b; Torgerson *et al.*, 1979; MacGregor and MacGregor, 1985).

To simulate the hydrolysis process, a random number was generated to select an element in the substrate array. If the element did not represent a glucose unit, a new element was chosen randomly until a glucose unit was selected. We assumed that this glucose unit was bound to the subsite at the right of the location of hydrolysis. In other words, the bond towards the non-reducing end might be hydrolysed. If there was no bond, because the glucose unit selected is a non-reducing end, this attack was called non-productive. If the bond was situated next to an α-1,6-linked glucose unit, we assumed that it could not be hydrolyzed (French *et al.*, 1972) and was therefore also non-productive. The bonds in maltose and maltotriose could also not be hydrolysed (Saito, 1973; Marchal *et al.*, 1999; Kandra *et al.*, 2002). It was assumed that the substrate binding mode with the highest value for $k_{+2,r,n} \cdot K_{r,n}$ had a chance of hydrolysis of 1 (Marchal *et al.*, 2003).

If this binding mode was achieved with substrate size o and with the reducing end located at position p, the chance of hydrolysis was defined as follows:

$$p_{r,n} = \frac{k_{+2,r,n} K_{r,n}}{k_{+2,p,o} K_{p,o}}$$

(4)

Note that the numerator is constant, whilst the denominator varies depending on substrate size and binding mode.

Besides a difference in affinity and hydrolysis rate, the influence of branch points (α-1,6-linkages) was also taken into account as described by Marchal *et al.* (2003). They distinguished three types of inhibition due to α-1,6-linkages. Inhibition type I is assumed to affect the enzyme during hydrolysis of α-1,4-linkages near a branch-starting glucose unit. In *Figure 1*, inhibition type I takes place in chains 2 and 3 close to glucose units labelled with index 4. In the vicinity of side branches, enzyme inhibition also takes place either towards the reducing end (type II) or towards the non-reducing end (type III) (see *Figure 1*). Inhibition was taken into account when an α-1,6-linkage is less than 5 glucose units apart from the location of hydrolysis (Marchal *et al.*, 2003). For the amylopectin molecule shown in *Figure 1*, at least one type of inhibition holds for each glucose unit. Each type of inhibition is described using an inhibition factor, k_{br_in}, which is defined as follows:

$$k_{br\_in} = 2 - exp(b_T y)$$

(5)

where b_T is the inhibition constant for the type of inhibition and y is the number of glucose units between the location of hydrolysis and the α-1,6-linked glucose unit. When k_{br_in} was smaller than 0, it was considered to be 0. The chance on hydrolysis $p_{r,n}$ was multiplied by ($1-k_{br\_in}$) for each type of inhibition. For more details on the inhibition by α-1,6-linked glucose units, we refer to Marchal *et al.* (2003).

To determine whether hydrolysis would take place, a random number between 0 and 1 was generated; if it was smaller than the chance of hydrolysis, the attack was productive and the bond was hydrolysed. This involved changing the glucose unit at subsite position +1 of the subsite map into a non-reducing end (unless a single glucose was split off) and converting the unit at subsite position -1 to a reducing end. The time was increased with t_p for a productive attack and t_{np} for a non-productive attack (Wojciechowski *et al.*, 2001).

The simulations were ended after a pre-defined model time of hydrolysis. At set intervals (to save disk space and calculation time), the content of the substrate matrix was analyzed to determine the saccharide composition and dextrose equivalent. The dextrose equivalent *DE* was calculated with:

$$DE = \frac{180.16 \cdot n_{re}}{162.14 \cdot n_{gl} + 18.02 \cdot n_{re}} \tag{6}$$

where n_{re} stands for the number of reducing ends and n_{gl} stands for the number of glucose units in the substrate matrix (Marchal *et al.*, 2003). Carbohydrates with a DP up to 7 (both branched and linear) were counted each time interval, because these carbohydrates could be measured with our HPLC system. If desired, all carbohydrates could be taken into account by the model, but this would require much more calculation time and disk space and this was therefore not attempted.

Materials and methods

Materials

Wheat starch (S5127) was obtained from Sigma-Aldrich (Steinheim, Germany) and it had a moisture content of 9.95 ± 0.43 w/w % (based on 22 measurements, 95 % confidence interval). The moisture content was determined by drying the wheat starch in a hot air oven at 105 °C or in a vacuum oven at 80 °C until the mass of the samples was constant in time. The water content of wheat starch was taken into account during all experiments. Thermostable α-amylase from *Bacillus licheniformis* (EC 3.2.1.1, Termamyl 120L, type XII-A) was obtained from Sigma-Aldrich Chemie B.V. (the Netherlands) and α-amylase from *Bacillus amyloliquefaciens* (BAN 480L) was donated by Novozymes (Bagsværd, Denmark). The enzyme concentration used during the experiments is expressed in mass percent of this enzyme stock solution per equivalent dry mass of substrate (w/w %). Fuming hydrochloric acid, sodium hydroxide, sodium chloride, calcium chloride dihydrate, calcium chloride and tri-sodium phosphate were bought from Merck (Darmstadt, Germany). Maleic acid (di-sodium salt) was obtained from Acros Organics (Geel, Belgium). Maltohexaose from Serva was obtained from Brunschwig Chemie BV (Amsterdam, the Netherlands). All chemicals were at least analytical grade. Milli-Q water was used for all experiments.

Microcon YM-30 centrifuge filters (Millipore Corporation, Bedford, MA, United States) were used to remove the enzyme from the hydrolysate. Before the actual filtration, these filters were washed by centrifugation with 500 μl milli-Q water during 40 minutes at 25 ºC and 13000 g.

Methods

Experimental set-up and sampling

For the validation of the model, hydrolysis experiments were carried out in a temperature-controlled batch reactor (liquid volume 200 ml) equipped with an anchor stirrer. Prior to enzymatic hydrolysis, the 10 w/w % wheat starch-water mixture containing 5.0 mM $CaCl_2$ was heated to approximately 90 °C and was kept at this temperature for one hour to ensure complete starch gelatinisation. After the gelatinisation treatment, the reactor content was cooled to 50 °C. When the temperature inside the reactor was 50 ± 1 °C, enzyme was added to the reactor (starting point of the hydrolysis reaction). The hydrolysis temperature in the reactor was kept at 50 ± 1 °C during hydrolysis experiments. The stirrer speed during gelatinisation and hydrolysis was equal to 300 rpm.

Hydrolysis of maltohexaose was carried out in a 1.5 ml safe-lock tube (Eppendorf AG, Hamburg, Germany). First, the reaction mixture excluding maltohexaose was heated to 50 °C. After this temperature was reached, maltohexaose was added to obtain a 10 w/w % maltohexaose-water mixture (starting point of the hydrolysis reaction). Hydrolyis was carried out at 50 ± 1 °C.

Samples were taken during the course of the experiments to determine the carbohydrate composition and the residual α-amylase activity. Due to the small sample volumes used during the maltohexaose hydrolysis experiment, the sample was first diluted to obtain a carbohydrate concentration of 10 g·l^{-1} and a NaOH concentration of 0.1 M (for analysis of the carbohydrate composition) or to obtain an enzyme concentration of 20 mg·l^{-1} (for enzyme activity measurements). All samples were frozen in liquid nitrogen to stop the hydrolysis reaction. The sample was kept in liquid nitrogen for at least 15 min and afterwards it was stored in a -80 °C freezer.

The samples that were taken during the experiment with maltohexaose could be used for analysis directly after defrosting. The samples taken during the other experiments had to be diluted first. These frozen samples were grinded in a mortar with a pestle while submerging the sample in liquid nitrogen. The remainder of the sample preparation

procedure used before analysis is reported elsewhere together with the procedures followed to determine the carbohydrate composition and the α-amylase activity (Baks *et al.*, 2007). The dextrose equivalent was calculated from the weight fractions of glucose to maltohexaose using the method developed by Kiser and Hagy (1979) and adapted by Baks *et al.* (2007).

The carbohydrate composition measurements were used to determine the weight fraction of a specific carbohydrate with the following equation:

$$x_{w,i} = \frac{C_{DPi}}{C_{tot} + M_{w,w} \cdot \left(\sum_{j=1}^{7} C_{m,DPj} \right)}$$ (7)

where C_{DPi} (g·l^{-1}) is the mass-based concentration of a carbohydrate with degree of polymerization i, $C_{m,DPj}$ (mol·l^{-1}) is the mole-based concentration of a carbohydrate with degree of polymerization j, C_{tot} (g·l^{-1}) is the total carbohydrate concentration, and $M_{w,w}$ is the molar mass of water (18 g·mol^{-1}). The total carbohydrate concentration was corrected for the increase in dry matter during the reaction caused by the formation of maltooligosaccharides smaller than maltooctaose. In case maltohexaose was used as a substrate, all reaction products can be quantified and equation 8 was used to calculate the oligosaccharide weight fraction:

$$x_{w,i} = \frac{C_{DPi}}{\left(\sum_{j=1}^{6} C_{DPj} \right)}$$ (8)

where C_{DPj} (g·l^{-1}) is the mass-based concentration of a carbohydrate with degree of polymerization j.

Model simulations

For each simulated starch hydrolysis process, a new starch substrate was built up with approximately 100,000 glucose units in total. For the modelling of amylopectin the chain length distribution as reported in *Table II* of Hizukuri and Maehara (1990) was used. For amylose, the distribution shown in *Figure 4* of Hanashiro and Takeda (1998) was incorporated.

Table 1: Subsite maps with the apparent binding energy per subsite (kJ·mol^{-1}) used for the model simulations from Kandra et al. (2002) for BLA, and from Allen and Thoma (1976b) for BAA. The location of hydrolysis is in between subsites -1 and +1, and the glucose unit with the reducing end must be located such that it is the outmost right glucose unit.

subsite	-6	-5	-4	-3	-2	-1	+1	+2	+3	+4
BLA	0	-11.1	-2.7	-5.1	-6.5	0	0	-5.1	-5.8[a]	8
BAA[b]	-4.48	-10.21	-0.67	-4.23	-9.54	13.81	-14.39	-7.2	-4.02	5.27

[a] For the modified subsite map of BLA, the binding energy of subsite +3 was set to 0 kJ·mol^{-1}.
[b] Including the acceleration factor, ΔG_a.

For the simulated hydrolysis of the substrate, the subsite map for *B. licheniformis* α-amylase (BLA) determined by Kandra *et al.* (2002) and the subsite map for *B. amyloliquefaciens* α-amylase (BAA) obtained by Allen and Thoma (1976b) were used (see *Table 1*). For both α-amylases, we used 0.1, 0.2, and 0.4 for respectively inhibition constants b_I, b_{II}, and b_{III} (Marchal *et al.*, 2003).

The results obtained with the simulations were compared to the experimental data to obtain values for t_p and t_{np}, by comparing initial rates of hydrolysis. Model simulations were performed three times and averaged (except for the modified subsite map of BLA, which was performed only once), neglecting small differences in the time intervals between the different simulations. For each individual simulation, the model time was then converted to actual reaction time by non-linear fitting of the modelled dextrose equivalent (in case the hydrolysis of starch was simulated) or maltohexaose weight fraction (in case maltohexaose hydrolysis was simulated) to the corresponding experimental values. The modelled data in the linear part of the curve were fitted to experimental data in the corresponding region. In case of maltohexaose, the first 6 h of hydrolysis were used for the fitting procedure. We used a ratio $t_p:t_{np}$ of 20:7, which was also used by Wojciechowski *et al.* (2001).

Matlab 7.0.1 (The MathWorks, Inc., Nattick, MA, United States) was used to perform the model simulations. The Matlab standard random number generator was changed to another state for each simulation.

Results

The manner in which the subsite mapping theory was applied in this article was similar to the approach of Marchal *et al.* (2003). However, we used a simpler, more efficient matrix representation of the substrate. Comparison of their results with ours (on the saccharide composition as function of the DE) showed that our model yielded comparable results. Time (not considered in the model by Marchal *et al.*) was incorporated in our model with use of the theory of productive and non-productive attack developed by Wojciechowski *et al.* (2001). In case enzyme deactivation would take place, the times required for productive and non-productive attack would increase. Enzyme activity measurements in time showed that enzyme deactivation was negligible at our reaction conditions (results not shown) and therefore enzyme deactivation was not taken into account.

Linear and branched carbohydrates with the same molecular weight cannot be separated with the HPLC column that was used for carbohydrate analysis. However, our stochastic model can discriminate between linear and branched carbohydrates. For hexasaccharides and heptasaccharides, the predicted weight fractions of both the linear carbohydrates and the total amount of carbohydrates (branched and linear) are shown. In principle, branched pentasaccharides are also formed, but their weight fractions were so low that they are not shown.

Enzymatic starch hydrolysis by BLA

Figure 2 shows the predicted and experimental results of the hydrolysis of wheat starch by BLA. *Figure 2A* shows that both the simulated and the experimentally obtained dextrose equivalent rapidly increased during the first stage of hydrolysis. However, this linear stage took about 120 minutes for the experimental data and 60 minutes for the simulated data. After this stage a more gradual increase of the dextrose equivalent was observed. The predicted dextrose equivalent was underestimated as compared to the experimental data.

In case of carbohydrates ranging from glucose to pentasaccharide, both the experimental and simulated weight fractions increased over the complete time course. Both the weight fractions of hexa- and heptasaccharide reached a maximum before they gradually started to decrease. Although the simulated data for BLA showed the same trends and order of magnitude as the experimental data, the absolute weight fractions of glucose, maltose (*Figure 2B*), maltotetraose and pentasaccharide (*Figure 2C*) were underestimated by the model. The predicted weight fraction of maltotriose was higher than the weight fraction that was determined experimentally (*Figure 2B*). The observed maximum in the

weight fraction vs. time curves of hexasaccharide and heptasaccharide were correctly predicted by our model (*Figure 2D*).
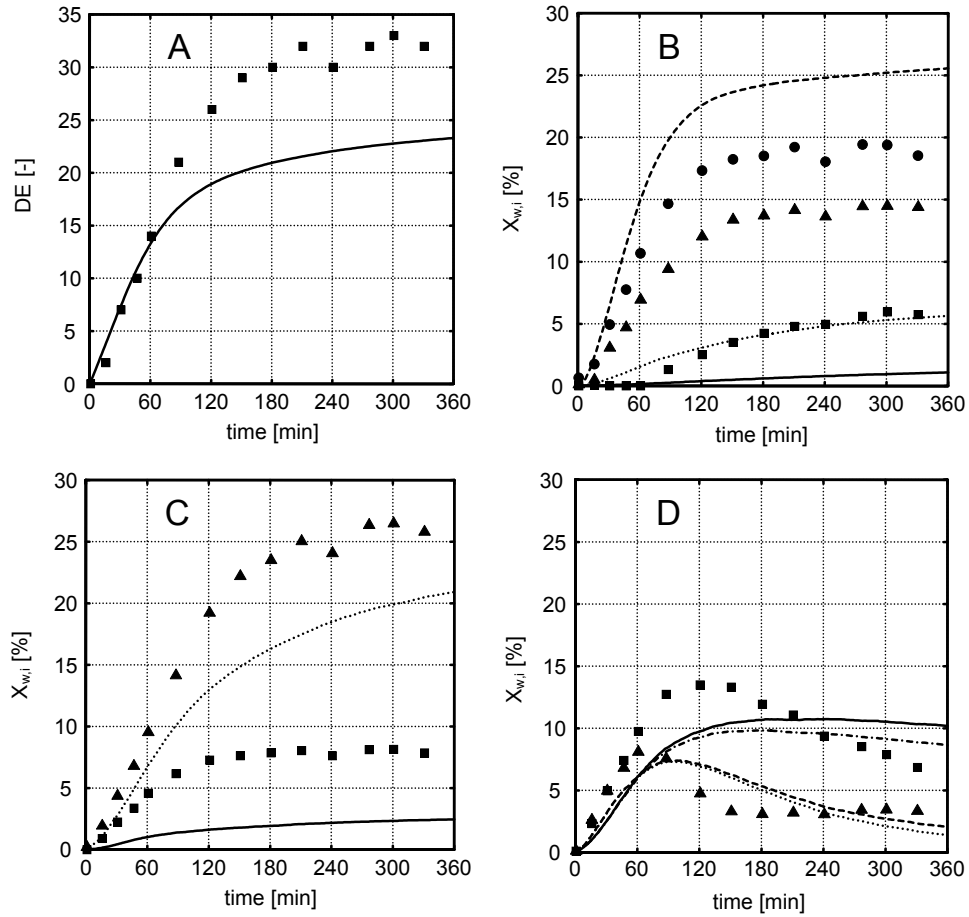

Figure 2: Experimental and predicted data obtained during enzymatic hydrolysis of 5 w/w % wheat starch with 0.01 w/w % BLA at 50 °C. Figure A contains the experimental (■) versus simulated (solid line) dextrose equivalent; Figure B contains the experimental weight fractions of glucose (■), maltose (▲) and maltotriose (●) versus simulated (respectively solid, dotted, and dashed line) weight fractions; Figure C contains the experimental weight fractions of maltotetraose (■) and total pentasaccharide (▲) versus simulated weight fractions (respectively solid and dotted line); Figure D contains the experimental weight fractions of hexasaccharide (■) and heptasaccharide (▲) versus simulated linear and total hexasaccharide (respectively dash-dotted and solid line) and linear and total heptasaccharide (respectively dotted and dashed line) weight fractions.

In case of hexasaccharide, however, a lower maximum value was predicted compared to the value that was found experimentally. In addition, the simulated weight fractions of

hexasaccharide and heptasaccharide decreased less rapidly after the maximum had been reached in comparison with the experimental data. Based on the model, it seems that the contribution of branched carbohydrates to the total amount of hexasaccharide and heptasaccharide is significant.

Enzymatic starch hydrolysis by BAA

Figure 3 shows the dextrose equivalent and weight fractions of several small carbohydrates based on experimental and simulated data for the hydrolysis of wheat starch by BAA. Both the experiment and the model predictions showed a dextrose equivalent that rapidly increased during the first half hour followed by a more gradual increase afterwards (*Figure 3A*). In general, the agreement between simulation and experiments is much better than with BLA, although the predicted dextrose equivalent was somewhat lower than the experimental dextrose equivalent when the time of hydrolysis exceeded one hour.

In *Figures 3B*, *3C* and *3D*, the simulated results show that the same trend and order of magnitude are found as observed during the experiment. However, the weight fractions of glucose, maltose (*Figure 3B*), and maltotetraose (*Figure 3C*) were underestimated by the model, whilst the maltotriose and pentasaccharide weight fractions were overestimated. The predicted weight fraction of hexa- and heptasaccharide, however, agreed well with the experimental values. Similar as observed during the simulations with BLA, we found that the contribution of branched carbohydrates to the total amount of hexasaccharide and heptasaccharide is significant.
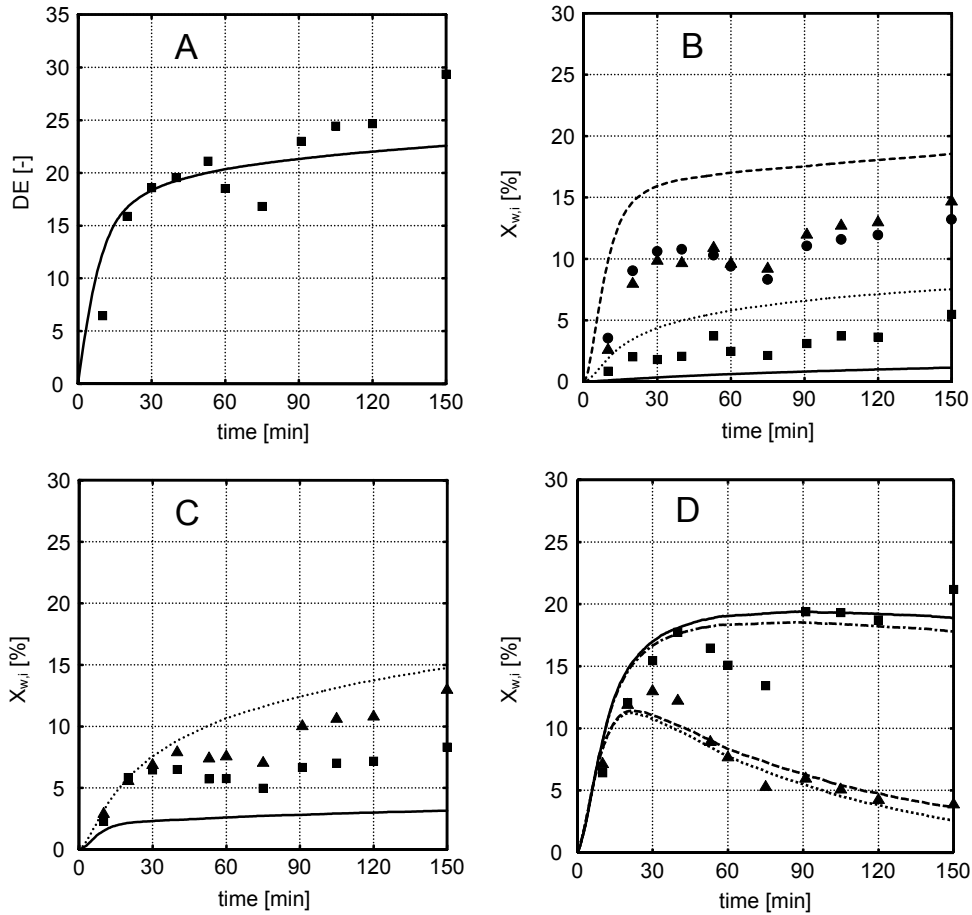
Figure 3: Experimental and predicted data obtained during enzymatic hydrolysis of 5 w/w % wheat starch with 0.01 w/w % BAA at 50 °C. Legend: see Figure 2.

Enzymatic maltohexaose hydrolysis by BAA

Enzymatic hydrolysis of maltohexaose with BAA resulted in a continuous increase in the weight fractions of all smaller carbohydrates during the complete time course of the experiment (*Figure 4*). The model predictions showed the same trend and the correct order of magnitude of the predicted weight fractions. However, the weight fraction of maltotriose was overestimated whilst the weight fraction of maltose and maltotetraose were underestimated. The predictions of the glucose, maltopentaose, and maltohexaose weight fractions were comparable to the corresponding experimental values.
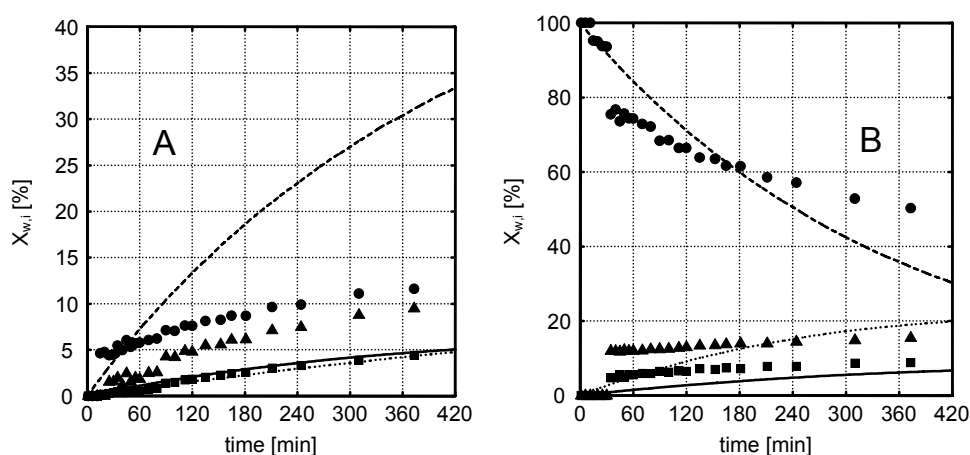
169

Figure 4: Experimental and predicted data obtained during enzymatic hydrolysis of 10 w/w % maltohexaose with 0.01 w/w % BAA at 50 °C. Figure A contains the experimental weight fractions of glucose (■), maltose (▲) and maltotriose (●) versus simulated (respectively solid, dotted, and dashed line) weight fractions; Figure B contains the experimental weight fractions of maltotetraose (■), maltopentaose (▲), and maltohexaose (●) versus simulated weight fractions (respectively solid, dotted, and dashed line).

Effect of BLA subsite map on enzymatic starch hydrolysis

According to the experimental data in *Figure 2B*, maltose and maltotriose were formed in approximately the same amounts when wheat starch is hydrolysed by BLA. As a result, one expects a negligible difference between the energy of binding of two or three glucose units at the left or right of the location of hydrolysis in the subsite map. The BLA subsite map obtained by Kandra *et al.* (2002) (*Table 1*) showed a clear preference for splitting off maltotriose from the reducing end as compared to maltose and other saccharides, because occupation of subsite +3 with binding energy -5.8 kJ·mol^{-1} results in a much lower total energy of binding. We therefore evaluated whether a better fit for maltose and maltotriose would be obtained when the binding energy of subsite +3 in the subsite map for BLA is set to 0 kJ·mol^{-1}. After modification of the subsite map, the dextrose equivalent agreed better with the experimental values (*Figure 2A* vs. *Figure 5A*) due to the increased glucose and maltose weight fraction (*Figure 2B* vs. *Figure 5B*). The simulated weight fractions glucose, maltose, maltotriose (*Figure 5B*) and pentasaccharide (*Figure 5C*) showed a reasonable agreement with experimental data after changing the subsite map. However, the modified subsite map did not lead to an improvement for maltotetraose (*Figure 5C*) and hexasaccharide and heptasaccharide (*Figure 5D*). These results were confirmed by the squared sum of differences between experimental and simulated data for the two subsite

170

maps as shown in *Table 2*. Note that the differences for maltotetraose, total hexasaccharide and total heptasaccharide were larger with the modified subsite map than with the original subsite map.
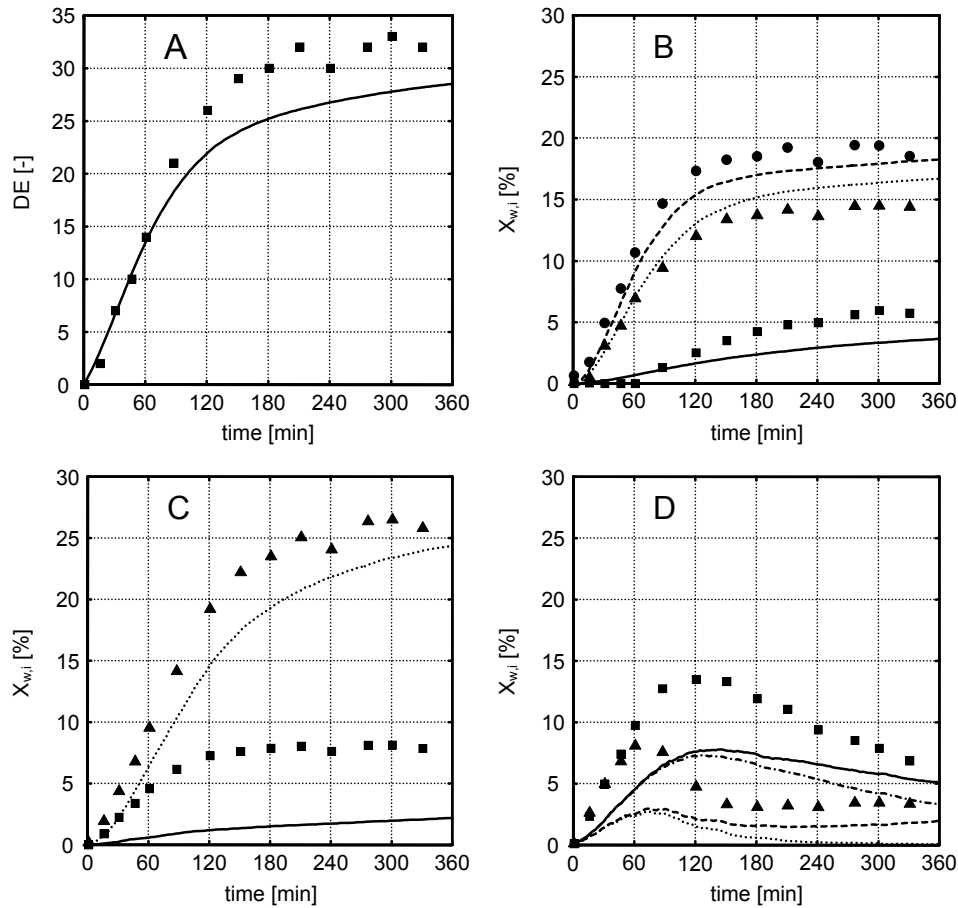

Figure 5: Experimental and predicted data (based on 1 simulation) obtained during enzymatic hydrolysis of 5 w/w % wheat starch with 0.01 w/w % BLA at 50 °C. For the simulated data, subsite +3 of the subsite map determined by Kandra et al. (2002) was set to 0 (see Table 1). Legend: see Figure 2.

Table 2: Squared sum of differences between experimental data points and corresponding model data (Figures 2-6) before and after changing the subsite map (BLA1 vs. BLA2; see Table 1), before and after changing tp:tnp (BAA1 = 20:7 and BAA2 = 66:1), and for hydrolysis of maltohexaose (BAA3, standard conditions).

	DE[a]	DP1[b]	DP2[b]	DP3[b]	DP4[b]	DP5[b]	DP6[b]	DP7[b]
BLA1	666.9	131.7	787.1	339.4	310.0	382.5	96.4	34.2
BLA2	174.1	33.5	24.7	28.2	358.8	144.2	218.1	116.2
BAA1	119.1	63.0	272.7	459.5	149.3	63.3	76.5	14.5
BAA2	70.5	46.6	192.4	589.8	127.6	252.2	107.4	68.4
BAA3	-	3.0	207.0	1371.3	287.0	593.5	1769.6	-

[a] Dextrose equivalent.

[b] DP1,…,DP7 stand for glucose, maltose, maltriose, maltotetraose, pentasaccharide, hexasaccharide, and heptasaccharide.

Effect of t_p:t_{np} ratio on enzymatic starch hydrolysis by BAA

The predictions shown in the previous figures were obtained with a fixed t_p:t_{np} ratio of 20:7 based on the article of Wojciechowski *et al.* (2001). *Figure 6* shows the results of a fit in which the t_p:t_{np} ratio was changed to 66:1. Changing the t_p:t_{np} ratio improved the fit between the experimental and modelled dextrose equivalent (*Figure 6A*). The predicted weight fractions of glucose, maltose (*Figure 6B*) and maltotetraose (*Figure 6C*) agreed better with the experimental data as compared to the predictions shown in *Figure 3*. However, the weight fractions of maltotriose (*Figure 6B*), pentasaccharide (*Figure 6C*), hexasaccharide and heptasaccharide (*Figure 6D*) deviated more from the experimental data compared to the predicted values obtained with the old tp:tnp ratio. The squared sums of differences between the experimental and simulated data for both fits are shown in *Table 2*. Based upon these values, it is difficult to decide which t_p:t_{np} ratio leads to the best predictions.
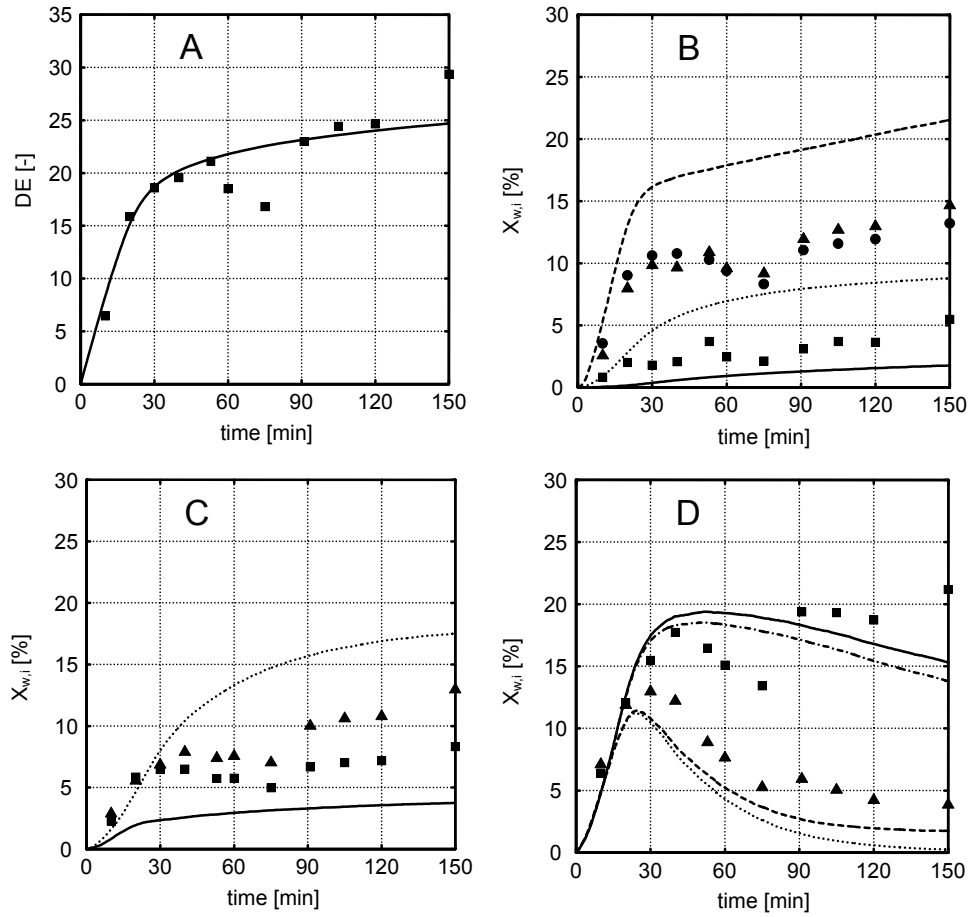
Figure 6: Experimental and predicted data obtained during enzymatic hydrolysis of 5 w/w % wheat starch with 0.01 w/w % BAA at 50 °C. The t_p:t_{np} ratio was changed from 20:7 to 66:1. Legend: see Figure 2.

Discussion

Although the predicted weight fractions of carbohydrates with a DP up to 7 were of the same order of magnitude as the experimentally determined weight fractions and they also showed the same trend, the absolute values were not predicted correctly. Deviations of the model data from the experimental data can be a result of several factors. The main factors that might cause these deviations are the substrate model, the subsite map, the hydrolysis behaviour of the α-amylase and the time scale.

173

Substrate model

The input for our amylopectin model was based on the chain length distribution of amylopectin in wheat starch and the model randomly inserted branch points. The model of Marchal *et al.* (2001) used a more structured distribution of branch points, which agrees better with the real structure of amylopectin. Use of our substrate model or use of the substrate model developed by Marchal *et al.* (2001) in our hydrolysis model resulted in approximately the same differences between the experiments and the model predictions. In case maltohexaose was used as a substrate, which is well defined and easy to model, the predicted values were still not comparable with the experimental values for all carbohydrates that were considered. Consequently, it seems that the substrate model did not cause the deviations between experimental and predicted weight fractions.

Subsite map

Another reason for the deviation between the predicted results and the experimental results can be caused by the subsite map that was used as these subsite maps might be affected by the type of substrate used to determine them. Torgerson *et al.* (1979) and Allen and Thoma (1976b) used radioactive oligosaccharides to determine the subsite maps of BAA. These radioactive oligosaccharides were assumed to be chemically similar to normal saccharides. Kandra *et al.* (2002) used 2-chloro-4-nitrophenyl (CNP) β-glycosides ranging from maltotetraose to maltodecaose to determine the subsite map of BLA. They mentioned that the CNP group can also interact with subsites +2 and +3, which might lead to deviations for the subsite map obtained using radioactive or normal oligosaccharides. Unfortunately, it has not been investigated whether different types of substrates would result in different subsite maps and different model predictions. In addition, the subsite maps were used in our model to predict the hydrolysis of a wide range of carbohydrates including large carbohydrates, while only small carbohydrates were used to determine these subsite maps.

The experimental results (*Figures 2-6*) indicate that maltose and maltotriose are formed in comparable amounts. Paolucci-Jeanjean *et al.* (2000) found similar results when cassava starch is hydrolysed by BLA at a higher temperature. However, the subsite map for BLA (Kandra *et al.*, 2002) clearly indicates the enzyme's preference to split off maltotriose from the reducing end; the lowest energy of binding at the right side of the location of hydrolysis can be obtained when subsites +1, +2 and +3 are filled. By setting the subsite energy of subsite +3 to 0, the influence of this subsite was illustrated. After this modification, the predicted weight fractions of maltose and maltotriose were comparable (*Figure 5*), leading

to a better description of the experimental data for maltose and maltotriose (see *Table 2*). To better fit the model data to the experimental data, a new subsite map could be obtained by fitting the model predictions to the experimental hydrolysis results. However, the validity of this approach is questionable given the large number of fit parameters that would be involved, and since our aim was to compose a model with a limited amount of independent experimental input, we did not consider this route.

Hydrolysis behaviour of α-amylase

Besides the hydrolysis behaviour of α-amylase incorporated in the subsite map, other specific hydrolysis phenomena may take place that were not taken into account in our model. For example, it is known that some α-amylases exhibit a repetitive-attack mechanism, which could give rise to higher amounts of maltose and glucose (MacGregor and MacGregor, 1985). This would also result in a higher dextrose equivalent. Furthermore, it is possible that carbohydrates form a non-productive complex with the enzyme without blocking the catalytic site and the subsites surrounding it. This resulting enzyme-carbohydrate complex might still be active, because in some cases it can still hydrolyse another substrate even at higher hydrolysis rates (Baks *et al.*, 2006). Once more, the predicted dextrose equivalent might increase leading to a better agreement between predicted and experimental values.

Finally, by having a purely random selection of an α-1,4-linkage for hydrolysis, it was assumed that the chance that an enzyme will attack an oligosaccharide is proportional to the number of glucose monomers it contains, and that all parts of the molecule are equally accessible to the enzyme. However, it might be possible that the volume occupied by branched and linear carbohydrates with the same degree of polymerisation differs, which might affect the chance that α-amylase encounters such a substrate. It should therefore be determined whether it is fair to assume that the chance of enzymatic hydrolysis of an oligosaccharide is proportional to the degree of polymerisation. It is unclear how such changes will affect the outcome of the model.

Time scale

For the model presented in this article, the t_p:t_{np} ratio of 20:7 was used that was proposed by Wojciechowski *et al.* (2001), but they did not mention how they determined this ratio. Since the BAA subsite map seemed to be more reliable than the BLA subsite map, it was decided to illustrate the effect of a different t_p:t_{np} ratio for the hydrolysis predictions with BAA. Changing this ratio indeed affected the outcome of the simulations and it should

therefore be investigated whether the t_p:t_{np} ratio can be determined independently instead of using a fit procedure to obtain this ratio. Molecular modelling might be used to determine the theoretical t_p:t_{np} ratio that is expected for various substrates with α-amylase. In addition, this ratio might also differ for different carbohydrates, because of variations in intra- and intermolecular mobility into and out of the enzyme's active site.

During wheat starch hydrolysis experiments, enzyme activity measurements indicated that the enzyme was stable at our reaction conditions. However, it is possible to include changes in the enzyme activity during hydrolysis. In case enzyme deactivation would take place, the actual values of t_p and t_{np} can be increased in time. The activity of BLA was studied quite extensively (De Cordt *et al.*, 1992; 1994; DeClerck *et al.*, 1997; Dobreva *et al.*, 1994; Fitter *et al.*, 2001; Ivanova *et al.*, 1993; Rodríguez *et al.*, 2006b; Tomazic and Klibanov, 1988; Violet and Meunier, 1989) and these articles can be used as a starting point. Various conditions, such as temperature, calcium concentration, pH, enzyme concentration and substrate concentration, determine the initial enzyme activity as well as the decrease of this activity in time. Obtaining a general equation for the activity based on all the factors described in literature is not a trivial task. It is simpler and more accurate to determine the enzyme activity at the specific reaction conditions and subsequently implement this information in the t_p:t_{np} ratio used in the model.

Conclusions

The stochastic model presented in this article shows that it is possible to use the subsite theory to predict the saccharide composition and dextrose equivalent in time for wheat starch hydrolysis with α-amylase. The relatively simple substrate model that was developed can be used as effective and efficient input for the hydrolysis model.

For both BAA and BLA, the predicted weight fractions and dextrose equivalents showed the same trend as the corresponding experimental values. Although the order of magnitude of the predictions was comparable with the experimentally determined values, the absolute values calculated with the model differed from the experimental results. The model can therefore be used to gain insight in the dynamic formation and breakdown of all carbohydrates during enzymatic starch hydrolysis, but it is not yet suitable for absolute predictions of the oligosaccharide concentrations and dextrose equivalent. To improve the model predictions, it seems to be necessary to obtain a subsite map that can be used for longer hydrolysis times and larger carbohydrates. Such a subsite map may be obtained by

fitting the model data to the experimental data. In addition, it may be useful to include the experimentally observed repetitive-attack mechanism for α-amylases in the model. Furthermore, a procedure should be developed to obtain a reliable ratio between the time required for the formation and break down of non-productive enzyme-substrate complexes and the time required for the formation of productive enzyme-substrate complexes and the subsequent release of the hydrolysis products. Research is also required to determine whether these reaction times depend on the carbohydrate chain length.

The model presented here was developed to describe the enzymatic hydrolysis of wheat starch by BAA and BLA, but it may well be converted to other depolymerase systems for which the subsite map is available. It is also be possible to include more than one enzyme in the model by the generation of an additional random number to select the enzyme that is going to interact with the substrate.

References

Allen JD, Thoma JA. 1976a. Subsite mapping of enzymes: depolymerase computer modelling. Biochem J 159:105-120.

Allen JD, Thoma JA. 1976b. Subsite mapping of enzymes: application of the depolymerase computer model to two α-amylases. Biochem J 159:121-132.

Baks T, Janssen AEM, Boom RM. 2006. A kinetic model to explain the maximum in α-amylase activity measurements in the presence of small carbohydrates. Biotechnol Bioeng 94:431-440.

Baks T, Kappen FHJ, Janssen AEM, Boom RM. 2007. Towards an optimal process for gelatinisation and enzymatic hydrolysis of highly concentrated starch-water mixtures. Accepted for publication in J Cereal Sci.

Brandam C, Meyer XM, Proth J, Strehaiano P, Pinguad H. 2003. An original kinetic model for the enzymatic hydrolysis of starch during mashing. Biochem Eng J 13:43-52.

Davies GJ, Wilson KS, Henrissat B. 1997. Nomenclature for sugar-binding subsites in glycosyl hydrolases. Biochem J 321:557-559.

De Cordt S, Vanhoof K, Hu J, Maesmans G, Hendrickx M, Tobback P. 1992. Thermostability of soluble and immobilized α-amylase from *Bacillus licheniformis*. Biotechnol Bioeng 40:396-402.

De Cordt S, Hendrickx M, Maesmans G, Tobback P. 1994. The influence of polyalcohols and carbohydrates on the thermostability of α-amylase. Biotechnol Bioeng 43:107-114.

Declerck N, Machius M, Chambert R, Wiegand G, Huber R, Gaillardin C. 1997. Hyperthermostable mutants of *Bacillus licheniformis* α-amylase: thermodynamic studies and structural interpretation. Protein Eng 10:541-549.

Dobreva E, Ivanova V, Emanuilova E. 1994. Effect of temperature on some characteristics of the thermostable α-amylase from *Bacillus licheniformis*. World J Microbiol Biotechnol 10:547-550.

Ellis RP, Cochrane MP, Dale MFB, Duffus CM, Lynn A, Morrison IM, Prentice RDM, Swanston JS, Tiller SA. 1998. Starch production and industrial use. J Sci Food Agric 77:289-311.

Fitter J, Herrmann R, Dencher NA, Blume A, Hauss T. 2001. Activity and stability of a thermostable α-amylase compared to its mesophilic homologue: mechanisms of thermal adaptation. Biochemistry 40:10723-10731.

French D, Smith EE, Whelan WJ. 1972. The structural analysis and enzymatic synthesis of a pentasaccharide alpha-limit dextrin formed from amylopectin by *Bacillus subtilis* alpha-amylase. Carbohydr Res 22:123-134.

Hanashiro I, Takeda Y. 1998. Examination of number-average degree of polymerization and molar-based distribution of amylose by fluorescent labelling with 2-aminopyridine. Carbohydr Res 306:421-426.

Hizukuri S, Maehara Y. 1990. Fine structure of wheat amylopectin: the mode of A to B chain binding. Carbohydr Res 206:145-159.

Hizukuri S. 1996. Starch: Analytical aspects. In: Eliasson AC, editor. Carbohydrates in food. New York: Marcel Dekker. 347-429.

Ivanova VN, Dobreva EP, Emanuilova EI. 1993. Purification and characterization of a thermostable alpha-amylase from *Bacillus licheniformis*. J Biotechnol 28:277-289.

Kandra L, Gyémánt G, Remenyik J, Hovánzski G, Lipták A. 2002. Action pattern and subsite mapping of *Bacillus licheniformis* α-amylase (BLA) with modified maltooligosaccharide substrates. FEBS Lett 518:79-82.

Kiser DL, Hagy RL. 1979. Estimation of dextrose equivalent value of starch hydrolysates from liquid chromatographic. In: Charalambous G, editor. Liquid chromatographic analysis of food and beverages (volume 2). New York: Academic Press. p 363-378.

Komolprasert V, Ofoly RY. 1991. Starch hydrolysis kinetics of *Bacillus licheniformis* α-amylase. J Chem Tech Biotechnol 51:209-223.

Kusunoki K, Kawakami K, Shiraishi F, Kato K, Kai M. 1982. A kinetic expression for hydrolysis of soluble starch by glucoamylase. Biotechnol Bioeng 24:347-354.

MacGregor EA, MacGregor AW. 1985. A model for the action of cereal alpha amylases on amylose. Carbohydr Res 142:223-236.

Marchal LM, van de Laar AMJ, Goetheer E, Schimmelpennink EB, Bergsma J, Beeftink HH, Tramper J. 1999. Effect of temperature on the saccharide composition obtained after α-amylolysis of starch. Biotechnol Bioeng 63:344-355.

Marchal LM, Zondervan J, Bergsma J, Beeftink HH, Tramper J. 2001. Monte Carlo simulation of the α-amylolysis of amylopectin potato starch. Part I: modelling of the structure of amylopectin. Bioprocess Biosyst Eng 24:163-170.

Marchal LM, Ulijn RV, de Gooijer CD, Franke GTh, Tramper J. 2003. Monte Carlo simulation of the α-amylolysis of amylopectin potato starch. Part II: α-amylolysis of amylopectin. Bioprocess Biosyst Eng 26:123-132.

Nakatani H. 1996. Monte Carlo simulation of multiple attack mechanism of α-amylase. Biopolymers 39:665-669.

Paolucci-Jeanjean D, Belleville MP, Zakhia N, Rios GM. 2000. Kinetics of cassava starch hydrolysis with Termamyl® enzyme. Biotechnol Bioeng 68:71-77.

Park JT, Rollings JE. 1994. Effects of substrate branching characteristics on kinetics of enzymatic depolymerization of mixed linear and branched polysaccharides: I. Amylose/Amylopectin α-amylolysis. Biotechnol Bioeng 44:792-800.

Rodríguez VB, Alameda EJ, Gallegos JFM, Requena AR, López AIG. 2006a. Enzymatic hydrolysis of soluble starch with an α-amylase from *Bacillus licheniformis*. Biotechnol Prog 22:718-722.

Rodríguez VB, Alameda EJ, Gallegos JFM, Requena AR, López AIG. 2006b. Thermal deactivation of a commercial α-amylase from *Bacillus licheniformis* used in detergents. Biochem Eng J 27:299-304.

Rollings JE, Thompson RW. 1984. Kinetics of enzymatic starch liquefaction: simulation of the high-molecular-weight product distribution. Biotechnol Bioeng 26:1475-1484.

Saito N. 1973. A thermophilic extracellular α-amylase from *Bacillus licheniformis*. Arch Biochem Biophys 155:290-298.

Thompson DB. 2000. On the non-random nature of amylopectin branching. Carbohydr Polym 43:223-239.

Tomazic SJ, Klibanov AM. 1988. Why is one *Bacillus* α-amylase more resistant against irreversible thermoinactivation than another? J Biol Chem 263:3092-3096.

Torgerson EM, Brewer LC, Thoma JA. 1979. Subsite mapping of enzymes. Use of subsite map to simulate complete time course of hydrolysis of a polymeric substrate. Arch Biochem Biophys 196:13-22.

Violet M, Meunier JC. 1989. Kinetic study of the irreversible thermal denaturation of *Bacillus licheniformis* α-amylase. Biochem J 263:665-670.

Wojciechowski PM, Koziol A, Noworyta A. 2001. Iteration model of starch hydrolysis by amylolytic enzymes. Biotechnol Bioeng 75:530-539.

Chapter 9

General discussion

Abstract

The results obtained in this thesis were used to determine alternative processes for gelatinisation and enzymatic hydrolysis at high starch concentrations. A fed-batch reactor concept was proposed in which either native or gelatinised starch (produced by an extruder) was added to the reactor. Alternatively, continuous processes were proposed by using a static mixer, a tubular reactor, a membrane reactor, or a packed bed reactor for hydrolysis of starch that was gelatinised in an extruder. Concepts of polymerisation reactors might also be interesting for gelatinisation and/or enzymatic hydrolysis of concentrated starch-water mixtures. The results reported in this thesis show that highly concentrated processing has potential for production of starch hydrolysates, for brewing, and for modification of starch in general. This may lead to more sustainable processing (less energy consumption, larger volumetric productivity, better use of substrate) and a wider range of products.

Introduction

Enzymatic hydrolysis of starch with use of α-amylase is encountered in day-to-day life for instance in the dishwasher during removal of stains with detergents or in our mouth during chewing of starch-based foods in the presence of saliva. The reaction is also important for food and non-food industries. For example, it is applied in the production of beer (mashing), bio-ethanol, and several commercially relevant hydrolysates (e.g. glucose syrup, used for soft drinks, baking, brewing, and fermentation; and maltodextrins, used for sports drinks, clinical feed formulations; raw materials for enzymic saccharification; thickening, filling, stabilising, etc.).

Before starch is enzymatically hydrolysed, it is common to gelatinise starch first to make it better accessible for the enzyme. The gelatinisation curves and phase diagrams in *Chapter 4* and *Chapter 5* showed that the degree of gelatinisation increased with an increasing temperature, an increasing pressure, and a decreasing starch concentration. In case native starch, high pressure gelatinised starch, and high temperature gelatinised were hydrolysed, we found that the hydrolysate composition was affected by the gelatinisation procedure (*Chapter 6*). The differences were explained by considering the accessibility of starch during the hydrolysis. Furthermore, since use of high pressure for hydrolysis did not lead to significantly different results in comparison to hydrolysis at atmospheric pressure (as long as gelatinization was complete), high pressure hydrolysis does not seem to offer much potential for enzymatic starch hydrolysis at a large scale (*Chapter 6*).

Industrial processes for gelatinisation and liquefaction of starch are usually carried out with a starch concentration of approximately 35 w/w % (Grafelman and Meagher, 1995), even though increasing the starch concentration can result in lower energy costs (Grafelman and Meagher, 1995), lower water consumption (Van der Veen, 2005), and higher enzyme stability (De Cordt *et al.*, 1994; Klibanov, 1983). In this thesis, high substrate concentrations (50-70 w/w %) were used by applying a twin screw extruder to gelatinise starch, to mix the enzyme with the gelatinised starch slurry, and thus to prepare the reaction mixture for enzymatic hydrolysis in a batch reactor (see *Chapter 7*).

According to *Chapter 4*, a higher starch concentration requires a higher temperature for complete gelatinisation. When an extruder is used for gelatinisation, the temperature required for complete gelatinisation can be decreased by increasing the screw speed (*Chapter 7*). The adapted Flory equation (*Chapter 4*), which describes gelatinisation curves

in absence of mechanical forces, therefore provides a high estimate for the temperature needed to completely gelatinise starch in the presence of shear forces.

The results obtained with extrusion (as described in *Chapter 7*) confirmed that higher substrate concentrations during enzymatic hydrolysis resulted in a higher stability for α-amylase from *B. licheniformis*. We also found that the volumetric productivity increased. The hydrolysate composition during enzymatic hydrolysis was not affected by increasing the substrate concentration from 10 to 60 w/w % (or higher) (*Chapter 7*).

The previous chapters reported on our contribution to the development of a process for gelatinisation and enzymatic hydrolysis at high starch concentrations. This chapter illustrates how our results may be applied in practice and it gives an overview of the remaining topics that have to be studied to develop useful processes for other applications.

Alternative processes for conversion of concentrated starch slurries

Enzymatic starch hydrolysis with α-amylase can be used to produce a wide variety of products (Kennedy *et al.*, 1988; Marchal, 1999), for example maltodextrins and glucose and maltose syrups. Maltodextrins can be produced using a twin screw extruder as described in *Chapter 7*. In case a high degree of hydrolysis is desired, for example for the production of maltose syrup, a longer reaction time is required and for that purpose a batch reactor can be used after the extruder (*Chapter 7*). Although the extruder combined with a batch reactor was proven to be successful, other reactor types or process configurations (*Figure 1*) might also be applicable for enzymatic hydrolysis of concentrated starch slurries.

An extruder coupled to a tubular reactor or a motionless mixer: Instead of using a batch reactor after an extruder, static or motionless mixers (Grafelman and Meagher, 1995; Lammers, 1995) or simple tubular reactors can also be used (*Figure 1A*). The extruder can be used to gelatinise starch, to mix the enzyme with the gelatinised starch-water mixture and to build up pressure to transport the starch slurry through the static mixer or tubular reactor.
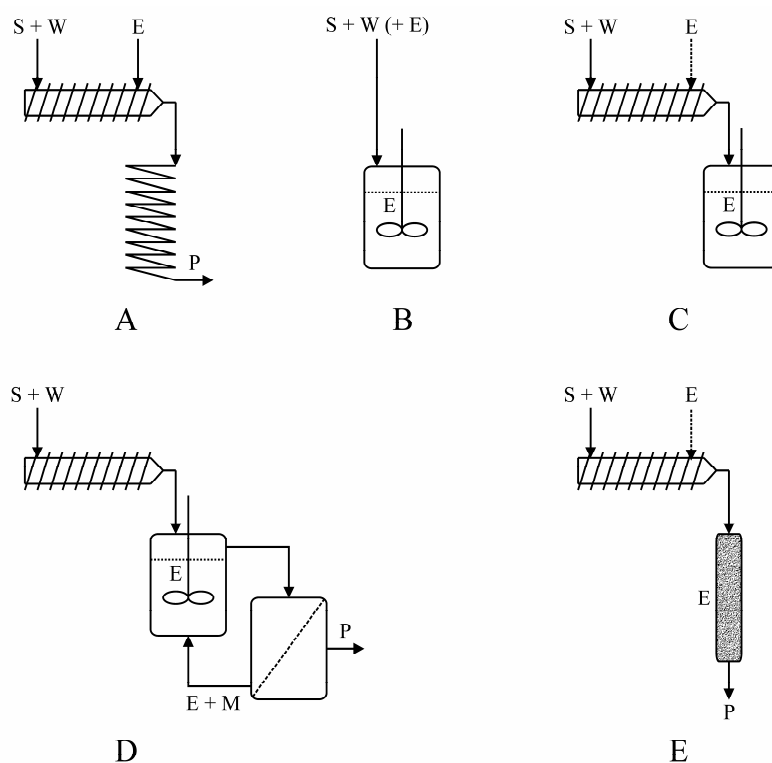
Figure 1: Schematic overview of alternative processes in which extruders are used to gelatinise starch and a tubular reactor or motionless mixer (Figure A), a fed-batch reactor (Figure C), a membrane reactor (Figure D), and a packed bed reactor with immobilized enzyme (Figure E) are used for enzymatic hydrolysis of concentrated starch slurries or a fed-batch reactor that is used for both process steps simultaneously (Figure 1B). For the fed-batch processes (Figures B and C) enzyme can be added during the process and/or enzyme can already be present in the reactor. Abbreviations: S = starch, W = water, E = enzyme, M = maltodextrins, P = product.

A fed-batch process: A fed-batch reactor can be used to carry out gelatinisation and enzymatic hydrolysis simultaneously (*Figure 1B*). The starch concentration should be high enough to provide stability for the enzyme throughout the process. However, the concentration should not be too high as an increased viscosity hinders proper mixing of the reaction mixture and it increases the gelatinisation temperature (*Chapters 4* and *5*). The rate at which starch should be added to the fed-batch reactor can be estimated by a stochastic model such as the one that was described in *Chapter 8*. When the hydrolysis reaction proceeds, the concentrations of glucose and other small carbohydrates increase, which leads to a higher gelatinisation temperature (Moates *et al.*, 1998; Perry and Donald, 2002; Sopade *et al.*, 2004) and a lower reaction rate (Yankov *et al.*, 1986). These findings were confirmed

by our own results. *Figure 2* shows the dextrose equivalent and the residual enzyme activity as function of time during enzymatic hydrolysis of starch in the presence of glucose. The differences are caused by the gelatinisation step prior to hydrolysis, which was either carried out in the presence of glucose or in the absence of glucose. Gelatinisation in the presence of glucose led to a lower dextrose equivalent during the subsequent hydrolysis step. Using a higher glucose concentration during the hydrolysis reaction, resulted in a lower dextrose equivalent as well (results not shown).

At 90 °C, a starch concentration of 8 w/w % is not sufficient to keep the enzyme stabile. The presence of glucose during gelatinisation did not affect the stability of the enzyme during hydrolysis. In the absence of substrate, the residual activity of the enzyme would be zero after two hours (results not shown).
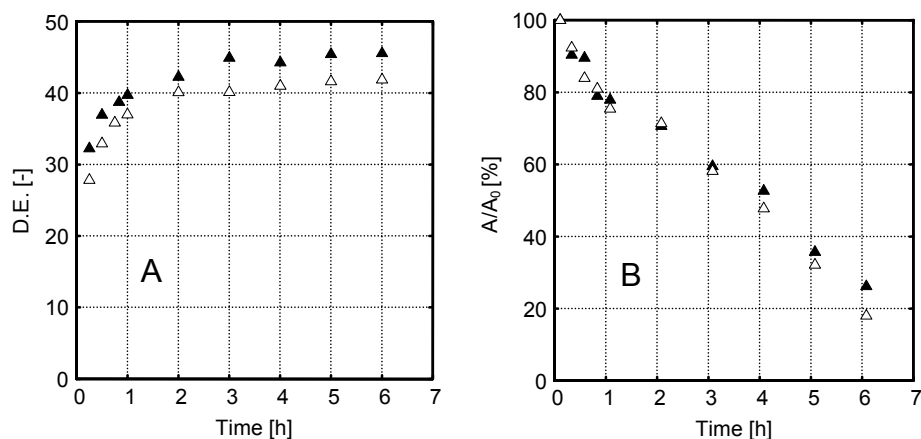
Figure 2: Dextrose equivalent (Figure A) and residual activity of α-amylase from B. licheniformis (Figure B) during enzymatic hydrolysis of 8 w/w % wheat starch with 20 w/w % glucose at 90 °C. Legend: Starch gelatinised in the absence (▲) and in the presence (△) of glucose.

Both literature and our own results indicate that the temperature in the fed-batch reactor is crucial. On the one hand, the temperature should be high enough to gelatinise starch completely in the presence of small carbohydrates. On the other hand, the temperature should not be too high to prevent substantial enzyme inactivation during the process. This trade-off can be minimised or avoided by using an extruder to provide a steady state supply of gelatinised starch to a batch reactor in which the enzymatic hydrolysis is carried out (*Figure 1C*).

An extruder coupled to a membrane reactor: The proposed fed-batch process in *Figure 1C* can be converted in a continuous process when a membrane reactor is used to keep the

enzyme and large carbohydrates in the hydrolysis reactor, while carbohydrates with the desired size can pass through the membrane (*Figure 1D*). Membrane reactors have already been used for the enzymatic hydrolysis of starch, but only at low substrate concentrations or for partially hydrolysed substrates (Darnoko *et al.*, 1989; Houng *et al.*, 1992; Paolucci-Jeanjean, 2000a,b; Sims and Cheryan, 1992). It should be investigated whether high starch concentrations can also be used without inhibition of mass transfer through the concentration polarization layer and the membrane due to the very high concentrations and without extensive fouling of the membrane.

An extruder coupled to a packed bed reactor: An extruder followed by a packed bed reactor can also be used (*Figure 1E*). The residence time in the packed bed with immobilised enzyme should be sufficient to attain the desired degree of hydrolysis (Hausser *et al.*, 1983). In this case, the reactor configuration proved to be useful for the hydrolysis of partially hydrolysed substrates (dextrose equivalent equal to 10) at a substrate concentration of 30 w/w %. It can, however, be expected that more highly concentrated starch-water mixtures cannot be easily processed in a packed bed reactor due to the high viscosities and lower mass transfer rates. However, by adding enzyme at the end of the extruder (see *Figure 1E*), part of the liquefaction reaction takes place in the extruder and the viscosity of the extrudate decreases. It should then be possible to handle these mixtures in a packed bed reactor. The packed bed reactor can then be operated with (for example) immobilised amyloglucosidase to carry out the saccharification reaction.

Polymerisation reactors: Highly viscous reaction mixtures are common in polymerisation reactions or polymer processing. Numerous reactor types have been developed to handle these mixtures, for example horizontal stirred tank reactors (Van der Gulik, 2002), static or motionless mixers placed behind an extruder (Grafelman and Meagher, 1995; Lammers, 1995), backmix reactors (Lu and Biesenberger, 1997), and hollow shaft reactors (Weickert, 1998). These reactor types might also be suitable for gelatinisation and/or hydrolysis of starch pastes at high starch concentrations. However, experiments need to be performed to determine whether concentrated starch mixtures can be handled in these reactors. Gelatinisation experiments are most suitable for this purpose since the highest viscosity is reached during this step.

Process applications following from this thesis

Production of starch hydrolysates

Although the process configuration described in *Chapter 7* can indeed be used to produce valuable hydrolysates, application of this extrusion-based process is not straightforward. Starch that is used in industry usually has a high moisture content as a result of pretreatment steps used for purification (sieving, steeping, grinding, and washing) (Simms, 1985) Working at higher starch concentrations might therefore require an additional drying step to remove part of the water. Although starch drying is a common procedure (Sriroth *et al.*, 1999; Van der Borght *et al.*, 2005), the costs of additional drying might be higher than the savings of using a process for concentrated starch slurries. Consequently, a prerequisite for applications at higher starch concentrations is that the treatment step prior to gelatinisation leads to a product stream that already has a high starch concentration. Recent developments (Peighambardoust *et al.*, 2006) indicate that it might well be possible to obtain purified starches using a lower amount of water.

Brewing

In this thesis, starch and α-amylase could be added individually and consequently gelatinisation and enzymatic hydrolysis can be optimised separately. In some other cases, the raw materials required for gelatinisation and enzymatic hydrolysis are only available as mixture, for example in the mashing step during brewing of beer. In the conventional brewing process, malted barley is the source for both the substrate and the enzymes. Malting consists of four steps: steeping to increase the moisture content; germination to make the barley kernel grow during which enzymes are produced and starch is made available for subsequent process steps; kilning to stop the growth in the barley kernel; and removal of rootlets formed during germination. After malting, the malt is mechanically broken down by milling. As a result of this step, smaller fragments are formed leading to an increased availability of the substrate for the enzymes. In the next step, called mashing, the product of the previous step (the grist) is mixed with water. During this step, starch is hydrolysed by various enzymes (including α-amylase) that are present in the grist. The results described in this thesis can be used for brewing purposes, especially for mashing.

Use of adjuncts: The amount of enzymes present in malt can easily hydrolyse the starch present in the malt, plus a significant fraction of added starch. Consequently, part of the

malt can be replaced by cheaper, unmalted starch sources (corn, rice, and sorghum). The unmalted cereals that replace part of the malt are called adjuncts. In a conventional brewing process, stirred batch vessels (adjunct cookers) are used to gelatinise the starch in the adjuncts. These adjunct cookers, however, are not able to handle concentrated starch slurries. A twin screw extruder can process much higher starch concentrations than a stirred vessel. Energy can be saved due to the lower amount of water that has to be heated and due to the lowering of the gelatinisation temperature as a result of application of shear (*Chapter 7*).

Increased volumetric production with fed-batch process: It is also possible to use the extruder to feed a continuous stream of gelatinised starch to a conventional mash tun. The mash tun is then operated as a fed batch reactor (see *Figure 1C*). In this case, the substrate concentration during mashing should be kept at a value that enables proper mixing by the stirrer while ensuring a sufficiently high reaction rate. It should be possible to reach higher hydrolysis yields and avoid peak viscosities in such a system. In addition, due to the presence of starch in the mash tun, enzymes remain more stable. However, it should still be verified whether the observed increase in enzyme stability (*Chapter 7*) will also be found in a concentrated mash with different enzymes that are less thermostable. In case a highly concentrated mashing system is implemented, the subsequent lautering or mash separation, where the mash is separated in spent grains (insoluble material) and wort (extract solution used for fermentation), is also affected. A different process should be developed to perform this separation step at a high concentration. A continuous filtration process suitable for high dry matter content and viscous media has already been developed (Hansen *et al.*, 2003). It is based on pressure driven filtration by pressing and removing the filter cake continuously and it appears to be suitable for our purpose. Alternatively, it is also possible to dilute the mash before lautering. In the latter case, a larger amount of water has to be heated during the subsequent boiling of wort together with hops, which will increase the energy consumption during this step.

Extrusion-based process for milling, mixing, and gelatinisation: The extruder may also be used for the milling step and subsequent addition of water. In case the amount of water is kept low, shear forces can lower the temperature required for complete gelatinisation while the high substrate concentration makes sure that the enzyme remains stable during gelatinisation. As a result, a lower mashing temperature can be used, because the substrate is already gelatinised in the extruder before the mixture is introduced to the mash tun. However, enzyme activity measurements should be carried out to determine whether the

enzyme stability of enzymes in the grist is comparable to the enzyme stability during our experiments.

Enzyme extraction: Deactivation of the enzymes during gelatinisation can be avoided by extraction of the enzymes from the malt prior to gelatinisation. Extraction of enzymes is a common procedure that has been applied to determine the enzyme activity in barley and wheat flours (for example, as described in the Ceralpha procedure). In case the enzymes can be extracted from the grist, starch and enzymes can be separated enabling independent optimisation of gelatinisation and enzymatic hydrolysis steps. A highly concentrated gelatinisation and mashing system can only be successful when the extraction procedure does not result in a dilute, aqueous enzyme solution.

Simultaneous hydrolysis and fermentation: Hydrolysis of native, ungelatinised starch with α-amylase from *B. licheniformis* resulted in a gradual increase of glucose, maltose, and maltriose, while the concentration of larger carbohydrates remained low (*Chapter 6*). It might be useful to integrate native starch hydrolysis with simultaneous fermentation to keep the concentration of glucose, maltose, and maltotriose low during fermentation to avoid inhibition of the yeast by these small carbohydrates (Verstrepen *et al.*, 2004). However, the activity of the enzyme at the fermentation temperature should still be investigated.

High pressure gelatinisation: It seems that use of high pressure for either gelatinisation or enzymatic hydrolysis with α-amylase from *B. licheniformis* did not lead to significantly different results in comparison to hydrolysis at atmospheric pressure. This line of application therefore shows limited potential. The process may, however, still be interesting for brewing. Heinz *et al.* (2005) showed that the stability of β-amylase from barley at 65°C increased when the pressure was increased from 0.1 to 100, 200, or 300 MPa. Buckow *et al.* (2007) found that the stability of α-amylase from barley at 60°C increased when the pressure was increased from 0.1 to 200 MPa. The results of Knorr *et al.* (2006) showed that starch in 5 w/w % barley malt suspension is gelatinised completely at temperatures below 65 °C after 15 min of pressures treatment (0-400 MPa) according to birefringence measurements. Based on the combined results of Heinz *et al.*, Buckow *et al.*, and Knorr *et al.*, one should be able to choose a pressure and temperature that results in complete starch gelatinisation without deactivation or with minor deactivation of α- and β-amylase. After gelatinisation, the pressure can be released and enzymatic hydrolysis of the completely gelatinised starch suspension can be continued at a lower temperature than the normal mashing temperature, because the substrate is already gelatinised. The drawback of high pressure gelatinisation is that pressure gelatinised starches are hydrolysed at a lower

reaction rate (*Chapter 6*). An advantage of high pressure gelatinisation is that a lower mashing temperature can be chosen leading to a higher enzyme stability throughout the mashing process. However, a lower mashing temperature might also lead to a lower hydrolysis rate and thus lower volumetric productivity.

Other applications

Starch, being the second most abundant biopolymer after cellulose, is widely used as a (renewable) feedstock for industrial processes (Röper, 2002). We have shown that it is possible to process 50-70 w/w % starch-water mixtures and to introduce an enzyme to the mixture with our extruder-based reaction setup (*Chapter 7*). This setup might also be useful for other reactions in which a concentrated starch slurry is modified or enzymatically broken down by addition of reactants or catalysts. In addition, this extruder-based setup might be useful for processing of other biopolymers. It might, for example, be used for (enzymatic) cellulose treatment for the production of bioethanol.

Conclusions

Although the process configuration described in *Chapter 7* proved to be successful for gelatinisation and enzymatic hydrolysis at high substrate concentrations, other process configurations seem to be feasible as well. In case a semi-continuous process is desired, an extruder can be used to produce gelatinised starch that is fed to a fed-batch reactor. Alternatively, starch can also be gelatinised and hydrolysed simultaneously by adding native, ungelatinised starch to a fed-batch reactor. Continuous processes can be developed by using a static mixer, a tubular reactor, a membrane reactor, or a packed bed reactor after production of gelatinised starch in an extruder. In addition, concepts of polymerisation reactors might be interesting for gelatinisation and enzymatic hydrolysis of concentrated starch-water mixtures.

The results reported in this thesis show that highly concentrated processing has potential for future industrial applications for the production of starch hydrolysates, for brewing, and for modification of starch in general. This may lead to more sustainable processing (less energy consumption, larger volumetric productivity, better use of substrate) and a wider range of products.

References

Buckow R, Weiss U, Heinz V, Knorr D. 2007. Stability and catalytic activity of α-amylase from barley malt at different pressure-temperature conditions. Biotechnol Bioeng 97:1-11.

Ceralpha: α-Amylase assay procedure (CER 07/00) Test Kit Booklet, Megazyme International Ireland Ltd., Bray, County Wicklow, Ireland.

Darnoko D, Cheryan M, Artz WE. 1989. Saccharification of cassava starch in an ultrafiltration reactor. Enzyme Microb Technol 11:154-159.

De Cordt S, Hendrickx M, Maesmans G, Tobback P. 1994. The influence of polyalcohols and carbohydrates on the thermostablity of α-amylase. Biotechnol Bioeng 43:107-114.

Fullbrook PD. 1984. The enzymic production of glucose syrups. In: Dziedzic SZ; Kearsley MW, editors. Glucose syrups: science and technology. London: Elsevier. 65-115.

Grafelman DD, Meagher MM. 1995. Liquefaction of starch by a single-screw extruder and post-extrusion static-mixer reactor. J Food Eng 24:529-542.

Hansen PB, Stubbe P, Birch H, Sørensen KG. 2003. A filtration method and apparatus, WO 03055570.

Hausser A, Goldberg B, Mertens J. 1983. An immobilized two-enzyme system (fungal α-amylase/glucoamylase) and its use in the continuous production of high conversion maltose-containing corn syrups. Biotech Bioeng 25:525–539.

Heinz V, Buckow R, Knorr D. 2005. Catalytic activity of β-amylase from barley in different pressure/temperature domains. Biotechnol progr 21:1632-1638.

Houng J-Y, Chiou J-Y, Chen K-C. 1992. Production of high maltose syrup using an ultrafiltration reactor. Bioprocess Eng 8:85–90.

Kennedy JF, Cabalda VM, White CA. 1988. Enzymic starch utilization and genetic engineering. Trends Biotechnol 6:184-189.

Klibanov AM. 1983. Stabilization of enzymes against thermal inactivation. Adv Appl Microbiol 29:1-28.

Knorr D, Heinz V, Buckow R. 2006. High pressure application for food biopolymers. BBA-Proteins Proteomics 1764:619-631.

Lammers G. 1995. Production of hydroxypropyl starch in a continuous static mixer reactor. PhD thesis, Universiteit of Groningen, Groningen, the Netherlands. 185 p.

Linko P, Linko Y-Y, Olkku J. 1983. Extrusion cooking and bioconversions. J Food Eng 2:243-257.

Lu Y, Biesenberger JA. 1997. Effect of reactor type on polymer product: A backmix reactor for polymerizations and other viscous reaction media. Polym Eng Sci 37:1036-1044.

Marchal LM. 1999. Towards a rational design of commercial maltodextrins: a mechanistic approach. PhD thesis, Wageningen University, Wageningen, the Netherlands. 197 p.

Moates GK, Parker R, Ring SG. 1998. Preferential solvent interactions and the dissolution of the B-type crystalline polymorph of starch in aqueous solutions. Carbohydr Res 313:225-234.

Paolucci-Jeanjean D, Belleville M-P, Rios GM, Zakhia N. 2000a. Kinetics of continuous starch hydrolysis in a membrane reactor. Biochem Eng J 6:233–238.

Paolucci-Jeanjean D, Belleville M-P, Rios GM, Zakhia N. 2000b. The effect of enzyme concentration and space time on the performance of a continuous recycle membrane reactor for one-step starch hydrolysis. Biochem Eng J 5:17-22

Peighambardoust SH, Van der Goot AJ, Hamer RJ, Boom RM. 2006. Process for the separation of gluten and starch, WO 2006123932.

Perry PA, Donald AM. 2002. The effect of sugars on the gelatinisation of starch. Carbohydr Polym 49:155-165.

Röper H. 2002. Renewable raw materials in Europe - Industrial utilisation of starch and sugar. Starch/Stärke 54:89-99.

Simms RL. 1985. The technology of corn wet milling, In: Van Beynum, GMA, Roels JA, editors. Starch conversion technology. New York: Marcel Dekker, 47-72.

Sims KA, Cheryan M. 1992, Hydrolysis of liquefied starch in a membrane reactor. Biotechnol Bioeng 39:960–967.

Sopade PA, Halley PJ, Junming LL. 2004. Gelatinisation of starch in mixtures of sugars. II. Application of differential scanning calorimetry. Carbohydr Polym 58:311-321.

Sriroth K, Walapatit S, Chollakup R, Chotineeranat S, Piyachomkwan K, Oates CG. 1999. An improved dewatering performance in cassava starch process by a pressure filter. Starch/Stärke 51:383-388.

Van der Borght A, Goesaert H, Veraverbeke WS, Delcour JA. 2005. Fractionation of wheat and wheat flour into starch and gluten: overview of the main processes and the factors involved. J Cereal Sci 41:221-237.

Van der Gullik GJS. 2002. Design and scale-up of polycondensation reactors : hydrodynamics in horizontal stirred tanks and pervaporation membrane modules. PhD thesis, Technical University Eindhoven, Eindhoven, the Netherlands. 157 p.

Van der Veen ME. 2005. Towards intensification of starch processing, PhD thesis, Wageningen University, Wageningen, the Netherlands. 104 p.

Verstrepen KJ, Iserentant D, Malcorps P, Derdelinckx G, Van Dijck P, Winderickx J, Pretorius IS, Thevelein JM, Delvaux FR. 2004. Glucose and sucrose: hazardous fast-food for industrial yeast? Trends Biotechnol 22:531-537.

Weickert G. 1998. Hollow shaft reactor: a useful tool for bulk polymerizations at high viscosities, temperatures, and polymerization rates. Ind Eng Chem Res 37:799-806.

Yankov D, Dobreva E, Beschkov V, Emanuilova E. 1986. Study of optimum conditions and kinetics of starch hydrolysis by means of thermostable α-amylase. Enzyme Microb Technol 8:665-667.

Summary

The enzymatic hydrolysis of starch is an important industrial process that is usually preceded by gelatinisation to make starch accessible for the enzyme. In industry, gelatinisation is usually carried out at concentrations of 30–35 w/w % starch (dry weight) in water. However, increasing the substrate concentration during gelatinisation and enzymatic hydrolysis can yield a higher productivity, a lower energy consumption, a lower water consumption, and a higher enzyme stability. Besides these advantages, working at higher starch concentrations also has some disadvantages. When the starch concentration increases, the temperature required to reach complete gelatinisation increases rapidly. Moreover, the viscosity of the starch slurry increases with increasing starch content and this complicates further processing. Conventional equipment used for gelatinisation and enzymatic hydrolysis cannot be used anymore at high substrate concentrations due to the increased viscosity and therefore a different process is needed to handle these concentrated starch slurries. The aim of this PhD project was therefore to develop a process for gelatinisation and enzymatic hydrolysis of wheat starch at high substrate concentrations (more than 40 w/w %) with α-amylase from *Bacillus licheniformis*. Measurements of the α-amylase activity, degree of gelatinisation, and carbohydrate composition are affected by the presence of high concentrations of carbohydrates. Consequently, measurement procedures used for aqueous solutions are often not applicable for concentrated starch-water mixtures. As a result, the effect of high substrate concentrations on measurement techniques for the degree of gelatinisation, and the enzyme activity and stability at high substrate concentrations had to be established.

The effects of high concentrations of carbohydrates on α-amylase activity measurements were described in *Chapters 2* and *3*. A simple kinetic model taking into account substrate inhibition and substrate competition was used to describe the observed phenomena for starch and maltodextrins (*Chapter 2*). For smaller carbohydrates, this model was not suitable and in *Chapter 3* a more general kinetic model was developed that can be used to describe all phenomena, including the observed maximum in the α-amylase activity measurements that was observed in the presence of several carbohydrates. Besides substrate inhibition and substrate competition, this model takes into account the formation of a carbohydrate-enzyme complex that remains active. The model that was developed was used

to correct for the presence of carbohydrates over a wide concentration range in order to obtain the true enzyme activity (*Chapters 6-8*).

Chapter 4 compares gelatinisation curves measured for aqueous (10 w/w %) and concentrated (60 w/w %) starch-water mixtures obtained with birefringence, differential scanning calorimetry, wide angle X-ray scattering, and amylose-iodine complex formation. If a 10 w/w % wheat starch-water mixture was used, each method resulted in approximately the same degree of gelatinisation vs. temperature curve. In case the gelatinisation of a 60 w/w % wheat starch-water mixture was followed as a function of the temperature, each method resulted in a different degree of gelatinisation vs. temperature curve. The differences between the methods were explained by considering the phenomena that take place during the gelatinisation at limiting water conditions. The Flory equation was adapted to provide a quantitative explanation for the curves describing the degree of starch gelatinisation as a function of the starch-water ratio and the temperature.

The results shown in *Chapter 4* are extended in *Chapter 5* by including the effect of pressure and treatment time on the degree of gelatinisation. These results were obtained with differential scanning calorimetry measurements for wheat starch-water mixtures with starch concentrations varying between 5 and 80 w/w %. A thermodynamic model based on the Gibbs energy difference was used to describe the degree of gelatinisation as a function of both pressure and temperature. The experimental and model data were used to construct a phase diagram for 5, 30, and 60 w/w % wheat starch-water mixtures. These phase diagrams can be used to estimate the degree of gelatinisation after applying a certain pressure and temperature on a starch-water mixture with starch concentrations in the range of 5 and 60 w/w %.

Starch can be gelatinised by means of a temperature increase (*Chapters 4* and *5*) or by means of a pressure increase (*Chapter 5*). A comparison between the effect of both gelatinisation methods on the hydrolysate composition and reaction rate during enzymatic hydrolysis of wheat starch with α-amylase from *B. licheniformis* was investigated in *Chapter 6*. We found that the hydrolysate composition was affected by the type of starch pretreatment and the enzyme addition point, but it was not affected by the hydrolysis pressure, as long as gelatinization was complete. The differences between thermally gelatinised, high pressure gelatinised and native starch were explained by considering the

accessibility of starch during the hydrolysis. These results showed that the hydrolysate composition could be influenced by choosing different process sequences and conditions.

With use of the analysis methods from *Chapters 2*, *3*, and *4* and the gelatinisation curves in *Chapter 4*, an extruder-based process was developed that is described in detail in *Chapter 7*. It consists of a twin-screw extruder used for gelatinisation and for mixing α-amylase with gelatinised starch and a batch reactor that was used for the enzymatic hydrolysis of the extrudate. High substrate concentrations (50-70 w/w %) could be handled with this setup. Gelatinisation experimenten showed that mechanical forces lowered the temperature required for complete gelatinisation. During hydrolysis experiments, high dextrose equivalents were observed even if starch was not completely gelatinised during extrusion. Due to high substrate concentrations, the residual α-amylase activity remained high throughout enzymatic hydrolysis, although high temperatures were used. Increased substrate concentrations did not affect the carbohydrate composition of the product.

Instead of carrying out a large number of hydrolysis experiments, it is faster and more efficient to use a kinetic model that is based on literature sources. In *Chapter 8*, a stochastic model was presented that can be used for this purpose. It predicts the formation and breakdown of all saccharides involved during enzymatic starch hydrolysis in time. This kinetic model takes into account the different affinity of α-amylase for different substrates by using the subsite mapping theory. In addition, the main structural characteristics of starch were also taken into account. The performance of the model was verified by comparing the modelled oligosaccharide composition and the dextrose equivalent in time with the corresponding experimental data.

The results shown in this thesis have potential for future industrial applications for the production of starch hydrolysates, for brewing, and, indirectly, for modification of starch, as described in *Chapter 9*. Alternative (semi-)continuous processes were also identified in this chapter. These processes make use of an extruder to gelatinise starch and a tubular mixer or motionless mixer, a fed-batch reactor, a membrane reactor, or a packed bed reactor with immobilized enzyme to hydrolyse the gelatinised starch slurry enzymatically. In addition, polymerisation reactors might be interesting concepts for gelatinisation and enzymatic hydrolysis of concentrated starch-water mixtures.

Samenvatting

De enzymatische hydrolyse van zetmeel is een belangrijk industrieel proces wat meestal vooraf wordt gegaan door de verstijfseling van zetmeel om zetmeel beschikbaar te maken voor enzymen. In de industrie wordt de verstijfseling meestal uitgevoerd met zetmeel-water mengsels met een concentratie van 30-35 massa-% zetmeel. Door de zetmeelconcentratie tijdens het verstijfselen en hydrolyseren te verhogen kan een hogere productiviteit, lagere energieconsumptie, lager water verbruik en hogere enzymstabiliteit bewerkstelligd worden. Naast deze voordelen zijn er helaas ook een aantal nadelen verbonden aan het werken bij hogere zetmeelconcentraties. Indien men de zetmeelconcentratie verhoogt, neemt ook de temperatuur toe die men nodig heeft om zetmeel volledig te verstijfselen. Daarnaast neemt ook de viscositeit van de zetmeel-watermengsels toe. Conventionele apparatuur kan bij verhoogde zetmeelconcentraties niet meer gebruikt worden door deze viscositeittoename. Hierdoor moet er andere apparatuur gezocht worden voor het verstijfselen en hydrolyseren van zetmeel bij hoge zetmeelconcentraties. Het doel van dit promotieonderzoek vloeit voort uit deze constatering: het ontwikkelen van een proces voor het verstijfselen en hydrolyseren van tarwezetmeel bij hoge zetmeelconcentraties (meer dan 40 massa-%) met α-amylase van *Bacillus licheniformis*. Aangezien analyses van de belangrijkste parameters binnen het proces (verstijfselingsgraad, α-amylase activiteit en de koolhydraatsamenstelling) beïnvloed worden door hoge koolhydraatconcentraties, kunnen analysemethoden ontwikkeld voor waterige oplossingen vaak niet toegepast worden. Om deze reden is het effect van hogere substraatconcentraties op het meten van de verstijfselingsgraad, de enzymactiviteit en de enzymstabiliteit onderzocht.

Het effect van hoge koolhydraatconcentraties op α-amylase activiteitsmetingen is beschreven in *hoofdstuk 2* en *3*. Door gebruik te maken van een eenvoudig model wat substraatinhibitie en substraatcompetitie meeneemt, was het mogelijk om de waargenomen activiteitsafname voor zetmeel en maltodextrine (partieel gehydrolyseerd zetmeel) te beschrijven (*hoofdstuk 2*). Dit model was niet geschikt voor het beschrijven van de metingen die waren waargenomen bij kleinere koolhydraten. Hiervoor is er een ander model ontwikkeld (*hoofdstuk 3*) waarmee ook het gemeten maximum in de α-amylase activiteitsmetingen in aanwezigheid van kleine koolhydraten verklaard kan worden. Naast substraatinhibitie en substraatcompetitie neemt dit model ook de vorming van actieve

enzym-koolhydraatcomplexen mee. Dit model was ontwikkeld om te corrigeren voor de aanwezigheid van koolhydraten voor een breed concentratiebereik om zo de echte enzymactiviteit te verkrijgen. De correctiemethode op basis van dit model is gebruikt in *hoofdstuk 6* tot en met *8*.

In *hoofdstuk 4* zijn verstijfselingsgrafieken vergeleken, die waren bepaald voor waterige (10 massa-%) en geconcentreerde (60 massa-%) zetmeel-watermengsels, met verschillende analysetechnieken (microscopie, 'differential scanning calorimetry' (DSC), 'wide angle X-ray scattering' en amylose-iodide complex vorming). Indien 10 massa-% zetmeel-watermengsels werden gebruikt, leverde iedere meetmethode ongeveer dezelfde grafieken voor de verstijfselingsgraad als functie van de temperatuur op. In het geval de verstijfselingsgraad van 60 massa-% zetmeel-watermengsels werd gevolgd als functie van de temperatuur, resulteerde iedere methode in een andere grafiek. De waargenomen verschillen tussen deze meetmethoden bij hoge zetmeelconcentraties zijn verklaard door te kijken naar de diverse verschijnselen die gedurende de verstijfseling plaatsvinden. Een aangepaste versie van de Flory-vergelijking is gebruikt voor een kwantitatieve verklaring van de grafieken waarin de verstijfselingsgraad was uitgezet tegen de temperatuur voor verschillende zetmeelconcentraties.

De resultaten uit *hoofdstuk 4* zijn verder uitgebreid in *hoofdstuk 5* door het effect van druk en behandeltijd op de verstijfselingsgraad mee te nemen. Deze resultaten zijn verkregen door de verstijfselingsgraad in mengsels met verschillende zetmeelconcentraties te meten m.b.v. DSC als functie van de druk, temperatuur en behandeltijd. Een thermodynamisch model, wat gebaseerd is op de Gibbs energie, is gebruikt om de verstijfselingsgraad als functie van druk en temperatuur te modelleren. Met behulp van de simulatiedata en de experimentele gegevens zijn er fasendiagrammen opgesteld voor 5, 30 en 60 massa-% tarwezetmeel-watermengsels. Deze diagrammen kunnen gebruikt worden om de verstijfselinsgraad af te schatten als functie van de druk en temperatuur voor tussenliggende zetmeelconcentraties.

Zetmeel kan men verstijfselen door de temperatuur te verhogen (*hoofdstuk 4* en *5*) en door de druk te verhogen (*hoofdstuk 5*). Het effect van deze verschillende verstijfselingscondities op de koolhydraatsamenstelling en reactiesnelheid gedurende de enzymatische hydrolyse van tarwezetmeel met α-amylase van *B. licheniformis* is beschreven in *hoofdstuk 6*. Tijdens de bijbehorende experimenten bleek dat de samenstelling van het reactiemengsel werd

beïnvloed door de verstijfselingstechniek en de locatie waarop het enzym werd toegevoegd. Echter, indien het substraat volledig verstijfseld was, werd de samenstelling niet beïnvloedt door een andere hydrolysedruk. De verschillende resultaten voor thermisch verstijfseld, hoge druk verstijfseld en natief zetmeel zijn verklaard door de beschikbaarheid van zetmeel tijdens de hydrolyse te beschouwen. De resultaten in dit hoofdstuk tonen aan dat de samenstelling van het reactiemengsel gedurende hydrolyse kan worden beïnvloed door verschillende verstijfselingsmethoden te kiezen.

Met gebruik van de meetmethoden beschreven in *hoofdstuk 2, 3* en *4* en de verstijfselingsgrafieken in *hoofdstuk 4* is een op extrusie gebaseerd proces ontwikkeld (*hoofdstuk 7*). Het bestaat uit een dubbelschroefsextruder die gebruikt werd voor het verstijfselen van zetmeel en het mengen van α-amylase met verstijfseld zetmeel en een batchreactor die gebruikt werd voor de hydrolyse van het verstijfselde zetmeel. Met dit proces was het mogelijk om zetmeel te verstijfselen en te hydrolyseren bij hoge zetmeelconcentraties (50-70 massa-%). Verstijfselingsexperimenten toonden aan dat mechanische krachten opgelegd op het substraat zorgden voor een verlaging van de temperatuur die nodig was voor volledige verstijfseling. Gedurende de hydrolyse-experimenten was het mogelijk om hydrolyseproducten te maken met een hoog dextrose equivalent, zelfs als het zetmeel niet volledig verstijfseld was. Hoge zetmeelconcentraties bleken de samenstelling van het reactieproduct niet te beïnvloeden.

In plaats van het uitvoeren van een groot aantal hydrolyse-experimenten is het sneller en efficiënter om een kinetisch model te gebruiken wat gebaseerd is op literatuurbronnen. In *hoofdstuk 8* is een model beschreven wat de vorming en afbraak van alle koolhydraten gedurende de hydrolyse kan voorspellen. Affiniteitsverschillen van α-amylase voor verschillende substraten zijn meegenomen in dit model door gebruik te maken van de zogenaamde 'subsite mapping'-theorie. Daarnaast zijn de belangrijkste aspecten van de zetmeelstructuur meegenomen in het model. De kwaliteit van de modelvoorspellingen is beoordeeld door de voorspelde oligosaccharide samenstelling en dextrose equivalent als functie van de tijd te vergelijken met experimentele waarden.

De resultaten uit dit proefschrift kunnen mogelijk worden toegepast n in industriële processen voor de productie van zetmeelhydrolysaten, voor bierbrouwen en, weliswaar indirect, voor het modificeren van zetmeel. Dit is beschreven in *hoofdstuk 9*. Daarnaast zijn er in dit hoofdstuk enkele andere (semi-)continu processen beschreven gebaseerd op een

extruder voor het verstijfselen van zetmeel gevolgd door een buisreactor of statische menger, een fed-batchreactor, een membraanreactor, of een gepakt bed met geïmmobiliseerd enzym voor de enzymatische hydrolyse van verstijfseld zetmeel. Verder worden polymerisatiereactoren nog genoemd, omdat zij wellicht ook bruikbaar kunnen zijn voor de verstijfseling en hydrolyse van zetmeel bij hoge zetmeelconcentraties.

Dankwoord

De vier jaar promotieonderzoek zijn voorbij gevlogen! Enerzijds doordat mijn promotieonderzoek erg leuk en leerzaam was, anderzijds door de leuke activiteiten die er op de vakgroep georganiseerd werden of waaraan meegedaan werd door de vakgroep. In het eerste jaar heb ik me echter ook dikwijls afgevraagd of ik wel 'op mijn plek zat' in Wageningen, waar het allemaal net wat anders was dan in Eindhoven. Terugkijkend denk ik dat ik door deze promotie juist veel nieuwe dingen heb geleerd en veel nieuwe, leuke mensen heb leren kennen. Allereerst wil ik dan ook al mijn collega's bedanken voor de leuke promotietijd!

De mensen waar je uiteraard veel mee te maken hebt, zijn je begeleiders. Anja: naast een kritische, hardwerkende (nooit hoefde ik lang te wachten op een goede correctie) begeleidster was je ook nog veel meer voor mij. Als ik het even niet zag zitten, zowel onderzoektechnisch als daarbuiten, kon ik altijd bij jou terecht voor een luisterend oor, advies en een opbeurend woord. Verder toon je altijd interesse in de mensen om je heen. Ik zal je dan ook zeker gaan missen! Remko: altijd vol vertrouwen en goede ideeën. Daarnaast wist je tijdens werkbesprekingen altijd verbazingwekkend snel hoe de vork in de steel zat en kon je daardoor ook vrijwel direct meedenken over oplossingen voor problemen, de vinger op de zere plek leggen of nieuwe onderzoeksplannen bedenken. Ik heb jullie manier van begeleiden altijd enorm gewaardeerd en ik realiseer me dat begeleiding die jullie me gaven een enorme luxe is en zeker niet vanzelfsprekend. Enorm bedankt daarvoor! Ik hoop dat we in de toekomst contact houden met elkaar.

Naast de begeleiding intern op de vakgroep, had ik ook nog een aantal externe begeleiders. De discussies en presentaties bij jullie vond ik erg leerzaam. August, Eric, Leen, Lex, Onno, Rolf en Willem: bedankt voor de vrijheid die jullie me gaven, jullie inbreng en jullie betrokkenheid bij het project.

Tijdens mijn promotie heb ik een aantal studenten mogen begeleiden. Het was erg leerzaam, maar ook heel erg leuk om samen met jullie te werken. Jullie hebben enorm veel werk verzet en dat heeft geleid tot mooie resultaten. Anja, Evelyn, Ikenna, Marieke, Raymond, Tamara en Jeroen: bedankt voor jullie inzet en gezelligheid!

Daarnaast kon ik ook altijd rekenen op de ondersteunende staf van proceskunde. Voor declaraties, computers, software, meetapparatuur, gereedschap, chemicaliën of laboratoriumbenodigdheden kon ik altijd bij een van jullie terecht! Joyce, Fred, Gerrit, Jos, Martin, Maurice, Pieter, Rouke, Sebastiaan: bedankt daarvoor!

Tijdens mijn promotie heb ik een gedeelte van de experimenten uitgevoerd bij het onderzoeksinstituut Agrotechnology & Food Innovations in Wageningen. Ondanks dat ik hier formeel niet werkte, kon ik toch rekenen op de hulp van diverse mensen. Jeroen: bedankt voor de nuttige discussies over zetmeel en zetmeelverstijfseling. Uiteindelijk ben ik door jou in contact gekomen met anderen binnen jullie instituut, wat heeft geleid tot een aantal artikelen. Frans: door jouw kennis en ervaring hebben we in een relatief korte tijd een hoop extrusiegegevens kunnen verkrijgen en een mooi artikel kunnen schrijven. Herman, Aldo en Guus: bedankt voor de hulp bij de DSC, 'compression molder' en WAXS metingen.

Een gedeelte van het onvermijdelijke promotieleed kon ik delen met de collega's tijdens het groepsoverleg (Daniel, Jan, Marieke, Maurice en Ruben). Bedankt voor de nuttige discussies en natuurlijk jullie geduld als ik in mijn enthousiasme net wat meer tijd nam voor de bespreking. Promotieleed hangt vreemd genoeg nogal eens samen met HPLC metingen. Maurice: jij wist de HPLC problemen altijd weer te verhelpen! Of de aandacht af te leiden door 's avonds af te spreken om spellen te spelen of films te kijken.

Verder wil ik graag mijn kamergenoten Martin, Dirk, Mohammed, Eduard, Sebastiaan, Jan-Willem en Cynthia bedanken voor de gezelligheid, maar ook voor het aanhoren van mijn (eindeloze?) geklets. Daarnaast weet ik nu een 'stuk' meer over algen, microfibrils en membranen!

Op de vakgroep waren er altijd wel mensen te vinden om buiten werktijd iets af te spreken. In eerste instantie hardlopen met Judy en Julita, daarna spinnen met Gerben en nog later wielrennen met de vakgroep (en anderen inmiddels). Voor mij waren deze sportmomenten noodzakelijk om af en toe afstand te nemen van mijn promotie. De 'stedentrips' samen met Cynthia, Detmer en Ronald, met daarbij als onbetwist hoogtepunt natuurlijk het bezoek aan Eindhoven, zorgden ook voor de nodige ontspanning! Erg jammer dat we daar nu niet meer zo vaak aan toe zullen komen! Daarnaast vond ik het eten bij de mensa, veelal vergezeld door Hylke en Sebastiaan, ook altijd erg gezellig.

Naast het contact met mijn collega's, heb ik de omgang met mijn huisgenoten in de Hoogstraat erg gewaardeerd. Mede dankzij jullie heb ik mijn draai in Wageningen kunnen vinden! Dorien, Femke, Marije, Mieke, Linette, Eelke, Gerben en Matthijs: bedankt voor de leuke tijd!

In de weekenden was ik vaak in Nuenen/Eindhoven te vinden. Niet voor niets, want bij velen kan ik terecht voor gezelligheid, afleiding en steun. Eefje, Elwin, Eva, Katja, Paul, Roland en Wouter: om wat voor reden we ook samen komen, ik vind het altijd enorm gezellig. Jeroen en Martijn: ik hoop dat we samen nog vaak bladerdeeg gaan eten (en radje draaien). Er moet natuurlijk ook gesurft worden! Rolf: ondanks dat je nu een gezin hebt, kan ik gelukkig nog regelmatig met jou op pad. Rob: je woont nu weliswaar in Frankrijk, toch hoop ik dat we contact houden. Walter: bedankt voor de getoonde interesse gedurende mijn promotie. Mark: bij wie kan ik beter terecht als ik een luisterend oor nodig heb, voor het inwinnen van advies, of om een activiteit te ondernemen! Ten slotte wil ik ook iedereen van de 'Albert Heijn' groep bedanken voor de gezelligheid.

Tijdens mijn studie op de TU/e heb ik veel tijd doorgebracht met Ard, Maurice, Sander en Twan. Vele uren zaten we te blokken in de collegezalen of zelfstudieruimtes. Dat is toch de basis geweest voor deze promotie en dat van grote waarde voor mij! Uit die periode (en plek) komen ook de eet-en-spellen avonden voort. Ida, Truusje, Wendy, Arno, Bas, Jaap, Jason en Thijs: hopelijk volgen er nog veel gezellige, competatieve, no-nonsense avonden waar er naast ruimte voor zieken ook altijd ruimte is voor wat serieuzere zaken!

Ten slotte mijn familie en in het speciaal mijn ouders en mijn broers bedanken. Jullie weten dat ik niet de makkelijkste persoon ben. Niet voor mezelf en ook niet altijd voor anderen. Desondanks hebben jullie me altijd gesteund, altijd vertrouwen in me gehad en me bovendien veel geleerd. Daarnaast kan ik altijd bij jullie terecht. Ik weet dat dit niet vanzelfsprekend is! De basis voor het slagen van deze promotie is dan ook gelegd door jullie. Ik hoop dat we in de toekomst, ondanks dat we niet dichtbij elkaar wonen, nog veel tijd samen door kunnen brengen!

Publications

Baks T, Janssen AEM, Boom RM. 2006. The effect of carbohydrates on α-amylase activity measurements. Enzyme Microb Technol 39:114-119.

Baks T, Janssen AEM, Boom RM. 2006. A kinetic model to explain the maximum in α-amylase activity measurements in the presence of small carbohydrates. Biotechnol Bioeng 94:431-440.

Baks T, Ngene IS, Van Soest JJG, Janssen AEM, Boom RM. 2007. Comparison of methods to determine the degree of gelatinisation for both high and low starch concentrations. Carbohydr Polym 67:481-490.

Baks T, Kappen FHJ, Janssen AEM, Boom RM. 2007. Towards an optimal process for gelatinisation and hydrolysis of highly concentrated starch-water mixtures with α-amylase from *B. licheniformis*. Accepted for publication in J Cereal Sci.

Baks T, Bruins ME, Janssen AEM, Boom RM. 2007. The effect of pressure and temperature on the gelatinisation of starch at various starch concentrations. Submitted for publication.

Baks T, Bruins ME, Matser AM, Janssen AEM, Boom RM. 2007. Effect of gelatinisation and hydrolysis conditions on the selectivity of starch hydrolysis with α-amylase from *B. licheniformis*. Submitted for publication.

Besselink T, Baks T, Janssen AEM, Boom RM. 2007. A stochastic model for predicting dextrose equivalent and saccharide composition during enzymatic starch hydrolysis. Submitted for publication.

Baks T, Janssen AEM, Boom RM. 2007. Process development for enzymatic starch conversion at high concentrations. Alternatives for brewing? Proceedings of 31st EBC congress, Venice, Italy.

Training activities

Discipline specific activities

Courses
Advanced Biocatalysis (BSDL, 2004)
A unified approach to mass transfer (OSPT, 2004)
Reaction kinetics in food science (VLAG, 2004)
Numerical methods in process technology (OSPT, 2005)
Summer course glycosciences (VLAG, 2006)

Meetings
Netherlands Process technology Symposium (2003, 2004, 2005, 2006)
Biocatalysis in Foods and Drinks Industries (2004, 2006)
Congress of European Brewery Convention (2007)

General courses
Organizing and guiding BSc and MSc students (OWU, 2003)
Time planning and project management (WGS, 2004)
VLAG PhD week (VLAG, 2004)
Result and development training (HRM, 2005)
Scientific writing (CENTA, 2005)
Giving lectures (OWU, 2006)
Career Perspectives (WGS, 2006)
Access First Career Workshop (Access First, 2007)

Optionals
Preparing PhD research proposal (2003)
Meetings and internship (2003-2007)
PhD study tour Canada (2004)
Case study prevention of biofilm formation on process equipment (2006)
PhD study tour Denmark and Sweden (2006)

Curriculum Vitae

Tim Baks was born in Eindhoven (the Netherlands) on the 24th of March 1979, but lived in a beautiful village near Eindhoven called Nuenen for the next 23 years. In 1991, he started his secondary education in Eindhoven at the Lorentz Lyceum (now called Lorentz Casimir Lyceum) where he received his diploma in 1997. In the same year, he started his MSc in Chemical Engineering and Chemistry at Eindhoven University of Technology. His MSc thesis (topic: phenol oxidation in a three phase slurry reactor) was carried out at the Chemical Reactor Engineering group. After obtaining his MSc degree (cum laude) in 2003, he became a PhD student at the Food and Bioprocess Engineering department at Wageningen University (2003-2007) focusing on enzymatic conversions in highly concentrated reaction systems and specifically the enzymatic hydrolysis of starch. The results obtained in this period are written in this thesis. On July 1st 2007, he started working at Akzo Nobel Chemicals as researcher chemical reaction engineering.

Tim Baks werd op 24 maart 1979 geboren in Eindhoven, maar hij heeft de eerste 23 jaar van zijn leven doorgebracht in het schitterende, nabijgelegen plaatsje Nuenen. In 1991 begon hij aan het Atheneum in Eindhoven op het Lorentz Lyceum (inmiddels Lorentz-Casimir Lyceum) waar hij in 1997 zijn diploma behaalde. In hetzelfde jaar begon hij aan de studie scheikundige technologie aan de Technische Universiteit in Eindhoven. Zijn afstudeerproject getiteld "phenol oxidation in a three phase slurry reactor" heeft hij uitgevoerd bij de vakgroep chemische reactoren. Nadat hij in 2003 cum laude afstudeerde, werd hij promovendus binnen de groep levensmiddelen- en bioproceskunde aan de Wageningen Universiteit (2003-2007) waar hij onderzoek heeft verricht naar enzymatische omzettingen in hooggeconcentreerde reactie systemen en specifiek naar de enzymatische hydrolyse van zetmeel. De resultaten die zijn verkregen in deze periode staan beschreven in dit proefschrift. Vanaf 1 juli 2007 is hij werkzaam bij Akzo Nobel Chemicals als onderzoeker chemische reactorkunde.